Avian Conservation Bioacoustics in Human-modified Landscapes: Community Responses to Forest Management and Riparian Urbanization in the Pacific Northwest

Giordano Jacuzzi

A dissertation

submitted in partial fulfillment of the

requirements for the degree of

Doctor of Philosophy

University of Washington

2026

Reading Committee:

Julian D. Olden, Chair

Sarah J. Converse

Beth Gardner

Joshua Lawler

Program authorized to offer degree:

School of Aquatic and Fishery Sciences

Chapter 1 © Copyright 2025
The authors, *Ecological Informatics*

Chapter 2 © Copyright 2026
The authors

Chapter 3 © Copyright 2026
The authors

All other materials © Copyright 2026
Giordano Jacuzzi

University of Washington

ABSTRACT

Avian conservation bioacoustics in human-modified landscapes:
Community responses to forest management and riparian urbanization in the Pacific Northwest

Giordano Jacuzzi

Chair of the Supervisory Committee:
Julian D. Olden
School of Aquatic and Fishery Sciences

The global loss of biodiversity is among the most central environmental challenges of the 21st century, and understanding the effects of land-use change and resource management on forest and riparian ecosystems is critical for the conservation of wildlife and ecosystem functions. Populations of many avian species in the Pacific Northwest have declined substantially over the past half century due to a legacy of habitat loss and degradation through forest management and urban development. These trends continue today despite the designation of late-successional reserves and general stability of early-seral habitat following the passage of the Northwest Forest Plan in 1994, and the increasing adoption of compact urban growth strategies and riparian protections—initiatives that have revolutionized land-use and resource management in the region. This points to an urgent need to better understand the processes that generate and maintain avian biodiversity and inform management strategies to ensure ecosystem integrity amid the ongoing biodiversity crisis.

Several practical challenges and knowledge gaps limit our current understanding of the relationships between forest and riparian management and avian communities. First, managers lack robust monitoring solutions that can operate at large spatiotemporal scales, and the promise of leveraging pre-trained bioacoustic classifiers with passive acoustic monitoring as an accessible and scalable method for rapid ecosystem surveillance remains unfulfilled due to poor generalization of classifiers in applied biodiversity surveys. Second, integrated forest management aims to balance biodiversity conservation with timber production and ecosystem service objectives, but the response of bird communities to habitat created through integrated forest management remains poorly understood, and uncertainties remain regarding the relative conservation value and ecological function of the developmental stages that constitute managed forest landscapes. Third, declines in insectivorous bird populations are attributed in part to parallel reductions in riparian habitat and the availability of aquatic prey, however, it remains unknown how urbanization alters aquatic subsidies and how these changes propagate to avian consumers, limiting our ability to anticipate future urbanization impacts and inform cross-boundary mitigation strategies.

I address these challenges by applying novel methods in passive acoustic monitoring, machine learning, and quantitative community ecology to enable the investigation of avian community responses to forest management and riparian urbanization in the Pacific Northwest. My first chapter demonstrates the use of a few-shot transfer learning approach to efficiently adapt a pre-trained bioacoustic classifier to a new domain with minimal local training data. I present an open-source workflow with guidelines for evaluating performance with ecologically meaningful metrics and training a model to improve performance for existing species and to add additional species or sounds of interest. In my second chapter, I employ a custom bioacoustic

classifier to survey breeding bird communities across a mosaic of forest developmental stages maintained by management in the Olympic Experimental State Forest, Washington. By leveraging multi-species occupancy models and multivariate analyses of community composition, I demonstrate the irreplaceable conservation value of mature primary forests and early-seral habitat and explore the importance of landscape management strategies that integrate both late-successional reserves and structurally enriched managed stands. Finally, in my third chapter I examine how aquatic insect communities, riparian vegetation, and urban land cover influence breeding bird assemblages across streams spanning an urbanization gradient in the Seattle metropolitan area. I use multi-species occupancy and structural equation modeling to reveal strong associations between stream biotic integrity and the richness of insectivore and migrant guilds, and report that the protection and restoration of riparian vegetation at both local and landscape scales may be necessary to maintain present-day avian richness levels in the face of projected urban expansion throughout the remainder of the century. Collectively, this research demonstrates the value of conservation bioacoustics for monitoring avian communities in human-modified landscapes and informing management strategies to protect avian biodiversity and ecosystem functions amidst continuing population declines.

TABLE OF CONTENTS

List of Figures ii

List of Tables v

Chapter 1. Few-shot transfer learning enables robust acoustic monitoring of wildlife communities at the landscape scale 1

1.1 Abstract 1
1.2 Introduction 2
1.3 Methods 6
1.4 Results 15
1.5 Discussion 24
1.6 Acknowledgements 35
1.7 Data availability 36
1.8 References 37
1.9 Appendix 1.1 43
1.10 Appendix 1.2 52

Chapter 2. Avian community responses to forest successional stage in a managed mosaic landscape 53

2.1 Abstract 53
2.2 Introduction 54
2.3 Methods 61
2.4 Results 74
2.5 Discussion 85
2.6 Acknowledgements 95
2.7 Data availability 96
2.8 References 97
2.9 Appendix 2.1 112
2.10 Appendix 2.2 125

Chapter 3. Aquatic insect subsidies mediate current and future urbanization effects on insectivorous birds across spatial scales 128

3.1 Abstract 128
3.2 Introduction 129
3.3 Methods 133
3.4 Results 144
3.5 Discussion 152
3.6 Acknowledgements 160
3.7 Data availability 160
3.8 References 161
3.9 Appendix 3.1 174
3.10 Appendix 3.2 186

LIST OF FIGURES

Figure 1.1: Domain shift between source and target domains. Species classes in the target region are shared, but the source domain may fail to account for variation in the target domain due to its novel acoustic context. 4
Figure 1.2: Conceptual diagram of the adapted convolutional neural network architecture. The source model extracts a feature embedding from the input audio segment spectrogram, which is associated with output class labels by a pre-trained classifier head. This classifier head is replaced with a new neural network trained on a small amount of local data from the target domain, changing the downstream output class labels. 13
Figure 1.3: Causes of confusion and performance error in the pre-trained source model, illustrated as associations between labels. Label nodes are grouped by type, order, and family (if applicable). A connection (i.e., edge) between nodes represents an incorrect prediction made at decision threshold $T_{0.5}$, with the light-colored terminus indicating the predicted label and the dark the true label. Nodes with many dark purple connections are labels frequently present in incorrect predictions and may serve as sources of confusion that define the unique acoustic context of the target domain. Node size is inversely related to precision-recall AUC, with poorly performing labels (low values) larger and well-performing labels (high values) smaller. Node alpha shading indicates the true presence of a label in the test data; the source model produces false positives for the absent species shown. 17
Figure 1.4: Differences in test performance between source (red) and target (blue) models with precision and recall across decision thresholds (top, bounded confidence scale) and prediction score distributions (bottom, logit scale), including both positive and negative samples, for selected species classes with high (A), moderate (B), and low (C) performance gains at the segment level. Classes achieved greater recall performance and improved precision stability across thresholds. Score distributions and paired precision-recall curves indicate that prediction scores generally shifted to lower and higher values for negative and positive samples, respectively, suggesting an improved ability to discriminate between samples that do and do not contain a species. Despite a small training sample size of 38, the Marbled Murrelet overcame previous signal confusions (shown by the low and jagged source model precision line). Performance for the Sooty Grouse also substantially improved AUC but continued to be challenged by signal confusion. The Golden-crowned Kinglet and Wilson's Warbler produced more bimodal score distributions and achieved gains from moderate source model performance to high target model performance. The Black-throated Gray Warbler already performed highly with the source model and achieved minimal gains in AUC at the segment level. However, improvements in recall and the shift in score distribution led to significant increases in accuracy at the site level (Table 1.1). The Belted Kingfisher did not substantially benefit from training due to a low training sample size and the presence of similar signals inducing frequent confusion. 22
Figure 2.1: Forest developmental stages maintained by integrated forest management in the Olympic Experimental State Forest, Washington, USA. Stages are stratified by stand age, representing a gradient of successional progression (A): stand initiation following variable retention harvest, stem exclusion, variable density thinning, and mature protected habitat reserve, including late-successional and old-growth forest. Examples of in-stand structure (B) and forest cover from satellite imagery (C) for each developmental stage. 58
Figure 2.2: Forest habitat and bioacoustic survey methodology to quantify avian community responses to integrated forest management. 224 site locations across the study area within the Olympic Experimental State Forest were sampled across stands of each management developmental stage (A). At each site an autonomous recording unit performed bioacoustic surveys for avian occurrence and measurements of environmental variables were taken at three spatial scales (B), the 100 m radius plot scale, the stand scale, and the species-specific home range scale. 62
Figure 2.3: Patterns in alpha and beta diversity across survey sites and developmental stages. (A) Posterior median species richness per site by stage (alpha diversity). (B) Non-metric multidimensional scaling (NMDS) ordination of assemblage composition based on Bray-Curtis dissimilarity. Points represent sites colored by

developmental stage with 95% confidence ellipses. (C) Beta diversity measured by pairwise dissimilarity between stages β_{BC} partitioned into species turnover β_{bal} and nestedness components β_{gra}. 76
Figure 2.4: Multi-species occupancy model coefficient estimates for effects of forest developmental stage proportion at the species-specific home range scale at the community, functional guild (A), and species (B) levels. Mean guild-level coefficients for three functional groupings are shown: community (comprising all species), nesting microhabitat (primary cavity, secondary cavity, tree, shrub, and ground nesting guilds), and foraging substrate (aerial, bark, ground, and foliage gleaning guilds). Posterior means and 95% and 50% Bayesian credible intervals (thin and thick lines, respectively) are shown in opaque color for guild-specific estimates (A) where the 50% BCI excludes zero, indicating probable effects, and for species-specific estimates (B) where the 95% BCI excludes zero, indicating strong effects. Covariates were *Z*-scored, and estimates are shown relative to stem exclusion as a baseline stage such that a positive effect indicates a greater probability of habitat use compared to stem exclusion. 80
Figure 2.5: Stage-specific mean community-level coefficient estimates for effects of local habitat structure at the plot scale: proportion of hardwood tree species, quadratic mean diameter, and tree density. Posterior means and 95% and 50% Bayesian credible intervals are shown in opaque color where the 50% BCI excludes zero, indicating probable effects. All covariates were *Z*-scored. 82
Figure 2.6: Relative conservation value of forest developmental stages for species and groups of conservation priority, as measured by marginal expected species richness when the home range comprises 100% of a given developmental stage for conservation priority species (A), and biological associates of early-seral (B) and old-forest habitat (C). Marginal predicted habitat use probability for conservation priority species across pairwise gradients of developmental stage composition (D) is calculated as weighted averages of stage-specific predictions proportional to home range composition. 84
Figure 3.1: Theoretical model illustrating pathways of influence, including trophic linkages and abiotic environmental effects, linking avian insectivores with aquatic macroinvertebrate prey, riparian vegetation, and urbanization stressors across multiple spatial scales. 131
Figure 3.2: Stream sampling methodology. Site locations in the Seattle metropolitan area (A) were sampled across an urbanization gradient of impervious surface cover (ISC) (B). At each site an autonomous recording unit was used to conduct a bioacoustic survey for avian occurrence, co-located with an in-stream macroinvertebrate survey to quantify the benthic index of biotic integrity (B-IBI) (C). Environmental measurements were taken from the riparian zone and connected stream segments and waterbodies, buffered by 100 m to include edge habitat, at local (C) and landscape (D) spatial extents. 135
Figure 3.3: Multi-species occupancy modeling results across functional groupings for the benthic index of biotic integrity (B-IBI). (A) Guild-level effects of B-IBI on occurrence probability (posterior means with 95% Bayesian credible intervals). (B) Mean marginal probabilities of occurrence for each guild in relation to B-IBI. Bold lines show responses for guild-level means with shaded 95% Bayesian credible intervals. Ghosted lines show responses for individual species members 145
Figure 3.4: Structural equation model illustrating pathways through which urban development (ISC) at local and landscape spatial scales directly and indirectly affected riparian vegetation (TCC), benthic macroinvertebrate prey diversity (B-IBI), and posterior estimates of species richness for the avian insectivore guild, based on data from remote sensing, in-stream surveys, and bioacoustic monitoring. Arrows represent causal pathways between predictor and response variables, with line thickness proportional to the mean estimated standardized effect size. R^2 values show the mean variance of endogenous variables explained by predictors. 147
Figure 3.5: Projected future changes in B-IBI (A) and avian insectivore richness (B) over time as a consequence of urban development under the B1 ICLUS scenario, illustrated using an SEM fit to the posterior mean richness. Mean trajectories across all surveyed stream sites are shown in bold color over individual site trajectories. (C,D) Predicted losses in B-IBI and richness in 2100 compared to present-day levels. 150
Figure 3.6: Predicted management action at local and landscape scales required to maintain present-day avian richness levels by year 2100, obtained from a sensitivity analysis of the SEM fit to the posterior mean

insectivore richness. (A) Local-only scenario, with commensurate increases in riparian vegetation from restoration implied. (B) Landscape-only scenario, with stream sites aligned with (A). (C) Predicted insectivore richness, using posterior mean SEM, across both spatial dimensions of impervious surface cover (ISC). Contours show equal levels of richness. Individual stream trajectories are shown with lines beginning at present-day conditions and ending at projected conditions in 2100 under a “no action” scenario. Streams shown in gray can fully mitigate reductions through single-scale management, at either the local or catchment scale. Those shown in red can only maintain richness via management at the local (triangle) or landscape (square) scale. Those shown in purple require management actions at both scales simultaneously..... 152

LIST OF TABLES

Table 1.1: Performance comparison between source and target models at the audio segment and site use levels. N indicates the number of examples for each class used to train the target model. Precision-recall AUC and F_1 score maximum are shown at the segment level. Accuracy at the site level indicates the percentage of sites correctly predicted for a species' presence and absence. Site level metrics were calculated using decision threshold $T_{0.9}$, which yielded the maximum total mean accuracy between both models and is coincidentally a widely used arbitrary threshold in bioacoustics studies. See Table A1.2 for the performance of alternative threshold values. Delta values are colored by target model performance with respect to the source model (green for improved performance, red for reduced performance, and white for approximately equal performance). Species are arranged by decreasing segment level ΔAUC..... 19

Table 1.2: Guidelines for few-shot transfer learning practitioners in bioacoustics research. 32

Table 2.1: Pairwise diversity metrics comparing assemblage composition among developmental stages, shown as posterior medians alongside 95% Bayesian credible intervals and posterior probabilities: species richness difference, $\Delta\alpha$, probability that richness of stage 1 exceeds stage 2, $P(\alpha_1 > \alpha_2)$, Bray-Curtis dissimilarity difference, $\Delta\beta_{BC}$, probability that between-stage dissimilarity exceeds within-stage dissimilarity, $P(\beta_{between} > \beta_{within})$, and Bray-Curtis dissimilarity β_{BC}, partitioned into components of species turnover (balanced variation), β_{bal}, and nestedness (use gradient), β_{gra}. 77

Table 3.1: Standardized path coefficients for guild-specific structural equation models. Coefficient posterior mean and 95% Bayesian credible intervals are shown. Component models relating the benthic index of biotic integrity (B-IBI) to landscape-scale impervious surface cover (ISC_{land}) and local-scale tree canopy cover (TCC_{local}), and TCC_{local} to ISC_{local}, shared an identical structure across all structural equation models. *f* is the proportion of the posterior with the same sign as the mean, reflecting uncertainty that an effect is positive or negative. 148

Chapter 1. FEW-SHOT TRANSFER LEARNING ENABLES ROBUST ACOUSTIC MONITORING OF WILDLIFE COMMUNITIES AT THE LANDSCAPE SCALE

Publication history: This study was co-authored with Julian D. Olden and has been published in *Ecological Informatics* (citation below).

Jacuzzi, G. & Olden, J.D. 2025. Few-shot transfer learning enables robust acoustic monitoring of wildlife communities at the landscape scale. *Ecological Informatics* 90 (Dec): 103294

1.1 ABSTRACT

Pre-trained classifiers for bioacoustic species detection have emerged as accessible tools for conservation and automated biodiversity monitoring at scale. Despite their wide use, these models are trained primarily on high-quality, weakly labeled species recordings from disparate regions that can fail to account for variation in passive ambient soundscape data due to poor signal-to-noise ratio and the presence of novel sounds such as abiotic noise and concurrent vocalizations. This domain shift may limit a pre-trained model's reliability and preclude its use in applied acoustic monitoring. Although relatively underexplored in bioacoustic monitoring, transfer learning may help overcome the limitations of existing pre-trained classifiers by enhancing predictive performance while avoiding the time, resources, and expertise required to develop entirely new models. We demonstrate the use of few-shot transfer learning as a strategy to efficiently adapt a pre-trained BirdNET source model to a new target domain with minimal local training data. We present an open-source workflow with guidelines to evaluate performance with ecologically meaningful metrics and train a target model with improved or missing classes for biotic and abiotic signals of interest. This process is demonstrated with an applied case study of community level acoustic monitoring across a managed temperate rainforest landscape in western Washington, United States.

The target model achieved a mean precision-recall AUC of 0.94 at the audio segment level and a mean accuracy of 92% at the site use level across trained avian species classes, an increase of 0.15 and 13% over the pre-trained source model, respectively. These improvements increased the probability of individual species detection and produced more accurate estimates of local species richness. Several species of high conservation and management priority that could not be reliably detected by the source model achieved high performance. Superior performance was achieved with an average of only 8 local training examples per species class. Training novel classes for other signals of interest (e.g., anurans, insects, aircraft, logging, rain) reduced confusion rates and mitigated the impact of the local environment on performance. Few-shot transfer learning leverages the learned knowledge of a pre-trained classifier to enable robust monitoring at the community level across the landscape and offers an approach that can be readily applied to other environments and taxa.

1.2 INTRODUCTION

Passive acoustic monitoring (PAM) is increasingly commonplace in the ecological sciences to inform wildlife management and conservation (Gibb et al., 2019; Oswald et al., 2022). Among the growing number of methods to navigate the vast quantities of acoustic data produced by PAM surveys, deep learning models such as convolutional neural networks have emerged as the leading tools used to automatically identify and label biotic signals for species detection (Stowell 2022; Oswald et al., 2022; Nieto-Mora et al., 2023). Far-reaching applications of these approaches include detecting rare and endangered species (Zhong et al., 2020a; Duarte et al., 2024), investigating animal behavior (Folliot et al., 2022), quantifying biodiversity patterns (Müller et al., 2023; Morales et al., 2022), and understanding responses of wildlife to environmental change (Larkin et al., 2024).

Developing deep learning models *de novo* is a persistent challenge for applied monitoring programs due to prohibitive requirements of time, data, processing power, and technical expertise (Kershenbaum et al., 2024; Oswald et al., 2022). This has sparked the burgeoning adoption of “off-the-shelf” classifier models that come pre-trained on vast quantities of bioacoustic data for different taxa from around the world (e.g., BirdNET, Merlin, Perch, Silbido)

(Stowell 2022). These openly available models are powerful and accessible, requiring minimal technical expertise to use, and are increasingly employed by researchers (Cole et al., 2022), managers (Sethi et al., 2021), and more than one million citizen scientists (Wood et al., 2022) to produce species detection histories. While pre-trained models can excel at classifying high-quality single-species recordings of a specific taxon, there is a growing appreciation that their performance degrades substantially for soundscape datasets generated from field surveys for conservation and management, where acoustic complexity often yields high rates of false positive and false negative errors (Kahl et al., 2021; Goëau et al., 2018; Pérez-Granados 2023). Compounding these challenges is the closed set of species vocalizations that pre-trained models support for identification, potentially excluding species and other acoustic signals of interest or conservation concern (e.g., illegal logging, hunting).

Reduced performance of a pre-trained classifier results from domain shift due to biases in the original data used to develop the model (Figure 1.1; Geirhos et al., 2023). Popular models such as BirdNET are trained primarily on a source domain of high-quality, “weakly labeled” (i.e., single-label) focal recordings assembled from disparate regions, often actively captured with a directional microphone and high signal-to-noise ratio (SNR) (Kahl et al., 2021). By contrast, the typical target domain of an applied PAM survey is very different, consisting of ambient soundscape recordings collected by passive omnidirectional microphones that contain diverse and novel biotic (i.e., species) and abiotic (e.g., geophonic and anthropogenic noise) signals that a pre-trained model has little or no “knowledge” of (Priyadarshani et al., 2018; van Merriënboer et al., 2024). As a result, low SNR and concurrent vocalizations are often implicated as the primary culprits of poor generalization of pre-trained models to scientific applications in field settings (Goëau et al., 2018). Because the data are drawn from two separate and distinct distributions, the source domain may fail to account for variation due to the novel acoustic context of the target domain (Figure 1.1).

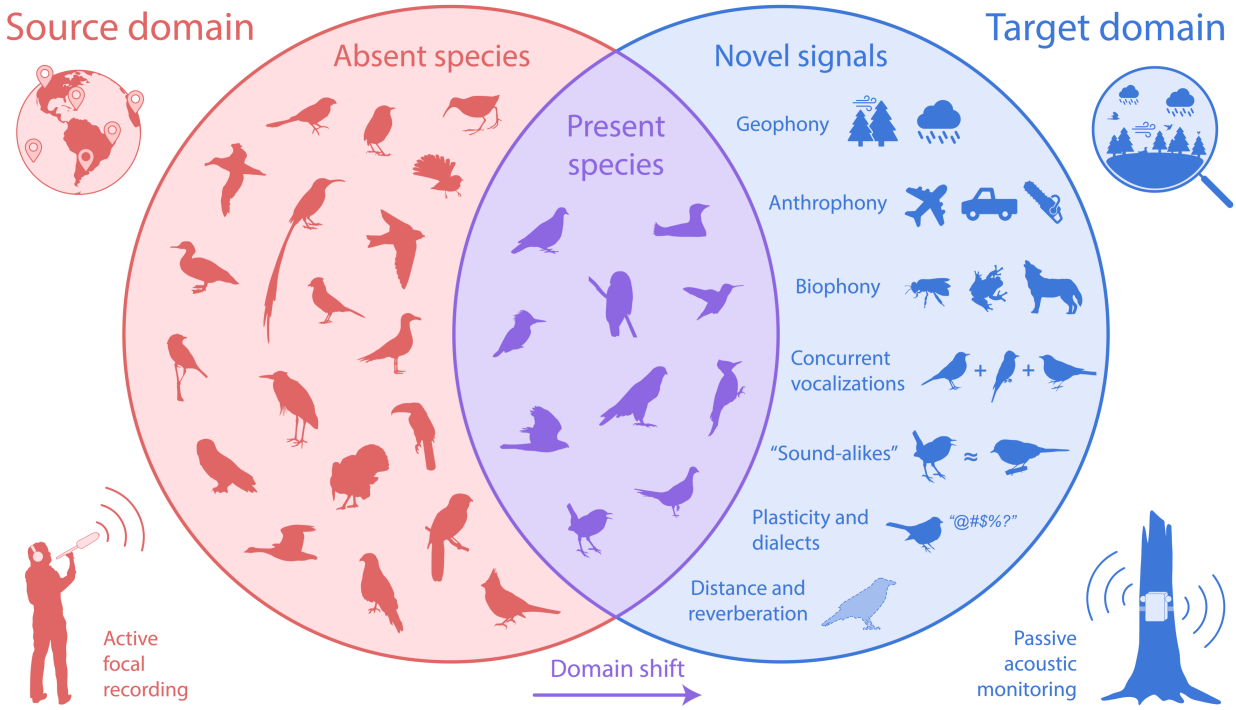

Figure 1.1: Domain shift between source and target domains. Species classes in the target region are shared, but the source domain may fail to account for variation in the target domain due to its novel acoustic context.

Limited reliability of pre-trained classifiers remains a perennial challenge to their application in ecology, potentially leading to poor detectability of particular species of high conservation priority and precluding the accurate estimation of assemblage structure (Lauha et al., 2022; Priyadarshani et al., 2018). Given the recent ubiquity of affordable autonomous recording units and the increasing use of pre-trained models to process PAM data, the implications of these limitations are increasingly relevant. Unaccounted errors from bioacoustic classification can produce incorrect detection histories, resulting in misleading ecological analyses and misinformed conservation and management actions. For example, a false negative evaluation of site occupancy (Type II error) for an endangered species in a working forest could mean the difference between habitat destruction and protection. Conversely, a false positive (Type I error) could divert limited conservation resources away from areas of need. At scale, these compounding errors could lead to the misclassification of a species as threatened, endangered, or recovering. For these reasons, the promise of leveraging pre-trained bioacoustic models with PAM as an accessible, scalable, and cost-effective method for rapid ecosystem

monitoring remains unfulfilled (Kershenbaum et al., 2024; Pérez-Granados 2023; Gibb et al., 2019; Besson et al., 2022).

Despite the limitations above, pre-trained convolutional neural networks often exhibit powerful feature recognition capabilities that can be utilized with *transfer learning* — the application of knowledge gained from one task to improve performance on another related task (Pan and Yang 2010; Yosinski et al., 2014). A feature embedding is a vector taken from an intermediate layer of a pre-trained source model that represents the salient characteristics of a given audio signal, and can be considered an acoustic "fingerprint" (Stowell 2022). High-quality feature embeddings from pre-trained image classifiers (e.g., ResNet, ImageNet) and bioacoustic classifiers (e.g., BirdNET) have been shown to enable efficient and superior transfer learning on novel bioacoustic classification tasks for a diverse variety of taxa (Ghani et al., 2023; Miyaguchi et al., 2023; Dufourq et al., 2022; Lauha et al., 2022) and rare species (Zhong et al., 2021), and in some cases outperform a bespoke regional model (Ghani et al., 2023). *Few-shot transfer learning* can take advantage of the existing feature recognition capabilities of a pre-trained source model as a foundation, re-training only the latter layers with a relatively small amount of local data to potentially produce a stronger model for a target domain (Ghani et al., 2023; Wang et al., 2020). By leveraging curated datasets, these studies suggest that few-shot transfer learning may overcome the challenge of poor pre-trained classifier performance precluding reliable ecological inference from field surveys.

Existing research has yet to report on the implementation of few-shot transfer learning with a pre-trained source model for downstream ecological analyses of PAM survey data at the community level. Changes in classifier performance and their implications for *in situ* monitoring are more clearly interpreted when quantified with ecologically meaningful metrics (e.g., error in prediction of site use or species richness, rather than only individual audio segment-level metrics), but have yet to be explored. As species detection history data in bioacoustic research are often aggregated from many individual audio segment detections derived from periods of continuous audio data, quantifying model performance at these levels is of great importance. Additionally, the extent to which few-shot transfer learning can reduce performance impacts incurred by low SNR and the presence of complex biotic (e.g., concurrent vocalizations) and abiotic (e.g., ambient and anthropogenic noise) signals commonly encountered in the field remains uninvestigated. Furthermore, wildlife managers and conservationists may seek to retain

existing relevant species classes from a pre-trained classifier for performance improvement (i.e., domain adaptation), while also expanding the list of classes of interest (e.g., transfer learning for novel taxa or anthropogenic signals). The present study aims to address these knowledge gaps, contributing to the growing body of work investigating practical applications of transfer learning in bioacoustics (e.g., Lauha et al., 2022; Dufourq et al., 2022; Ghani et al., 2023).

This study demonstrates the application of few-shot transfer learning in a real-world monitoring scenario, leveraging PAM data from an avian monitoring program across a managed temperate rainforest landscape in western Washington, USA, as a case study. We show how this method can effectively adapt the popular BirdNET pre-trained classifier source model, widely considered the state-of-the-art for general bird species identification, to an applied domain with a limited sample of training data collected from a study region. Our objectives were to: 1) quantify the performance of the source model in an applied monitoring survey using metrics at the audio segment (i.e., individual vocalization), site use, and community levels; 2) identify drivers of prediction error, including causes of confusion for the source model and signals that define the unique acoustic context of the target domain; and 3) improve performance by leveraging few-shot transfer learning to enable robust detection of species across the community and additional signals of management interest. We outline a process for evaluating classifier performance with ecologically meaningful metrics, identifying causes of prediction error, and training improved or missing classes for the detection of species and other abiotic signals (both anthropogenic and geophonic) of interest. We show how the proposed workflow for few-shot transfer learning can enable robust acoustic community monitoring and may be readily applied to other taxa, environments, and applied monitoring scenarios

1.3 METHODS

1.3.1 Study region and sampling design

Acoustic surveys were conducted in collaboration with the Washington State Department of Natural Resources (WADNR) across the Olympic Experimental State Forest, a 270,000-acre managed temperate rainforest located on the western Olympic Peninsula of Washington state, USA (47.71341ºN, 124.07945ºW). The landscape comprises a mosaic of coniferous forest

patches of varying successional stages and habitat structures ranging from early seral timber plantation to protected old-growth. The region experiences ample rainfall, windstorms, frequent aircraft flyovers, and active timber harvest, creating a challenging acoustic environment. WADNR manages an ongoing passive acoustic monitoring program surveying forest patches across the landscape to determine biotic diversity and occupancy of several avian species of high conservation and management priority (Minkova et al., 2020, Minkova et al., 2024). Patches are stratified by four habitat types: early seral (0-24 years), mid seral (25-79), mid seral subjected to commercial thinning within the last 25 years, and late seral (80-300). These habitat types represent a gradient of increasing structural complexity ranging from open canopy with tree seedlings, grasses, forbs, and shrubs to multi-layered closed canopy dominated by Douglas fir (*Pseudotsuga menziesii*) and western hemlock (*Tsuga heterophylla)*.

Survey effort for the monitoring program varies by season across more than 200 individual acoustic survey sites. Locations for survey sites are randomly placed within available patches, subject to minimum distance buffers from patch edges, paved roads, streams, and other sites. Survey sites consist of a 100-meter radius circular plot centered on one Song Meter Mini autonomous recording unit (ARU) (Wildlife Acoustics, Massachusetts, USA) installed on a tree at breast height. Plot size reflects the estimated effective detection range for most species with the ARU model employed (Minkova et al. 2020). ARUs are configured for a 32 kHz sampling rate, default 18 dB gain setting, and single-channel mono audio recording. Due to the limited availability of ARUs, a common challenge in acoustic surveys, a rotating deployment schedule is used to record acoustic data continuously (24 hours per day) at a site for 10 days (the maximum time achievable before battery depletion). This intensive continuous recording schedule ensures complete temporal coverage of all sound events at a site to better understand model performance across the entire deployment duration and facilitates flexibility of the survey data in supporting further ecological research (Minkova et al. 2020). More detailed information regarding sampling design for the broader monitoring program, including site selection and recording schedule, can be found in Minkova et al. (2020).

To assist in processing the vast amounts of PAM data produced by this program into species detection histories, the present study sought to utilize BirdNET with few-shot transfer learning to develop a robust bioacoustic classifier model for acoustic monitoring of wildlife in the region. We obtained a stratified random selection from the collection of sites monitored by

WADNR throughout the 2020 avian breeding season (April to July) to obtain a representative sample of forest habitat types and time periods for model performance evaluation. Survey effort was consistent across all sites during the 2020 season of the monitoring program, but not in subsequent years. As such, the 2020 season was evaluated to obtain broad temporal coverage across the breeding season with a balanced sample of habitat types and survey duration per site. One site was randomly chosen per habitat type per month, yielding 16 sites for evaluation

1.3.2 Transfer learning workflow

The workflow we developed is divided into four steps: 1) quantify source model performance in the target domain; 2) identify causes of error that define the unique acoustic context of the target domain and determine classes for improvement; 3) implement few-shot transfer learning to develop a target model; and 4) quantify target model performance. We first processed all raw continuous audio data with the open-source Python BirdNET model (version 2.4; Kahl et al., 2021) to obtain a time series of prediction scores for avian species per site from 3-second audio segments (the detection interval supported by BirdNET). Default sensitivity and overlap parameter settings (1.0 and 0.0, respectively) were used to evaluate the model's performance in its standard configuration, reflecting common usage and enabling direct comparison of results with existing literature. The source model was modified to produce continuous prediction scores on both the raw logit and bounded confidence (i.e., the sigmoid of the logit score ranging from 0.0 to 1.0, exclusive) scales. We limited the output class labels of the model to a subset of 95 species that was determined could reasonably be encountered in the study area (Table A1.1), specifically species associated with forest, woodland, and early seral habitats with breeding ranges overlapping with the study region as informed by observation data from the Washington Department of Fish and Wildlife (Johnson and O'Neil, 2001) and eBird (Fink et al., 2023). This list was amended and validated by two local expert wildlife biologists.

Model performance evaluation

We assembled a test dataset by annotating a subset of 3-second audio segments for each species across a representative sample of habitats and time periods. One site was randomly chosen per habitat type per month, yielding 16 sites, from which a subset of audio segments was obtained. Direct random sampling of segments from the raw audio data mirrors the distribution of scores for a given species class at the consequence of heavily skewing the test dataset towards low

confidence (i.e., likely negative) predictions, which are ubiquitous in continuous PAM data (Wood and Kahl 2024). As such, we randomly selected segments for each species class at each site from confidence score bins stratified by ranges (0.0–0.1), N=1, and [0.1–1.0), N=6. In addition, the segments with the highest and lowest confidence scores were also chosen, yielding 8-9 segments per species per site, or roughly 140 segments per species in total. This stratified sampling produced a test dataset representing the full range of confidence scores while mitigating the overabundance of negative samples at extremely low confidence values in the raw PAM data.

We manually annotated each segment using Raven Pro software (version 1.6, Cornell Lab of Ornithology 2024) after repeatedly listening to the recording and viewing its spectrogram to determine the true presence or absence of any vocalizing species or other acoustic events. One observer annotated each discrete event in the segment (i.e., "strong" labeling, van Merriënboer et al., 2024), including all vocalizing species (regardless of representation in the original list of species labels) and abiotic signals including, for example, wind, rain, and anthropogenic noise (see Table A1.1 for a list of all biotic and abiotic labels used). Segments were also labeled for the presence of artifacts due to audio data capture or processing, such as signal truncation at the edge of segment windows or digital clipping, and poor signal-to-noise ratio when no discrete sound event was present (i.e., the ambient noise floor). Segments from which the presence or absence of the predicted species could not be definitively determined were labeled as "unknown" and excluded from subsequent model performance evaluations. Segments from which the absence of the predicted species could be definitively determined, but the identity of other species could not be, were labeled as "not target" and only included in performance evaluations for the predicted species class. A second trained observer then independently verified the labels, correcting any that were determined to be made in error. When needed, both observers consulted the Peterson Field Guide to Bird Sounds (Pieplow 2024), regional bioacoustic recordings from the Macaulay Library (Cornell Lab of Ornithology 2024) and the continuous raw audio data to aid in species identification. The resulting collection of annotations and their associated audio segments comprised our held-out test dataset. As annotations were pooled and species were present in (and absent from) more segments than the approximately 140 that were randomly sampled per species, this test dataset totaled roughly 2,450 samples for evaluation per species class.

Source model performance for each species class was quantified with the test dataset using metrics considered best practice for bioacoustic classifier evaluation, namely precision, recall (i.e., sensitivity), F_1 score, and area under the precision-recall curve (Knight et al., 2017). Precision (how many predicted species detections were true presences) and recall (how many true presences were predicted) were calculated at both the audio segment and site use levels across decision threshold values T_x where $x \in (0.0,1.0)$, such that any prediction with a score greater than or equal to a given threshold was interpreted as a species presence. The area under the precision-recall curve and maximum F_1 score were calculated at the segment level to quantify overall performance and the balance between precision and recall, respectively. Following Knight et al. (2017), we employed precision-recall AUC (hereafter AUC) as the primary evaluation metric for segment level performance to account for the inherent class imbalance in bioacoustic monitoring data and reflect how well the model maintains precision across thresholds, particularly for classes in the minority. Receiver operating characteristic (ROC) AUC, average precision (AP), and a suite of other conventional metrics were also calculated for ease of comparison with other studies (Table A1.1).

At the site level, species presence or absence was determined by manually validating all segments from the raw audio monitoring data for each class label that was not already found present in the test dataset, excluding segments with a confidence score less than 0.1 to mitigate the overabundance of negative samples and render manual review feasible, while also reflecting the default range of predictions reported by BirdNET (Kahl et al., 2021). Site precision (how many sites predicted present by the model were truly occupied), recall (how many sites truly occupied were predicted present), and accuracy (how many sites were correctly predicted as either present or absent) were calculated across a range of decision thresholds from $T_{0.5}$ to $T_{0.95}$ in increments of 0.05. Absent species classes were excluded from mean recall calculations due to a lack of present examples. We also evaluated the performance of class-specific optimized thresholds to maximize segment-level precision while retaining the highest possible recall performance T_P, and to maximize F_1 score T_{F1}. Together, these predicted presence-absence data were used to estimate species richness per site (i.e., a measure of α-diversity) and compared against the observed true species richness.

Causes of performance error

For all biotic and abiotic labels, we quantified the frequency of occurrence in incorrectly classified species predictions (false positives and false negatives) using a 0.5 decision threshold ($T_{0.5}$) on bounded (sigmoid transformed) confidence scores, treating each species class prediction as an independent binary classification task. The resulting matrix summarized patterns of confusion between classes by counting how often sounds that were not truly produced by a species occurred in incorrect predictions for that species. We then visualized these relationships between labels with hierarchical edge bundling, organizing labels by type, order, and family. This allowed us to identify recurrent sources of confusion and novel signals that define the unique acoustic context of the target domain. We also quantified total accuracy, false positive rate, and false negative rate at the site use level to investigate the role of α-diversity (species richness) and structural complexity (proxied by a numerically encoded gradient of forest seral stage) in performance error.

We then assembled a list of target class labels (both biotic and abiotic) for further training with few-shot transfer learning according to the following criteria: 1) high relevance for management or conservation objectives; or 2) insufficient source model performance (specifically, precision-recall AUC < 0.8); or 3) the class is a recurrent source of confusion for other classes or a novel and commonly encountered signal in the target domain (specifically, if the class is present in multiple incorrectly predicted segments at $T_{0.5}$).

Few-shot transfer learning

We assembled a training dataset by using confirmed examples of target class labels from the test dataset as temporal references to the raw continuous audio data from which to identify and extract additional examples. For each target class, an expert observer 1) randomly selected one site at which the target class was present, 2) randomly selected a positive example from the test data as a reference (including those that were predicted as the target class and those that were predicted as a confusing class but were truly the target class), and 3) extracted all 3-second examples from within ±1 minutes of the reference, excluding any audio data already present in the test dataset. Steps 1-3 were repeated until at least 125 positive examples were collected, where possible, ensuring 100 examples could be used in training and 25 in validation (constituting an 80/20% split). If less than 125 examples were collected this way, additional examples were extracted from the hour-long recording period containing each reference. In

addition, all audio segments confirmed to have no signals of interest were extracted as examples of the ambient noise floor (i.e., silence).

We took advantage of the knowledge present in the pre-trained source model to retrain the model's classification ability for the target classes by using this small amount of data from the target domain. The BirdNET source model uses a conventional neural network architecture comprised, at a high level, of feature extraction and classification steps (Figure 1.2). This process converts input audio segment data to a spectrogram, which is passed to a convolutional model that extracts feature maps by applying filters in a series of layers that transform the input data. Deeper layers identify increasingly abstract features, culminating in a feature embedding representing salient information about the input data in a compact, vectorized form. A fully connected classifier head (a feed-forward neural network) is then trained to associate feature embeddings with classification labels. Finally, an output layer applies a sigmoid activation to produce confidence score predictions. To adapt the classifier to our target domain, we used the BirdNET-Analyzer training API (Kahl et al., 2021) to preserve (or “freeze”) the existing convolutional feature extraction layers and replace the classifier head with a new neural network (i.e., a fully-connected layer and zero or more hidden layers followed by sigmoid activation functions) trained simultaneously on all target classes with our small collection of few-shot training data (Figure 1.2).

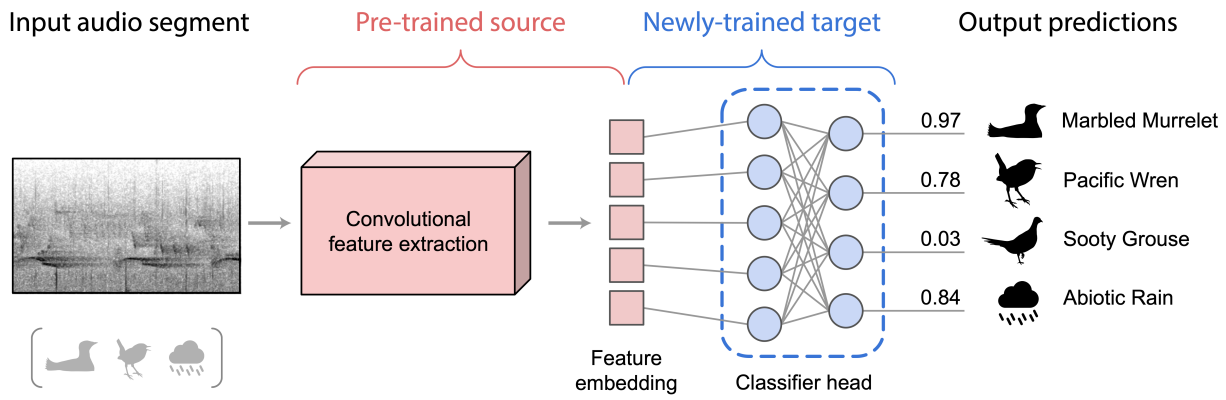

Figure 1.2: Conceptual diagram of the adapted convolutional neural network architecture. The source model extracts a feature embedding from the input audio segment spectrogram, which is associated with output class labels by a pre-trained classifier head. This classifier head is replaced with a new neural network trained on a small amount of local data from the target domain, changing the downstream output class labels.

Data was split into sets for model training and cross-validation (80% and 20%, respectively) with iterative stratification to ensure that each fold had approximately the same class distribution as the original dataset (Sechidis et al., 2011). We performed 5-fold cross-validation to ensure that every example taken from the training dataset was used for both training and model validation. The new classifier head was trained with TensorFlow (Abadi et al., 2015) using a binary cross-entropy loss function and Adam optimizer over a maximum of 50 epochs, with early stopping once 5 consecutive epochs resulted in no improvement in minimum validation loss. The model weights from the epoch with the minimum validation loss were retained. The mean validation performance for each class was calculated across all folds to estimate the average class and overall model performance using the same audio segment and site use metrics described previously.

Validation performance informed the iterative development of the model, including hyperparameter selection and architecture design. Hyperparameters subjected to tuning included batch size, learning rate, number of layers in the classifier head network architecture (one or two), and number of hidden units in a two-layer network. The effect of hyperparameter choice on performance was quantified through a linear search, holding other values constant to find an optimal setting for each hyperparameter independently. Combinations of these settings were then evaluated to identify an optimal tuning for the final model.

The final target model was trained on all available data (excluding the held-out test dataset), again performing iterative stratification to mirror the class distribution of the original dataset. This resulted in a modest class imbalance of roughly 15:1, with majority class Western Flycatcher (N=328) and minority class Belted Kingfisher (N=22), and a median of 131 (mean 142) positive examples for each class overall. The model was trained for 15 epochs (the average number at which minimum loss occurred across validation iterations) with a batch size of 10, a learning rate of 0.001, and a single-layer neural network architecture (i.e., no hidden units).

Performance metrics for the final target model were quantified with the original test dataset at the segment and site levels to estimate real-world performance on unseen data. We also compared shifts in the distribution of prediction scores between source and target models on the raw logit and bounded confidence scales to further investigate the ability of the models to discriminate between audio segments that do and do not contain a species. Additionally, we quantified performance across the avian community by constructing a model ensemble that combined predictions from the source and target models such that confidence scores for shared classes were only retained from the target model.

To investigate the effect of training sample size on transfer learning performance, we also conducted experiments for different quantities of training data collected per class (N≈1,5,10,25,50,100) randomly chosen from the available examples. Note that N is effectively a rough approximation of the number of examples used per class because the required number of examples for some rare or infrequently vocalizing species were not available, and multiple class labels are often present in a given example. The same validation set (roughly 25 validation examples per class, constituting an 80/20% split for model N≈100) was used for each model in the experiment to enable early stopping of training and direct comparison of performance results. Hyperparameters were fixed to mirror the final target model, with batch size 10, learning rate 0.001, and a single-layer network architecture.

1.4 RESULTS

1.4.1 Source model performance

Of the 95 species under consideration across the 16 sites, 56 were determined to be present through manual review. A lack of sufficient positive examples for several species (American Crow, American Goldfinch, Bald Eagle, MacGillivray's Warbler, Northern Goshawk, Red-tailed Hawk, Sharp-shinned Hawk, Yellow Warbler) presented the possibility of strong bias in performance metrics due to high variance at small positive sample sizes (N≤5). For this reason, these 8 species and any determined not present at any sites (N=39) were excluded from consideration for transfer learning and subsequent segment-level performance calculations, unless noted otherwise. However, false positives did occur for absent species (discussed in detail below).

Among the remaining 48 bird species present in the study area, segment level precision-recall AUC values for the BirdNET source model ranged from 0.37 to 1.0, with a mean of 0.82, indicating moderate model performance (Table A1.1). Similarly, F_1 score maximum ranged from 0.42 to 0.97, with a mean of 0.78. While most species classes had AUC values greater than 0.8 (e.g., Common Raven, American Robin, Barred Owl), roughly one-third of species performed below this benchmark. Notably, several species of high conservation or management priority were not consistently detected, such as the Marbled Murrelet (0.46) and Golden-crowned Kinglet (0.75). Optimized class-specific decision thresholds to maximize precision T_P (i.e., precision = 1.0) resulted in an average recall of 0.43, while optimized thresholds to maximize F_1 score T_{F1} resulted in an average precision of 0.79 and also recall of 0.79.

Among all thresholds, the source model achieved a maximum mean accuracy of 89% at the site use level across all 95 species at $T_{0.8}$, a maximum mean precision of 0.92 at $T_{0.95}$, and a maximum mean recall of 0.97 at T_{F1} (Table A1.2). These metrics indicate relatively high site level performance for most species classes, although error rates exceeded 10% for roughly one-third of species classes ($T_{0.8}$). Notably, due to low precision or recall, the model could not reliably predict site use for several species of high conservation or management priority, such as the Marbled Murrelet and Wilson's Warbler (accuracy 33% and 77%, respectively). Additionally, high false positive rates for particular absent species, such as the Great Horned Owl, resulted in

low site accuracy. Segment level AUC was directly related to site level accuracy, with species performing poorly at the segment level generally tending to also perform poorly at the site level.

1.4.2 Causes of performance error

Habitat type did not exhibit an apparent effect on the total site error rate (i.e., accuracy). However, we found evidence for positive relationships between α-diversity and false positive rate (Pearson's $r = 0.6$, $p = 0.01$) and structural complexity and false negative rate ($r = 0.56$, $p = 0.02$). Habitats with the greatest species richness (early seral) produced the highest false positive rates, while habitats with the most heterogeneous environmental structure (late seral) produced the highest false negative rates (Table A1.3).

Abiotic signals, in particular rain, wind, and aircraft noise, were the most frequent signals present in incorrect predictions across all species classes (Figure 1.3). Other abiotic signals caused confusion in the prediction of one or more particular species, such as the warning beep of a vehicle in reverse yielding extremely confident prediction scores (up to 0.99) for the Northern Saw-whet Owl. Low SNR due to signal distance, environmental reverberation, and the ambient noise floor was also strongly associated with incorrect predictions, often resulting in the misclassification of similar biotic signals (for example, a distant Common Raven labeled as a Northern Pygmy-Owl). The prevalence of these labels among predictions for species with low AUC values suggests that ambient noise and novel abiotic signals (both geophonic and anthropogenic) are primary drivers of error and causes of confusion for the source model, as illustrated by the high density of bundled edges linking the abiotic label group to other biotic labels in Figure 1.3. Artifacts due to audio data capture or processing, such as signal truncation at the edge of segment windows or digital clipping, were also a source of confusion, albeit much less often.

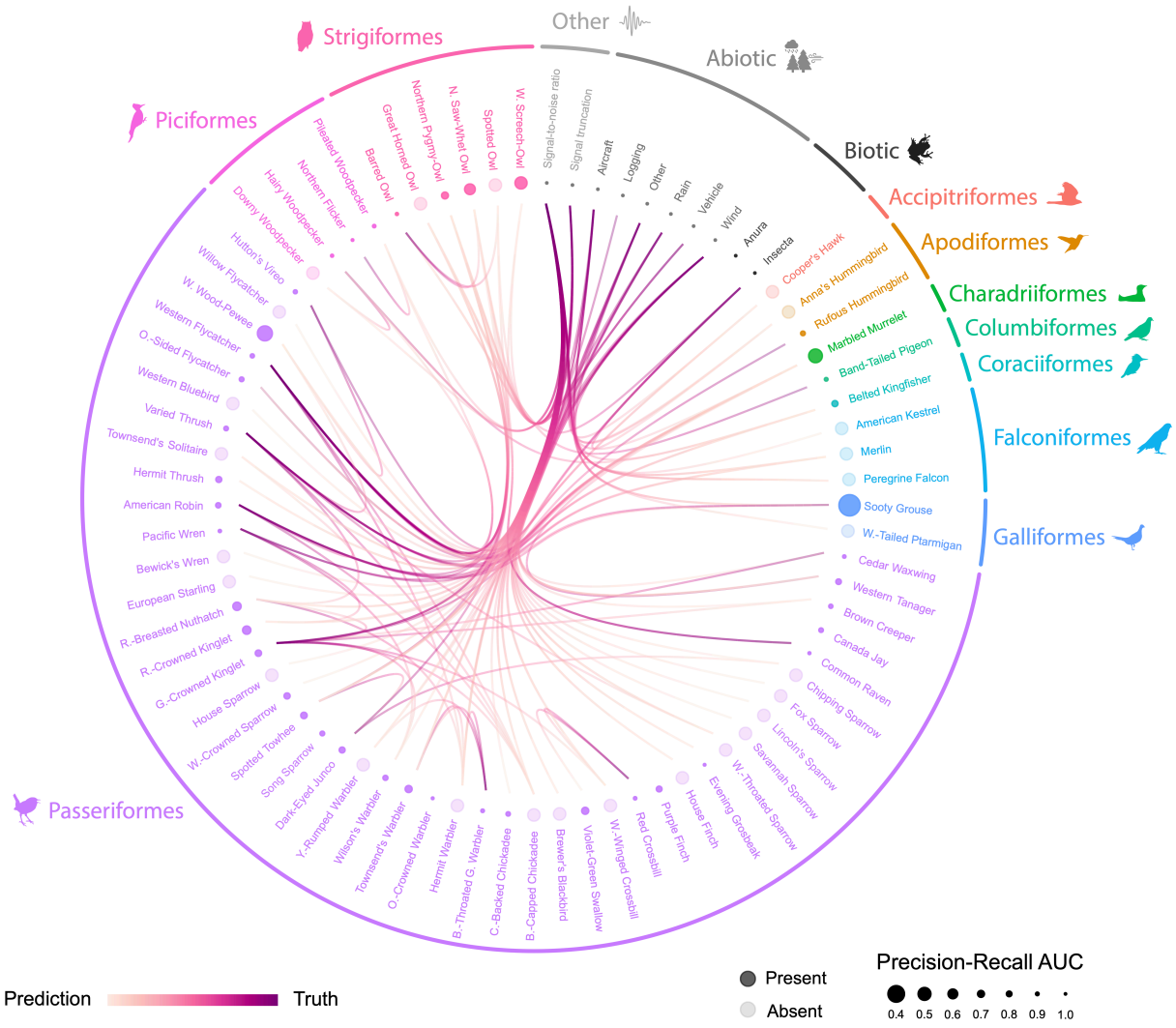

Figure 1.3: Causes of confusion and performance error in the pre-trained source model, illustrated as associations between labels. Label nodes are grouped by type, order, and family (if applicable). A connection (i.e., edge) between nodes represents an incorrect prediction made at decision threshold $T_{0.5}$, with the light-colored terminus indicating the predicted label and the dark the true label. Nodes with many dark purple connections are labels frequently present in incorrect predictions and may serve as sources of confusion that define the unique acoustic context of the target domain. Node size is inversely related to precision-recall AUC, with poorly performing labels (low values) larger and well-performing labels (high values) smaller. Node alpha shading indicates the true presence of a label in the test data; the source model produces false positives for the absent species shown.

Novel biotic signals also impacted performance, such as the sounds of insect flight for the Great Horned Owl song (high confidence scores up to 0.95) or the Douglas Squirrel's *chatter* calls for the Northern Flicker's *keek* series (low confidence scores near and below 0.5).

Confusion was also present within and between biotic groups, displayed as connections within and between grouped species in Figure 1.3. For example, juvenile Barred Owl *shriek* calls were consistently mistaken for those of a Spotted Owl, and Wilson's Warbler and Pacific Wren *jit* calls were often confused for one another, despite highly confident predictions. Similarly, species that exhibit mimicry (such as the Steller's Jay's imitation of the Red-tailed Hawk) could not always be definitively identified during manual review but are also suspected to pose difficulties for classification.

The presence of concurrent vocalizations also challenged the performance of the source model, often either reducing confidence scores overall or resulting in highly confident incorrect predictions. For example, simultaneous combinations of multiple passerine songs (e.g., American Robin, Varied Thrush, Pacific Wren, etc.) consistently resulted in extremely confident but incorrect prediction scores for the Marbled Murrelet *keer* (up to 0.99). While common and highly vocal species such as these were also frequently present in incorrect predictions across many other labels, this primarily reflects their prevalence in the acoustic environment rather than implicating their role in widespread classifier confusion.

Several poorly performing species classes lacked strong confusion relationships with another signal, suggesting a domain shift due to within-species signal variation (illustrated as labels with low AUC yet few connections in Figure 1.3). For example, a majority of the Western Wood-pewee vocalizations in the data occurred early in the breeding season when songs are more variable and plastic. Similarly, the White-crowned Sparrow, which exhibits high geographic variation in song structure, could use a local dialect in the study region that may not be reflected in the source domain

1.4.3 Target model training and performance

The target class labels chosen for transfer learning that met the criteria outlined previously (section 2.2.2) consisted of 37 pre-existing species (Table 1.1) and 7 novel signals (rain, wind, aircraft, logging, vehicles, anurans, and insects). Hyperparameter choice and model architecture of the convolutional neural network had a substantial impact on target model development performance (Table A1.4), A standard learning rate of 0.001 and batch size of 10 resulted in optimal validation performance when training with roughly 100 examples per class. Higher learning rates led to faster model convergence but reduced training stability and increased risk of

overfitting. Larger batch sizes resulted in slightly reduced performance, while smaller sizes reduced training stability. We found that using a multi-layer neural network architecture did not substantially improve performance, and we opted to use a single-layer design (i.e., no hidden units) in the final target model to reduce the risk of overfitting with our relatively small training dataset.

			Segment level						Site level ($T_{0.9}$)								
Class			Precision-Recall AUC			F1 Score Maximum			Accuracy			Precision			Recall		
Common name	Scientific name	N	Δ	Source	Target	Δ	Source	Target	Δ	Source	Target	Δ	Source	Target	Δ	Source	Target
Marbled Murrelet	*Brachyramphus marmoratus*	38	0.54	0.46	1.00	0.50	0.50	1.00	0.54	0.33	0.87	0.53	0.27	0.80	0.20	0.60	0.80
Western Screech-owl	*Megascops kennicottii*	37	0.49	0.51	1.00	0.50	0.50	1.00	0.00	0.79	0.79	-0.33	1.00	0.67	0.25	0.25	0.50
Sooty Grouse	*Dendragapus fuliginosus*	253	0.43	0.37	0.80	0.32	0.43	0.74	0.33	0.47	0.80	-0.17	1.00	0.83	0.64	0.27	0.91
Northern Pygmy-owl	*Glaucidium californicum*	179	0.41	0.59	1.00	0.33	0.67	1.00	0.14	0.73	0.87	0.17	0.33	0.50	0.00	1.00	1.00
Western Wood-pewee	*Contopus sordidulus*	40	0.31	0.43	0.74	0.32	0.42	0.74	-0.07	0.93	0.86	-0.50	1.00	0.50	0.00	0.50	0.50
Red-Breasted Nuthatch	*Sitta canadensis*	148	0.28	0.66	0.95	0.29	0.64	0.93	0.00	0.79	0.79	-0.05	0.80	0.75	0.11	0.89	1.00
Northern Saw-whet Owl	*Aegolius acadicus*	43	0.27	0.63	0.90	0.25	0.57	0.82	0.06	0.88	0.94	0.50	0.50	1.00	-0.50	1.00	0.50
Ruby-crowned Kinglet	*Corthylio calendula*	43	0.25	0.66	0.91	0.27	0.67	0.93	0.00	1.00	1.00	0.00	1.00	1.00	0.00	1.00	1.00
White-crowned Sparrow	*Zonotrichia leucophrys*	61	0.23	0.77	1.00	0.18	0.82	1.00	0.06	0.94	1.00	0.00	1.00	1.00	0.50	0.50	1.00
Townsend's Warbler	*Setophaga townsendi*	74	0.23	0.72	0.95	0.24	0.67	0.91	0.08	0.92	1.00	0.00	1.00	1.00	0.12	0.88	1.00
Violet-green Swallow	*Tachycineta thalassina*	34	0.22	0.72	0.94	0.16	0.73	0.89	0.00	0.91	0.91	0.00	1.00	1.00	0.00	0.67	0.67
Dark-eyed Junco	*Junco hyemalis*	167	0.22	0.77	0.99	0.23	0.71	0.95	0.14	0.86	1.00	0.00	1.00	1.00	0.14	0.86	1.00
Hermit Thrush	*Catharus guttatus*	58	0.21	0.78	0.99	0.19	0.75	0.94	0.17	0.75	0.92	0.00	1.00	1.00	0.50	0.25	0.75
Golden-crowned Kinglet	*Regulus satrapa*	238	0.15	0.75	0.90	0.14	0.70	0.83	0.06	0.94	1.00	0.00	1.00	1.00	0.06	0.94	1.00
Song Sparrow	*Melospiza melodia*	128	0.15	0.85	1.00	0.18	0.80	0.98	0.07	0.93	1.00	0.00	1.00	1.00	0.33	0.67	1.00
American Robin	*Turdus migratorius*	167	0.15	0.82	0.96	0.16	0.74	0.90	0.13	0.87	1.00	0.00	1.00	1.00	0.13	0.87	1.00
Wilson's Warbler	*Cardellina pusilla*	95	0.14	0.83	0.96	0.07	0.83	0.90	0.22	0.67	0.89	0.00	1.00	1.00	0.25	0.62	0.88
Spotted Towhee	*Pipilo maculatus*	232	0.13	0.75	0.88	0.16	0.70	0.86	-0.36	0.93	0.57	-0.60	1.00	0.40	0.25	0.75	1.00
Purple Finch	*Haemorhous purpureus*	128	0.12	0.79	0.91	0.14	0.76	0.91	0.00	0.81	0.81	0.00	1.00	1.00	0.00	0.57	0.57
Olive-sided Flycatcher	*Contopus cooperi*	135	0.10	0.85	0.95	0.08	0.83	0.92	0.00	0.93	0.93	0.00	1.00	1.00	0.00	0.80	0.80
Western Tanager	*Piranga ludoviciana*	148	0.09	0.80	0.89	0.12	0.74	0.86	0.14	0.73	0.87	-0.13	1.00	0.87	0.31	0.69	1.00
Hutton's Vireo	*Vireo huttoni*	137	0.07	0.89	0.96	0.09	0.81	0.90	0.13	0.87	1.00	0.00	1.00	1.00	0.14	0.86	1.00
Band-tailed Pigeon	*Patagioenas fasciata*	125	0.07	0.91	0.97	0.04	0.88	0.92	0.69	0.31	1.00	0.00	1.00	1.00	0.73	0.27	1.00
Pileated Woodpecker	*Dryocopus pileatus*	90	0.06	0.93	0.99	0.09	0.88	0.97	0.19	0.62	0.81	0.00	1.00	1.00	0.19	0.62	0.81
Rufous Hummingbird	*Selasphorus rufus*	163	0.05	0.85	0.91	0.07	0.81	0.88	-0.06	1.00	0.94	-0.20	1.00	0.80	0.00	1.00	1.00
Black-throated Gray Warbler	*Setophaga nigrescens*	130	0.05	0.92	0.98	0.05	0.86	0.92	0.43	0.50	0.93	0.00	1.00	1.00	0.43	0.50	0.93
Red Crossbill	*Loxia curvirostra*	128	0.05	0.93	0.98	0.07	0.88	0.96	0.73	0.27	1.00	0.00	1.00	1.00	0.73	0.27	1.00
Varied Thrush	*Ixoreus naevius*	307	0.05	0.86	0.91	0.05	0.78	0.83	0.00	1.00	1.00	0.00	1.00	1.00	0.00	1.00	1.00
Western Flycatcher	*Empidonax difficilis*	328	0.04	0.88	0.92	0.03	0.81	0.84	0.12	0.88	1.00	0.00	1.00	1.00	0.12	0.88	1.00
Swainson's Thrush	*Catharus ustulatus*	139	0.04	0.93	0.97	0.04	0.88	0.92	0.22	0.64	0.86	0.00	1.00	1.00	0.27	0.55	0.82
Pacific Wren	*Troglodytes pacificus*	301	0.04	0.95	0.98	0.03	0.89	0.92	0.00	1.00	1.00	0.00	1.00	1.00	0.00	1.00	1.00
Barred Owl	*Strix varia*	125	0.02	0.95	0.97	0.03	0.90	0.93	0.12	0.88	1.00	0.00	1.00	1.00	0.14	0.86	1.00
Belted Kingfisher	*Megaceryle alcyon*	22	0.02	0.77	0.79	0.02	0.73	0.75	-0.06	0.94	0.88	-0.17	1.00	0.83	0.00	0.83	0.83
Hairy Woodpecker	*Dryobates villosus*	125	0.01	0.95	0.97	0.01	0.92	0.93	0.06	0.94	1.00	0.00	1.00	1.00	0.06	0.94	1.00
Northern Flicker	*Colaptes auratus*	134	0.01	0.98	0.99	0.03	0.93	0.95	0.50	0.50	1.00	0.00	1.00	1.00	0.53	0.47	1.00
Hammond's Flycatcher	*Empidonax hammondii*	132	0.01	0.92	0.92	0.03	0.86	0.89	0.00	0.93	0.93	-0.17	1.00	0.83	0.20	0.80	1.00
Common Raven	*Corvus corax*	132	0.00	0.99	0.99	0.01	0.96	0.97	0.12	0.88	1.00	0.00	1.00	1.00	0.12	0.88	1.00
MEAN		**134.16**	**0.15**	**0.79**	**0.94**	**0.15**	**0.76**	**0.91**	**0.13**	**0.79**	**0.92**	**-0.03**	**0.94**	**0.91**	**0.19**	**0.71**	**0.90**

Table 1.1: Performance comparison between source and target models at the audio segment and site use levels. N indicates the number of examples for each class used to train the target model. Precision-recall AUC and F_1 score maximum are shown at the segment level. Accuracy at the site level indicates the percentage of sites correctly predicted for a species' presence and absence. Site level metrics were calculated using decision threshold $T_{0.9}$, which yielded the maximum total mean accuracy between both models and is coincidentally a widely used arbitrary threshold in bioacoustics studies. See Table A1.2 for the performance of alternative threshold values. Delta values are colored by target model performance with respect to the source model (green for improved performance, red for reduced performance, and white for approximately equal performance). Species are arranged by decreasing segment level ΔAUC.

The final target model achieved a mean precision-recall AUC of 0.94 at the segment level across the pre-existing species classes, an increase of approximately 0.15 over the source model (Table 1.1). Combining predictions between models as an ensemble yielded a mean AUC of 0.91 for all avian species present across the study region. The target model increased AUC for all but one species class, Common Raven, which maintained parity with the source model. Similarly, the mean F_1 score maximum of 0.91 rose by 0.15 compared to the source model. This improved performance reflects increases in both model recall and precision across decision thresholds

(Figure 1.4, A1.1). Class prediction score distributions shifted between models as well, with confidence and logit scores from the target model generally shifting to lower and higher values for negative and positive samples, respectively (Figure 1.4, A1.2). The most prominent gains occurred for classes that the source model struggled to predict reliably due to high confusion rates, with the greatest improvement for the Marbled Murrelet (Table 1.1). However, the poorest performing classes, e.g. Western Wood-pewee (AUC 0.74) and Sooty Grouse (0.8), continued to mirror those most challenging for the source model. The 7 novel classes achieved excellent performance with mean AUC and F_1 scores of 0.96 and 0.91, respectively. Optimized class-specific decision thresholds T_P resulted in a mean recall of 0.71, while thresholds T_{F1} yielded a mean precision of 0.92 and recall of 0.89. Further segment level performance metrics for all classes, including ROC AUC and average precision AP, can be found in Table A1.1 and Figure A1.1.

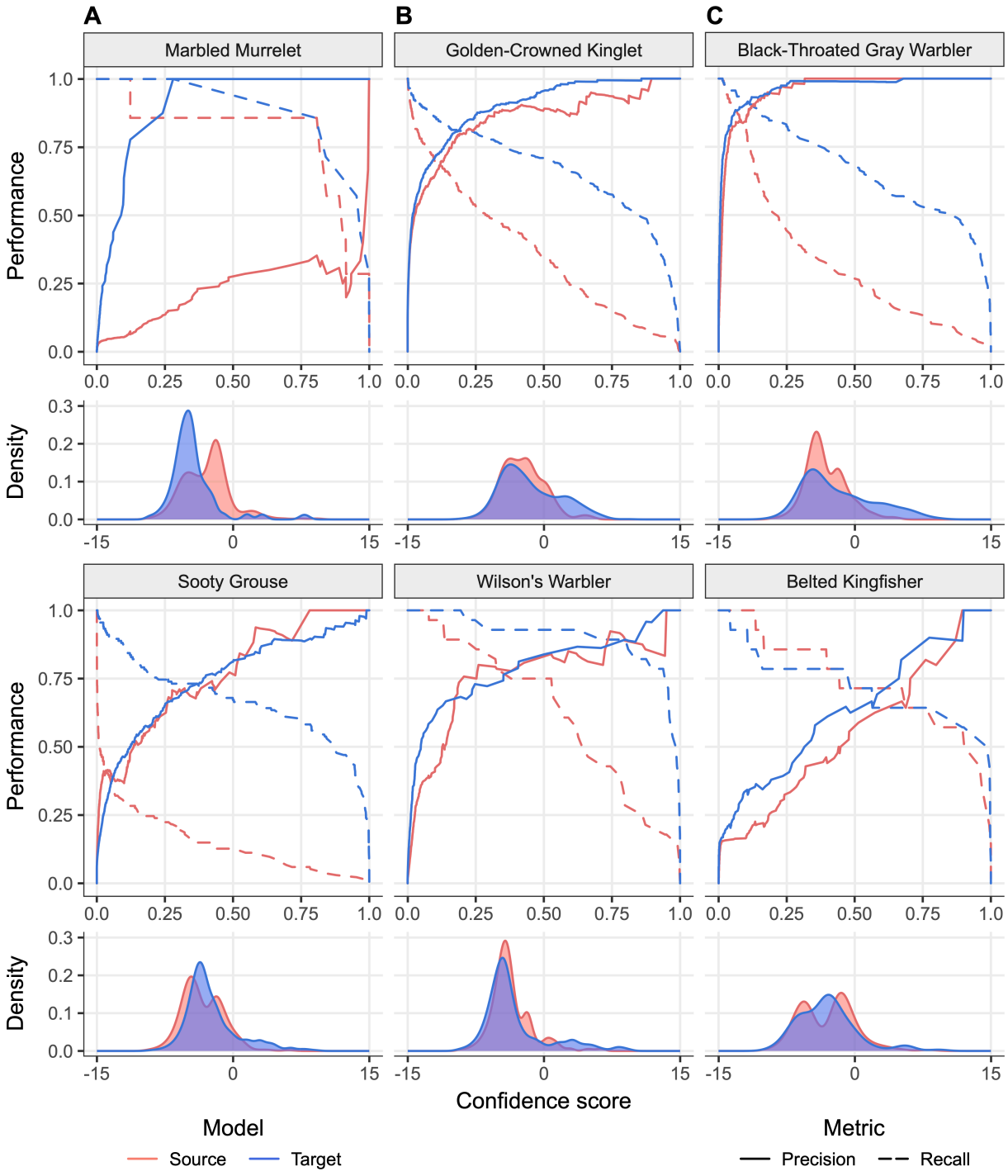
A
B
C
Marbled Murrelet
Golden-Crowned Kinglet
Black-Throated Gray Warbler
Sooty Grouse
Wilson's Warbler
Belted Kingfisher
Performance
Density
Confidence score
Model
Source
Target
Metric
Precision
Recall

Figure 1.4: Differences in test performance between source (red) and target (blue) models with precision and recall across decision thresholds (top, bounded confidence scale) and prediction score distributions (bottom, logit scale), including both positive and negative samples, for selected species classes with high (A), moderate (B), and low (C) performance gains at the segment level. Classes achieved greater recall performance and improved precision stability across thresholds. Score distributions and paired precision-recall curves indicate that prediction scores generally shifted to lower and higher values for negative and positive samples, respectively, suggesting an improved ability to discriminate between samples that do and do not contain a species. Despite a small training sample size of 38, the Marbled Murrelet overcame previous signal confusions (shown by the low and jagged source model precision line). Performance for the Sooty Grouse also substantially improved AUC but continued to be challenged by signal confusion. The Golden-crowned Kinglet and Wilson's Warbler produced more bimodal score distributions and achieved gains from moderate source model performance to high target model performance. The Black-throated Gray Warbler already performed highly with the source model and achieved minimal gains in AUC at the segment level. However, improvements in recall and the shift in score distribution led to significant increases in accuracy at the site level (Table 1.1). The Belted Kingfisher did not substantially benefit from training due to a low training sample size and the presence of similar signals inducing frequent confusion.

At the site use level, the target model achieved the highest mean accuracy of 92% at $T_{0.9}$, with roughly half of the species classes predicted with zero error, indicating high performance (Table 1.1). Using the same threshold, the combined model ensemble yielded 91% mean site accuracy across all present species. The target model increased or maintained accuracy for all but four species classes (Western Wood-pewee, Spotted Towhee, Rufous Hummingbird, and Belted Kingfisher). Improvements in accuracy were primarily due to substantial gains in recall, with reduced false negative rates across most species classes. The target model outperformed the source model in recall at all decision thresholds and achieved the highest mean precision of 0.95 at $T_{0.95}$ (Table A1.2). By comparison, the source model achieved a maximum mean site accuracy of 89% and maximum precision of 0.95 at T_P for the same species classes. Using species-specific optimized segment level thresholds T_P and T_{F1} did not improve overall site level performance for the target model compared to arbitrary thresholding at $T_{0.9}$.

The target model achieved higher precision at the site level for certain species classes that the source model struggled to reliably predict (e.g., Marbled Murrelet). However, precision for some species decreased at $T_{0.9}$ due to increased false positive rates (see Spotted Towhee, Western Wood-pewee, Rufous Hummingbird, and Belted Kingfisher classes in Table 1.1). Subsequent confusion analysis attributes these errors to audio segments with low SNR, signal truncation, and novel variation, leading to overly confident prediction outliers. For example, Varied Thrush *trill*

calls, which were underrepresented in the training data, were consistently mistaken for the Spotted Towhee's song. Insufficient performance may also reflect a lack of sufficient training data for other species (e.g., Belted Kingfisher, N = 22).

Precision improved for several underperforming classes when applying a more conservative decision threshold of $T_{0.95}$, but accuracy decreased for other more stable classes. Similarly, post-processing predictions (e.g., by only retaining predictions for a species that were made multiple times at a site) improved precision by filtering out outliers while incurring a relatively minor impact to recall.

The target model's improvements in site accuracy also produced more accurate estimates of species richness, i.e. α-diversity (Table A1.5). At the site assemblage level, the decision threshold to maximize accuracy ($T_{0.9}$) resulted in average α-diversity estimates of 96% of the truth, a 4% increase over the source model's performance ($T_{0.8}$) for the same set of species classes. For both models, lower thresholds and class-specific thresholds (T_P, T_{F1}) generally resulted in overestimates of α-diversity, while higher thresholds resulted in underestimates. Lastly, the effects of habitat α-diversity on false positive rates and structural complexity on false negative rates for trained species classes were less pronounced or unapparent with the target model (Pearson's r = 0.45, p = 0.08 and r = 0.13, p = 0.64, respectively). Error was generally reduced and exhibited less variation in performance across habitat types compared to the source model (Table A1.3).

Training sample size was strongly associated with model performance, following a positive decelerating monotonic relationship (Figure A1.3). Small initial increases in sample size resulted in disproportionately large performance gains, with diminishing returns as sample size increased further. Mean AUC exceeded the source model at an average of 8 training samples per class, and a mean AUC of 0.9 was achieved with 16 training samples per class. Several species classes achieved superior performance with as few as 5 samples (e.g., Red Crossbill, Violet-green Swallow). Performance plateaued for most classes between 50 and 75 samples.

1.5 DISCUSSION

1.5.1 Model performance and design

As the number, scale, and ecological scope of bioacoustic monitoring initiatives and datasets produced by research networks and citizen science programs continue to increase, so do the challenges of obtaining the computational power and analytical capabilities needed to efficiently and accurately process PAM data (Kershenbaum et al., 2024; Nieto-Mora et al., 2023). While pre-trained classifier models are increasingly employed to meet these challenges, poor domain generalization and restriction to a closed set of supported taxa severely limit a model's reliability for drawing ecological or conservation inferences from predictions. Our study demonstrates that few-shot transfer learning can effectively adapt a pre-trained source model to an applied passive acoustic monitoring domain, resulting in more robust species detection histories across the audible community.

Performance improvements at the audio segment (i.e., vocalization) level reflect increases in both precision and recall across trained avian species classes for the target classifier model (Table 1.1, Figure A1.1). Achieving a high (mean 0.9) precision-recall AUC with an average of only 16 training examples per class demonstrates the predictive utility of a source model with strong feature-recognition capabilities, such as BirdNET, infused with a small amount of local data through few-shot transfer learning. Shifts in prediction score distributions for the target model toward lower and higher confidence values also indicate an improved ability to distinguish between positive and negative samples (Figure 1.4, A.2). Although precision at the site use level did not improve on average (for reasons discussed below), gains in recall were substantial, resulting in higher site accuracy overall (i.e., lower error) (Table 1.1). Achieving these gains with minimal training data corroborates previous reports that the probability of detection can be significantly increased for monitoring applications where recordings of a species of interest are scarce, i.e. for rare or understudied species (Dufourq et al., 2022; Zhong et al., 2021). Our findings bolster a small but growing body of research demonstrating improvements in species detectability and classification accuracy through transfer learning (e.g., Ghani et al., 2023; Miyaguchi et al., 2023; Lauha et al., 2022).

Species classes from the source model that benefited most from transfer learning generally suffered from low precision due to frequent confusion with other signals (e.g., Marbled Murrelet, Northern Saw-whet Owl), low recall from poor SNR, or a combination thereof. Conversely, only limited gains were achieved for species classes that performed highly with the source model (Table 1.1). Species with more unique vocalizations or stereotyped repertoires achieved high performance with few training samples. By contrast, species with diverse songs and call types, plastic calls early in the breeding season, or vocalizations with high similarity to other signals required more training examples to ensure sufficient model performance. For example, training with only 10 samples of the Pileated Woodpecker (a limited repertoire of stereotyped, simple vocalizations) yielded an AUC greater than 0.95, while roughly 100 samples of the Pacific Wren (an extremely large repertoire regularly modulated with complex variations) were required to achieve the same performance (Figure A1.3). While high performance (mean AUC 0.9) was achieved for most species classes by training with an average of only 16 samples per class, this variation in performance among classes suggests that such a small number of samples should be regarded only as a lower bound for model training. Relatedly, inconsistent variation in performance across sample sizes for some species classes (e.g., Western Wood-pewee, Northern Saw-whet Owl; Figure A1.3) highlights the strong influence of relatively few training examples at small sample sizes and class imbalances on performance stability.

These findings point to the need for obtaining the highest number of training samples feasible to achieve acceptable performance for a given model application, reduce the risk of overfitting, and maintain class balance while also ensuring that the examples are sufficiently diverse to account for variation within and between class signals (Oswald et al., 2022). An investigation of model performance for specific bird species illustrates the importance of these recommendations. For example, classes in the target model that performed poorly in site level precision suffered from a dearth of training examples overall (Belted Kingfisher), a lack of examples for particular calls or songs within a larger repertoire (Spotted Towhee in relation to Varied Thrush), high natural variation in vocalizations (Western Wood-pewee), or continued confusion due to poor SNR or signal truncation. Similar findings have been shown for other taxonomic groups, including primates (Dufourq et al., 2022), cetaceans (Zhong et al., 2020a), amphibians (Zhong et al., 2020b), and bats (Franco and Lipani, 2020). Care should be taken to curate a training database that is sufficiently representative of the variation present within the

target domain. Although increasing the number of training examples led to improved performance, asymptotes indicate the possibility of maximizing the potential of training data for certain classes (Figure A1.3), perhaps due to training samples not being varied or representative enough to fully resolve sources of signal confusion. For example, performance for the Sooty Grouse plateaued at AUC 0.8 with approximately 100 training samples, continuing beyond this point to exhibit confusion with noise from distant aircraft, rapid gusts of wind, and heavy rain (Table A1.3). Obtaining more diverse training samples for underperforming classes and confusing signals in our model would likely improve these shortcomings.

Classification performance at the segment level was generally correlated with performance at the site level, but with some notable exceptions. Very conspicuous or abundant species (e.g., Golden-crowned Kinglet) by nature of their frequent vocalizations presented more opportunities for detection and thus achieved high site level accuracy for the source model despite modest segment level AUC (Table 1.1). By contrast, less conspicuous (e.g., Marbled Murrelet) and highly mobile species (e.g., Red Crossbill) offered fewer opportunities for detection, often with lower confidence scores, resulting in low site level accuracy despite high segment level AUC for the source model (Table 1.1). These latter species classes benefited most from the target model's improvements in recall.

The complexity and variation inherent in passive acoustic soundscapes are leading impediments to model generalization in applied monitoring scenarios (Priyadarshani et al., 2018; van Merriënboer et al., 2024; Goëau et al., 2018). We found that the source model's ability to generalize was confronted with two primary challenges: 1) similar signals presented in a new acoustic context, and 2) novel signals the model had little or no previous "knowledge" of. For example, vocalizations with poor SNR (due to distance, reverberation, or geophony), concurrent vocalizations of multiple individuals, high plasticity, regional dialects, and "sound-alike" interspecific vocalizations (e.g., mimicry and the many variations of songbird *jit* and *chip* calls) all presented familiar signals but in a more acoustically complex context, leading either to reduced precision from confusion or reduced recall from low confidence scores. Correspondingly, novel signals such as anthropogenic noise from vehicles and logging and biophony from insects, anurans, and squirrels often reduced precision by yielding highly confident, but incorrect, predictions for species classes. This resulted in high false positive rates for several absent species, such as the Great Horned Owl. While the absence of these species

precludes training of a target model with local examples of their vocalizations, the target model's ability to identify novel confusing signals can assist in identifying these false positives. Although data processing artifacts such as signal truncation were not among the leading sources of error, their influence could also be mitigated, for example, by overlapping segment windows and averaging class predictions over time (e.g., via the BirdNET overlap parameter). Finally, post-processing model predictions (e.g., culling class outliers rarely detected at a site) may further strengthen model precision with a minor impact to recall.

Our finding that abiotic signals and ambient noise were the most prominent drivers of error for the source model suggest that efforts to reduce their influence on model predictions will result in the greatest gains in performance. While the presence of specific novel signals unique to a monitoring site can have substantial effects on individual species classes (Figure 1.3), the influence of common sources of confusion on poor performance is mitigated by the target model. This corroborates previous findings that poor SNR and ambient noise are primary culprits in reduced performance (Pérez-Granados 2023; Wood et al., 2021) and contributes to the small but growing body of research exploring the specific biotic and abiotic signals and mechanisms that drive this variation, and subsequently the common problems that PAM practitioners may encounter in the field (Priyadarshani et al., 2018). Reductions in error for species classes that had frequent confusions in the source model confirm that training with examples of confusing signals and ambient background noise is important, in addition to training on the poorly performing classes themselves (Kershenbaum et al., 2024). This also improves the model's ability to detect vocalizations in recordings with adverse acoustic conditions that would otherwise typically be discarded (e.g., Cole et al., 2022).

A fundamental challenge in scaling up bioacoustic species detection probabilities to entire communities is the influence of the unique qualities of a soundscape, including multiple vocalizing species and acoustic propagation through the environment (Sueur et al., 2008; Gibb et al., 2019). We found evidence for a positive relationship between α-diversity and false positive rate, such that sites with greater species richness yielded higher false positive rates (Table A1.3). We posit that this is because increased vocalization of different species results in more opportunities for signal confusion. Similarly, we found evidence for a positive relationship between habitat structural complexity (proxied by forest seral stage) and false negative rate, such that sites with more heterogeneous environmental structure yielded higher false negative rates

(Table A1.3). In this case, a more acoustically complex environment results in more opportunities for a signal to be attenuated due to sound absorption, reflection, or poor SNR from ambient geophony (van Merriënboer et al., 2024). These effects were diminished in the target model, with lower error and variation across habitat types suggesting a reduced influence of the monitoring environment itself on performance.

While it is well recognized that decision threshold tuning is essential to optimize pre-trained model performance (Pérez-Granados 2023; Cole et al., 2022), this study showed that a threshold optimizing classification performance at the segment level will not necessarily improve performance at the site level (Table A1.2). This is due to the presence of variation in raw acoustic monitoring data that is not fully accounted for in a limited test dataset, including the detectability and call rate of individuals. Furthermore, the best choice of threshold depends highly on the goals of a study. For example, a multi-species occupancy study may use conservative thresholds to prioritize precision as long as recall is adequate to yield sufficient species detection probabilities, knowing that the hierarchical model will account for imperfect detection (Cole et al., 2022). Conversely, a study searching audio data for vocalizations of a particular rare or cryptic species may benefit from a more liberal threshold to ensure that false negatives are minimized (Zhong et al., 2021; Kershenbaum et al., 2024). While these thresholding techniques can lead to increased efficiency when processing acoustic data, studies employing automated species detection models should still manually validate results to ensure accuracy. An increasingly common approach used in scenarios where predictions cannot feasibly be manually reviewed at scale (e.g., large surveys involving vast quantities of data or numbers of species) is to convert prediction scores into true positive probabilities through a logistic regression fit to a subsample of validated data (Wood and Kahl 2024). This method can yield probabilistic score thresholds and offers a more quantitatively robust approach to deriving binary species detection histories from model predictions than conventional arbitrary thresholding.

Design of the convolutional neural network architecture and tuning of training hyperparameters played important roles in optimizing model performance (Table A1.4). Increased learning rate may result in faster convergence, but at the cost of reduced learning stability and increased risk of overfitting to the training data. Changes in batch size can present similar tradeoffs in performance and learning stability, and should be explored in further investigations of the relationship between training sample size and performance. Increasing the

complexity of the classifier head network architecture (i.e., adding additional layers and hidden units) may not necessarily lead to gains in performance substantial enough to warrant the increased risk of overfitting. However, the interaction between training set size and classification head complexity with respect to classifier performance warrants further investigation. We suggest validating model development with early stopping to prevent overfitting and inform an appropriate number of epochs for training the final model. While the settings presented here may yield sufficient performance in other similar transfer learning applications, alternative configurations should be explored to ensure an optimal design is found.

The potential benefit of other machine learning and model configuration techniques beyond the scope of this study warrants further investigation. For example, training data augmentation (e.g., through shifts in time and pitch, spectrogram transformation, noise simulation, or signal mixup) could substantially expand the effective number of training samples and improve class balance (Dufourq et al., 2022; Zhong et al., 2021). Additionally, employing "active learning" techniques to optimize training data annotation could reduce model development time (Kath et al., 2024). Furthermore, while we chose to retain the convolutional layers of the source model in their entirety, these layers could be fine-tuned to produce feature embeddings more closely adapted to the target domain. However, the present study corroborates previous findings that the existing BirdNET feature embeddings are sufficient for highly performant transfer learning across diverse taxa, which similarly reported that ROC AUC values greater than 0.9 can be achieved with as little as 4 training samples (Ghani et al., 2023). Finally, increasing the BirdNET model overlap parameter value can increase temporal detection resolution, potentially influencing precision and recall, while adjusting the sensitivity parameter will change the relative spread of low- and high-confidence prediction scores, and thus the specific threshold value calculated to achieve a particular performance metric (Kahl et al., 2021). The potential of these various approaches to further enhance model performance is a promising area for future investigation.

1.5.2 Important considerations for performance evaluation

Several considerations concerning model performance evaluation should be mentioned. First, sample size and variation can have a substantial effect on estimated performance metrics. In particular, estimates of precision and recall become unstable at small positive sample sizes,

introducing bias in AUC due to high variance. Therefore, while ideal AUC and F_1 values of 1.0 report exceptional model performance (see, for example, Marbled Murrelet and Western Screech-Owl, rare species in the study region, Table 1.1), they suggest a degree of bias due to the reduced quantity of positive samples for the associated classes in the test dataset. Similarly, evaluation samples with very little variation can introduce bias in estimation (e.g., anuran vocalizations from a limited number of individuals, Figure A1.1, A1.3). Detections for these classes should therefore be interpreted with caution, and transfer learning practitioners should strive to assemble evaluation datasets with sample size and variation sufficient to achieve stability in estimates of performance metrics. In addition, vocalization samples collected from our target domain do not represent the comprehensive repertoire of each species. As such, performance comparisons between models were made only using examples of the same set of signals (i.e., primary song and call types). Finally, a fully unbiased evaluation of model performance would ideally be conducted with a random selection of samples taken directly from the raw PAM data. However, this can heavily skew the distribution of a test dataset towards overabundant negative samples, potentially requiring an exceptionally large sample size to obtain enough positive examples to evaluate performance across the full range of confidence scores for each species, and ultimately rendering manual review infeasible (Wood and Kahl 2024). We addressed this by randomly sampling from score bins stratified across the full range of confidence scores, sacrificing a representative distribution of the raw monitoring data in favor of a representative range of scores and the practical feasibility of required manual review effort.

Separation of training, validation, and held-out test data is critical in machine learning to develop a generalizable model and obtain an unbiased estimation of its performance on unseen data (Kershenbaum et al., 2024; Oswald et al., 2022). Although we ensured this separation, our decision to sample training, validation, and test data from the same set of sites may introduce a degree of bias in the model, leading to overfitting. For example, including multiple vocalizations from the same individual in both the training and test datasets can skew results due to temporal autocorrelation between samples, inflating performance estimates (Oswald et al., 2022). Maintaining complete independence of sites between datasets would have resulted in an insufficient number of examples for uncommon species classes, precluding estimation of performance at the community level and transfer learning. We reduced this bias by sampling across multiple sites, habitat types, and months within the breeding season.

Lastly, model performance can vary over both space and time. In practice, performance metrics and optimal decision thresholds may differ not only by class but by survey site and potentially over time due to variation in the local acoustic environment. Therefore, arbitrary and class-specific decision thresholds implicitly assume consistent model performance across space (survey sites) and time (within the individual survey period and the breeding season). Moreover, using metrics from this study to estimate expected performance on other unseen data (i.e., other sites or monitoring years) assumes that model performance across the sites sampled during the 2020 breeding season sufficiently indicates performance across different sites and time periods. While we have demonstrated a capacity for the target model to mitigate the influence of local environmental variation on performance, suggesting improved generalization among sites, variation in performance across seasons remains to be quantified. Adjustments to explicitly account for such spatiotemporal variation in model performance could be determined through further manual validation, integrated modeling, or by incorporating contextual information (e.g., Singer et al., 2024; Jeantet and Dufourq 2023)

1.5.3 Guidelines for transfer learning in practice

We offer a set of guidelines to practitioners employing few-shot transfer learning in bioacoustics (Table 1.2) and discuss several of these recommendations in more detail below. To determine target classes for training, identify species that perform insufficiently with a source model by calculating performance metrics, and consider prioritizing species of high relevance for management or conservation objectives. Metrics should be evaluated at ecologically meaningful levels relevant to a study, for example, both the audio segment and site use levels, as high segment performance does not necessarily result in high site performance (e.g., Black-throated Gray Warbler, Table 1.1). Low precision suggests frequent signal confusion and false positives, low recall suggests a species may not be detected at sites where it is truly present, and low AUC indicates poor overall performance (van Merriënboer et al., 2024; Kershenbaum et al., 2024). To reduce signal confusion, ensure that ambient noise and sources of common confusion that define the distinct acoustic context of a study area are also included in training as either negative species class examples or unique classes themselves (Kershenbaum et al., 2024). The method outlined previously to evaluate classifier model performance can be used to identify the

dominant signals present within a target domain and prioritize signals for monitoring and improvement.

Guideline	
Select an appropriate source model	Begin with a pre-trained source model that provides powerful feature recognition capabilities and an accessible development API (e.g., BirdNET, ResNet).
Evaluate model performance in context	Evaluate model performance using established metrics (e.g., precision-recall AUC, F_1 score, etc.) at ecologically meaningful levels relevant to the study (for example, both audio segment and site use levels). Consider that model performance can vary substantially over both space and time, and estimates of performance metrics are more stable at greater sample sizes.
Prioritize classes for training	Prioritize classes for training with the greatest potential for gain. These may be species with low source model performance, species of high conservation or management importance, or other acoustic signals relevant to a study that are not natively supported for detection by a source model.
Consider performance-effort tradeoff	When selecting classes and acquiring training samples, consider the cost-benefit tradeoff between model performance capabilities and requirements for annotation effort and data. Consider that training sample size can have a dramatic impact on performance, but this effect may vary widely among species and depending on the acoustic environment.
Obtain representative training data	Obtain training data that are representative of the range of variation in acoustic signals and conditions throughout the study area.
Train on drivers of error	Include training examples of the leading drivers of classification error (e.g., abiotic noise, "soundalike" species) to improve model discrimination between commonly confused signals.
Balance training data, when feasible	A training data set balanced between classes is desirable to prevent biases in training (i.e., toward more abundant common species over rare species) and improve inference of model strength from performance metrics.
Ensure independence of data	Ensure independence of training, validation, and held-out test data to develop a generalizable model and an unbiased estimation of its performance on unseen data.
Tune model architecture and hyperparameters	Explore the benefits of adjusting model architecture design and hyperparameter settings, and the use of other machine learning techniques (e.g., training data augmentation).
Leverage model strengths with an ensemble	A target model can be used together with a pre-trained source model in a model ensemble to achieve robust signal detection across the entire acoustic community of interest.

Table 1.2: Guidelines for few-shot transfer learning practitioners in bioacoustics research.

Consider that a cost-benefit tradeoff exists. Increasing the number of classes and quantity of training examples for a model improves its capabilities and performance but substantially increases annotation time and data requirements. However, excessively reducing the number of classes and quantity of data will limit performance, negating the benefit of developing a new model. The number of training samples required to achieve sufficient performance will vary among species and signal types (Ghani et al., 2023; Dufourq et al., 2022). Moreover, what a researcher deems “sufficient performance” highly depends on the goals and needs of a particular study. Therefore, classes chosen and samples acquired for transfer learning should be selected purposefully with these factors in mind.

A machine learning model is only as strong as the data it is trained with. Training, validation, and held-out test data should be kept independent. These data should be representative of the scope of variation in acoustic signals and conditions throughout the study area. They should ideally be balanced between classes to prevent biases in training (Dufourq et al., 2022; Kershenbaum et al., 2024). If a model is trained to recognize only a specific song or call type for a species, performance for that signal may improve, but the model cannot detect other signals from the species (van Merriënboer et al., 2024).

Lastly, a model ensemble should be used in practice. Rather than modifying the source model directly, the transfer learning approach we demonstrate produces a new model for the target domain for a particular set of classes. Unless this new model supports all classes of monitoring interest, it should be used in conjunction with the source model to ensure complete class coverage. This can be done with a model ensemble that combines predictions from both the target and source model to produce a final prediction (Pan and Yang 2010), for example, via a weighted average based on performance or class-specific replacement, as in this study. Our results support previous studies demonstrating that a model ensemble can achieve better overall performance than a single model can independently (Redgwell et al., 2009), in this case by combining the strengths of the source model (i.e., preexisting classes with sufficient performance) and the target model (i.e., novel classes and improved performance for select preexisting classes). However, using a model ensemble will increase processing time, as both models must be run to produce detection histories for the entire acoustic community

1.5.4 Implications for bioacoustic monitoring

Methods for rigorous bioacoustic classifier model evaluation and optimization in applied scenarios are essential as pre-trained models are increasingly used in research, management, and citizen science (Cole et al., 2022; Sethi et al., 2021; Wood et al., 2022; Nieto-Mora et al., 2023). While the pre-trained BirdNET source model performed moderately well in our study region, it could not consistently detect one-third of avian species present, including several of high conservation and management priority. Additionally, high false positive rates for several absent species resulted in frequent “false alarms.” Weak model performance for individual species scaled up to inaccurate estimates of species diversity. Considered together, these limitations highlight the critical importance of validating the performance of a pre-trained “off-the-shelf”

model before drawing ecological or conservation inferences from its predictions (Sandfort et al., 2024). These results also point to the need for increased scrutiny of species detections reported by citizen scientists, often determined with pre-trained models (e.g., Merlin) applied in challenging acoustic environments.

Our results demonstrate the use of few-shot transfer learning to produce a robust classifier for monitoring avian communities at a landscape scale. A model developed with this approach can reduce errors in predicted species detection histories and enable more efficient manual validation of detections. Improved performance at the audio segment (i.e., vocalization) level increases the detection probabilities of both common and rare species and supports scientific investigations of animal behavior and communication. Improved performance at the site use level provides more accurate estimates of species diversity and community composition. This results in a more reliable model for applied monitoring scenarios to better inform confident ecological analyses and subsequent conservation and management actions (Gibb et al., 2019).

The primary benefit of few-shot transfer learning is the comparatively small data, time, and processing power required to produce a robust model compared to parameterizing and training an entirely new model. While our study region is home to almost one hundred well-studied avian species, other regions worldwide support many more soniferous species and are challenged by resource limitations that make the conventional development of a local classifier model intractable. As such, transfer learning may provide a fast track to performant acoustic monitoring in regions with limited data and technologies for bioacoustic classification.

Transfer learning also offers opportunities to expand acoustic monitoring capabilities beyond the scope of a pre-trained model to new environments and taxa. Our target model performed well in the study region despite the challenging acoustic environment of a temperate rainforest with regular rainfall, windstorms, aircraft flyovers, active logging, concurrent vocalizations, complex environmental structure, and generally poor SNR. This suggests that a regional model adapted with transfer learning may improve monitoring efforts in other acoustically challenging environments, such as tropical rainforests, free-flowing waterways, and urbanized terrestrial and aquatic environments dominated by anthropogenic noise. Relatedly, our model's high performance on insect, anuran, geophonic, and anthropogenic signal classes confirms previous findings that feature embeddings produced by the BirdNET source model

capture a diverse range of acoustic variation that is readily applicable to non-avian taxa and abiotic signals (Ghani et al., 2023).

Despite the advantages of using transfer learning in bioacoustics models, we recognize that its execution still requires a degree of technical expertise in machine learning that managers and conservationists may lack (Kershenbaum et al., 2024). For this reason, we provide the workflow outlined in this study as an open-source repository (see Data Availability section; Jacuzzi 2025), including all associated Python and R code, reproducible programming examples, and a graphical user interface for processing audio data via a model ensemble with no programming required (Figure A1.4). This and other open-source software for model evaluation and development, such as BirdNET-Analyzer (Kahl et al., 2021; Symes et al., 2024) and OpenSoundscape (Lapp et al., 2023), can serve as helpful resources to onboard new machine learning practitioners and develop models that produce robust ecological data. Future efforts to make machine learning model evaluation and training more accessible to researchers and managers (e.g., through user interfaces or wrappers for the R programming language) should be prioritized to encourage adoption and better utilize the immense value of these technologies.

1.6 ACKNOWLEDGEMENTS

We gratefully acknowledge student technicians from the University of Washington for their assistance with data annotation: Summer Delehanty, Stevan Pekich, Iris Haley, Mirella Brannon, Jack McKenzie, and Jessica Robinson. We thank the Washington State Department of Natural Resources for providing acoustic monitoring data from the Olympic Experimental State Forest and wildlife biologists Scott Gremel (National Park Service) and Scott Horton (WADNR) for their expertise in validating the regional list of avian species. Teodora Minkova, Lauren Kuehne, and Daniel Donato provided valuable input on the manuscript. We also thank four anonymous reviewers for their helpful suggestions in improving the manuscript. Attributions for art used in figure illustrations can be found in Appendix 1.2.

1.7 DATA AVAILABILITY

Code for the transfer learning workflow, programming examples, and the graphical user interface for ensemble model prediction, as well as all data required for the reproduction of results from this study, are available at the open-source repository github.com/giojacuzzi/few-shot-transfer-learning-bioacoustics (doi.org/10.5281/zenodo.15694435, Jacuzzi 2025) which leverages BirdNET-Analyzer (Kahl et al., 2021) as a dependency.

1.8 REFERENCES

Abadi, M., Agarwal, A., Barham, P., Brevdo, E., Chen, Z., Citro, C., Corrado, G.S., Davis, A., Dean, J., Devin, M., Ghemawat, S., Goodfellow, I., Harp, A., Irving, G., Isard, M., Jia, Y., Jozefowicz, R., Kaiser, L., Kudlur, M., Levenberg, J., Mane, D., Monga, R., Moore, S., Murray, D., Olah, C., Schuster, M., Shlens, J., Steiner, B., Sutskever, I., Talwar, K., Tucker, P., Vanhoucke, V., Vasudevan, V., Viegas, F., Vinyals, O., Warden, P., Wattenberg, M., Wicke, M., Yu, Y., Zheng, X., 2015. TensorFlow: Large-Scale Machine Learning on Heterogeneous Distributed Systems.

Besson, M., Alison, J., Bjerge, K., Gorochowski, T.E., Høye, T.T., Jucker, T., Mann, H.M.R., Clements, C.F., 2022. Towards the fully automated monitoring of ecological communities. Ecology Letters 25, 2753–2775. https://doi.org/10.1111/ele.14123

Cole, J.S., Michel, N.L., Emerson, S.A., Siegel, R.B., 2022. Automated bird sound classifications of long-duration recordings produce occupancy model outputs similar to manually annotated data. Ornithological Applications 124, 1–15. https://doi.org/10.1093/ornithapp/duac003

Cornell Lab of Ornithology, Cornell University, Interactive Sound Analysis Software [WWW Document], n.d. URL https://www.ravensoundsoftware.com/ (accessed 10.31.24).

Duarte, A., Weldy, M.J., Lesmeister, D.B., Ruff, Z.J., Jenkins, J.M.A., Valente, J.J., Betts, M.G., 2024. Passive acoustic monitoring and convolutional neural networks facilitate high-resolution and broadscale monitoring of a threatened species. Ecological Indicators 162, 112016. https://doi.org/10.1016/j.ecolind.2024.112016

Dufourq, E., Batist, C., Foquet, R., Durbach, I., 2022. Passive acoustic monitoring of animal populations with transfer learning. Ecological Informatics 70, 101688. https://doi.org/10.1016/j.ecoinf.2022.101688

Fink, D., Auer, T., Johnston, A.,Strimas-Mackey, M., Ligocki, S., Robinson, O., Hochachka, W., Jaromczyk, L.,Crowley, C., Dunham, K., Stillman, A., Davies, I., Rodewald, A., Ruiz-Gutierrez, V., Wood, C.. 2023. eBird Status and Trends, Data Version: 2022; Released: 2023. Cornell Lab of Ornithology, Ithaca, New York. https://doi.org/10.2173/ebirdst.2022

Folliot, A., Haupert, S., Ducrettet, M., Sèbe, F., Sueur, J., 2022. Using acoustics and artificial intelligence to monitor pollination by insects and tree use by woodpeckers. Science of The Total Environment 838, 155883. https://doi.org/10.1016/j.scitotenv.2022.155883

Franco, M., Lipani, C., 2020. Automated monitoring of bat species in Belgium. Ecole polytechnique de Louvain, Catholic University of Louvain.

Geirhos, R., Jacobsen, J.-H., Michaelis, C., Zemel, R., Brendel, W., Bethge, M., Wichmann, F.A., 2020. Shortcut learning in deep neural networks. Nat Mach Intell 2, 665–673. https://doi.org/10.1038/s42256-020-00257-z

Ghani, B., Denton, T., Kahl, S., Klinck, H., 2023. Global birdsong embeddings enable superior transfer learning for bioacoustic classification. Sci Rep 13, 22876. https://doi.org/10.1038/s41598-023-49989-z

Gibb, R., Browning, E., Glover-Kapfer, P., Jones, K.E., 2019. Emerging opportunities and challenges for passive acoustics in ecological assessment and monitoring. Methods in Ecology and Evolution 10, 169–185. https://doi.org/10.1111/2041-210X.13101

Goëau, H., Kahl, S., Glotin, H., Planqué, B., Vellinga, W.-P., Joly, A., 2018. Overview of BirdCLEF 2018: Monospecies vs. Sundscape Bird Identification. Presented at the Working Notes of CLEF 2018 - Conference and Labs of the Evaluation Forum, Avignon, France, September 10-14, 2018.

Jacuzzi, G, 2025. giojacuzzi/few-shot-transfer-learning-bioacoustics: 1.0. Zenodo. https://doi.org/10.5281/zenodo.15694435

Jeantet, L., Dufourq, E., 2023. Improving deep learning acoustic classifiers with contextual information for wildlife monitoring. Ecological Informatics 77, 102256. https://doi.org/10.1016/j.ecoinf.2023.102256

Johnson, D.H., O'Neil, T.A. (Eds.), 2001. Wildlife-habitat relationships in Oregon and Washington, 1st ed. ed. Oregon State University Press, Corvallis.

Kahl, S., Wood, C.M., Eibl, M., Klinck, H., 2021. BirdNET: A deep learning solution for avian diversity monitoring. Ecological Informatics 61, 101236. https://doi.org/10.1016/j.ecoinf.2021.101236

Kath, H., Serafini, P.P., Campos, I.B., Gouvêa, T.S., Sonntag, D., 2024. Leveraging transfer learning and active learning for data annotation in passive acoustic monitoring of wildlife. Ecological Informatics 82, 102710. https://doi.org/10.1016/j.ecoinf.2024.102710

Kershenbaum, A., Akçay, Ç., Babu-Saheer, L., Barnhill, A., Best, P., Cauzinille, J., Clink, D., Dassow, A., Dufourq, E., Growcott, J., Markham, A., Marti-Domken, B., Marxer, R., Muir, J., Reynolds, S., Root-Gutteridge, H., Sadhukhan, S., Schindler, L., Smith, B.R., Stowell, D., Wascher, C.A.F., Dunn, J.C., 2024. Automatic detection for bioacoustic research: a practical guide from and for biologists and computer scientists. Biological Reviews. https://doi.org/10.1111/brv.13155

Lapp, S., Rhinehart, T., Freeland-Haynes, L., Khilnani, J., Syunkova, A., Kitzes, J., 2023. OpenSoundscape: An open-source bioacoustics analysis package for Python. Methods in Ecology and Evolution 14, 2321–2328. https://doi.org/10.1111/2041-210X.14196

Larkin, J.T., McNeil, D.J., Chronister, L., Akresh, M.E., Cohen, E.B., D'Amato, A.W., Fiss, C.J., Kitzes, J., Larkin, J.L., Parker, H.A., King, D.I., 2024. A large-scale assessment of eastern whip-poor-will (*Antrostomus vociferus*) occupancy across a gradient of forest management intensity using autonomous recording units. Journal of Environmental Management 366, 121786. https://doi.org/10.1016/j.jenvman.2024.121786

Lauha, P., Somervuo, P., Lehikoinen, P., Geres, L., Richter, T., Seibold, S., Ovaskainen, O., 2022. Domain-specific neural networks improve automated bird sound recognition already with small amount of local data. Methods in Ecology and Evolution 13, 2799–2810. https://doi.org/10.1111/2041-210X.14003

Macaulay Library, n.d. URL https://www.macaulaylibrary.org/ (accessed 10.31.24).

Minkova, T.V., Kuehne, L.M., Donato, D., 2020. Using Passive Acoustic Monitoring to evaluate sustainability of forest management. Study Plan. Washington State Department of Natural Resources.

Minkova, T.V., Devine, W.D., Martens, K.D. 2024. T3 Watershed Experiment in the Olympic Experimental State Forest: 2016-2023 Implementation Report. Washington State Department of Natural Resources, Forest Resources Division, Olympia, WA.

Miyaguchi, A., Zhong, N., Gustineli, M., Hayduk, C., 2023. Transfer Learning with Semi-Supervised Dataset Annotation for Birdcall Classification. https://doi.org/10.48550/arXiv.2306.16760

Morales, G., Vargas, V., Espejo, D., Poblete, V., Tomasevic, J.A., Otondo, F., Navedo, J.G., 2022. Method for passive acoustic monitoring of bird communities using UMAP and a deep

neural network. Ecological Informatics 72, 101909. https://doi.org/10.1016/j.ecoinf.2022.101909

Müller, J., Mitesser, O., Schaefer, H.M., Seibold, S., Busse, A., Kriegel, P., Rabl, D., Gelis, R., Arteaga, A., Freile, J., Leite, G.A., de Melo, T.N., LeBien, J., Campos-Cerqueira, M., Blüthgen, N., Tremlett, C.J., Böttger, D., Feldhaar, H., Grella, N., Falconí-López, A., Donoso, D.A., Moriniere, J., Buřivalová, Z., 2023. Soundscapes and deep learning enable tracking biodiversity recovery in tropical forests. Nat Commun 14, 6191. https://doi.org/10.1038/s41467-023-41693-w

Nieto-Mora, D.A., Rodríguez-Buritica, S., Rodríguez-Marín, P., Martínez-Vargaz, J.D., Isaza-Narváez, C., 2023. Systematic review of machine learning methods applied to ecoacoustics and soundscape monitoring. Heliyon 9, e20275. https://doi.org/10.1016/j.heliyon.2023.e20275

Oswald, J.N., Van Cise, A.M., Dassow, A., Elliott, T., Johnson, M.T., Ravignani, A., Podos, J., 2022. A Collection of Best Practices for the Collection and Analysis of Bioacoustic Data. Applied Sciences 12, 12046. https://doi.org/10.3390/app122312046

Pan, S.J., Yang, Q., 2010. A Survey on Transfer Learning. IEEE Transactions on Knowledge and Data Engineering 22, 1345–1359. https://doi.org/10.1109/TKDE.2009.191

Pérez-Granados, C., 2023. BirdNET: applications, performance, pitfalls and future opportunities. Ibis 165, 1068–1075. https://doi.org/10.1111/ibi.13193

Pieplow, N., 2016. Peterson Field Guide to Bird Sounds | Bird Academy • The Cornell Lab [WWW Document]. URL https://academy.allaboutbirds.org/peterson-field-guide-to-bird-sounds/ (accessed 10.31.24).

Priyadarshani, N., Marsland, S., Castro, I., 2018. Automated birdsong recognition in complex acoustic environments: a review. Journal of Avian Biology 49, jav-01447. https://doi.org/10.1111/jav.01447

Redgwell, R.D., Szewczak, J.M., Jones, G., Parsons, S., 2009. Classification of Echolocation Calls from 14 Species of Bat by Support Vector Machines and Ensembles of Neural Networks. Algorithms 2, 907–924. https://doi.org/10.3390/a2030907

Sandfort, R., Uhlhorn, B., Geißler, G., Lyhne, I., Jiricka-Pürrer, A., 2024. AI will change EA practice – but are we ready for it? A call for discussion based on developments in

collecting and processing biodiversity data. Impact Assessment and Project Appraisal 42, 200–208. https://doi.org/10.1080/14615517.2024.2318684

Sechidis, K., Tsoumakas, G., Vlahavas, I., 2011. On the Stratification of Multi-label Data, in: Gunopulos, D., Hofmann, T., Malerba, D., Vazirgiannis, M. (Eds.), Machine Learning and Knowledge Discovery in Databases. Springer, Berlin, Heidelberg, pp. 145–158. https://doi.org/10.1007/978-3-642-23808-6_10

Sethi, S. S., Fossøy, F., Cretois, B. & Rosten, C. M., n.d. Management-relevant applications of acoustic monitoring for Norwegian nature – The Sound of Norway. Norwegian Institute for Nature Research NINA Report 2064.

Singer, D., Hagge, J., Kamp, J., Hondong, H., Schuldt, A., 2024. Aggregated time-series features boost species-specific differentiation of true and false positives in passive acoustic monitoring of bird assemblages. Remote Sensing in Ecology and Conservation 10, 517–530. https://doi.org/10.1002/rse2.385

Stowell, D., 2022. Computational bioacoustics with deep learning: a review and roadmap. PeerJ 10, e13152. https://doi.org/10.7717/peerj.13152

Sueur, J., Pavoine, S., Hamerlynck, O., Duvail, S., 2008. Rapid Acoustic Survey for Biodiversity Appraisal. PLOS ONE 3, e4065. https://doi.org/10.1371/journal.pone.0004065

Symes, L., Sugai, L. S., Gottesman, B., Pitzrick, M., Wood, C., & Charif, R., 2024. Acoustic analysis with BirdNET and (almost) no coding: practical instructions (Version 1.0). Zenodo. https://doi.org/10.5281/zenodo.8415090

van Merriënboer, B., Hamer, J., Dumoulin, V., Triantafillou, E., Denton, T., 2024. Birds, bats and beyond: evaluating generalization in bioacoustics models. Front. Bird Sci. 3. https://doi.org/10.3389/fbirs.2024.1369756

Wang, Y., Yao, Q., Kwok, J.T., Ni, L.M., 2020. Generalizing from a Few Examples: A Survey on Few-shot Learning. ACM Comput. Surv. 53, 63:1-63:34. https://doi.org/10.1145/3386252

Wood, C. M., and S. Kahl. 2024. Guidelines for appropriate use of BirdNET scores and other detector outputs. Journal of Ornithology 165:777–782. https://doi.org/10.1007/s10336-024-02144-5

Wood, C.M., Kahl, S., Rahaman, A., Klinck, H., 2022. The machine learning–powered BirdNET App reduces barriers to global bird research by enabling citizen science participation. PLOS Biology 20, e3001670. https://doi.org/10.1371/journal.pbio.3001670

Yosinski, J., Clune, J., Bengio, Y., Lipson, H., 2014. How transferable are features in deep neural networks? https://doi.org/10.48550/arXiv.1411.1792

Zhong, M., Castellote, M., Dodhia, R., Lavista Ferres, J., Keogh, M., Brewer, A., 2020a. Beluga whale acoustic signal classification using deep learning neural network models. The Journal of the Acoustical Society of America 147, 1834–1841. https://doi.org/10.1121/10.0000921

Zhong, M., LeBien, J., Campos-Cerqueira, M., Dodhia, R., Lavista Ferres, J., Velev, J.P., Aide, T.M., 2020b. Multispecies bioacoustic classification using transfer learning of deep convolutional neural networks with pseudo-labeling. Applied Acoustics 166, 107375. https://doi.org/10.1016/j.apacoust.2020.107375

Zhong, M., Taylor, R., Bates, N., Christey, D., Basnet, H., Flippin, J., Palkovitz, S., Dodhia, R., Lavista Ferres, J., 2021. Acoustic detection of regionally rare bird species through deep convolutional neural networks. Ecological Informatics 64, 101333. https://doi.org/10.1016/j.ecoinf.2021.101333

1.9 APPENDIX 1.1

Table A1.1: Audio segment level performance metrics for source and target models. Columns are *model*, the model evaluated (i.e. source or target); *label*, the name of the class label; *PR_AUC*, the precision-recall area under the curve; *ROC_AUC*, the receiver operating characteristic area under the curve; *AP*, average precision (weighted mean of precisions achieved at each threshold); *f1_max*, the maximum F_1 score achieved; *Tp*, the decision threshold to maximize precision; *r_Tp*, the recall performance at threshold *Tp*; *Tf1*, the decision threshold to maximize F_1 score; *p_Tf1* and *r_Tf1*, the precision and recall performance at threshold *Tf1*, respectively; *N_pos* and *N_neg*, the number of positive and negative samples of the class available for evaluation.

model	label	PR_AUC	ROC_AUC	AP	f1_max	Tp	r_Tp	Tf1	p_Tf1	r_Tf1	N_pos	N_neg
source	american crow	0.67	0.98	0.67	0.8	0.6	0.67	0.6	1	0.67	3	2419
source	american goldfinch	0.45	0.99	0.48	0.57	0.93	0.25	0.36	0.67	0.5	4	2423
source	american kestrel										0	2428
source	american robin	0.82	0.96	0.81	0.74	0.21	0.21	0.01	0.71	0.77	318	2252
source	anna's hummingbird										0	2452
source	bald eagle	1	1	1	1	0.71	1	0.71	1	1	5	2428
source	band-tailed pigeon	0.91	1	0.91	0.88	0.46	0.15	0.03	0.83	0.93	103	2378
source	barred owl	0.95	1	0.95	0.9	0.73	0.51	0.16	0.85	0.95	74	2345
source	belted kingfisher	0.77	1	0.78	0.73	0.89	0.57	0.89	1	0.57	14	2447
source	bewick's wren										0	2428
source	black swift										0	2407
source	black-capped chickadee										0	2454
source	black-headed grosbeak	0.85	1	0.85	0.78	0.45	0.41	0.17	0.68	0.93	27	2408
source	black-throated gray warb	0.92	1	0.92	0.86	0.32	0.37	0.06	0.84	0.89	137	2343
source	brewer's blackbird										0	2432
source	brown creeper	0.88	1	0.88	0.83	0.96	0.33	0.23	0.78	0.88	33	2402
source	brown-headed cowbird										0	2432
source	bullock's oriole										0	2433
source	canada jay	0.86	1	0.86	0.81	0.88	0.15	0.13	0.71	0.94	34	2401
source	cedar waxwing	0.93	1	0.93	0.88	0.71	0.74	0.51	0.97	0.8	35	2409
source	chestnut-backed chickad	0.87	0.99	0.87	0.81	0.62	0.57	0.17	0.77	0.85	47	2397
source	chipping sparrow										0	2427
source	common raven	0.99	1	0.99	0.96	0.19	0.79	0.01	0.96	0.97	137	2333
source	common yellowthroat										0	2427
source	cooper's hawk										0	2473
source	dark-eyed junco	0.77	0.99	0.78	0.71	0.85	0.3	0.35	0.95	0.57	37	2412
source	downy woodpecker										0	2433
source	european starling										0	2413
source	evening grosbeak	0.98	1	0.98	0.93	0.54	0.66	0.22	0.91	0.95	65	2386
source	fox sparrow										0	2461
source	golden eagle										0	2401
source	golden-crowned kinglet	0.75	0.94	0.75	0.7	0.9	0.07	0.17	0.77	0.63	282	2309
source	great horned owl										0	2452
source	hairy woodpecker	0.95	1	0.95	0.92	0.71	0.47	0.04	0.9	0.93	91	2351
source	hammond's flycatcher	0.92	1	0.92	0.86	0.48	0.75	0.31	0.94	0.8	20	2451
source	hermit thrush	0.78	1	0.79	0.75	0.67	0.5	0.4	0.75	0.75	8	2440
source	hermit warbler										0	2474
source	house finch										0	2436
source	house sparrow										0	2438
source	house wren										0	2431
source	hutton's vireo	0.89	0.98	0.89	0.81	0.22	0.55	0.04	0.86	0.77	110	2345
source	lincoln's sparrow										0	2454
source	macgillivray's warbler	0.55	1	0.57	0.67	0.99	0.5	0.99	1	0.5	2	2458
source	marbled murrelet	0.46	0.99	0.48	0.5	1	0.29	0.81	0.35	0.86	7	2468
source	merlin										0	2443
source	mourning dove										0	2416
source	northern flicker	0.98	1	0.98	0.93	0.28	0.72	0.1	0.91	0.95	102	2346
source	northern goshawk	0.42	0.99	0.44	0.5	0.98	0.33	0.98	1	0.33	3	2456
source	northern pygmy-owl	0.59	1	0.61	0.67	0.87	0.5	0.87	1	0.5	2	2405
source	northern saw-whet owl	0.63	1	0.64	0.57	0.99	0.33	0.87	0.8	0.44	9	2424
source	olive-sided flycatcher	0.85	1	0.85	0.83	0.65	0.67	0.3	0.83	0.83	12	2443
source	orange-crowned warbler	0.97	1	0.97	0.91	0.49	0.73	0.28	0.83	1	15	2426
source	pacific wren	0.95	0.99	0.95	0.89	0.88	0.21	0.05	0.89	0.89	227	2255
source	pacific-slope flycatcher	0.88	0.97	0.88	0.81	0.66	0.19	0.04	0.85	0.78	328	2250
source	peregrine falcon										0	2437
source	pileated woodpecker	0.93	1	0.93	0.88	0.63	0.61	0.35	0.88	0.88	33	2404
source	pine siskin	0.92	1	0.92	0.82	0.41	0.59	0.25	0.84	0.8	51	2406
source	purple finch	0.79	0.99	0.79	0.76	0.35	0.61	0.23	0.81	0.72	18	2411
source	red crossbill	0.93	0.99	0.93	0.88	0.4	0.44	0.12	0.88	0.89	90	2359
source	red-breasted nuthatch	0.66	1	0.67	0.64	0.97	0.31	0.61	0.75	0.56	16	2446
source	red-breasted sapsucker										0	2422
source	red-eyed vireo										0	2431
source	red-tailed hawk	1	1	1	1	0.94	1	0.94	1	1	1	2463
source	red-winged blackbird										0	2416
source	ruby-crowned kinglet	0.66	1	0.68	0.67	0.72	0.38	0.58	0.71	0.62	8	2450
source	ruffed grouse										0	2416
source	rufous hummingbird	0.85	0.99	0.85	0.81	0.4	0.61	0.22	0.84	0.78	49	2410
source	savannah sparrow										0	2432
source	sharp-shinned hawk	1	1	1	1	0.95	1	0.95	1	1	2	2441
source	song sparrow	0.85	1	0.85	0.8	0.29	0.31	0.09	0.85	0.76	29	2392
source	sooty grouse	0.37	0.77	0.37	0.43	0.78	0.06	0.03	0.41	0.45	134	2394
source	spotted owl											2444
source	spotted towhee	0.75	0.98	0.75	0.7	0.75	0.16	0.14	0.65	0.74	74	2417
source	steller's jay	0.89	0.99	0.89	0.84	0.94	0.16	0.1	0.78	0.91	102	2364
source	swainson's thrush	0.93	1	0.93	0.88	0.26	0.56	0.05	0.85	0.92	66	2366
source	townsend's solitaire											2455
source	townsend's warbler	0.72	0.99	0.73	0.67	0.87	0.47	0.43	0.59	0.76	17	2444
source	tree swallow											2423
source	turkey vulture											2403
source	varied thrush	0.86	0.94	0.86	0.78	0.41	0.34	0.03	0.79	0.77	492	2208
source	vaux's swift	1	1	1	0.97	0.16	0.94	0.14	0.99	0.96	69	2355
source	violet-green swallow	0.72	1	0.74	0.73	0.93	0.22	0.29	0.62	0.89	9	2429
source	warbling vireo	0.89	1	0.89	0.8	0.29	0.64	0.23	0.89	0.73	22	2414
source	western bluebird											2428
source	western screech-owl	0.51	1	0.53	0.5	0.85	0.29	0.38	0.6	0.43	7	2411
source	western tanager	0.8	0.99	0.8	0.74	0.81	0.35	0.18	0.68	0.8	40	2401
source	western wood-pewee	0.43	0.99	0.45	0.42	0.7	0.22	0.27	0.33	0.56	9	2445
source	white-crowned sparrow	0.77	1	0.79	0.82	0.63	0.29	0.2	0.7	1	7	2416
source	white-tailed ptarmigan											2416
source	white-throated sparrow											2442
source	white-winged crossbill											2455
source	willow flycatcher											2423
source	wilson's warbler	0.83	1	0.83	0.83	0.95	0.18	0.26	0.8	0.86	28	2416
source	yellow warbler	1	1	1	1	0.4	1	0.4	1	1	4	2415
source	yellow-rumped warbler											2470
target	abiotic aircraft	0.98	0.99	0.98	0.92	0.69	0.55	0.17	0.9	0.94	395	2109
target	abiotic logging	0.92	0.99	0.92	0.84	0.83	0.41	0.06	0.83	0.85	112	2220
target	abiotic rain	0.97	1	0.97	0.92	0.67	0.73	0.3	0.97	0.88	213	2124
target	abiotic vehicle	0.96	1	0.96	0.95	0.68	0.42	0.11	0.97	0.92	40	2222
target	abiotic wind	0.96	0.99	0.96	0.89	0.9	0.29	0.19	0.9	0.88	251	2135
target	american robin	0.96	0.99	0.96	0.9	0.29	0.69	0.07	0.93	0.87	321	2095
target	band-tailed pigeon	0.98	1	0.98	0.93	0.96	0.65	0.51	0.92	0.94	103	2218
target	barred owl	0.97	1	0.97	0.93	0.99	0.66	0.51	0.91	0.95	74	2189
target	belted kingfisher	0.79	1	0.8	0.75	0.9	0.57	0.77	0.9	0.64	14	2295
target	biotic anuran	1	1	1	1	0.99	1	0.99	1	1	31	2217
target	biotic insect	0.9	0.97	0.9	0.83	0.65	0.54	0.21	0.9	0.76	258	2118
target	black-throated gray warb	0.98	1	0.98	0.92	0.68	0.57	0.06	0.89	0.96	137	2186
target	common raven	0.98	1	0.98	0.96	0.49	0.89	0.23	0.98	0.95	148	2168
target	dark-eyed junco	0.99	1	0.99	0.95	0.5	0.89	0.19	0.92	0.97	38	2250
target	golden-crowned kinglet	0.9	0.97	0.9	0.84	0.86	0.49	0.26	0.88	0.8	284	2154
target	hairy woodpecker	0.97	1	0.97	0.93	0.97	0.66	0.3	0.92	0.93	91	2195
target	hammond's flycatcher	0.92	1	0.93	0.89	0.69	0.8	0.46	0.94	0.85	20	2293
target	hermit thrush	0.99	1	0.99	0.94	0.96	0.88	0.04	0.89	1	8	2283
target	hutton's vireo	0.97	1	0.97	0.9	0.75	0.7	0.08	0.87	0.95	110	2190
target	marbled murrelet	1	1	1	1	0.28	1	0.28	1	1	7	2309
target	northern flicker	0.99	1	0.99	0.95	0.36	0.91	0.36	1	0.91	102	2191
target	northern pygmy-owl	1	1	1	0.97	0.95	0.94	0.91	0.94	1	16	2274
target	northern saw-whet owl	0.92	1	0.92	0.84	0.96	0.7	0.39	0.89	0.8	10	2267
target	olive-sided flycatcher	0.95	1	0.95	0.92	0.81	0.83	0.68	0.92	0.92	12	2288
target	pacific wren	0.98	1	0.98	0.92	0.68	0.78	0.2	0.89	0.96	228	2101
target	pacific-slope flycatcher	0.92	0.98	0.92	0.84	0.92	0.35	0.16	0.83	0.86	329	2093
target	pileated woodpecker	0.99	1	0.99	0.98	0.72	0.97	0.72	1	0.97	33	2249
target	purple finch	0.91	1	0.91	0.91	0.77	0.83	0.77	1	0.83	18	2254
target	red crossbill	0.98	1	0.98	0.96	0.93	0.8	0.63	0.97	0.94	90	2204
target	red-breasted nuthatch	0.95	1	0.95	0.93	0.88	0.88	0.88	1	0.88	16	2289
target	ruby-crowned kinglet	0.92	1	0.92	0.93	0.77	0.88	0.77	1	0.88	8	2291
target	rufous hummingbird	0.91	0.99	0.91	0.88	0.89	0.62	0.48	0.9	0.86	50	2252
target	song sparrow	1	1	1	0.98	0.39	0.97	0.39	1	0.97	29	2237
target	sooty grouse	0.82	0.97	0.82	0.76	0.99	0.23	0.42	0.81	0.72	134	2238
target	spotted towhee	0.89	0.99	0.89	0.86	1	0.17	0.52	0.94	0.8	75	2259
target	swainson's thrush	0.97	1	0.97	0.92	0.38	0.83	0.3	0.98	0.86	66	2207
target	townsend's warbler	0.95	1	0.96	0.91	0.91	0.82	0.36	0.94	0.88	17	2284
target	varied thrush	0.92	0.96	0.92	0.83	0.68	0.57	0.22	0.92	0.76	491	2053
target	violet-green swallow	0.94	1	0.95	0.89	0.93	0.67	0.69	0.89	0.89	9	2271
target	western screech-owl	1	1	1	1	0.8	1	0.8	1	1	7	2254
target	western tanager	0.89	0.99	0.89	0.86	0.94	0.65	0.7	0.89	0.82	40	2245
target	western wood-pewee	0.74	0.99	0.75	0.74	0.74	0.56	0.28	0.7	0.78	9	2290
target	white-crowned sparrow	1	1	1	1	0.85	1	0.85	1	1	7	2262
target	wilson's warbler	0.97	1	0.97	0.9	0.94	0.79	0.62	0.87	0.93	28	2260

Table A1.2: Site use level performance metrics across decision thresholds for source and target models. Metrics are shown for the source model considering all species, as well as for the source model and target model considering only those species classes shared by both. T_p and T_{f1} specify the performance using a class-specific threshold to optimize precision and F_1 score, respectively.

	Mean accuracy			Mean precision			Mean recall		
Threshold	**Source (all sp.)**	**Source**	**Target**	**Source (all sp.)**	**Source**	**Target**	**Source (all sp.)**	**Source**	**Target**
0.5	0.834	0.826	0.797	0.618	0.797	0.73	0.953	0.948	0.97
0.55	0.849	0.834	0.806	0.669	0.837	0.736	0.94	0.934	0.96
0.6	0.863	0.847	0.826	0.689	0.857	0.752	0.932	0.925	0.96
0.65	0.874	0.831	0.844	0.735	0.881	0.775	0.893	0.893	0.951
0.7	0.879	0.829	0.861	0.751	0.888	0.8	0.874	0.87	0.929
0.75	0.885	0.836	0.885	0.774	0.905	0.831	0.859	0.854	0.925
0.8	0.894	0.842	0.896	0.828	0.924	0.866	0.841	0.844	0.918
0.85	0.892	0.824	0.903	0.84	0.928	0.885	0.795	0.782	0.9
0.9	0.879	0.791	0.924	0.878	0.943	0.913	0.72	0.71	0.899
0.95	0.854	0.743	0.911	0.92	0.929	0.954	0.597	0.61	0.858
Tp	0.877	0.895	0.889	0.714	0.953	0.875	0.891	0.865	0.892
Tf1	0.855	0.854	0.806	0.639	0.81	0.755	0.975	0.962	0.968

Table A1.3: Accuracy, false positive rate, and false negative rate at the site use level across the gradient of habitat types, structural complexity, and α-diversity. “All species” includes all species classes under evaluation, while “shared species” includes only those species classes shared by both the source and target model.

			Mean error rate				Mean false positive rate				Mean false negative rate			
			All species		Shared species		All species		Shared species		All species		Shared species	
Str. complex.	**Mean α**	**Habitat**	**Source**	**Ensemble**	**Source**	**Target**	**Source**	**Ensemble**	**Source**	**Target**	**Source**	**Ensemble**	**Source**	**Target**
Very high	29	Late-seral (Mature)	0.14	0.1	0.21	0.1	0.05	0.06	0.04	0.06	0.09	0.04	0.17	0.04
High	29	Mid-seral (Thinned)	0.1	0.06	0.19	0.08	0.03	0.02	0.05	0.05	0.07	0.03	0.14	0.03
Low	37	Early-seral (Stand init.)	0.14	0.12	0.15	0.08	0.08	0.07	0.05	0.03	0.07	0.04	0.1	0.05
Mid	27	Mid-seral (Comp. excl.)	0.07	0.05	0.11	0.06	0.03	0.03	0.04	0.02	0.03	0.02	0.07	0.04
		SD	0.04	0.03	0.05	0.02	0.02	0.02	0.01	0.02	0.03	0.01	0.04	0.01

Table A1.4: Effect of hyperparameter value on PR AUC performance of sample size experiment model N≈100. The number of hidden units reflects the number of layers in the classifier head network architecture (0 hidden units for a one-layer network, and 128 or more for a two-layer network).

Learning rate	PR AUC	Batch size	PR AUC	Hidden units	PR AUC
0.0001	0.633	1	0.961	0	0.957
0.001	0.957	5	0.952	128	0.956
0.005	0.962	10	0.961	256	0.957
0.01	0.919	25	0.959	512	0.961
		50	0.959	1024	0.957
		75	0.961	2048	0.959
		100	0.957		

Table A1.5: Mean site level species richness estimates across decision thresholds for source and target models. Delta quantities are calculated relative to the observed (naïve) species richness. *Tp* and *Tf1* specify the performance using a class-specific threshold to optimize precision and F_1 score, respectively.

	Δ Species richness		Δ Species richness %	
Threshold	**Source**	**Target**	**Source**	**Target**
0.5	8.4	11.7	127.6	139.3
0.55	6.6	10.3	121.3	134.3
0.6	4.9	8.9	116.1	129.9
0.65	2.6	6.8	108.5	122
0.7	1.3	5.3	103.7	117.6
0.75	-0.3	3.6	98.8	112.2
0.8	-2.3	1.8	92.3	106.3
0.85	-3.9	0.3	86.7	101.1
0.9	-6.4	-1.3	78.7	95.9
0.95	-10.5	-4	65.1	86.7
Tp	2.1	5	106.6	116.2
Tf1	9.1	11.8	130.4	140

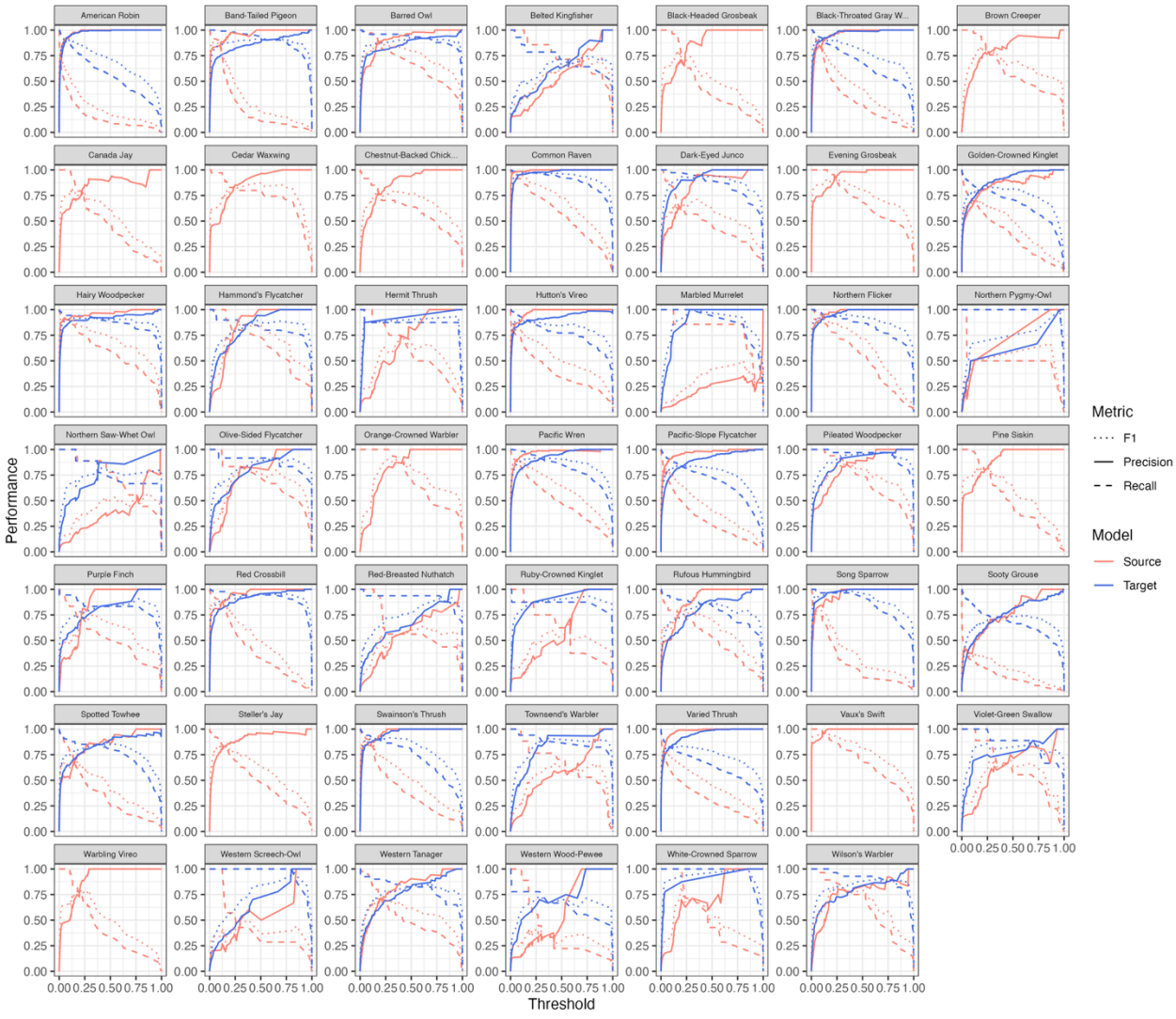

Figure A1.1: Differences in precision, recall, and F_1 performance across decision thresholds between source (red) and target (blue) models for all present classes. The target model generally achieved greater recall across thresholds and more stabilized precision. Novel target classes show high performance metrics, indicating the relevance of source model feature embeddings to non-avian taxa and signals of interest.

Figure A1.2: Differences in class prediction score distributions on the logit scale between source (red) and target (blue) models. Scores from the target model generally shift to lower and higher values for negative and positive samples, respectively.

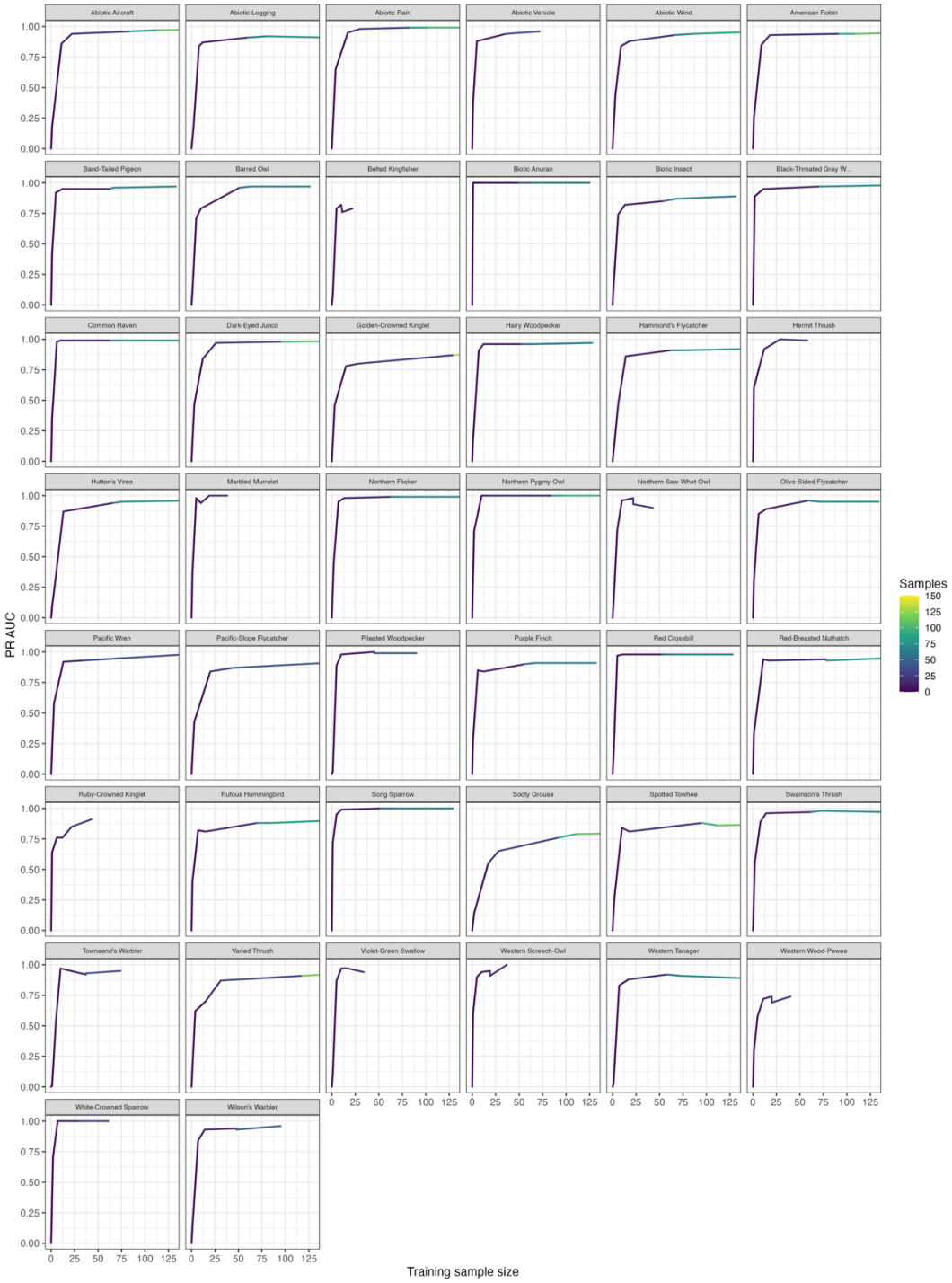

Figure A1.3: Relationships between training sample size and precision-recall AUC performance. Precision-recall AUC performance across models from the sample size experiment (N≈1,5,10,25,50,100) and the final target model (N≈125) are shown. Training sample size and model performance generally follow a positive decelerating monotonic trend.

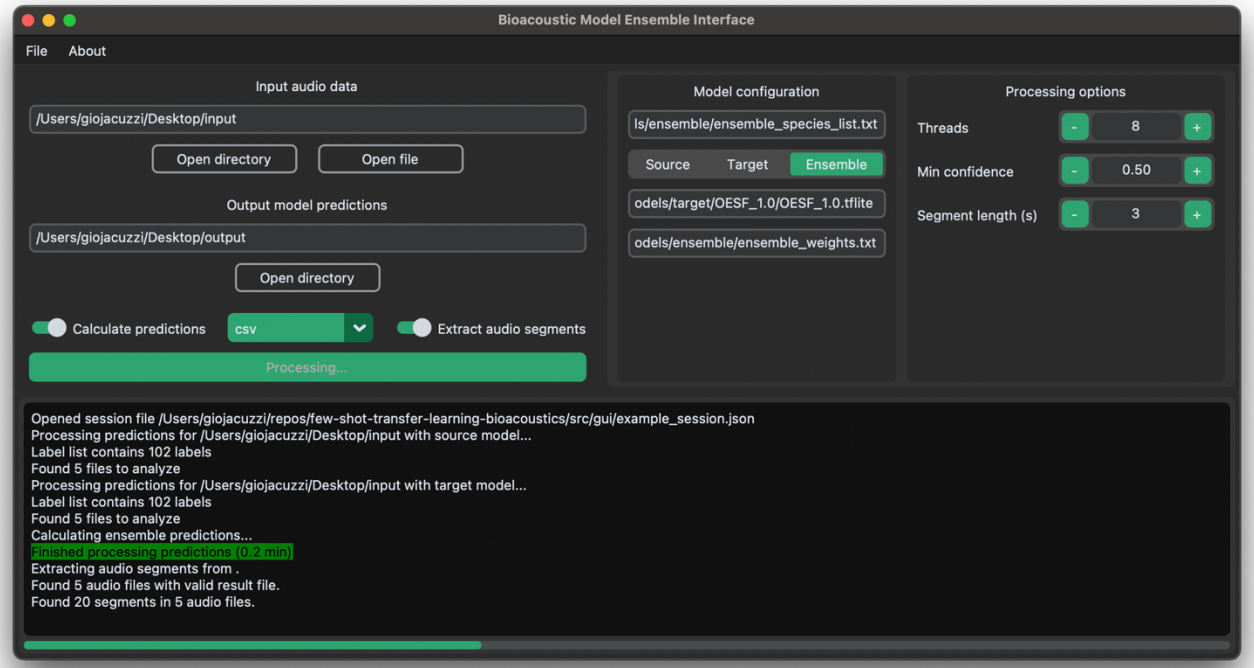

Figure A1.4: Open-source graphical user interface for processing audio data. The application can be used to generate species detection predictions with a either a source BirdNET model, a target model, or both through a model ensemble (with provided weights). Audio segments for predictions can be extracted automatically.

1.10 APPENDIX 1.2

Artist attribution: Silhouette images for wildlife species were obtained from PhyloPic (Michael Keesey, 2024, https://www.phylopic.org/) and were created by Alexandre Vong (*Diomedea exulans*), Andy Wilson (*Accipiter cooperii, Branta canadensis, Cardinalis cardinalis, Crotophaga sulcirostris, Dryocopus pileatus, Megaceryle alcyon, Turdus migratorius, Tyrannus tyrannus, Zonotrichia leucophrys*), Anthony Caravaggi (*Troglodytes troglodytes*), Campbell Fleming (*Promerops cafer*), Edwin Price (*Bubo magellanicus, Meleagris gallopavo, Pteroglossus pluricinctus, Tachycineta leucopyga*), Felix Vaux (*Rhipidura fuliginosa*), Ferran Sayol (*Accipiter, Aegotheles savesi, Corvus corax, Falco peregrinus peregrinus, Larus, Patagioenas, Rallus, Regulus regulus, Sciurus vulgaris*), Francesco "Architetto" Rollandin (Turdidae), Gabriela Palomo-Munoz (*Phasianus colchicus*), Kai Caspar (*Mergus merganser*), Margot Michaud (*Calypte anna*), Mattia Menchetti (*Apis mellifera*), Matías Muñoz (*Brachyramphus marmoratus*), Rebecca Groom (*Ardea cinerea*), Sam Jones (*Myioborus miniatus*), T. Michael Keesey (photo by Darren Swim) (*Cyanocitta cristata bromia*), Tracy A. Heath (*Canis lupus monstrabilis*), Will Booker (*Hyla versicolor*), Wynston Cooper (photo) and Albertonykus (silhouette) (*Xenicus gilviventris*), xgirouxb (*Bubo scandiacus*), and others (*Saxicola rubicola*).

Images and icons for abiotic acoustic signals and illustration were obtained from FlatIcon (Freepik Company, 2024, https://flaticon.com/) and were created by Ahmad Yafie (Plane), Indygo (Music) Fantasyou (Windy), bqlqn (Rainy), Victoruler (Forest), Andrejs Kirma (Pickup), Nuricon (Chainsaw), and Freepik (Location).

Chapter 2. AVIAN COMMUNITY RESPONSES TO FOREST SUCCESSIONAL STAGE IN A MANAGED MOSAIC LANDSCAPE

Publication history: This study was co-authored with Teodora Minkova, Lauren M. Kuehne, Daniel C. Donato, Sarah J. Converse, and Julian D. Olden. At the time this dissertation was published, this chapter was in preparation for publication.

2.1 ABSTRACT

Integrated forest management strategies aim to reconcile biodiversity conservation and timber production objectives by maintaining a landscape mosaic of productive and reserved stands across successional stages, under the assumption that habitat heterogeneity expands ecological niche availability. However, the response of bird communities to forest habitat created through management remains poorly understood, limiting our ability to anticipate how integrated forest management influences avian diversity and ecological function. We conducted four years of bioacoustic surveys (2020-2023) in the Olympic Experimental State Forest, Washington state, USA, to assess breeding bird communities in early-seral stand initiation, mid-seral stem exclusion, variable-density thinned, and mature (late-successional and old-growth) forest developmental stages.

Multi-species occupancy modeling and multivariate analyses revealed pronounced differences in habitat use probability and assemblage composition across stages driven by species turnover along a disturbance gradient. Mature and stand initiation emerged as complementary stages that contributed most to diversity, maximized the use probability of conservation priority species, and supported a broad range of ecological functions: mature supported primary cavity excavators and bark foragers, while stand initiation supported early-seral shrub and ground nesters, aerial foragers, and foliage gleaners. By contrast, stem exclusion stands contributed least to avian diversity by failing to support diverse functional niches. Variable density thinning increased species richness but did not substantially shift assemblage

composition or functional diversity toward mature forest conditions within 25 years post-harvest. Variation in local habitat structure and tree species composition strongly modulated within-stage use, underscoring potential pathways for experimental prescriptions to further integrate conservation and timber production objectives. Our results reaffirm the irreplaceable conservation value of mature primary forests and early-seral habitat, and emphasize the importance of landscape management strategies that integrate both late-successional reserves and structurally enriched managed stands.

2.2 INTRODUCTION

Forests harbor the majority of the world's terrestrial biodiversity (UN, 2020), and forest habitat conversion and degradation are primary drivers of global biodiversity decline (Grantham et al., 2020; Betts et al., 2017). Many foresters continue to meet rising global demand for wood products with intensive plantation management practices intended to optimize tree growth and harvest efficiency while consequently simplifying and homogenizing wildlife habitat (Puettmann et al., 2009). Although the resulting degradation and fragmentation of habitat is implicated as a leading cause of wildlife population declines in managed landscapes (Betts et al., 2022), market projections and renewed interests in extractive timber harvesting on previously protected lands suggest that conventional forest plantations will continue to expand globally (USA, 2025; UN, 2020; Jürgensen et al., 2014). Because biodiversity cannot be conserved effectively in protected areas alone (Maxwell et al., 2020; Loiseau et al., 2021), understanding how biological communities are influenced by integrated forestry practices that include both protected and productive areas is critical to support ecosystem integrity in managed forest landscapes.

Forest-breeding bird populations across North America have experienced precipitous declines over the past half-century, with approximately two-thirds of western forest bird species continuing to decline (North American Bird Conservation Initiative (NABCI), 2025; Rosenberg et al., 2019). In the Pacific Northwest these trends are associated with habitat loss and degradation from a legacy of unsustainable timber management converting native forests to even-aged industrial plantations (DeMeo et al., 2018). Today, forests cover roughly half of Washington and Oregon's land area, the majority being unreserved and susceptible to harvest

(Oswalt et al., 2019), with coniferous monoculture plantations and frequent harvest rotations producing forests much younger and simpler in habitat structure than those generated under natural disturbance regimes (Franklin et al., 2002; Hagar, 2007). The disruption of these regimes, which once maintained a landscape of mixed coniferous and broadleaf forests across early- and late-successional stages, has reduced biological complexity and contributed to observed bird declines of both old-forest and early-seral associates (Phalan et al., 2019; NABCI, 2025). These declines threaten the integrity of ecosystem functions and services provided by birds (Spies et al., 2018; Cushman & McGarigal, 2003), including forest regeneration through seed dispersal and pollination, regulation of insect pests through insectivory, ecosystem engineering through cavity excavation, and contribution to nutrient cycling processes (Whelan et al., 2015; Sekercioglu, 2006; Sekercioglu et al., 2004).

Forestry directly influences avian community assembly by manipulating environmental conditions relevant to ecological niche requirements both within a forest stand and across the landscape (Sallabanks & Arnett, 2005; Cody, 1985; Burivalova et al., 2015; Wells et al., 2012). Habitat selection by birds is generally considered a hierarchical process operating at multiple spatial scales, from a species' biogeographic range to microhabitat used for nesting or foraging (Battin & Lawler, 2006. Cushman & McGarigal, 2004; Wiens, 1989a). Fine-scale vegetation changes alter the composition of local foraging resources (small vertebrates, invertebrates, fruit, and nectar) alongside structural features required for perching and nesting (Sallabanks & Arnett, 2005; Wiens, 1989b). These proximate factors alter local avian assemblage composition and directly influence food availability and breeding success, mechanisms that can ultimately determine the health and viability of avian populations (Martin, 1995; Cody, 1985). Across forested landscapes, topography and the broad-scale composition, configuration, and connectivity of forest stands influence the dispersal of individuals and the assembly of regional avian communities (McGarigal & McComb, 1995; Turner & Gardner, 2015; Wiens, 1989b).

Deficits of critical old-growth and late-successional habitat resulting from unsustainable timber harvest in the Pacific Northwest have severely threatened the persistence of species such as the northern spotted owl, *Strix occidentalis caurina*, and marbled murrelet, *Brachyramphus marmoratus* (Thomas et al., 1990; FEMAT, 1993). The impending threat of extirpation and concurrent societal shifts in priorities for forest ecosystems culminated in the passage of the Northwest Forest Plan in 1994, a sweeping restructuring of federal land management to halt

clearcutting and protect threatened species by establishing late-successional reserves and expanding restorative forestry practices while also contributing to economic sustainability in the region (Thomas et al., 2006; Raphael, 2006). This transformation to integrated forest management coincided with the emergence of "ecological forestry," a suite of novel conservation and silvicultural strategies that attempts to reconcile ecological and production objectives by developing habitat heterogeneity at both the stand and landscape scales (Franklin et al., 2018).

Within a forest stand, increasing structural complexity is expected to expand resource variety and support a diversity of ecological niches, promoting species richness (alpha diversity) and ecological function (Franklin et al., 2002; Lindenmayer et al., 2006). Silvicultural prescriptions more closely resembling natural disturbance regimes, such as the retention of old live trees, snags, and woody debris, are critical to mitigate declines in richness and abundance following harvest (Franklin & Donato, 2020; Price et al., 2020; Donato et al., 2012). Variable density thinning can accelerate the development of mature vegetation structure in plantation stands, restoring habitat heterogeneity and enhancing richness (Carey, 2003; Hagar et al., 2004; Cahall et al., 2013; Thomas et al., 2006) while also providing commercial harvest and promoting merchantable tree growth. Recognizing that no single silvicultural strategy can provide suitable habitat for all species (Hansen et al., 1995; Chambers et al., 1999), ecological forestry at the landscape scale attempts to integrate conservation and economic production by maintaining a portfolio of unmanaged reserves and managed stands subjected to harvest (Franklin et al., 2018; Lindenmayer & Franklin, 2002). Inspired by the habitat heterogeneity and intermediate disturbance hypotheses (MacArthur & MacArthur, 1961; Connell, 1978), this shifting mosaic of successional stages is expected to promote a diversity of distinct assemblages through species turnover (beta diversity; Duflot et al., 2022; Franklin et al., 2018; Legendre, 2014), supporting birds ranging from fast-colonizing early-seral migrants to native old-forest obligates (Swanson et al., 2014; Cushman & McGarigal, 2003; Ruggiero et al., 1991).

Integrated forest management practitioners have increasingly employed ecological forestry methods in an attempt to reconcile biodiversity conservation and ecosystem service (e.g., timber production) objectives by managing for a diversity of forest developmental stages and structures across the landscape (Franklin & Johnson, 2012). For example, the Olympic Experimental State Forest is managed by the Washington State Department of Natural Resources under the assumption that "landscapes managed for a fairly even apportionment of forest cover

among stands in all stages of development, from stand initiation to old growth, will support desirable levels of both commodities and ecosystem functions" (Figure 2.1; WADNR 1997). Yet despite the designation of late-successional reserves and increasing adoption of integrated forest management following the passage of the Northwest Forest Plan, conservation challenges persist as populations of avian species associated with both old and early-seral forest continue to decline in the region (Phalan et al., 2019; NABCI, 2025; Rosenberg et al., 2019). Production of timber remains a leading objective for state and federal forests, and the primary focus of private industrial forest lands, and a central but unproven assumption underpinning this management strategy is that it is possible to produce economic value through timber harvest while simultaneously providing habitat with sufficient ecological function for particular species of conservation priority (Betts et al., 2021; Stokely et al., 2021; WADNR, 1997). Although the broad habitat associations of forest birds in the region are mostly known (Carey, 2003; Ruggiero et al., 1991; Mannan, 1980), their response to habitat structure created through management is not (Sallabanks & Arnett, 2005; Nott et al., 2005). Uncertainties remain regarding the relative conservation value and ecological function of the developmental stages that constitute managed forest landscapes (Arcilla & Strazds, 2023).

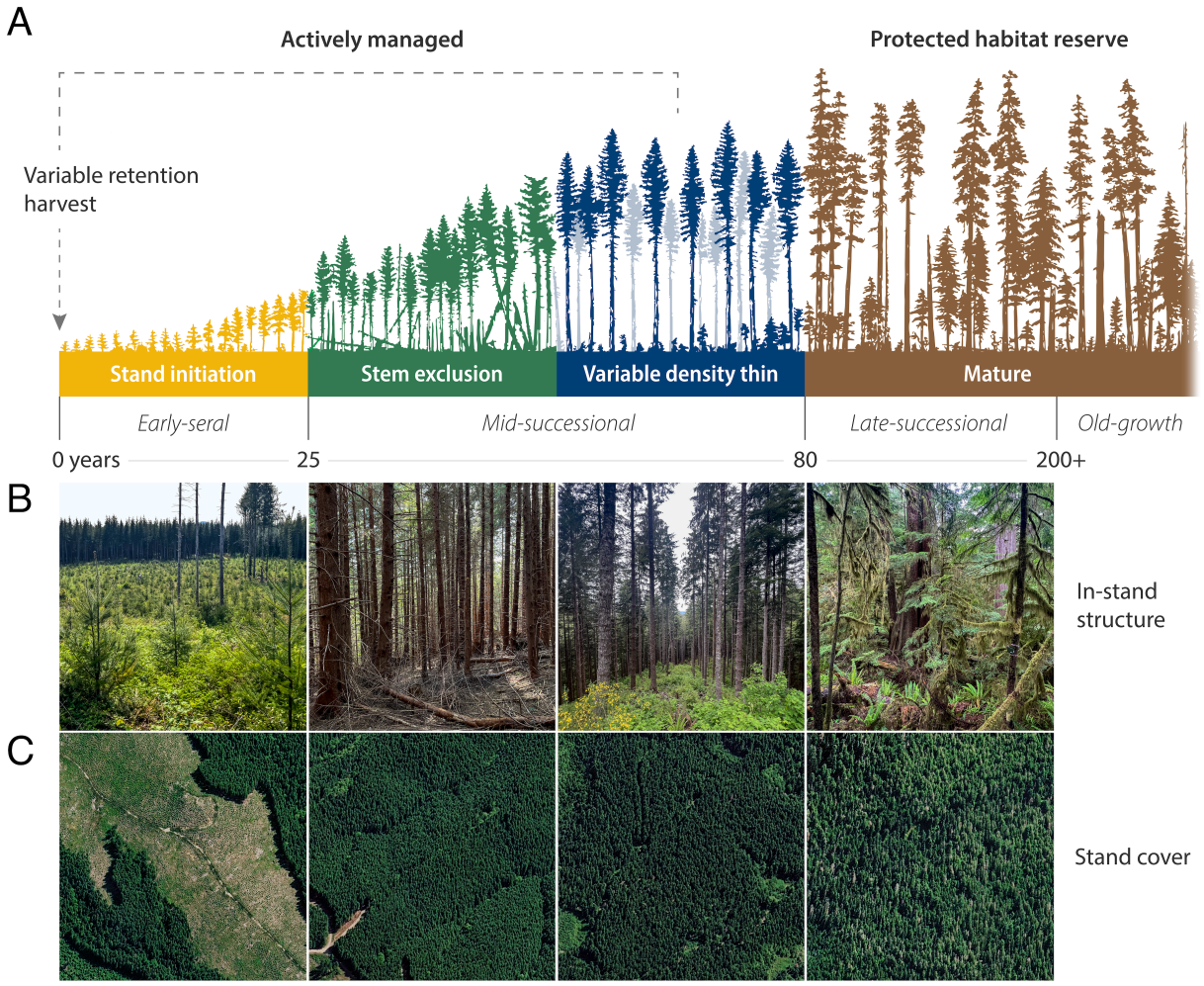

Figure 2.1: Forest developmental stages maintained by integrated forest management in the Olympic Experimental State Forest, Washington, USA. Stages are stratified by stand age, representing a gradient of successional progression (A): stand initiation following variable retention harvest, stem exclusion, variable density thinning, and mature protected habitat reserve, including late-successional and old-growth forest. Examples of in-stand structure (B) and forest cover from satellite imagery (C) for each developmental stage.

Previous investigations of avian responses to managed habitat have been limited in spatiotemporal scale and taxonomic and functional scope. Studies at landscape scales are rare due to a lack of broad-scale forest inventory data at fine spatiotemporal resolutions relevant to individual species (Betts et al., 2022; Sallabanks & Arnett, 2005), and traditional point-count surveys and habitat assessments are costly and labor-intensive, often constraining replicates in space and time (Ruggiero et al., 1991; Hansen et al., 1995). This can reduce statistical power and the probability of rare species detection, biasing estimates of species richness and composition

(Bryant et al., 1993) and failing to capture long-term responses to common silvicultural prescriptions such as variable density thinning (Willis et al., 2018; Cahall et al., 2013). Research has also tended to focus on a small number of threatened focal species or common diurnal species (Akresh et al., 2023; Sallabanks et al., 2000; Marzluff et al., 2000), overlooking species not listed at the federal or state levels that can have disproportionately influential roles in ecosystem functioning (Basile, 2022), and obscuring community- and guild-level responses (Martins et al., 2025).

Critically, taxonomic richness and composition metrics alone may be insufficient to detect consequential changes in diversity and ecosystem functioning under forest management (Hillebrand et al., 2017; Burivalova et al., 2015; Cadotte, 2011), as silvicultural prescriptions can maintain species richness while reducing functional diversity (Ibarra et al., 2017), compromising the resilience of forest ecosystem functions. Because birds exhibit highly variable and species-specific relationships with forest structure, responses of functional guilds are recognized as valuable lenses through which to examine the ecological underpinnings of niche differentiation and community assembly (Mason et al., 2005) and reveal broader effects of management on ecosystem function and trophic structure (Sallabanks & Arnett, 2005; Sekercioglu, 2006; Sekercioglu et al., 2004; Simberloff, 1991). Therefore, understanding how managed forest conditions influence functional diversity as well as species loss (alpha diversity) and turnover (beta diversity), is critical to support managers working to ensure ecosystem integrity amid ongoing population declines (Socolar et al., 2016; Jones et al., 2022).

Recent technological and methodological advances present novel opportunities to address these challenges. Passive acoustic monitoring has emerged as an effective method for non-invasive avian surveys across large spatiotemporal and taxonomic scales (Shonfield & Bayne, 2017), improving detection probability and sample size relative to traditional point-count methods (Darras et al., 2018), and is particularly well-suited to forest environments where most detections rely on auditory cues (Brewster & Simons, 2009). Combined with machine learning algorithms for automated species identification, this approach can vastly increase survey replicates and improve precision of occupancy and diversity estimates (Jacuzzi & Olden, 2025; Martins et al., 2025; Cole et al., 2022). Complementary advances in remote sensing now provide fine-resolution measurements of forest structure across entire landscapes (NAIP, 2026; Hansen et

al., 2013), while multi-species occupancy models enable rigorous community-level inference with direct implications for management (Sauer et al., 2012; Zipkin et al., 2010).

In this study, we aim to leverage these advances to quantify avian community responses to integrated forest management in the Olympic Experimental State Forest, a successional mosaic landscape in Washington, USA. We compare habitat use at community, guild, and species levels across stands stratified by four developmental stages: stand initiation, stem exclusion, variable density thinned, and mature forest deferred from harvest (Figure 2.1), with particular focus on species of conservation priority (defined as listed threatened, endangered, and candidate species at the state or federal level, as well as common birds in steep decline identified by the North American Bird Conservation Initiative). Under the hypothesis that maintaining a greater diversity of structurally complex forest developmental stages across the landscape results in greater taxonomic and functional biodiversity and fewer losses of conservation priority species, we predict that:

1. *Avian species composition will vary across forest stages*, such that beta diversity will be driven by species turnover rather than nestedness, and thinned assemblages will be more similar to mature than to stem exclusion assemblages.
2. *Nesting microhabitat and foraging substrate guild membership will predict species-level habitat use probability*, such that guild-level differences in mean habitat use will vary by stage according to the structural features each stage provides.
3. *Stages will differ in conservation value*, such that stand initiation and mature stages will have the greatest habitat use among species of conservation priority, while stem exclusion forest will have the least.
4. *Greater structural complexity and tree species diversity will promote increased community-level habitat use within each stage*.

2.3 METHODS

2.3.1 Study area and site selection

The study took place in the Olympic Experimental State Forest (OESF) in Washington, USA (Figure 2.2A). The OESF is a 270,000-acre (1090 km^2) working forest consisting of state trust lands administered by the Washington State Department of Natural Resources (WADNR), located on the western Olympic Peninsula adjacent to the Olympic National Park, Olympic National Forest, and Quinault Indian Nation. Residing in the temperate rainforest zone of the Coast Range ecoregion, the regional maritime climate produces abundant precipitation (203 to 355 cm per year) and a long growing season, resulting in a highly productive environment with rapid growth rates (1.2 meters per year for young trees). Common tree species include western hemlock (*Tsuga heterophylla*), Douglas-fir (*Pseudotsuga menziesii*), and Sitka spruce (*Picea sitchensis*). Elevation ranges from 60 to 1,155 meters, with red alder (*Alnus rubra*) and western redcedar (*Thuja plicata*) growing in wetter areas at lower elevations, and Pacific silver fir (*Abies amabilis*) at higher elevations.

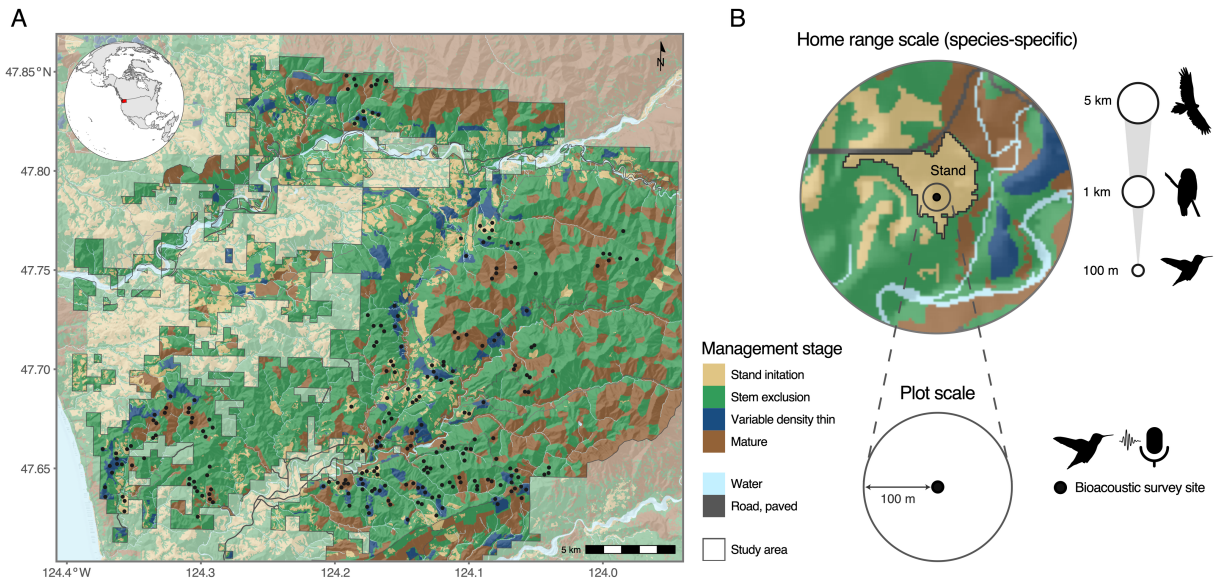

Figure 2.2: Forest habitat and bioacoustic survey methodology to quantify avian community responses to integrated forest management. 224 site locations across the study area within the Olympic Experimental State Forest were sampled across stands of each management developmental stage (A). At each site an autonomous recording unit performed bioacoustic surveys for avian occurrence and measurements of environmental variables were taken at three spatial scales (B), the 100 m radius plot scale, the stand scale, and the species-specific home range scale.

Approximately 1% of timberland within the OESF is harvested annually through a combination of sustainable regeneration harvest and commercial thinning. WADNR has a legal obligation to manage state trust lands to generate revenue for beneficiaries (e.g., counties, public schools), primarily through timber sales, while also complying with state laws and the federal Endangered Species Act. The WADNR Habitat Conservation Plan calls for an adaptive management approach for state lands (WADNR, 1997), with research and monitoring focused in the OESF to formally address uncertainties in forest management practices and continually incorporate findings to improve the management strategy. The present study is nested within a broader management experiment conducted by WADNR with the objective to develop silvicultural practices and watershed management approaches that maximize both environmental and economic outcomes in working forests (Minkova et al., 2024). The study area comprises five administrative units (Copper Mine, Kalaloch, Queets, Upper Clearwater, and Willy Huel), encompassing roughly 170,000 acres (686 km^2) in total.

WADNR maintains a patchwork of forest stands varying in succession across the OESF (Figure 2.2A), which we stratified by four developmental stages (Oliver, 1980; Powell, 2012): stand initiation, stem exclusion, stands subjected to variable density thinning within the last 25 years, and mature (including both late-successional and old-growth forest substages). This classification includes three managed second-growth stages that originated from silviculture prescriptions, i.e., the active planting or tending of trees after a harvest disturbance, and one unmanaged primary forest stage deferred from harvest (mature). Measurements characterizing within-stand habitat conditions are provided in Figure A2.1 and described in detail under "Multi-scale environmental predictors". Together, these stages provide a representative gradient of forest conditions and dynamics, as maintained by management, across both reserved and unreserved areas (Figure 2.1).

Stand initiation patches are early-seral plantation habitats ranging from 1-24 years in age post-harvest, comprising 8% of the study area. Variable retention harvest maintains riparian zones and a small number of trees as biological legacies (Franklin & Donato, 2020), resulting in irregularly-shaped patches with high edge contrast. Planted western hemlock and Douglas fir trees are actively tended and competing vegetation suppressed with herbicide. Habitat is characterized by small conifers alongside broadleaf red alder pioneers, abundant early-seral shrubs and herbs, very few snags, and little downed wood. *Stem exclusion* patches are mid-successional habitats ranging from 25-79 years in age, comprising 60% the landscape due to extensive clearcut logging in the 1970s-80s. Conifers dominate as even-aged trees compete strongly for light in increasingly narrow growing spaces, and canopy closure suppresses understory vegetation and red alder persistence while producing the highest density of merchantable trees and snags among all stages. *Variable density thinning* is frequently applied to second-growth stands between 40-55 years in age to accelerate the development of mature forest habitat and restore structural diversity that would otherwise take decades to develop (Thomas et al., 2006; Carey, 2003). Selective harvesting to form gaps reintroduces light and space, promotes understory reinitiation, and redistributes growth to trees of highest conservation or production value. Thinned stands are subsequently either commercially harvested roughly 20 years following treatment or deferred from harvest for development as mature forest habitat. Variable retention harvest typically occurs at the stem exclusion and thinned stages of development, resetting a forest patch to the stand initiation stage and representing a conventional short rotation

age of 40-50 years. Patches reserved as protected habitat progress to the *mature* stage, encompassing both late-successional and old-growth forest (roughly 10% and 12% of the study area, respectively). Late-successional habitats are at least 80 years in age, regenerated naturally after a severe 1921 windstorm on the Olympic Peninsula. Self-thinning promotes the development of understory vegetation and increases vertical heterogeneity. Old-growth stands at least 200 years in age once dominated the landscape and are now deferred permanently from harvest as protected species habitat. These remnant primary forest patches host a diversity of live and dead structural features and tree species, including Pacific silver fir and western redcedar. Collectively, mature forest habitat is characterized by high snag density and the greatest downed wood volume, largest trees, and greatest variation in tree height among developmental stages, reflecting structural complexity.

We divided the study area into 16 watersheds, each encompassing multiple forest stands at varying developmental stages ranging from 2.2 to 10.8 km^2 in size. Passive acoustic recordings were made with autonomous recording units (ARUs) throughout the breeding season (April-August) of 2020-2023 at 224 sites distributed among stand initiation (n = 34), stem exclusion (83), variable density thinned (51), and mature (56) stands, with mature sites including both late-successional (31) and old-growth (25) forest (Figure 2.2, Table A2.1). Each site was defined as a 100-m radius plot centered on a Songmeter SM4 or SM Mini ARU (installed on a marked tree at breast height; Wildlife Acoustics Inc.), representing both local habitat conditions and the ARU's effective detection range (Kuehne et al., 2019). Within each watershed, up to four stands per habitat type were randomly selected, with up to four sites randomly distributed within each stand, subject to minimum buffers from other sites (250 m), edges and paved roads (100 m), and streams (60 m). Not all watersheds contained all developmental stages or sufficient contiguous area for four independent sites, so sites were distributed across stands as necessary and totals varied by watershed. ARUs recorded continuously at 32 kHz for 10-day deployment periods with two-day intervals for retrieval and redeployment. Limitations in available personnel precluded annual surveys of all sites, and a small number of survey days were missed due to equipment malfunction or site inaccessibility.

2.3.2 Bioacoustic species detection

Acoustic survey data were processed with an ensemble of convolutional neural networks trained on data from the study area to enable robust acoustic monitoring of wildlife communities at the landscape scale (Jacuzzi & Olden 2025). This classifier leverages a pre-trained BirdNET model (version 2.4; Kahl et al., 2021) with transfer learning to greatly improve the probability of individual species detection and estimation of species richness across heterogeneous forest conditions, achieving a mean precision-recall AUC of 0.94. Detection predictions were produced for 95 species comprising the regional species pool, based on historical observations from the study area and the Cornell Laboratory's eBird regional occurrence database (Fink et al., 2025). We applied the classifier with default analysis parameters, generating continuous prediction scores at 3-second intervals for each species.

Given that the predictions resulting from the classifier encompassed over 93,000 hours of acoustic data, far exceeding feasibility for manual review for true detections, we used Platt scaling (Platt, 1999) to calibrate prediction scores to true positive probabilities following Wood and Kahl (2024). This method fits a species-specific logistic regression model to a manually validated dataset of positive and negative examples, relating a score value *s* to the probability that a prediction is a true positive detection, such that $logit(p) = \ln\left(\frac{p}{1-p}\right) = \beta_0 + \beta_{\text{score}} * s$, which, for a given probability *p*, can be solved for the associated threshold *t*, as in $t = \frac{\ln\left(\frac{p}{1-p}\right) - \beta_0}{\beta_{\text{score}}}$.

The validation dataset was assembled by aurally and visually reviewing spectrograms of randomly selected predictions for each species across the full score range with Raven Pro (version 1.6; K. Lisa Yang Center for Conservation Bioacoustics, 2024), until at least 100 positive examples were obtained (the total number of detections validated per species ranged from 3194 to 3580). Species-specific probability thresholds were then derived by fitting logistic regression models to these validation data, subject to a minimum threshold of 0.5 representing the classifier's decision boundary between putative true-positive and false-positive detections. Only predictions with a true positive probability exceeding 95% were retained as detections. As species chosen for automated detection at this threshold exhibited extremely high classifier specificity (mean precision 0.99), this is likely an underestimate of the effective true positive rate. Additionally, strong species sensitivity (mean recall 0.67) suggests that false negative rates are sufficient to support automated detection. For species of exceptional conservation priority or

with insufficient validation data or performance to support automated detection, predictions with scores above 0.5 were exhaustively manually reviewed (Table A2.2). The resulting presence-absence data represented putative detection histories for each species across all sites, surveys, and years.

2.3.3 Multi-scale environmental predictors

The spatial scales at which forest management operates, and birds interact with forest habitat, informed the scales of our investigation. Avian occurrence may be driven by a combination of habitat characteristics at local, neighborhood, and landscape scales (Galitsky & Lawler, 2015; Cushman & McGarigal, 2004; Wiens 1989a). Most small birds appear to distinguish habitats by their structural characteristics (Cody, 1985), while larger birds can be influenced more by habitat area and landscape context (Thornton & Fletcher, 2014). As such, we consider the environment of the study area as hierarchically organized at three spatial scales — plot, stand, and home range— such that the home range may contain multiple stands, and a stand contains one or more plots (Figure 2.2B).

We define a *plot* as the environment within the fixed 100-m radius site buffer containing an ARU at its center. A plot serves as the finest spatial grain of measurement, reflecting local habitat characteristics that can be directly manipulated by management, and corresponds roughly to the ARU's effective detection range and the home range size of most passerines in the study region (Kuehne et al., 2019; Billerman et al., 2026; Brown, 1985). We define a *stand* as a contiguous discrete area (i.e. patch) of the same forest developmental stage maintained by management, reflecting conditions across a single management unit. Riparian management zones for rivers and perennial fish-bearing streams were treated as stand boundaries as they support distinct riparian vegetation constituting different habitat, while non-fish-bearing and intermittent streams were not. We also recognized paved roads as stand boundaries but excluded unpaved roads because we expected them to appear to birds as gaps in the forest, being narrow (roughly 3 m wide) and rarely driven.

For each site, we defined a *home range* scale as a species-specific fixed radius area centered on the site that represents broader conditions in the surrounding forest landscape, or “neighborhood,” that a species is expected to interact with (Addicott et al., 1987). The spatial scale at which birds perceive and interact with surrounding habitat is correlated with dispersal

ability, in which morphological traits such as body mass and hand-wing index can serve as a species-level proxy (Thornton & Fletcher 2014; Claramunt, 2021). To account for scarce direct estimates of species-specific dispersal distances, we related measurements of these traits from the AVONET trait database (Tobias et al., 2022) to existing documented home range sizes within the region (Billerman et al., 2026; Brown, 1985), excluding the Marbled Murrelet as an outlier with an unusually large home range from a combination of mature forest nesting and marine foraging behaviors (Meyer et al., 2002). We modeled home range radius as a function of log-transformed body mass and hand-wing index using a generalized linear model with a gamma error distribution and log link to account for the positive and right-skewed response variable (n = 23). The best-supported model via AIC_c included body mass as the sole predictor (pseudo-R^2 = 0.72; Table A2.4). We used this model to predict unknown species-specific home range sizes (Figure A2.2), subject to a minimum radius of 100 m corresponding to the local plot scale.

We identified a suite of candidate environmental predictors of habitat use (Table A2.3) from a literature review of forest bird habitat relationships. To characterize local habitat conditions associated with each stage and establish ground-truthed field measurements for validation against remotely-sensed data, we measured habitat elements at the plot scale for a random sample of 141 sites across developmental stages (Figure A2.1). These variables included basal area, quadratic mean diameter, and stem density across multiple tree size classes; tree species composition; canopy closure, lift and height; the amount of standing snags and down dead wood; and understory composition, height, and cover. The full site habitat sampling protocol can be found in Minkova et al., (2020).

To quantify forest conditions at the plot, stand, and home range scales we obtained topographic and vegetation data layers from the WADNR Remotely Sensed Forest Resource Inventory System (WADNR, 2026). These data are derived from light detection and ranging (LiDAR) and digital aerial photogrammetry, and include raster layers at approximately 20 m resolution. We excluded layers having poor agreement (Pearson's $r < 0.6$) with field measurements within the study area or from previous validation efforts across state forest lands (Ricklefs, 2026). To account for variation in habitat structure and landscape composition over time due to management activities and succession, all variables were calculated at time steps corresponding to the most recently available biennial remote sensing data.

At the plot scale we calculated basal area, quadratic mean diameter, and stem density (mean and coefficient of variation); hardwood composition; canopy closure and height; and standing snag and down dead wood volume. We classified stands by developmental stage using field inspection, management history, and tree core inventories where available, and calculated stand area and core area (stand area minus a 50-m edge buffer; Kremsater & Bunnell, 1999). For unmeasured stands or those outside WADNR ownership, developmental stage was inferred from stand age estimated as a function of height and climate relationships (Ricklefs, 2026). At each species-specific home range scale, we characterized landscape composition and configuration by the proportional abundance of each forest developmental stage, the aggregation index, shape index, and tree height-weighted edge density (Ene & McGarigal, 2023). Additional contextual variables included elevation, distance to stand edge, distance to the nearest paved road, and distance to the nearest perennial fish-bearing stream.

Cross-scale correlations arising from spatial autocorrelation between environmental variables at different scales can obscure habitat associations (Battin & Lawler, 2006). We explored variation and collinearity among candidate variables, excluding those with little (i.e., uniform) variation among sites and selecting from among highly correlated variables (Pearson's $r > 0.8$) to facilitate interpretability and relevance to avian habitat features commonly manipulated by management. At the plot scale, basal area, quadratic mean diameter, and tree density were strongly correlated across size classes, and we constrained all three to trees ≥ 15 cm diameter at breast height to represent merchantable timber targeted by silvicultural prescriptions. Tree density was strongly correlated with canopy cover, quadratic mean diameter with height, and basal area with all except tree density. As tree number, size, and species composition are fundamental aspects of stand structure manipulated by management (Sallabanks & Arnett, 2005; Hansen et al., 1995), we retained tree density, quadratic mean diameter, and hardwood proportion as plot-scale predictors.

Across home range scales, the proportion of stem exclusion forest was strongly correlated with the proportions of stand initiation and variable-density thinned forest, reflecting proportional replacement within a stem exclusion-dominated landscape. Stand initiation forest was strongly correlated with edge density, reflecting the fragmented and irregularly shaped patches produced by variable retention harvest. Aggregation and shape indices were additionally correlated with stage proportions at the extremes of home range size (e.g., passerines, birds of

prey), such that smaller extents yield more homogenous stage distributions that inflate aggregation, while larger extents capture greater landscape heterogeneity, confounding configuration metrics with spatial scale. We ultimately retained the following as the most parsimonious habitat predictors for subsequent modeling: proportion of stand initiation, thinned, and mature forest (home range scale); tree density, quadratic mean diameter, and hardwood proportion (plot scale); and elevation, distance to the nearest paved road, and distance to the nearest perennial fish-bearing stream. Variance inflation factors confirmed negligible cross-scale multicollinearity (VIF < 5).

2.3.4 Functional guilds

Because birds exhibit highly variable species-specific relationships with forestry, guild-level responses offer a valuable lens for quantifying niche differentiation and revealing broader effects on ecosystem function (Sallabanks & Arnett, 2005; Simberloff & Dayan, 1991). To investigate variation in responses across functional groups within the broader avian community, we categorized species by two functional groupings—nesting microhabitat and foraging substrate—as informed by AVONET (Tobias et al., 2022) and literature reviews from the Birds of the World database (Billerman et al., 2026). The nesting microhabitat grouping comprises five individual guilds—primary cavity excavators, secondary cavity, tree, shrub, and ground nesters—representing the diversity of nesting microhabitats provided by forest structural features. The foraging substrate grouping comprises four guilds—aerial foragers, bark foragers, foliage gleaners, and ground foragers—reflecting the range of substrates through which birds acquire food. Guilds within groupings with low membership ($n < 3$) resulting in high posterior uncertainty were excluded from analysis.

2.3.5 Multi-species occupancy modeling

To estimate effects of forest conditions on species- and guild-specific habitat use we developed a series of multi-species occupancy models (MSOM). Each MSOM is a Bayesian hierarchical model that accounts for the imperfect detection of species by explicitly modeling both a latent biological occurrence process and an observational detection process (Royle & Dorazio, 2005; MacKenzie et al., 2002), while treating species-specific occurrence and detection parameters as random effects linked across functional guilds through guild-specific distributions. Compared to a traditional single-species occupancy model, this increases precision of parameter estimates

through the "borrowing" of information across multiple species within a shared community hierarchy, improving inferences for rare or elusive species with limited observational data and extending inference to the guild and community levels. This also enables the robust estimation of species richness and composition (Royle & Dorazio, 2005), and offers a practical framework for predicting the effect of management scenarios on ecological communities (Sauer et al., 2012; Zipkin et al., 2010).

We developed a unique MSOM for each functional grouping (nesting microhabitat and foraging substrate), as well as a community grouping including all species, following Pacifici et al., (2014). The occurrence of species *i* at site *j* during season *t* is modeled as a Bernoulli random variable z_{ijt} with probability of presence ψ_{ijt}. Detection or nondetection of a species at a site during survey *k* is similarly treated as a Bernoulli random variable y_{ijkt}. When a species is present ($z_{ijt} = 1$), it is detected during a survey with probability p_{ijkt}. When absent ($z_{ijt} = 0$), detection probability is assumed to be zero. An observed detection history is then conditional on species presence through the product $z_{ijt}\, p_{ijkt}$, such that $y_{ijkt} \mid z_{ijt} \sim \text{Bernoulli}(z_{ijt}\, p_{ijkt})$. The ecological occurrence state process is modeled as:

(1)

$$\begin{aligned} logit(\psi_{ijt}) = {} & u_i + \alpha_{1,i} * \text{Initiation}_{ijt} + \alpha_{2,i} * \text{Thinned}_{ijt} + \alpha_{3,i} * \text{Mature}_{ijt} + \alpha_{4,s[j]i} \\ & * \text{Density}_{jt} + \alpha_{5,s[j]i} * \text{QMD}_{jt} + \alpha_{6,s[j]i} * \text{Hardwood}_{jt} + \alpha_{7,i} * \text{Elevation}_j + \alpha_{8,i} \\ & * \text{Road}_j + \alpha_{9,i} * \text{Stream}_j + \alpha_{10,i} * \text{Year}_t \end{aligned}$$

$$u_i \sim \text{Normal}\left(\mu^{(u)}_{g[i]}, \sigma^{(u)}_{g[i]}\right)$$

$$\alpha_{a,i} \sim \text{Normal}\left(\mu^{(\alpha)}_{a,g[i]}, \sigma^{(\alpha)}_{a,g[i]}\right), a = 1, \ldots, 10$$

where $s[j]$ is the numerically-encoded forest developmental stage of site *j* and $g[i]$ is the guild membership of species *i* under the functional grouping of the model. u_i is a species-specific occurrence intercept drawn from a guild-specific normal distribution with mean $\mu^{(u)}_{g[i]}$ and standard deviation $\sigma^{(u)}_{g[i]}$. Species-specific occurrence coefficients $\alpha_{a,i}$ are likewise modeled as guild-level random effects, corresponding to home range-scale continuous proportion of stand initiation, variable density thinned, and mature forest ($\alpha = 1,2,3$), treating stem exclusion as the

implicit reference condition representing the background landscape; plot-scale and stage-specific effects of tree density, quadratic mean diameter (QMD), and proportion of hardwood species (α = 4,5,6); and elevation, distance to the nearest paved road, distance to the nearest stream, and year (α = 7,8,9,10). Because we anticipate trends in occurrence for several species to change over time due to ongoing increases and declines in local populations (e.g., Marbled Murrelet, Barred Owl; Lorenz et al., 2021; Dugger et al., 2015), we modeled a linear effect of year as a continuous covariate. All covariates were *Z*-scored prior to model fitting.

Covariates influencing species detectability were also obtained for each survey day at each site from the Daymet surface weather model (Thornton & Devarakonda, 2026), including maximum temperature (ºC) and amount of precipitation (mm). The observation process is modeled as:

(2)

$$logit(p_{ijkt}) = v_{i,s[j]} + \beta_{1,i} * \text{Temperature}_{jkt} + \beta_{2,i} * \text{Precipitation}_{jkt} + \beta_{3,i} * \text{Day}_{jkt} + \beta_{4,i} * \text{Day}^2_{jkt}$$

$$v_{i,s[j]} \sim \text{Normal}\left(\mu^{(v)}_{g[i]}, \sigma^{(v)}_{g[i]}\right)$$

$$\beta_{b,i} \sim \text{Normal}\left(\mu^{(\beta)}_{b,g[i]}, \sigma^{(\beta)}_{b,g[i]}\right), b = 1, \ldots, 4$$

where $v_{i,s[j]}$ and $\beta_{b,i}$ are species-level random effects drawn from guild-specific distributions, with coefficients corresponding to (*Z*-scored) temperature, precipitation, and a quadratic effect of ordinal date to capture seasonal variation in detection probability.

We assigned weakly informative normal(0, 2.25^2) hyperpriors on the logit scale to the guild-level means of all occurrence and detection parameters and associated covariate effects, following Broms et al., (2016) and Northrup and Gerber (2018). For the corresponding guild-level standard deviations we specified half-Cauchy(0, 2.25) hyperpriors on the logit scale. Prior to model fitting, all variables were standardized to have a mean of zero and unit variance. We performed our Bayesian analysis using Markov chain Monte Carlo with JAGS (Plummer, 2023), and processed results through jagsUI (Kellner & Meredith, 2026). Convergence was assessed through Gelman-Rubin diagnostics and visual inspection of chain histories, and model fit was

evaluated using deviance-based posterior predictive checks (Broms et al., 2016). Full model specifications and MCMC configurations are provided in Appendix 2.2.

Most passerines and small birds within the region exhibit home range sizes comparable to the effective detection area of an ARU (Billerman et al., 2026; Brown, 1985) and could therefore be interpreted as occupying a site. However, many other species regularly move beyond this spatial extent, violating the assumption of site closure to changes in occupancy between surveys. We relax this requirement by assuming random movement into and out of the site (MacKenzie & Royle, 2005) but therefore interpret our models as estimating the probability of a site being used by species during the breeding season, rather than occupied.

2.3.6 Avian conservation value of developmental stages

We compared differences in habitat suitability for species and groups of conservation priority between developmental stages using marginal use probabilities under a range of environmental conditions within the species-specific home range scale. We defined a group of regional "conservation priority species" including listed threatened, endangered, and candidate species at the state or federal level, as well as common birds in steep decline identified by the North American Bird Conservation Initiative as experiencing accelerating short-term losses or having declined continentally by an estimated 50% or more since 1970 (NABCI, 2025; Partners in Flight (PIF), 2026). We also explored responses for biological associates of early-seral and old-forest habitat, respectively, as two additional groups of conservation and management interest (Phalan et al., 2019; Sallabanks & Arnett, 2005).

We compared expected group richness across stages under scenarios in which the stage comprised 100% of the home range, holding plot-scale habitat parameters at their stage-specific means and all remaining parameters at their overall means. We estimated posterior expected richness per group as the sum of predicted habitat use probabilities for all member species of group g, such that $R_g = \Sigma_{i \in g} \psi_i$.

We further explored marginal habitat use responses across a simulated gradient of forest developmental stage composition to predict how species-specific use probability is expected to change as the home range shifts from one stage to the other. For each pair of adjacent developmental stages (stand initiation to competitive exclusion, competitive exclusion to thinned, and thinned to mature), we varied home range composition from 0 to 100% in equal

increments, respectively. At each increment along the gradient we calculated a weighted average of use probabilities under each stage weighted by the proportion of the home range containing that stage, holding plot-scale habitat parameters at their stage-specific means and all remaining parameters at their overall means. The resulting gradient identified stages that maximize or minimize predicted habitat use probability for each conservation priority species. While this approach simulates changes in use as a function of spatial variation within the home range, it is analogous to changes from the replacement of habitat over time to succession and management intervention: the progression of stand initiation to stem exclusion; the application of variable density thinning to stem exclusion; and the retention of thinned stands for the restoration of mature habitat.

2.3.7 Multivariate assemblage composition analyses

Our MSOMs enable the robust estimation of alpha and beta diversity through explicit modeling of imperfect detection and partial pooling of species-level parameters within a shared hierarchical structure (Royle & Dorazio, 2005; Noble et al., 2024). We retained posterior distributions of latent occurrence states from the community (all species) model, averaged across years, to reflect frequency of species-specific habitat use, propagating both parametric uncertainty and seasonal stochasticity through analyses of assemblage composition. Alpha diversity (species richness) at each site was estimated as the sum of occurrence probabilities across species for each posterior iteration, and stage-level differences were evaluated by comparing posterior distributions of mean richness. Beta diversity (dissimilarity between sites, β_{BC}) was quantified using the Bray-Curtis metric (Oksanen et al., 2026), computed from occurrence probabilities for each posterior iteration, yielding a posterior distribution of pairwise β_{BC} values among sites. Pairwise differences in assemblage composition between stages were evaluated by computing the posterior probability that mean between-stage dissimilarity exceeded mean within-stage dissimilarity, estimated as the proportion of posterior iterations in which $\bar{\beta}^{(x)}_{BC,between} - \bar{\beta}^{(x)}_{BC,within} > 0$, where $\bar{\beta}^{(x)}_{BC,between}$ and $\bar{\beta}^{(x)}_{BC,within}$ are the mean pairwise Bray-Curtis dissimilarity across between- and within-stage site pairs at iteration *x*. Differences in within-stage dissimilarity between stages were evaluated as the proportion of posterior iterations in which $\bar{\beta}^{(x)}_{BC,s} - \bar{\beta}^{(x)}_{BC,s'} > 0$, where $\bar{\beta}^{(x)}_{BC,s}$ is the mean pairwise dissimilarity among sites within stage *s*. Finally, differences in multivariate dispersion between stages were evaluated as the

proportion of posterior iterations in which $\bar{d}_s^{(x)} - \bar{d}_{s'}^{(x)} > 0$, where $\bar{d}_s^{(x)}$ is the mean distance of sites in stage *s* to their multivariate centroid (Oksanen et al., 2026). Ordination of the posterior mean dissimilarity matrix with non-metric multidimensional scaling visualized the rank order of dissimilarities among sites belonging to each stage.

We partitioned dissimilarity into components of turnover (species replacement) and nestedness (species loss) by adapting the abundance-based framework of Baselga (2013) to posterior site use probabilities. By accounting for quantitative differences in occurrence over time (e.g., between transient and consistently breeding species), this approach preserves temporal variation and posterior uncertainty that would otherwise be obscured by binary summaries of presence-absence biasing estimates of diversity (Liu et al., 2005). Species turnover is captured by the balanced variation component β_{bal}, whereby species use probabilities are substituted from one set of species to another between sites, while species nestedness is captured by the use gradient component β_{gra}, whereby species use probabilities are systematically reduced from one site to another. The relative magnitude of these components can indicate the influence of environmental filtering versus habitat quality in structuring assemblage composition, and has direct implications for the conservation and restoration of habitat to conserve metacommunity diversity (Legendre, 2014).

2.4 RESULTS

2.4.1 Assemblage composition and diversity

We observed 72 species from 71,655 putative detections and 3,799 total survey occasions spanning roughly 91,000 hours of acoustic data across 224 sites (Table A2.2). Species represented 28 families across 10 orders consisting of *Passeriformes* (67%), *Accipitriformes* (7), *Strigiformes* (7), *Piciformes* (6), *Caprimulgiformes* (4), and *Columbiformes*, *Galliformes*, *Charadriiformes*, *Coraciiformes*, and *Falconiformes* (9, collectively). A total of 16 conservation priority species were present, including listed, candidate, and watch list species (Washington Department of Fish and Wildlife, 2025; NABCI, 2025): Marbled Murrelet (*Brachyramphus marmoratus*), American Goshawk (*Accipiter gentilis*), Rufous Hummingbird (*Selasphorus*

rufus), Evening Grosbeak (*Coccothraustes vespertinus*), Olive-sided Flycatcher (*Contopus cooperi*) and Vaux's Swift (*Chaetura vauxi*). The most common species observed were the American Robin (*Turdus migratorius*), Common Raven (*Corvus corax*), Evening Grosbeak (*Coccothraustes vespertinus*), Pacific Wren (*Troglodytes pacificus*), Steller's Jay (*Cyanocitta stelleri*), and Varied Thrush (*Ixoreus naevius*), having occurred at every site at least once during the study.

We derived estimates of species-specific occurrence and detectability for 66 species with sufficient observations for multi-species occupancy modeling (being observed at more than 2 sites). Convergence was confirmed for each MSOM grouping (all species, nesting, and foraging guilds) via Gelman-Rubin statistics ($\hat{R} < 1.1$) and visual inspection of chain histories. Bayesian posterior predictive checks ($p = 0.42–0.49$) indicated sufficient fit. We report results as posterior medians alongside 95% Bayesian credible intervals (CI). Probability of detection varied greatly among species, but environmental and temporal effects were broadly consistent at the community level. Community detectability was reduced in closed-canopy stages (stem exclusion, thinned, mature), decreased with amount of precipitation, and increased with temperature (Figure A2.4A, Table A2.5). Marginal predictions of detection probability as a function of survey day and squared survey day using averaged stage-specific detection intercepts revealed a maximum in detectability in early June, coinciding with peak breeding and fledging periods for most birds in the region (Figure A2.4B). Occurrence probability at the community level remained stable across breeding seasons, though we found evidence for a small yearly decrease in the mean occurrence of ground foragers, increase in the mean occurrence of aerial foragers (Figure A2.4C), and also for yearly decreases in occurrence of the Marbled Murrelet and Pine Siskin, and increase in occurrence of the Barred Owl.

Alpha diversity varied across developmental stages (Figure 2.3A). Stand initiation sites consistently supported the greatest species richness, with 8-10 more species than closed-canopy stages (posterior probability $P = 1.0$; median 43.81; SD 0.6). By contrast, stem exclusion sites supported the lowest number of species on average (median 34.27; SD 0.39), with richness increasing progressively from mature (35.26; 0.56) to thinned (36.15; 0.49) stages. However, pairwise differences among closed-canopy stages were small: thinned sites were consistently more species-rich than stem exclusion ($P = 1.0$; $\Delta\alpha = 1.87$, CI 0.89-2.9), while mature-thinned

and mature-stem exclusion comparisons were statistically indistinguishable, with posterior differences overlapping zero (P = 0.91 and 0.95, respectively; Table 2.1).

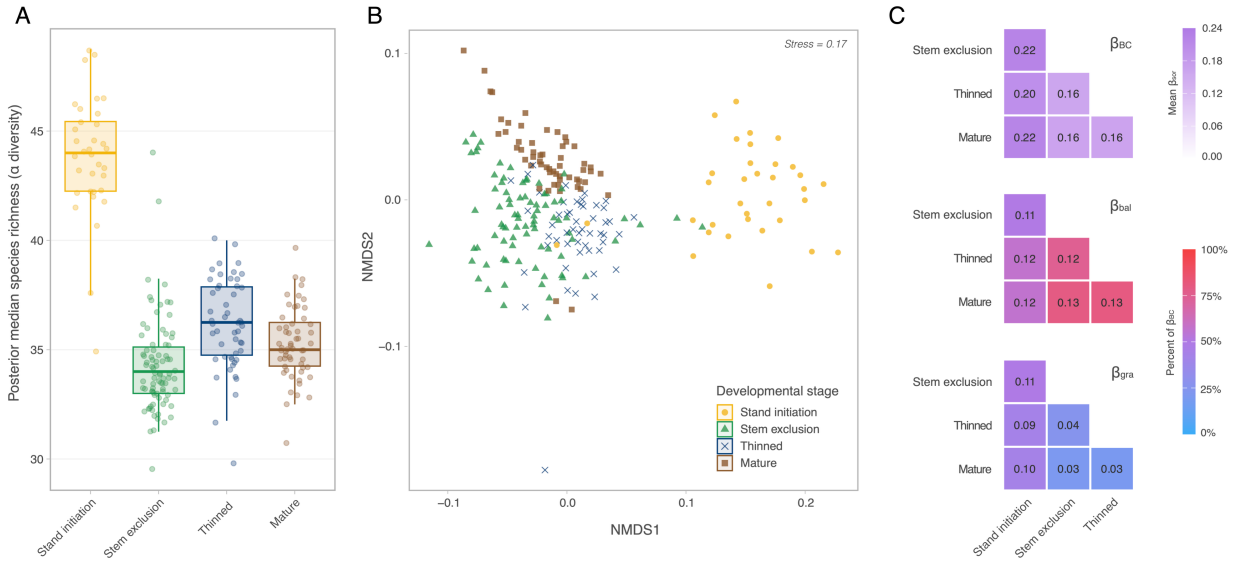

Figure 2.3: Patterns in alpha and beta diversity across survey sites and developmental stages. (A) Posterior median species richness per site by stage (alpha diversity). (B) Non-metric multidimensional scaling (NMDS) ordination of assemblage composition based on Bray-Curtis dissimilarity. Points represent sites colored by developmental stage with 95% confidence ellipses. (C) Beta diversity measured by pairwise dissimilarity between stages β_{BC} partitioned into species turnover β_{bal} and nestedness components β_{gra}.

Assemblages varied widely across the landscape (β_{BC} = 0.951, CI 0.95-0.953), with developmental stage explaining one quarter of the variation in taxonomic composition (R^2 = 0.27, CI 0.25-0.30) and between-stage dissimilarity exceeding within-stage dissimilarity for all pairwise stage comparisons (P = 1.0, Table 2.1). Stand initiation was compositionally distinct from all closed-canopy stages ($\Delta\beta_{BC}$ = 0.05-0.075). By contrast, stem exclusion, thinned, and mature stages showed comparatively weak pairwise dissimilarities ($\Delta\beta_{BC}$ = 0.01-0.02), indicating detectable but modest compositional differences. Similarly, mature substages (late-successional and old-growth) hosted statistically distinguishable but largely overlapping assemblages with the weakest compositional dissimilarities (P = 1.0, $\Delta\beta_{BC}$ = 0.005). Stand age similarity predicted compositional similarity among stand initiation sites (median Spearman r_s = 0.57, P = 1), and weakly among closed-canopy sites (r_s = 0.14–0.18, P > 0.99).

Stage 1	Stage 2	$\Delta\alpha$	$P(\alpha_1 > \alpha_2)$	$\Delta\beta_{BC}$	$P(\beta_{between} > \beta_{within})$	β_{BC}	β_{bal}	β_{gra}
Stand initiation	Stem exclusion	9.54 (8.29, 10.92)	1.000	0.068 (0.059, 0.077)	1.000	0.222 (0.213, 0.231)	0.112 (50.4%)	0.110 (49.6%)
Stand initiation	Thinning	7.66 (6.27, 9.10)	1.000	0.053 (0.045, 0.063)	1.000	0.202 (0.193, 0.213)	0.115 (57.0%)	0.087 (43.0%)
Stand initiation	Mature	8.54 (7.03, 10.12)	1.000	0.075 (0.064, 0.870)	1.000	0.220 (0.210, 0.231)	0.125 (56.7%)	0.096 (43.3%)
Thinning	Stem exclusion	1.87 (0.89, 2.90)	1.000	0.008 (0.004, 0.013)	1.000	0.160 (0.153, 0.168)	0.120 (74.9%)	0.040 (25.1%)
Mature	Stem exclusion	0.99 (–0.15, 2.24)	0.954	0.011 (0.007, 0.019)	1.000	0.163 (0.155, 0.172)	0.129 (79.5%)	0.033 (20.3%)
Mature	Thinning	0.88 (–0.48, 2.17)	0.907	0.018 (0.012, 0.026)	1.000	0.163 (0.155, 0.173)	0.131 (80.2%)	0.032 (19.8%)

Table 2.1: Pairwise diversity metrics comparing assemblage composition among developmental stages, shown as posterior medians alongside 95% Bayesian credible intervals and posterior probabilities: species richness difference, $\Delta\alpha$, probability that richness of stage 1 exceeds stage 2, $P(\alpha_1 > \alpha_2)$, Bray-Curtis dissimilarity difference, $\Delta\beta_{BC}$, probability that between-stage dissimilarity exceeds within-stage dissimilarity, $P(\beta_{between} > \beta_{within})$, and Bray-Curtis dissimilarity β_{BC}, partitioned into components of species turnover (balanced variation), β_{bal}, and nestedness (use gradient), β_{gra}.

Stand initiation and mature hosted the most dissimilar assemblages overall ($\Delta\beta_{BC}$ = 0.075, CI 0.064-0.087; β_{BC} = 0.22, CI 0.21-0.23), while among closed-canopy stages mature and thinned assemblages were the most dissimilar ($\Delta\beta_{BC}$ = 0.018, CI 0.012-0.026; β_{BC} = 0.163), and stem exclusion and thinned the most similar ($\Delta\beta_{BC}$ = 0.008, CI 0.004-0.013; β_{BC} = 0.16). We found no evidence that thinned assemblages were more similar to mature than to stem exclusion assemblages (P = 0.2), and dissimilarity between thinned and mature assemblages did not decrease with time since thinning (up to 25 years; P = 0.02). Within-stage dissimilarity and multivariate dispersion did not differ consistently among stages, with small pairwise posterior differences largely overlapping zero, and only stem exclusion displaying tendency toward greater dispersion than mature forest (P = 0.99). Ordination of the posterior mean dissimilarity matrix with non-metric multidimensional scaling reinforced these patterns (Figure 2.3B).

Beta diversity decomposition revealed that differences in assemblages across the landscape were driven by species turnover (β_{bal} = 0.928, CI 0.92-0.931) rather than nestedness (β_{gra} = 0.023, CI 0.02-0.27). This pattern held between closed-canopy stages, with turnover

accounting for 75-80% of dissimilarity, indicating closed-canopy assemblages are distinct rather than species-poor subsets (Figure 2.3C). Dissimilarity between stand initiation and closed-canopy stages, however, was driven by a mixture of turnover (50-57%) and nestedness (43-50%), indicating filtering of species by canopy closure from the stand initiation pool (Figure 2.3E). Turnover was highest between mature-stem exclusion and mature-thinned assemblages (80%), while nestedness was highest between stand initiation and stem exclusion (50%). Dissimilarity within each developmental stage was primarily driven by turnover (77-80%).

The spatial context of a forest stand within the surrounding landscape also influenced assemblage composition. Assemblages at sites surrounded by more stand initiation or mature habitat within the mean species home range extent were more similar to the average assemblages of those stages (median Spearman r_s = –0.33 and –0.15, respectively; P = 1). By contrast, stem exclusion and thinned forest proportions did not show this pattern (r_s = 0.0, –0.2, P = 0.5, 0.71, respectively).

2.4.2 Habitat use by species and functional guilds

Forest developmental stage strongly influenced habitat use probability across the community, with substantial variation between functional guild (Figure 2.4A, Table A2.6) and species responses (Figure 2.4B) further revealing determinants of assemblage composition. MSOM developmental stage covariates indicated the effect of each stage on habitat use relative to stem exclusion, as measured by the proportion of that stage within the species-specific home range. The signs of coefficient posterior means for developmental stage were consistent across the three MSOM specifications (community, nesting microhabitat, foraging substrate) for the majority of species-covariate combinations (79%; Figure A2.3), with nearly all directional responses in agreement for species where at least one credible interval excluded zero (97%). Disagreements were concentrated among species whose estimates broadly overlapped zero in all models.

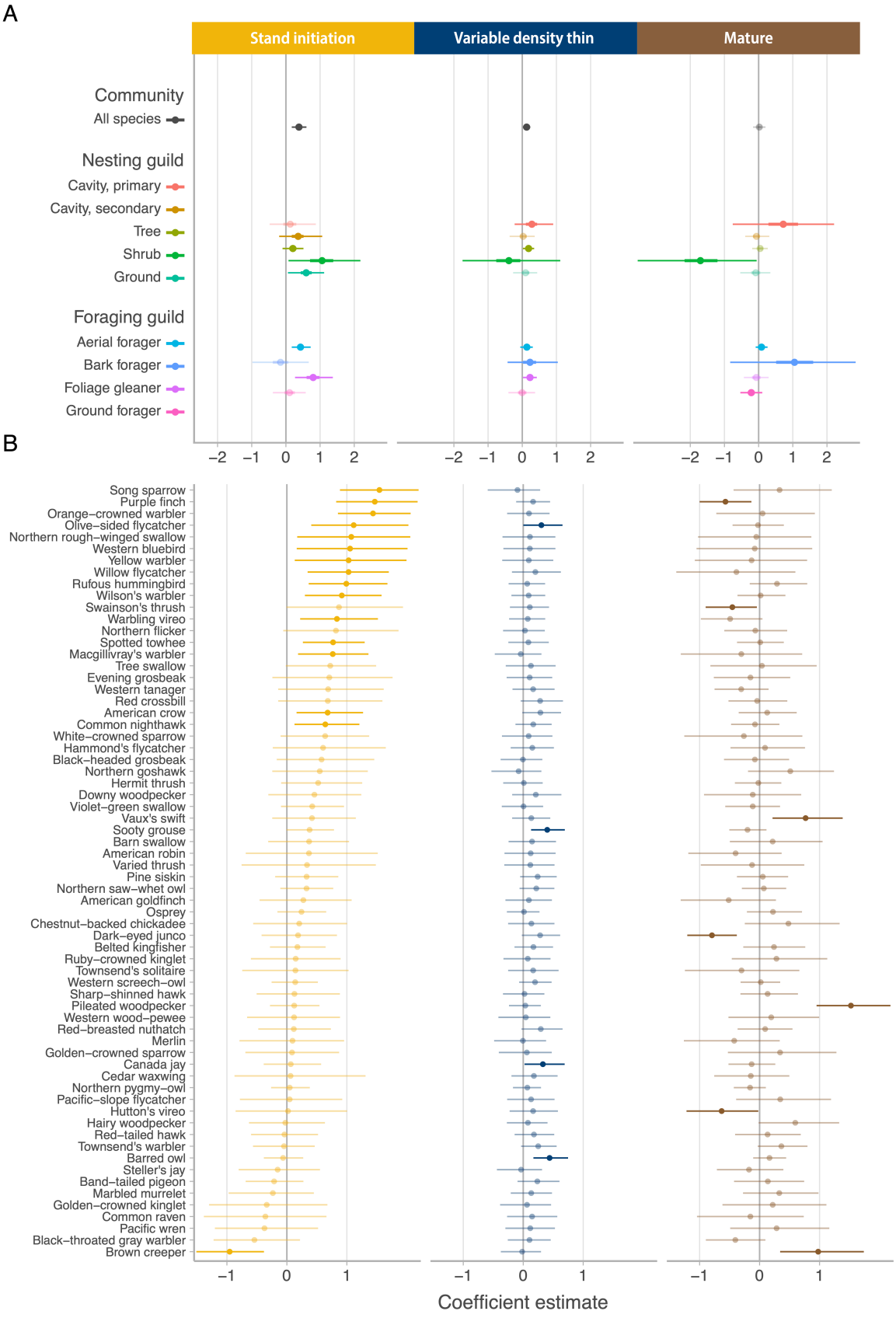
A
Stand initiation
Variable density thin
Mature
Community
All species
Nesting guild
Cavity, primary
Cavity, secondary
Tree
Shrub
Ground
Foraging guild
Aerial forager
Bark forager
Foliage gleaner
Ground forager
−2 −1 0 1 2
B
Song sparrow
Purple finch
Orange−crowned warbler
Olive−sided flycatcher
Northern rough−winged swallow
Western bluebird
Yellow warbler
Willow flycatcher
Rufous hummingbird
Wilson's warbler
Swainson's thrush
Warbling vireo
Northern flicker
Spotted towhee
Macgillivray's warbler
Tree swallow
Evening grosbeak
Western tanager
Red crossbill
American crow
Common nighthawk
White−crowned sparrow
Hammond's flycatcher
Black−headed grosbeak
Northern goshawk
Hermit thrush
Downy woodpecker
Violet−green swallow
Vaux's swift
Sooty grouse
Barn swallow
American robin
Varied thrush
Pine siskin
Northern saw−whet owl
American goldfinch
Osprey
Chestnut−backed chickadee
Dark−eyed junco
Belted kingfisher
Ruby−crowned kinglet
Townsend's solitaire
Western screech−owl
Sharp−shinned hawk
Pileated woodpecker
Western wood−pewee
Red−breasted nuthatch
Merlin
Golden−crowned sparrow
Canada jay
Cedar waxwing
Northern pygmy−owl
Pacific−slope flycatcher
Hutton's vireo
Hairy woodpecker
Red−tailed hawk
Townsend's warbler
Barred owl
Steller's jay
Band−tailed pigeon
Marbled murrelet
Golden−crowned kinglet
Common raven
Pacific wren
Black−throated gray warbler
Brown creeper
−1 0 1
Coefficient estimate

Figure 2.4: Multi-species occupancy model coefficient estimates for effects of forest developmental stage proportion at the species-specific home range scale at the community, functional guild (A), and species (B) levels. Mean guild-level coefficients for three functional groupings are shown: community (comprising all species), nesting microhabitat (primary cavity, secondary cavity, tree, shrub, and ground nesting guilds), and foraging substrate (aerial, bark, ground, and foliage gleaning guilds). Posterior means and 95% and 50% Bayesian credible intervals (thin and thick lines, respectively) are shown in opaque color for guild-specific estimates (A) where the 50% BCI excludes zero, indicating probable effects, and for species-specific estimates (B) where the 95% BCI excludes zero, indicating strong effects. Covariates were *Z*-scored, and estimates are shown relative to stem exclusion as a baseline stage such that a positive effect indicates a greater probability of habitat use compared to stem exclusion.

Stand initiation promoted broadly convergent patterns of habitat use across the community, with positive or neutral responses among nesting microhabitat and foraging substrate guilds contributing to a positive community mean effect (Figure 2.4A). Shrub and ground nesters responded most strongly, while tree and secondary cavity nesters showed weak positive trends and primary cavity excavators no clear response. Likewise, foliage gleaners and aerial foragers showed similarly strong responses, whereas bark and ground foragers were unresponsive. At the species level, early-seral (e.g., Spotted Towhee), forest-edge (Orange-crowned Warbler), and open-habitat (Song Sparrow) associates all showed strong affinity for stand initiation. Positive coefficient estimates across most members of the community indicate consistently lower habitat use probability in stem exclusion stands by comparison. The Brown Creeper was the only species to show a strong aversion to stand initiation.

Mature forest, by contrast, showed high divergence in guild-specific responses, with large coefficient magnitudes cancelling out at the community level but indicating strong signals among particular guilds and species (Figure 2.4A, B). Primary cavity excavators were the most strongly affiliated nesting guild, with the Pileated Woodpecker showing the strongest stage-specific response of any species. Within this guild, however, substantial species-specific variation revealed divergent associations between associates of late-successional forest (Hairy Woodpecker) and open woodlands (Northern Flicker). By contrast, shrub nesters such as the Swainson's Thrush showed strong aversion to mature forest. Among foraging guilds, bark foragers such as the Brown Creeper were most strongly associated with mature forest. Again, substantial within-guild variation indicated divergence between late-successional (e.g., Pileated Woodpecker) and open-woodland associates (e.g., Downy Woodpecker). Ground foragers such as Dark-eyed Junco trended negative, while foliage gleaners and aerial foragers showed no

discernable response. Species-level responses indicated that mature stands strongly promoted use of old-forest structural obligates (Brown Creeper, Vaux's Swift), while filtering out species associated with forest edges (Purple Finch), early- (Dark-eyed Junco), and mid-successional stages (Hutton's Vireo).

Variable density thinning of stem-exclusion forest had a positive but weak effect on community-wide habitat use probability, driven by generally modest, uncertain responses across nesting and foraging guilds (Figure 2.4A). Thinned stands tended to promote the occurrence of primary cavity excavators and suppress shrub nesters, while also supporting foliage gleaners, mirroring mature and stand initiation stages, respectively. Smaller coefficient magnitudes, however, indicated comparatively weaker effects. Species-specific effects were similarly modest and uncertain, with three notable exceptions: the Barred Owl, Gray Jay (Canada Jay), and Sooty Grouse each showed a clear and unique association with thinned forest not observed in other developmental stages.

Stem exclusion sites suppressed community-wide occurrence relative to other developmental stages, with generally comparable or weaker associations among nesting and foraging guilds, except for shrub nesters. We found weak positive but uncertain species-specific effects for generalists (Steller's Jay, Common Raven) and dense mid-successional second growth associates (Hutton's Vireo, Black-throated Gray Warbler).

Variation in habitat structure at the local plot scale also strongly modulated habitat use probability within each stage (Figure 2.5, Table A2.6). Greater broadleaf hardwood proportion (predominantly red alder) consistently promoted community-wide habitat use across all developmental stages, with this effect being most pronounced in closed-canopy stages. Tree nesters and foliage gleaners were the clearest drivers of this pattern, though weakly positive or neutral associations extended across nearly all nesting and foraging guilds.

Tree size (quadratic mean diameter of merchantable trees) had a strong negative effect on community-wide use of thinned forest—the greatest magnitude of any plot-scale coefficient. This response was driven by tree nesters, ground foragers, and foliage gleaners. By contrast, tree size trended weakly positive in stand initiation and had no discernable community-wide effect in stem exclusion or mature forest. However, increased tree size tended to suppress the use of stand initiation sites by primary cavity nesters specifically.

Tree density showed divergent effects across developmental stages, promoting habitat use in mature forest while weakly suppressing use in stand initiation and stem exclusion stages. In mature forest, higher tree density most clearly benefitted tree nesters, while in stand initiation it suppressed tree nesters, secondary cavity nesters, and ground foragers. Ground foragers also tended to respond negatively to tree density with the stem exclusion stage.

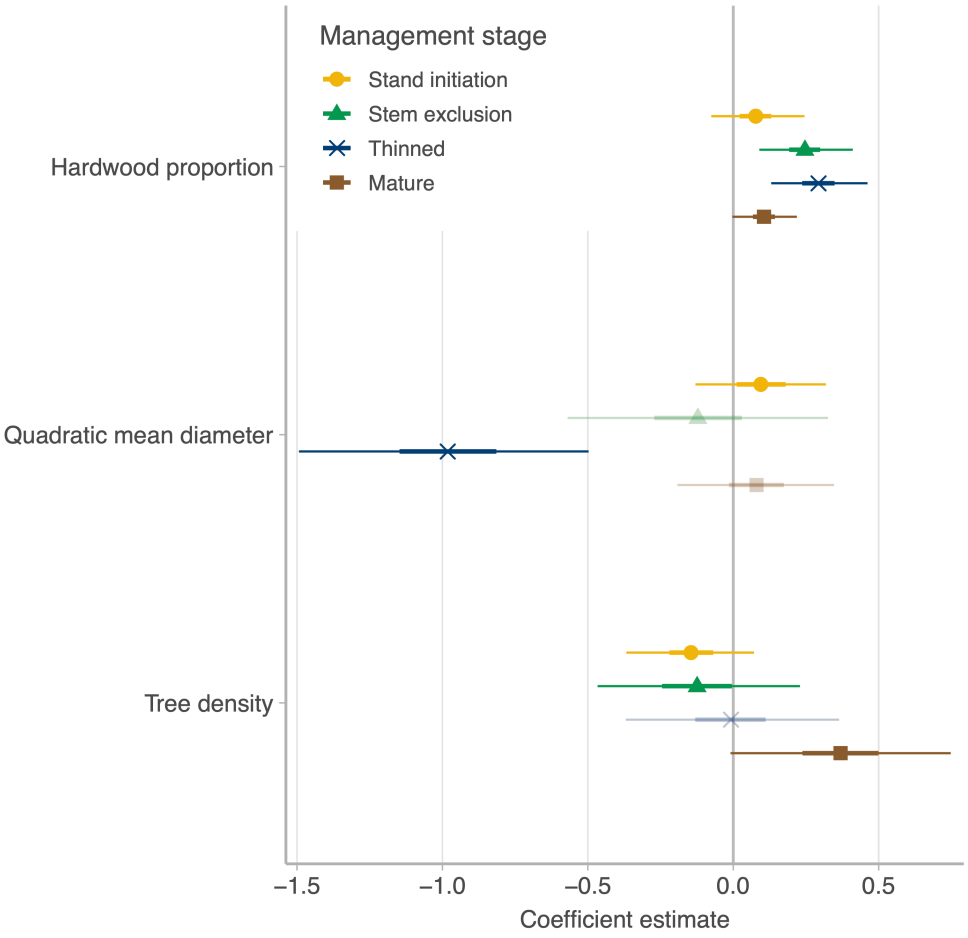

Figure 2.5: Stage-specific mean community-level coefficient estimates for effects of local habitat structure at the plot scale: proportion of hardwood tree species, quadratic mean diameter, and tree density. Posterior means and 95% and 50% Bayesian credible intervals are shown in opaque color where the 50% BCI excludes zero, indicating probable effects. All covariates were *Z*-scored.

Site elevation and proximity to paved roads and streams had weak and uncertain effects on habitat use at the community level and highlighted within-guild heterogeneity in species-specific responses (Figure A2.4C, Table A2.6). Elevation demonstrated strong positive

relationships with montane and subalpine associates such as the Canada Jay (Gray Jay) and Red-breasted Nuthatch, and strong negative relationships with lowland and riparian associated species such as the Belted Kingfisher and Hutton's Vireo. Increased site proximity to paved roads promoted the occurrence of disturbance-tolerant and edge-associated species (American Crow, Orange-crowned Warbler), while tending to be negatively associated with the occurrence of primary cavity excavators. No strong evidence was found for an effect of stream proximity at the community or guild levels once elevation and forest stage were accounted for, with the Belted Kingfisher, a riparian obligate, showing the only unequivocal response.

2.4.3 Habitat use by conservation priority species across developmental stages

Marginal predictions of habitat use across developmental stages for species and groups of conservation priority served as indicators of each stage's relative benefit in support of avian species and community diversity. Stand initiation and mature stages harbored the greatest expected number of priority species by promoting comparatively high probabilities of habitat use across early-seral and old-forest associates, respectively (Figure 2.6). Stand initiation maximized use probability for warblers, flycatchers, and open-canopy associates, while old-forest associates nearly all reached their highest expected use in the mature stage. However, responses for Marbled Murrelet and American Goshawk were highly uncertain, reflecting species rarity and a scarcity of observations. Variable density thinning produced a modest but uncertain increase in priority species richness compared to stem exclusion. The Olive-sided Flycatcher exhibited the most notable gains, more than doubling in expected use probability in mid-successional stands. By contrast, stem exclusion forest did not enhance use probability for any priority species relative to other stages. For example, our results suggest that the Rufous Hummingbird is roughly 3 times more likely to use a 100 m radius stand initiation patch than stem exclusion. Similarly, the Pileated Woodpecker is 1.6 times more likely to use a contiguous stand of mature forest than stem exclusion. For several species—Rufous Hummingbird, Pileated Woodpecker, Vaux's Swift, and Pine Siskin—multimodal responses were apparent, indicating frequent use of multiple developmental stages. By contrast, the Evening Grosbeak, Chestnut-backed Chickadee, and Golden-crowned Kinglet were ubiquitous across the landscape and showed no clear affiliation to a particular stage.

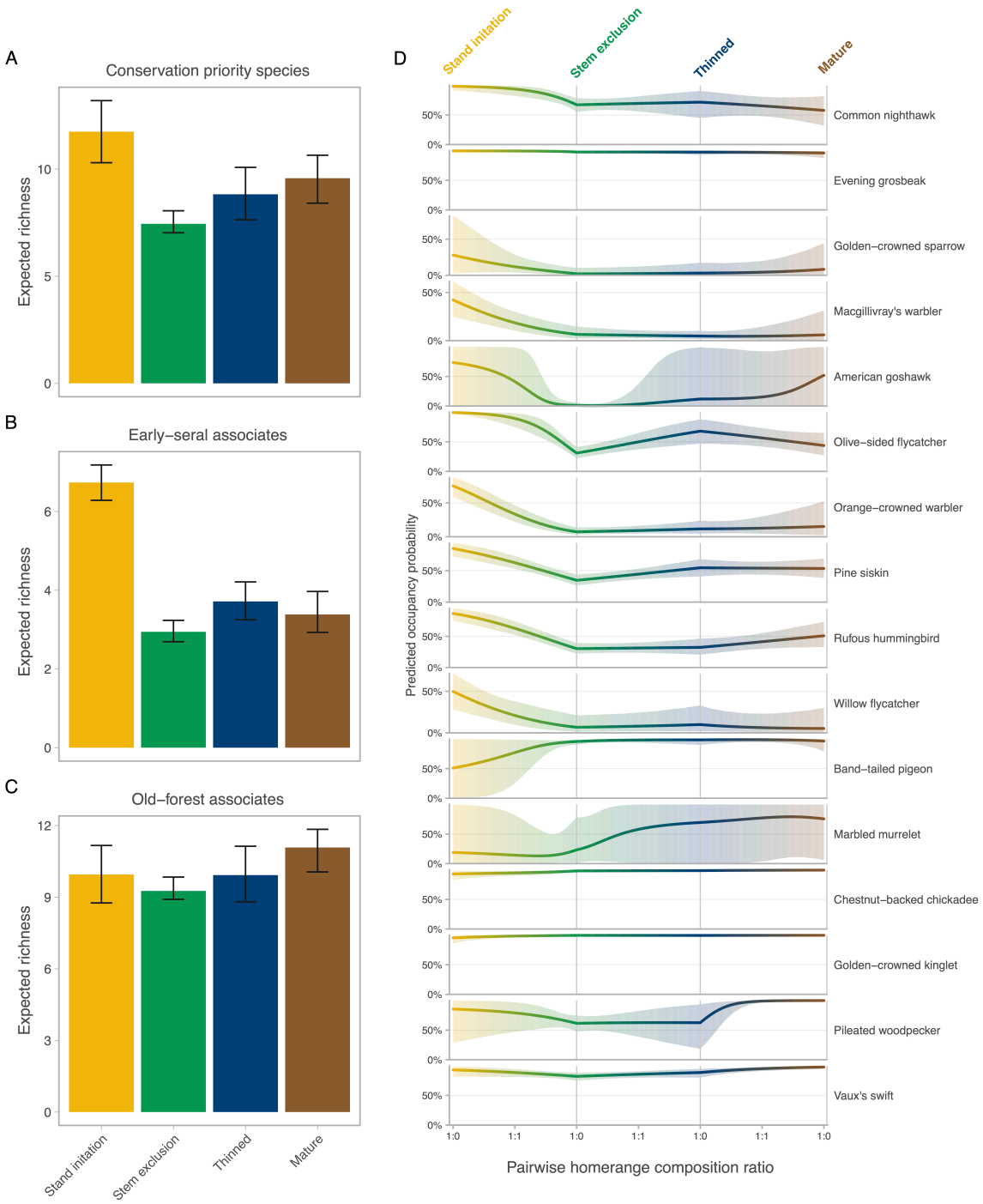

Figure 2.6: Relative conservation value of forest developmental stages for species and groups of conservation priority, as measured by marginal expected species richness when the home range comprises 100% of a given developmental stage for conservation priority species (A), and biological associates of early-seral (B) and old-forest habitat (C). Marginal predicted habitat use probability for conservation priority species across pairwise gradients of developmental stage composition (D) is calculated as weighted averages of stage-specific predictions proportional to home range composition.

2.5 DISCUSSION

Central to ecological forestry and integrated forest management is the hypothesis that maintaining a diversity of developmental stages and structures across a landscape will promote biodiversity and conservation of priority species (Franklin et al., 2018; Lindenmayer & Franklin 2002). By investigating community-wide habitat use patterns across a managed successional mosaic landscape, our study builds on a strong foundation of ecological and ornithological research in the region (e.g., Sallabanks & Arnett, 2005; McGarigal & McComb 1995; Ruggiero et al., 1991), while extending inference to the community level by using new monitoring technologies with a multi-species occupancy modeling framework. We found that forest developmental stage is a fundamental determinant of avian assemblage composition, organizing distinct assemblages along an environmental gradient of disturbance and canopy closure. Nesting and foraging strategies structure much of this variation, with guild-specific patterns of habitat use tracking the resources characteristic of a given stage.

Forest habitat in the mature and stand initiation stages supported a broad range of complementary ecological functions and together maximized the probability of habitat use for species and groups of conservation priority. By contrast, secondary forest plantation stands in the stem exclusion phase contributed the least to avian diversity and conservation, failing to support a diverse array of functional niches. Variable density thinning produced modest gains in community-wide alpha diversity but did not substantially shift guild-level habitat use or assemblage composition toward mature forest conditions within 25 years post-harvest. These patterns highlighted clear contrasts in expected conservation value across the landscape in response to management prescription and habitat reservation. Variation in local habitat structure also modulated within-stage habitat use, highlighting the potential ecological benefits of targeted silvicultural prescriptions. Our results provide empirical evidence supporting the hypothesis that integrated forest management can promote avian diversity and ecological functions through the provision of mature and early-seral habitat (Duflot et al., 2022; Franklin et al., 2018; Cushman & McGarigal 2003). However, given mid-successional plantation stands that dominate the landscape hosted the lowest levels of taxonomic and functional diversity, and variable density thinning prescriptions were unable to rapidly recover the functional associates of late-successional forest, these findings highlight inherent limitations in the conservation value of

second growth forest stands managed primarily for timber production (Spies et al., 2018; Hagar, 2007; Sallabanks & Arnett, 2005)

2.5.1 Variation in assemblage composition and diversity among developmental stages

Variation in assemblage composition (beta diversity) among sites was driven primarily by species turnover rather than by nestedness, pointing to environmental filtering as a leading process shaping community assembly across the landscape (Baselga, 2013; Legendre, 2014). However, the magnitude of these components varied between stages, indicating differences in the relative influence of environmental conditions versus habitat quality and species dispersal (Figure 2.3C, Table 2.1). Most notably, we found that canopy closure was the primary environmental axis structuring assemblage composition.

Variable retention harvest, followed by stand initiation, creates ephemeral openings of early-seral habitat and high edge density within an otherwise contiguous forest canopy, promoting colonization by pioneering vegetation and an influx of early-seral (e.g., Spotted Towhee), forest edge (Orange-crowned Warbler), and open-habitat (Song Sparrow) associates (Swanson et al., 2014). The availability of early-seral foraging and nesting resources was reflected in strong responses by aerial foragers (e.g., Olive-sided Flycatcher), foliage gleaners (Swainson's Thrush) and shrub (Willow Flycatcher) and ground (Wilson's Warbler) nesting guilds (Figure 2.4). This influx of disturbance-tolerant species increased alpha diversity and produced assemblages with the highest pairwise dissimilarity to all other developmental stages, driven by both species turnover and nestedness. Turnover captured the use of novel early-seral specialists, while nestedness reflected a substantial compositional overlap with closed-canopy assemblages. As high nestedness suggests that differences in habitat quality or dispersal ability influences assembly (Baselga, 2013; Legendre, 2014), we suggest this overlap reflects both the use of stand initiation habitat by forest interior species and the ubiquity of generalists across all developmental stages. Canopy closure acts as an environmental filter, reducing richness through the exclusion of open-forest obligates, and this effect was most pronounced in stem exclusion stands where tree density and canopy cover reach their maximum.

Despite containing broadly similar pools of forest-interior species, stem exclusion, thinned, and mature stages each harbored distinct assemblages rather than species-poor subsets of one another. Which species persist under different management conditions varied

substantially, as species turnover accounted for a large majority of the dissimilarity between closed-canopy stages. Mature forests deferred from harvest as protected habitat harbored the most distinct assemblages, characterized by late-successional specialists and high divergence in guild-specific responses (Figure 2.4). Old-forest structural obligates such as the Vaux's Swift and Brown Creeper reached their highest habitat use probabilities in mature stands, underscoring the role of large snags, mature trees, and downed wood in supporting these species, and reinforcing the importance of retaining biological legacies in secondary forest maintained for timber production (Franklin & Donato, 2020; Price et al., 2020; Donato et al., 2012; Hanle et al., 2019). Primary cavity excavators were likewise most strongly affiliated with this stage, suggesting that maintaining late-successional habitat may be critical to safeguard the persistence of both primary cavity nesters as well as obligate secondary cavity nesters that depend on previously excavated sites (Trzcinski et al., 2021). Divergence in guild-specific responses indicated strong environmental niche filtering, promoting the use of late-successional interior forest specialists while suppressing shrub nesters (e.g., Swainson's Thrush) and species affiliated with forest edges (Purple Finch), early-seral (Dark-eyed Junco), and dense plantation habitat (Hutton's Vireo).

Although secondary forests in the stem exclusion stage tended to support the least species richness among all developmental stages, the remaining species were not simply a species-poor subset of the broader avian community. Several forest generalists (Steller's Jay, Common Raven) and mid-successional associates (Hutton's Vireo, Black-throated Gray Warbler) reached their greatest marginal use probability in stem exclusion habitat, though were commonly observed throughout other developmental stages as well. This suggests that mid-successional plantation forest conditions may select for species affiliated with, or tolerant of, dense second growth habitat, while not providing the resources necessary for specialist species found in other developmental stages that rely on absent structural features and vegetation. As a consequence, while stem exclusion assemblages were compositionally distinct, they hosted the lowest richness of conservation priority species among all developmental stages (Figure 2.6A).

Variable density thinning introduced structural heterogeneity and understory vegetation to plantation stands, promoting modest increases in community-wide use probability within 25 years after harvest across most foraging and nesting guilds. Cumulatively, these trends manifested in higher species richness, consistent with previous reports on the ecological benefits of thinning (Carey, 2003; Hagar et al., 2004; Cahall et al., 2013; Thomas et al., 2006). Thinned

stands partially resembled mature forest in promoting primary cavity excavators and suppressing shrub nesters, and stand initiation in promoting foliage gleaners, though consistently smaller coefficient magnitudes indicate comparatively weaker effects (Figure 2.4). Despite approaching late-successional structure and comparable species richness, thinned and mature stands were the most compositionally dissimilar among closed-canopy stages. Instead, thinned assemblages most closely resembled those of stem exclusion habitat, reflecting deficits in vertical heterogeneity, snags, and downed wood. Unique species-specific responses reinforce these differences, strongly supporting the Olive-sided Flycatcher, Canada Jay, and Sooty Grouse, and maximizing Barred Owl habitat use. Although variable density thinning is widely prescribed to accelerate structural development toward mature forest conditions, our results suggest that the resources required to support old-forest associates take considerably longer to develop. In addition, thinning may inadvertently promote the colonization of species directly at odds with old-growth ecological conservation, such as the Barred Owl, which we address below.

Most species were not exclusively affiliated with a particular developmental stage. This reflects both the widespread occurrence of species common to Pacific Northwest forests (e.g., Pacific Wren, Varied Thrush, Western Flycatcher), as well as the frequent use of multiple forest habitats. For example, several species were observed often in both mature and stand initiation stands. Vaux's Swifts, while dependent on large forest snags for breeding and nesting, frequently congregate at forest openings and edges to exploit areas abundant in flying insects (Bull & Beckwith, 1993). Rufous Hummingbirds, the only nectarivore we encountered, are dependent on flowering plants in forest openings but often nest in mature forest (Ruggiero et al., 1991). Similarly, the Hairy and Pileated Woodpeckers, while associated with mature forest, may use open habitat when snags and dead wood are present (Ripper et al., 2007; Raley & Aubry, 2006). These findings align with a growing body of evidence that some mature forest birds may use early-successional habitat during the post-fledging period for abundant food resources and escape cover not available near the nest site (Vitz & Rodewald, 2021; Chandler et al., 2012). This reinforces the merit of retaining biological legacies during harvest, and more broadly supports the ecological benefits of habitat heterogeneity at the landscape scale (Cushman & McGarigal, 2003). Moreover, these patterns underscore the importance of considering the full life histories and spatial scales relevant to individual species when designing habitat management strategies.

These results highlight the potential of forest management to bolster ecosystem function amid ongoing avian declines by creating habitat conditions that promote both the breadth and redundancy of functional traits. Habitats promoting high redundancy, where co-occurring species share similar traits, may have greater resilience to species loss as persisting species are able to maintain critical ecosystem processes despite local extirpations (Biggs et al., 2020). Strong convergent guild responses (e.g., aerial insectivores in stand initiation habitat) exemplify this. Conversely, habitats characterized by low redundancy and high functional uniqueness are more vulnerable to functional degradation, as the loss of even a single species may disproportionately disrupt ecological processes (Mouillot et al., 2013). For example, primary cavity excavators were most often observed in mature forest stands, though limited to a comparatively small number of species. The loss of unique functional traits may compromise the sustainability of ecosystem processes even if taxonomic richness remains high, as evidenced by thinned stands exhibiting greater alpha diversity than mature yet comparatively weaker responses across functional guilds. As such, forest stands supporting unique functional diversity should be priorities for conservation, as they provide irreplaceable habitats that sustain ecosystem processes. Where habitat conditions cannot support particular traits, as in the plantation stem exclusion stage, restoration (e.g., structural enhancement) may aid in maintaining ecosystem functions.

2.5.2 Ecological potential of silvicultural prescriptions to manipulate local habitat structure and landscape context

Our analyses of within-stage beta diversity and structural variation highlight the potential of silvicultural prescriptions to influence avian habitat use. We suggest turnover-driven compositional variation within each stage is a function of heterogeneity in local habitat structure over time due to stand growth and management history, as well as the spatial context of the stand within the broader landscape. Indeed, despite classification by management into discrete developmental stages for human purposes, forest development occurs along a continuous gradient of succession that is influenced by the age of individual tree and vegetation cohorts within a stand. Stand age similarity was correlated with compositional similarity within each developmental stage, and mature substages (late-successional and old-growth) hosted statistically distinguishable, though broadly similar, assemblages. These patterns reflect the influence of successional progression (e.g., grass-forb to shrub-seedling) and active management

prescriptions in shaping bird assemblages over time. Relatedly, we found that variation in tree species composition and local habitat structure at the plot scale modulated habitat use within developmental stages (Figure 2.5).

Greater proportions of hardwood tree species consistently supported increased occurrence across the community regardless of stage, indicating that the maintenance of monoculture coniferous plantation stands dominated by western hemlock and Douglas fir negatively influences habitat use for many species. This effect was most clear for the tree nesting guild, which may benefit from structural variation introduced by broadleaf trees (Hagar, 2007). This suggests that polyculture prescriptions integrating deciduous pioneer tree species such as red alder may be particularly effective in promoting use of mid-successional stands.

Structural complexity also influenced guild-specific habitat use within each developmental stage. Increased merchantable tree density reduced use in stand initiation and stem exclusion stages, particularly among tree nesters and ground foragers, as competition among planted trees suppressed the shrub layer and homogenized structural complexity. By contrast, increased density strongly promoted use of mature habitat, where stand density is correlated with greater compositional and structural heterogeneity across canopy layers and foraging substrates. Increased quadratic mean diameter (QMD) within thinned stands elicited a strong negative community response driven by tree nesters, foliage gleaners, and ground foragers. We suggest this reflects the dynamics of structural recovery, whereby thinning initially drives a short-term influx of several open-canopy associates, followed by a delayed response of comparatively fewer species linked to recovering and mature vegetation. Species with strong negative responses to QMD included forest edge (Steller's Jay) and open canopy associates (Dark-eyed Junco, Common Nighthawk), while those with positive responses were affiliated with shrubs (Wilson's Warbler) and mature trees (Brown Creeper). These findings are consistent with documented variation in species-specific responses to thinning over time (Cahall et al., 2013) and may be compounded by direct disturbance (soil compaction, slash accumulation) temporarily degrading conditions for ground foragers.

Community-wide and species-specific responses to variable density thinning underscore the capacity of silvicultural prescriptions to shape community assembly, promoting and suppressing habitat suitability for particular species and functional guilds. Strategic silvicultural prescriptions can support the conservation of at-risk species, as evidenced by the doubling of

olive-sided flycatcher habitat use probability in thinned stands, and the ecological benefits of legacy features maintained under variable retention harvest (Franklin & Donato, 2020; Price et al., 2020; Hanle et al., 2019). However, any management strategy will inherently benefit some species while hindering others (Hansen et al., 1995), both directly through manipulation of foraging and nesting resources and indirectly by altering species interactions (Wiens, 1989b). This tension is exemplified by the Barred Owl (*Strix varia*), whose occurrence probability was maximized in thinned stands, likely reflecting its preference for open understory conditions that facilitate hunting maneuverability and its broad use of younger forest types (Hamer et al., 2007). Given that Barred Owl presence is a primary driver of Northern Spotted Owl (*Strix occidentalis caurina*) decline (Dugger et al., 2015), this creates a direct management challenge: thinning prescribed to accelerate the development of late-successional habitat for Spotted Owl recovery may inadvertently promote colonization by its most significant competitor. This finding merits further investigation, but highlights the importance of aligning silvicultural strategies with clearly defined species and community conservation priorities (Arcilla & Strazds, 2023; Hansen et al., 1995).

The spatial context of a forest stand within the broader landscape also influenced assemblage composition. For example, assemblages at sites surrounded by more stand initiation or mature habitat were more similar to the average assemblages of those stages, indicating dispersal of open-habitat associates and species with large home ranges into adjacent stands. By contrast, we did not see this pattern for the proportion of nearby stem exclusion or thinned habitat. As the dominant background matrix hosting the lowest richness and narrowest functional niche space, stem exclusion provides comparatively less compositional diversity to shape assemblages in adjacent stands, while the absence of a thinned forest effect likely reflects the high compositional similarity between thinned and stem exclusion stages.

Similarly, home range-scale predictors of forest composition revealed contrasts in stage-specific habitat affiliations that were obscured when considering the local developmental stage of a site alone. For example, the marbled murrelet was detected primarily in stand initiation stands, presumably in transit between coastal foraging grounds and mature forest nest sites (Meyer et al., 2002), yet analysis of landscape composition at the home range scale revealed that the proportion of nearby mature forest was the true driver of occurrence. Accounting for the multiple spatial

scales at which birds interact with and depend on their environment is imperative when inferring habitat associations from species observations (Battin & Lawler, 2006).

Furthermore, these patterns underscore the importance of considering the ecological effects of management actions on the broader "neighborhood" beyond the stand itself (Lindenmayer & Franklin, 2002). For example, our models suggest that spatially allocating late-successional stands near preexisting old-growth habitat, both within the OESF and the adjacent Olympic National Park, may enhance connectivity and effective habitat area for sensitive species. Conversely, management actions that expand paved road networks are expected to favor disturbance-tolerant and edge-associated species while reducing the occurrence of primary cavity excavators.

2.5.3 Conservation implications for integrated forest management

When the objective of forest management is to provide habitat for the greatest number of bird species, with priority for those of conservation concern, our results support the preservation of large continuous tracts of mature forest, maintenance of complex early-seral habitat, and restoration of structural heterogeneity in even-aged mid-successional plantations. At the landscape scale, forests dominated by a single developmental stage are expected to reduce avian diversity compared to those containing a mosaic of successional stages (Duflot et al., 2022; Franklin et al., 2018; Cushman & McGarigal, 2003). Similarly, within a forest stand, homogenous structural and compositional conditions are expected to narrow available ecological niches compared to habitat with a range of tree size classes, densities, and horizontal and vertical structures (Hansen et al., 1995; Chambers et al., 1999). The importance of conserving late-successional and old-growth forest for avian biodiversity is well established, and indeed has directed forest management strategy in the region since the passage of the Northwest Forest Plan (Thomas et al., 2006; Phalan et al., 2019). Meanwhile, sharp declines in early-seral ecosystems and associated bird assemblages have also been concentrated in the Coast Range ecoregion (Phalan et al., 2019), spurring growing efforts to restore complex early-seral habitat. Our results provide evidence for the unique assemblages fostered by early-successional habitat in managed landscapes, though efforts to restore early-seral ecosystems, if they come at the expense of mature forest conservation rather than being concentrated in existing plantation stands, will have negative effects on landscape avian diversity.

Both species- and guild-level habitat use patterns reinforce the growing body of evidence that mature and early-seral forests are ecologically irreplaceable habitats for maintenance of avian biodiversity in the region (Swanson et al., 2014; Cushman & McGarigal 2003; Ruggiero et al., 1991). Occupying opposite ends of the successional spectrum, stand initiation and mature stages supported the most dissimilar assemblages of any pairwise comparison, together spanning the full range of nesting and foraging strategies and promoting complementary ecological functions. These stages also exhibited the greatest avian conservation value by supporting the highest habitat use probabilities for species and groups of conservation priority (Figure 2.6). Mature forest is critical for the persistence of native endangered (e.g., Marbled Murrelet), candidate (American Goshawk), and keystone species and ecosystem engineers (Pileated Woodpecker). Meanwhile, neotropical migrants (e.g., Olive-sided Flycatcher) and open-canopy forest associates (Pine Siskin) experiencing alarming population declines used stand initiation habitat at much higher rates than other developmental stages. Both stages together maximized the occurrence of the Rufous hummingbird and Vaux's swift, at-risk species of high regional concern (PIF, 2026).

When management strategies include objectives for both economic production and biodiversity conservation, a likely effective strategy is to defer mature forest from harvest and manage for secondary forest habitat that maintains structural heterogeneity as plantation cohorts age. Our results suggest that the current regional dominance of mid-successional monoculture plantation forest serves to reduce avian habitat use and degrade matrix quality, likely posing consequences for avian population stability (Betts et al., 2022). The importance of species turnover in structuring beta diversity, strong differences in functional group responses, and species-specific use patterns spanning multiple developmental stages together support the hypothesis that maintaining a portfolio of habitat conditions is needed to conserve diversity across a landscape managed for both ecological and economic outcomes. Patterns in species nestedness between open- and closed-canopy stages further suggest that dispersal and habitat quality influence community structure, such that a proportion of species-rich early-seral habitat should be maintained in the landscape, while mid-successional plantation stands warrant restoration as degraded habitats. This supports previous findings that managed landscapes composed of a mixture of successional stages harbor greater species richness (Phalan et al., 2019; Cushman & McGarigal 2003), and avian biodiversity is likely to benefit from the

management of plantation forests to support both early-seral and late-successional ecosystems (Franklin et al., 2018; Lindenmayer & Franklin 2002).

The optimal landscape proportion of reserves (protected areas for biodiversity), intensive management (productive areas optimized for timber yields), and extensive management (i.e., ecological forestry) to integrate conservation and economic goals is the subject of ongoing research and debate (Betts et al., 2021; Arroyo-Rodríguez et al., 2020). The relative capacity of "land sharing", "land sparing", and "Triad" zoning to maximize both production and conservation objectives in the region warrants further study (Tittler et al., 2016). Prolonged harvest rotations may maintain larger proportions of mature forest in the landscape over time, promoting biodiversity (akin to the assemblages we observed in 80 year late-successional stands) and bolstering ecosystem functions while producing the same or greater levels of timber output (Petersson et al., 2023). Restoration and structural enrichment of forest plantations through silvicultural strategies such as complex early-seral development or variable density thinning may be critical to conserve diversity and ecological functions in managed forest landscapes, though experimental approaches to ecological forestry may yield unintended ecological effects, warranting further study and active management (Franklin & Johnson, 2012). Within the limitations of ownership objectives, management actions that prioritize at-risk species that are particularly sensitive to forestry and exhibiting precipitous population declines (Arcilla & Strazds, 2023; Sallabanks & Arnett, 2005) will help to maintain these species and prevent reductions to biodiversity.

We acknowledge two limitations of our study that constrain ecological inference. First, our interpretation of habitat associations is limited by the absence of demographic data and direct breeding observations. While bioacoustic species detection is particularly well-suited to heterogenous forest environments (Brewster & Simons, 2009), vocalization behavior may be influenced by biotic interactions and distance from the home range center (Rugg et al., 2025). As such, a greater number of survey replicates would increase the probability of detection for rare species. Furthermore, while our multi-species occupancy framework accounts for imperfect detection, occurrence during the breeding season does not necessarily indicate high habitat quality (Van Horne, 1983; Jones, 2001) and may include transient visitors. Furthermore, source-sink dynamics in human-modified landscapes may promote high use of areas that function as ecological traps where local vital rates are insufficient to sustain viable populations (Battin,

2004). However, our findings support a large body of research demonstrating robust associations of avian communities in mature and early-seral temperate forests (e.g., Swanson et al., 2014; Cushman & McGarigal, 2003; Ruggiero et al., 1991). Second, we observed interannual changes in occurrence probability for the Marbled Murrelet, Pine Siskin (decline), and Barred Owl (increase) that align with known population trends and range expansion, respectively. Indeed, Marbled Murrelet populations are expected to continue to decline in the region as a consequence of reductions in core nesting habitat (Lorenz et al., 2021; Peery & Jones, 2016). However, given the limited temporal scope of our study and high parameter uncertainty for the Marbled Murrelet due to low detection rates, we acknowledge that these effects capture seasonal variation rather than long-term trends and should be interpreted with caution.

2.5.4 Conclusion

Our study suggests that integrated forest management can enhance avian diversity and ecological functions by maintaining structurally complex mature and early-seral habitats in the landscape. However, reduced diversity in productive plantation stands that dominate the region, and the limited capacity of variable density thinning prescriptions to recover ecological functions within 25 years, highlight an inherent tradeoff between timber production and biodiversity conservation objectives. Our results reaffirm the irreplaceable conservation value of mature primary forests and early-seral habitat, and emphasize the importance of landscape management strategies that integrate both late-successional reserves and structurally-enriched managed stands. Experimental prescriptions that restore in-stand structural and compositional heterogeneity and retain key habitat features may offer promising pathways toward further integrating these two objectives, but warrant careful monitoring for unintended consequences.

2.6 ACKNOWLEDGEMENTS

Funding for this study was provided by the Future Rivers National Science Foundation program, the School of Aquatic and Fishery Sciences, University of Washington, and the Earthwatch Institute. We thank Jeffrey Ricklefs and Warren Devine for their assistance in procuring Washington State Department of Natural Resources (WADNR) remotely sensed forest resource inventory system data, Travis West and Kristopher Bryan for their assistance in validating

species detections, and all WADNR technicians that conducted habitat surveys and autonomous recording unit deployments. We also thank Sarah Converse, Beth Gardner, and Joshua Lawler for their guidance in formal analysis. Attributions for photos and graphical elements used in figures can be found in Appendix 2.1.

2.7 Data availability

All data and code required to reproduce the results of the study are available at the open-source repository github.com/giojacuzzi/avian-acoustic-monitoring-oesf. Remote sensing data were obtained from the Washington State Department of Natural Resources Forest Resource Inventory (WADNR, 2026).

2.8 REFERENCES

Addicott, John F., John M. Aho, Michael F. Antolin, Dianna K. Padilla, John S. Richardson, and Daniel A. Soluk. 1987. “Ecological Neighborhoods: Scaling Environmental Patterns.” Oikos 49 (3): 340–46. https://doi.org/10.2307/3565770.

Arcilla, Nico, and Māris Strazds. 2023. “Ten Principles for Bird-Friendly Forestry: Conservation Approaches in Natural Forests Used for Timber Production.” Birds 4 (2): 245–61. https://doi.org/10.3390/birds4020021.

Arroyo-Rodríguez, Víctor, Lenore Fahrig, Marcelo Tabarelli, et al., 2020. “Designing Optimal Human-Modified Landscapes for Forest Biodiversity Conservation.” Ecology Letters 23 (9): 1404–20. https://doi.org/10.1111/ele.13535.

Baselga, Andrés. 2013. “Separating the Two Components of Abundance-Based Dissimilarity: Balanced Changes in Abundance vs. Abundance Gradients.” Methods in Ecology and Evolution 4 (6): 552–57. https://doi.org/10.1111/2041-210X.12029.

Basile, Marco. 2022. “Rare Species Disproportionally Contribute to Functional Diversity in Managed Forests.” Scientific Reports 12 (April): 5897. https://doi.org/10.1038/s41598-022-09624-9.

Battin, James. 2004. “When Good Animals Love Bad Habitats: Ecological Traps and the Conservation of Animal Populations.” Conservation Biology 18 (6): 1482–91. https://doi.org/10.1111/j.1523-1739.2004.00417.x.

Battin, James, and Joshua J. Lawler. 2006. “Cross-Scale Correlations and the Design and Analysis of Avian Habitat Selection Studies.” The Condor: Ornithological Applications 108 (1): 59–70. https://doi.org/10.1093/condor/108.1.59.

Betts, Matthew G., Benjamin T. Phalan, Christopher Wolf, et al., 2021. “Producing Wood at Least Cost to Biodiversity: Integrating Triad and Sharing–Sparing Approaches to Inform Forest Landscape Management.” Biological Reviews 96 (4): 1301–17. https://doi.org/10.1111/brv.12703.

Betts, Matthew G., Christopher Wolf, William J. Ripple, et al., 2017. “Global Forest Loss Disproportionately Erodes Biodiversity in Intact Landscapes.” Nature 547 (7664): 441–44. https://doi.org/10.1038/nature23285.

Betts, Matthew G., Zhiqiang Yang, Adam S. Hadley, et al., 2022. “Forest Degradation Drives Widespread Avian Habitat and Population Declines.” Nature Ecology & Evolution 6 (6): 709–19. https://doi.org/10.1038/s41559-022-01737-8.

Biggs, Christopher R., Lauren A. Yeager, Derek G. Bolser, et al., 2020. “Does Functional Redundancy Affect Ecological Stability and Resilience? A Review and Meta-Analysis.” Ecosphere 11 (7): e03184. https://doi.org/10.1002/ecs2.3184.

Billerman, S. M., B. K. Keeney, G. M. Kirwan, F. Medrano, N. D. Sly, and M. G. Smith. 2026. “Birds of the World.” Cornell Laboratory of Ornithology. https://doi.org/10.2173/bow.

Brewster, Jerome P., and Theodore R. Simons. 2009. “Testing the Importance of Auditory Detections in Avian Point Counts.” Journal of Field Ornithology 80 (2): 178–82. https://doi.org/10.1111/j.1557-9263.2009.00220.x.

Broms, Kristin M., Mevin B. Hooten, and Ryan M. Fitzpatrick. 2016. “Model Selection and Assessment for Multi-Species Occupancy Models.” Ecology 97 (7): 1759–70.

Brown, E. R. 1985. Management of Wildlife and Fish Habitats in Forests of Western Oregon and Washington. PB-94-188075/XAB. U.S. Department of Agriculture, Forest Service. https://www.osti.gov/biblio/7110353.

Bryant, Andrew A., Jean-Pierre L. Savard, and Ronal T. McLaughlin. 1993. Avian Communities in Old-Growth and Managed Forests of Western Vancouver Island British Columbia. No. 167. Canadian Wildlife Service. https://publications.gc.ca/collections/collection_2018/eccc/cw69-5/CW69-5-167-eng.pdf.

Bull, Evelyn L., and Roy C. Beckwith. 1993. “Diet and Foraging Behavior of Vaux’s Swifts in Northeastern Oregon.” The Condor 95 (4): 1016–23. https://doi.org/10.2307/1369437.

Burivalova, Zuzana, Tien Ming Lee, Xingli Giam, Çağan Hakkı Şekercioğlu, David S. Wilcove, and Lian Pin Koh. 2015. “Avian Responses to Selective Logging Shaped by Species Traits and Logging Practices.” Proceedings of the Royal Society B: Biological Sciences 282 (1808): 20150164. https://doi.org/10.1098/rspb.2015.0164.

Cadotte, Marc W., Kelly Carscadden, and Nicholas Mirotchnick. 2011. “Beyond Species: Functional Diversity and the Maintenance of Ecological Processes and Services.” Journal of Applied Ecology 48 (5): 1079–87. https://doi.org/10.1111/j.1365-2664.2011.02048.x.

Cahall, Rebecca E., John P. Hayes, and Matthew G. Betts. 2013. “Will They Come? Long-Term Response by Forest Birds to Experimental Thinning Supports the ‘Field of Dreams’

Hypothesis." Forest Ecology and Management 304 (September): 137–49. https://doi.org/10.1016/j.foreco.2013.04.042.

Carey, A. B. 2003. "Biocomplexity and Restoration of Biodiversity in Temperate Coniferous Forest: Inducing Spatial Heterogeneity with Variable-Density Thinning." Forestry 76 (2): 127–36. https://doi.org/10.1093/forestry/76.2.127.

Chambers, Carol L., William C. McComb, and John C. Tappeiner II. 1999. "Breeding Bird Responses to Three Silvicultural Treatments in the Oregon Coast Range." Ecological Applications 9 (1): 171–85. https://doi.org/10.1890/1051-0761(1999)009%255B0171:BBRTTS%255D2.0.CO;2.

Chandler, Carlin C., David I. King, and Richard B. Chandler. 2012. "Do Mature Forest Birds Prefer Early-Successional Habitat during the Post-Fledging Period?" Forest Ecology and Management 264 (January): 1–9. https://doi.org/10.1016/j.foreco.2011.09.018.

Claramunt, Santiago. 2021. "Flight Efficiency Explains Differences in Natal Dispersal Distances in Birds." Ecology 102 (9): e03442. https://doi.org/10.1002/ecy.3442.

Cody, Martin L. 1985. Habitat Selection in Birds. Academic Press. https://shop.elsevier.com/books/habitat-selection-in-birds/cody/978-0-12-178080-7.

Cole, Jerry S., Nicole L. Michel, Shane A. Emerson, and Rodney B. Siegel. 2022. "Automated Bird Sound Classifications of Long-Duration Recordings Produce Occupancy Model Outputs Similar to Manually Annotated Data." Ornithological Applications 124 (2): duac003. https://doi.org/10.1093/ornithapp/duac003.

Connell, Joseph H. 1978. "Diversity in Tropical Rain Forests and Coral Reefs." Science 199 (4335): 1302–10. https://doi.org/10.1126/science.199.4335.1302.

Cushman, Samuel A., and Kevin McGarigal. 2003. "Landscape-Level Patterns of Avian Diversity in the Oregon Coast Range." Ecological Monographs. 73(2): 259-281., 259–81. https://doi.org/10.1890/0012-9615(2003)073%255B0259:lpoadi%255D2.0.co;2.

Cushman, Samuel A., and Kevin McGarigal. 2004. "Hierarchical Analysis of Forest Bird Species–Environment Relationships in the Oregon Coast Range." Ecological Applications 14 (4): 1090–105. https://doi.org/10.1890/03-5131.

Darras, Kevin, Péter Batáry, Brett Furnas, et al., 2018. "Comparing the Sampling Performance of Sound Recorders versus Point Counts in Bird Surveys: A Meta-Analysis." Journal of Applied Ecology 55 (6): 2575–86. https://doi.org/10.1111/1365-2664.13229.

DeMeo, Tom, Ryan Haugo, Chris Ringo, et al., 2018. “Expanding Our Understanding of Forest Structural Restoration Needs in the Pacific Northwest.” Northwest Science 92 (1): 18–35. https://doi.org/10.3955/046.092.0104.

Donato, Daniel C., John L. Campbell, and Jerry F. Franklin. 2012. “Multiple Successional Pathways and Precocity in Forest Development: Can Some Forests Be Born Complex?” Journal of Vegetation Science 23 (3): 576–84. https://doi.org/10.1111/j.1654-1103.2011.01362.x.

Dorazio, Robert M., and J. Andrew Royle. 2005. “Estimating Size and Composition of Biological Communities by Modeling the Occurrence of Species.” Journal of the American Statistical Association 100 (470): 389–98. https://doi.org/10.1198/016214505000000015.

Duflot, Rémi, Lenore Fahrig, and Mikko Mönkkönen. 2022. “Management Diversity Begets Biodiversity in Production Forest Landscapes.” Biological Conservation 268 (April): 109514. https://doi.org/10.1016/j.biocon.2022.109514.

Dugger, Katie M., Eric D. Forsman, Alan B. Franklin, et al., 2016. “The Effects of Habitat, Climate, and Barred Owls on Long-Term Demography of Northern Spotted Owls.” The Condor: Ornithological Applications 118 (1): 57–116. https://doi.org/10.1650/CONDOR-15-24.1.

Ene, Eduard, and Kevin McGarigal. 2023. “FragStats.” FragStats. https://fragstats.org/index.php/fragstats-metrics/patch-based-metrics/area-and-edge-metrics.

Food and Agriculture Organization and the United Nations Environment Programme. 2020. The State of the World’s Forests 2020. Forests, Biodiversity and People. The State of the World’s Forests (SOFO) 2020. FAO and UNEP. https://doi.org/10.4060/ca8642en.

Fink, D., A. Johnston, M. Strimas-Mackey, et al., 2025. “eBird Status and Trends, Data Version: 2023.” eBird Status and Trends, Cornell Lab of Ornithology. https://doi.org/10.2173/WZTW8903.

Forest Ecosystem Management Assessment Team. 1993. Forest Ecosystem Management: An Ecological, Economic, and Social Assessment. https://www.fs.usda.gov/r6/reo/library/downloads/documents/FEMAT-1993-Report.pdf.

Franklin, Jerry F., and Daniel C. Donato. 2020. “Variable Retention Harvesting in the Douglas-Fir Region.” Ecological Processes 9 (1): 8. https://doi.org/10.1186/s13717-019-0205-5.

Franklin, Jerry F., and K. Norman Johnson. 2012. “A Restoration Framework for Federal Forests in the Pacific Northwest.” Journal of Forestry 110 (8): 429–39. https://doi.org/10.5849/jof.10-006.

Franklin, Jerry F., K. Norman Johnson, and Deborah L. Johnson. 2018. Ecological Forest Management. Waveland Press. https://www.waveland.com/browse.php?t=730.

Franklin, Jerry F., Thomas A. Spies, Robert Van Pelt, et al., 2002. “Disturbances and Structural Development of Natural Forest Ecosystems with Silvicultural Implications, Using Douglas-Fir Forests as an Example.” Forest Ecology and Management, Forest Ecology in the next Millennium : Putting the long view into Practice, vol. 155 (1): 399–423. https://doi.org/10.1016/S0378-1127(01)00575-8.

Galitsky, Christina, and Joshua J. Lawler. 2015. “Relative Influence of Local and Landscape Factors on Bird Communities Vary by Species and Functional Group.” Landscape Ecology 30 (2): 287–99. https://doi.org/10.1007/s10980-014-0138-4.

Grantham, H. S., A. Duncan, T. D. Evans, et al., 2020. “Anthropogenic Modification of Forests Means Only 40% of Remaining Forests Have High Ecosystem Integrity.” Nature Communications 11 (1): 5978. https://doi.org/10.1038/s41467-020-19493-3.

Hagar, Joan C. 2007. “Wildlife Species Associated with Non-Coniferous Vegetation in Pacific Northwest Conifer Forests: A Review.” Forest Ecology and Management, Biodiversity Management in Pacific Northwest Forests: Strategies and Opportunities., vol. 246 (1): 108–22. https://doi.org/10.1016/j.foreco.2007.03.054.

Hagar, Joan, Shay Howlin, and Lisa Ganio. 2004. “Short-Term Response of Songbirds to Experimental Thinning of Young Douglas-Fir Forests in the Oregon Cascades.” Forest Ecology and Management 199 (2): 333–47. https://doi.org/10.1016/j.foreco.2004.05.054.

Hamer, Thomas E., Eric D. Forsman, and Elizabeth M. Glenn. 2007. “Home Range Attributes and Habitat Selection of Barred Owls and Spotted Owls in an Area of Sympatry.” The Condor 109 (4): 750–68. https://doi.org/10.1650/0010-5422(2007)109%255B750:HRAAHS%255D2.0.CO;2.

Hanle, Juliana, Marlyse C. Duguid, and Mark S. Ashton. 2020. “Legacy Forest Structure Increases Bird Diversity and Abundance in Aging Young Forests.” Ecology and Evolution 10 (3): 1193–208. https://doi.org/10.1002/ece3.5967.

Hansen, Andrew J., William C. McComb, Robyn Vega, Martin G. Raphael, and Matthew Hunter. 1995. “Bird Habitat Relationships in Natural and Managed Forests in the West Cascades of Oregon.” Ecological Applications 5 (3): 555–69. https://doi.org/10.2307/1941966.

Hansen, M. C., P. V. Potapov, R. Moore, et al., 2013. “High-Resolution Global Maps of 21st-Century Forest Cover Change.” Science 342 (6160): 850–53. https://doi.org/10.1126/science.1244693.

Hillebrand, Helmut, Bernd Blasius, Elizabeth T. Borer, et al., 2018. “Biodiversity Change Is Uncoupled from Species Richness Trends: Consequences for Conservation and Monitoring.” Journal of Applied Ecology 55 (1): 169–84. https://doi.org/10.1111/1365-2664.12959.

Ibarra, José Tomás, Michaela Martin, Kristina L. Cockle, and Kathy Martin. 2017. “Maintaining Ecosystem Resilience: Functional Responses of Tree Cavity Nesters to Logging in Temperate Forests of the Americas.” Scientific Reports 7 (1): 4467. https://doi.org/10.1038/s41598-017-04733-2.

Jacuzzi, Giordano, and Julian D. Olden. 2025. “Few-Shot Transfer Learning Enables Robust Acoustic Monitoring of Wildlife Communities at the Landscape Scale.” Ecological Informatics 90 (December): 103294. https://doi.org/10.1016/j.ecoinf.2025.103294.

Jones, Gavin M., Berry Brosi, Jason M. Evans, et al., 2022. “Conserving Alpha and Beta Diversity in Wood-Production Landscapes.” Conservation Biology: The Journal of the Society for Conservation Biology 36 (3): e13872. https://doi.org/10.1111/cobi.13872.

Jones, Jason. 2001. “Habitat Selection Studies in Avian Ecology: A Critical Review.” The Auk 118 (2): 557–62. https://doi.org/10.1093/auk/118.2.557.

Jürgensen, C., W. Kollert, and A. Lebedys. 2014. Assessment of Industrial Roundwood Production from Planted Forests. FAO Planted Forests and Trees Working Paper FP/48/E. Food and Agriculture Organization of the United Nations.

K. Lisa Yang Center for Conservation Bioacoustics at the Cornell Lab of Ornithology. 2026. Raven Pro: Interactive Sound Analysis Software (Version 1.6.5). The Cornell Lab of Ornithology, released. https://www.ravensoundsoftware.com/.

Kahl, Stefan, Connor M. Wood, Maximilian Eibl, and Holger Klinck. 2021. “BirdNET: A Deep Learning Solution for Avian Diversity Monitoring.” Ecological Informatics 61 (March): 101236. https://doi.org/10.1016/j.ecoinf.2021.101236.

Kellner, Ken, and Mike Meredith. 2026. jagsUI: A Wrapper Around “rjags” to Streamline “JAGS” Analyses. V. 1.6.3. Released January 10. https://cran.r-project.org/web/packages/jagsUI/index.html.

Kremsater, Laurie, and Fred Bunnell. 1999. “Edge Effects: Theory, Evidence and Implications to Management of Western North American Forests.” Forest Fragmentation: Wildlife and Management Implications, January 1, 117–53.

Kuehne, L., L. Giannone, C. Zwierzynski. 2019. Comparison of Songmeter4, AudioMoth, and Swift recording units in forested and clear-cut areas. Unpublished Report.

Legendre, Pierre. 2014. “Interpreting the Replacement and Richness Difference Components of Beta Diversity.” Global Ecology and Biogeography 23 (11): 1324–34. https://doi.org/10.1111/geb.12207.

Lindenmayer, D. B., J. F. Franklin, and J. Fischer. 2006. “General Management Principles and a Checklist of Strategies to Guide Forest Biodiversity Conservation.” Biological Conservation 131 (3): 433–45. https://doi.org/10.1016/j.biocon.2006.02.019.

Lindenmayer, David B., and Jerry F. Franklin. 2002. Conserving Forest Biodiversity: A Comprehensive Multi-Scaled Approach. Island Press. https://andrewsforest.oregonstate.edu/publications/3559.

Liu, Canran, Pam M. Berry, Terence P. Dawson, and Richard G. Pearson. 2005. “Selecting Thresholds of Occurrence in the Prediction of Species Distributions.” Ecography 28 (3): 385–93. https://doi.org/10.1111/j.0906-7590.2005.03957.x.

Loiseau, Nicolas, Wilfried Thuiller, Rick D. Stuart-Smith, et al., 2021. “Maximizing Regional Biodiversity Requires a Mosaic of Protection Levels.” PLOS Biology 19 (5): e3001195. https://doi.org/10.1371/journal.pbio.3001195.

Lorenz, Teresa, Martin G. Raphael, Richard D. Young, Deanna Lynch, S. Kim Nelson, and William R. McIver. 2021. Status and Trend of Nesting Habitat for the Marbled Murrelet under the Northwest Forest Plan, 1993 to 2017. U.S. Department of Agriculture, Forest Service, Pacific Northwest Research Station. https://research.fs.usda.gov/treesearch/63314.

MacArthur, Robert H., and John W. MacArthur. 1961. “On Bird Species Diversity.” Ecology 42 (3): 594–98. https://doi.org/10.2307/1932254.

MacKenzie, Darryl I., James D. Nichols, Gideon B. Lachman, Sam Droege, J. Andrew Royle, and Catherine A. Langtimm. 2002. “Estimating Site Occupancy Rates When Detection Probabilities Are Less Than One.” Ecology 83 (8): 2248–55. https://doi.org/10.1890/0012-9658(2002)083%255B2248:ESORWD%255D2.0.CO;2.

Mackenzie, Darryl I., and J. Andrew Royle. 2005. “Designing Occupancy Studies: General Advice and Allocating Survey Effort.” Journal of Applied Ecology 42 (6): 1105–14. https://doi.org/10.1111/j.1365-2664.2005.01098.x.

Mannan, R. William. 1980. Assembalges of Bird Species in Western Coniferous Old-Growth Forests. INT-GTR-86. Workshop Proceedings: Management of Western Forests and Grasslands for Nongame Birds. U.S. Department of Agriculture, Forest Service, Intermountain Forest and Range Experiment Station. https://doi.org/10.2737/INT-GTR-86.

Martin, Thomas E. 1995. “Avian Life History Evolution in Relation to Nest Sites, Nest Predation, and Food.” Ecological Monographs 65 (1): 101–27. https://doi.org/10.2307/2937160.

Martins, Frederico Carvalho, Pedro Segurado, and João Tiago Marques. 2025. “Acoustic Detection and Occupancy Models: A Systematic Review with Insights for Future Monitoring Programs.” Ecological Indicators 179 (October): 114081. https://doi.org/10.1016/j.ecolind.2025.114081.

Marzluff, John M., Martin G. Raphael, and Rex Sallabanks. 2000. “Understanding the Effects of Forest Management on Avian Species.” Wildlife Society Bulletin (1973-2006) 28 (4): 1132–43.

Mason, Norman W. H., David Mouillot, William G. Lee, and J. Bastow Wilson. 2005. “Functional Richness, Functional Evenness and Functional Divergence: The Primary Components of Functional Diversity.” Oikos 111 (1): 112–18. https://doi.org/10.1111/j.0030-1299.2005.13886.x.

Maxwell, Sean L., Victor Cazalis, Nigel Dudley, et al., 2020. “Area-Based Conservation in the Twenty-First Century.” Nature 586 (7828): 217–27. https://doi.org/10.1038/s41586-020-2773-z.

McGarigal, Kevin, and William C. McComb. 1995. “Relationships Between Landscape Structure and Breeding Birds in the Oregon Coast Range.” Ecological Monographs 65 (3): 235–60. https://doi.org/10.2307/2937059.

Meyer, Carolyn B., Sherri L. Miller, and C. John Ralph. 2002. “Multi-Scale Landscape and Seascape Patterns Associated with Marbled Murrelet Nesting Areas on the U.S. West Coast.” Landscape Ecology 17 (2): 95–115. https://doi.org/10.1023/A:1016574928706.

Minkova, Teodora V., Lauren M. Kuehne, and Daniel Donato. 2020. Using Passive Acoustic Monitoring to Evaluate Sustainability of Forest Management. Study Plan. Washington State Department of Natural Resources. https://www.dnr.wa.gov/publications/lm_oesf_pac_sp.pdf.

Minkova, Teodora V., Tracy Petroske, Bill Wells, Bernard Bormann, and Courtney Bobsin. 2024. T3 Watershed Experiment in the Olympic Experimental State Forest 2016-2023 Implementation Report. Washington State Department of Natural Resources. https://www.dnr.wa.gov/publications/lm_oesf_t3_imp_rpt.pdf.

Mouillot, David, David R. Bellwood, Christopher Baraloto, et al., 2013. “Rare Species Support Vulnerable Functions in High-Diversity Ecosystems.” PLoS Biology 11 (5): e1001569. https://doi.org/10.1371/journal.pbio.1001569.

National Agriculture Imagery Program. 2026. “USGS EROS Archive - Aerial Photography.” U.S. Geological Survey. https://www.usgs.gov/centers/eros/science/usgs-eros-archive-aerial-photography-national-agriculture-imagery-program-naip.

Noble, Ciar D., Carlos A. Peres, and James J. Gilroy. 2024. “Accounting for Imperfect Detection When Estimating Species-area Relationships and Beta-diversity.” Ecology and Evolution 14 (7): e70017. https://doi.org/10.1002/ece3.70017.

North American Bird Conservation Initiative. 2025. State of the Birds. https://www.stateofthebirds.org/2025.

Northrup, Joseph M., and Brian D. Gerber. 2018. “A Comment on Priors for Bayesian Occupancy Models.” PLOS ONE 13 (2): e0192819. https://doi.org/10.1371/journal.pone.0192819.

Nott, M. Philip, David F. Desante, Peter Pyle, and Nicole Michel. 2005. Pacific Northwest Forest Bird Population Declines: Formulating Population Management Guidelines from

Landscape-Scale Ecological Analyses of MAPS Data from Avian Communities on Seven National Forests in the Pacific Northwest. The Institute for Bird Populations.

Oksanen, Jari, Gavin L. Simpson, F. Guillaume Blanchet, et al., 2026. Vegan: Community Ecology Package. V. 2.7-3. Released March 4. https://cran.r-project.org/web/packages/vegan/index.html.

Oliver, Chadwick Dearing. 1980. "Forest Development in North America Following Major Disturbances." Forest Ecology and Management 3 (January): 153–68. https://doi.org/10.1016/0378-1127(80)90013-4.

Oswalt, Sonja, W. Brad Smith, Patrick D. D. Miles, and Scott A. Pugh. 2019. "Forest Resources of the United States, 2017: A Technical Document Supporting the Forest Service 2020 RPA Assessment." Gen. Tech. Rep. WO-97. Washington, DC: U.S. Department of Agriculture, Forest Service, Washington Office. 97. https://doi.org/10.2737/WO-GTR-97.

Pacifici, Krishna, Elise F. Zipkin, Jaime A. Collazo, Julissa I. Irizarry, and Amielle DeWan. 2014. "Guidelines for a Priori Grouping of Species in Hierarchical Community Models." Ecology and Evolution 4 (7): 877–88. https://doi.org/10.1002/ece3.976.

Partners in Flight Databases. 2026. Avian Conservation Assessment Database Scores. https://pif.birdconservancy.org/avian-conservation-assessment-database-scores/.

Peery, M. Zach, and Gavin M. Jones. 2016. "Using Population Viability Analyses to Assess the Potential Effects of Washington DNR Forest Management Alternatives on Marbled Murrelets." Washington State Department of Natural Resources.

Petersson, Lisa, Delphine Lariviere, Emma Holmström, Matts Lindbladh, and Adam Felton. 2023. "Potential Implications of Shortened Rotation Length for Forest Birds, Bryophytes, Lichens and Vascular Plants: An Example from Southern Swedish Production Forests." PLOS ONE 18 (12): e0289835. https://doi.org/10.1371/journal.pone.0289835.

Phalan, Benjamin T., Joseph M. Northrup, Zhiqiang Yang, et al., 2019. "Impacts of the Northwest Forest Plan on Forest Composition and Bird Populations." Proceedings of the National Academy of Sciences 116 (8): 3322–27. https://doi.org/10.1073/pnas.1813072116.

Platt, John. 2000. "Probabilistic Outputs for Support Vector Machines and Comparisons to Regularized Likelihood Methods." Adv. Large Margin Classif. 10 (June).

Plummer, Martyn. 2023. “JAGS - Just Another Gibbs Sampler.” https://mcmc-jags.sourceforge.io/.

Powell, David C. 2012. A Stage Is A Stage Is A Stage…Or Is It? Successional Stages, Structural Stages, Seral Stages. Nos. F14-SO-WP-SILV-10. USDA Forest Service.

Price, Karen, Kiri Daust, Erica Lilles, and Anne-Marie Roberts. 2020. “Long-Term Response of Forest Bird Communities to Retention Forestry in Northern Temperate Coniferous Forests.” Forest Ecology and Management 462 (April): 117982. https://doi.org/10.1016/j.foreco.2020.117982.

Puettmann, Klaus J., K. David Coates, and Christian Messier. 2009. A Critique of Silviculture: Managing for Complexity. Island Press. https://legado.moodle.ufsc.br/pluginfile.php/1935344/mod_resource/content/1/Klaus%20J%20Puettmann_%20K%20%20Dave%20Coates_%20Christian%20C%20Messier-A%20critique%20of%20silviculture%20_%20managing%20for%20complexity-Island%20Press%20%20%282009%29.pdf.

Raley, Cathy, and K. B. Aubry. 2006. “Foraging Ecology of Pileated Woodpeckers in Coastal Forests of Washington.” The Journal of Wildlife Management. 70(5): 1266-1275. https://research.fs.usda.gov/treesearch/29698.

Raphael, Martin G. 2006. “Conservation of the Marbled Murrelet under the Northwest Forest Plan.” Conservation Biology 20 (2): 297–305. https://doi.org/10.1111/j.1523-1739.2006.00382.x.

Ricklefs, Jeffrey. 2026. Remotely Sensed Forest Resource Inventory System (RS-FRIS). Washington State Department of Natural Resources. Unpublished report.

Ripper, Dana, James C. Bednarz, and Daniel E. Varland. 2007. “Landscape Use by Hairy Woodpeckers in Managed Forests of Northwestern Washington.” The Journal of Wildlife Management 71 (8): 2612–23. https://doi.org/10.2193/2005-487.

Rosenberg, Kenneth V., Adriaan M. Dokter, Peter J. Blancher, et al., 2019. “Decline of the North American Avifauna.” Science 366 (6461): 120–24. https://doi.org/10.1126/science.aaw1313.

Rugg, Natalie M., Cara L. Appel, Julianna M. A. Jenkins, Chris McCafferty, Taal Levi, and Damon B. Lesmeister. 2025. “Decoding Owl Calls: Refining Occupancy Inference From

Passive Acoustic Monitoring." Ecology and Evolution 15 (10): e72255. https://doi.org/10.1002/ece3.72255.

Ruggiero, Leonard F., Keith B. Aubry PhD, Andrew B. Carey, and Mark H. Huff. 1991. "Wildlife and Vegetation of Unmanaged Douglas-Fir Forests." Gen. Tech. Rep. PNW-GTR-285. Portland, OR: U.S. Department of Agriculture, Forest Service, Pacific Northwest Research Station. 533 p 285. https://doi.org/10.2737/PNW-GTR-285.

Sallabanks, Rex, and Edward B. Arnett. 2005. "Accommodating Birds in Managed Forests of North America: A Review of Bird-Forestry Relationships." In: Ralph, C. John; Rich, Terrell D., Editors 2005. Bird Conservation Implementation and Integration in the Americas: Proceedings of the Third International Partners in Flight Conference. 2002 March 20-24; Asilomar, California, Volume 1 Gen. Tech. Rep. PSW-GTR-191. Albany, CA: U.S. Dept. of Agriculture, Forest Service, Pacific Southwest Research Station: P. 345-372 191. https://research.fs.usda.gov/treesearch/31705.

Sallabanks, Rex, Edward B. Arnett, and John M. Marzluff. 2000. "An Evaluation of Research on the Effects of Timber Harvest on Bird Populations." Wildlife Society Bulletin (1973-2006) 28 (4): 1144–55.

Sauer, John R., Peter J. Blank, Elise F. Zipkin, Jane E. Fallon, and Frederick W. Fallon. 2013. "Using Multi-Species Occupancy Models in Structured Decision Making on Managed Lands." The Journal of Wildlife Management 77 (1): 117–27. https://doi.org/10.1002/jwmg.442.

Sekercioglu, Cagan H. 2006. "Increasing Awareness of Avian Ecological Function." Trends in Ecology & Evolution 21 (8): 464–71. https://doi.org/10.1016/j.tree.2006.05.007.

Sekercioglu, Cagan H., Gretchen C. Daily, and Paul R. Ehrlich. 2004. "Ecosystem Consequences of Bird Declines." Proceedings of the National Academy of Sciences of the United States of America 101 (52): 18042–47. https://doi.org/10.1073/pnas.0408049101.

Shonfield, Julia, and Erin Bayne. 2017. "Avian Conservation and Ecology: Autonomous Recording Units in Avian Ecological Research: Current Use and Future Applications." Avian Conservation and Ecology 12 (1). https://doi.org/10.5751/ACE-00974-120114.

Simberloff, D., and T. Dayan. 1991. "The Guild Concept and the Structure of Ecological Communities." Annual Review of Ecology, Evolution, and Systematics 22 (Volume 22, 1991): 115–43. https://doi.org/10.1146/annurev.es.22.110191.000555.

Socolar, Jacob B., James J. Gilroy, William E. Kunin, and David P. Edwards. 2016. “How Should Beta-Diversity Inform Biodiversity Conservation?” Trends in Ecology & Evolution 31 (1): 67–80. https://doi.org/10.1016/j.tree.2015.11.005.

Spies, Thomas, Paul F. Hessburg PhD, Carl N. Skinner, et al., 2018. “Chapter 3: Old Growth, Disturbance, Forest Succession, and Management in the Area of the Northwest Forest Plan.” In: Spies, T.A.; Stine, P.A.; Gravenmier, R.; Long, J.W.; Reilly, M.J., Tech. Coords. 2018. Synthesis of Science to Inform Land Management within the Northwest Forest Plan Area. Gen. Tech. Rep. PNW-GTR-966. Portland, OR: U.S. Department of Agriculture, Forest Service, Pacific Northwest Research Station: 95-243. 966: 95–243.

Stokely, Thomas D., Urs G. Kormann, Jake Verschuyl, et al., 2022. “Experimental Evaluation of Herbicide Use on Biodiversity, Ecosystem Services and Timber Production Trade-Offs in Forest Plantations.” Journal of Applied Ecology 59 (1): 52–66. https://doi.org/10.1111/1365-2664.13936.

Swanson, Mark E., Nichole M. Studevant, John L. Campbell, and Daniel C. Donato. 2014. “Biological Associates of Early-Seral Pre-Forest in the Pacific Northwest.” Forest Ecology and Management 324 (July): 160–71. https://doi.org/10.1016/j.foreco.2014.03.046.

Thomas, Jack Ward, Eric D. Forsman, Joseph B. Lint, E. Charles Meslow, Barry B. Noon, and Jared Verner. 1990. A Conservation Strategy for the Northern Spotted Owl. Interagency Scientific Committee to Address the Conservation of the Northern Spotted Owl. https://www.fws.gov/media/conservation-strategy-northern-spotted-owl.

Thomas, Jack Ward, Jerry F. Franklin, John Gordon, and K. Norman Johnson. 2006. “The Northwest Forest Plan: Origins, Components, Implementation Experience, and Suggestions for Change.” Conservation Biology 20 (2): 277–87. https://doi.org/10.1111/j.1523-1739.2006.00385.x.

Thornton, Daniel H., and Robert J. Fletcher Jr. 2014. “Body Size and Spatial Scales in Avian Response to Landscapes: A Meta-Analysis.” Ecography 37 (5): 454–63. https://doi.org/10.1111/j.1600-0587.2013.00540.x.

Thornton, M. M., and R. Devarakonda. 2026. “Daymet: Daily Surface Weather Data on a 1-Km Grid for North America, Version 4 R1.” https://doi.org/10.3334/ORNLDAAC/2129.

Tittler, Rebecca, Christian Messier, and Rosa C. Goodman. 2016. “Triad Forest Management: Local Fix or Global Solution.” In Ecological Forest Management Handbook. CRC Press.

Tobias, Joseph A., Catherine Sheard, Alex L. Pigot, et al., 2022. “AVONET: Morphological, Ecological and Geographical Data for All Birds.” Ecology Letters 25 (3): 581–97. https://doi.org/10.1111/ele.13898.

Trzcinski, M. Kurtis, Kristina L. Cockle, Andrea R. Norris, Max Edworthy, Karen L. Wiebe, and Kathy Martin. 2022. “Woodpeckers and Other Excavators Maintain the Diversity of Cavity-Nesting Vertebrates.” Journal of Animal Ecology 91 (6): 1251–65. https://doi.org/10.1111/1365-2656.13626.

Turner, Monica G., and Robert H. Gardner. 2015. Landscape Ecology in Theory and Practice: Pattern and Process. Springer New York. https://doi.org/10.1007/978-1-4939-2794-4.

United States, Executive Office of the President. 2025. Immediate Expansion of American Timber Production – The White House. Executive Order 14225. https://www.whitehouse.gov/presidential-actions/2025/03/immediate-expansion-of-american-timber-production/.

Van Horne, B. 1983. “Density as a Misleading Indicator of Habitat Quality.” The Journal of Wildlife Management 47 (4): 893–901. https://doi.org/10.2307/3808148.

Vitz, Andrew C., and Amanda D. Rodewald. 2007. “Vegetative and Fruit Resources as Determinants of Habitat Use by Mature-Forest Birds During the Postbreeding Period.” The Auk 124 (2): 494–507. https://doi.org/10.1093/auk/124.2.494.

Washington State Department of Natural Resources. 1997. “Final Habitat Conservation Plan.” https://dnr.wa.gov/forest-resources/habitat-conservation-state-trust-lands.

Washington State Department of Natural Resources. 2026. “Raster All RS FRIS Rasters.” https://geo.wa.gov/maps/wadnr::raster-all-rs-fris-rasters/about.

Wells, K., R. B. O’Hara, S. M. Böhm, et al., 2012. “Trait-Dependent Occupancy Dynamics of Birds in Temperate Forest Landscapes: Fine-Scale Observations in a Hierarchical Multi-Species Framework.” Animal Conservation 15 (6): 626–37. https://doi.org/10.1111/j.1469-1795.2012.00560.x.

Whelan, Christopher J., Çagan H. Şekercioglu, and Daniel G. Wenny. 2015. “Why Birds Matter: From Economic Ornithology to Ecosystem Services.” Journal of Ornithology 156 (S1): 227–38. https://doi.org/10.1007/s10336-015-1229-y.

Wiens, J. A. 1989. “Spatial Scaling in Ecology.” Functional Ecology 3 (4): 385–97. https://doi.org/10.2307/2389612.

Wiens, John A. 1989. The Ecology of Bird Communities: Volume 2: Processes and Variations. Vol. 2. Cambridge Studies in Ecology. Cambridge University Press. https://doi.org/10.1017/CBO9780511608568.

Willis, John L., Scott D. Roberts, and Constance A. Harrington. 2018. “Variable Density Thinning Promotes Variable Structural Responses 14 years after Treatment in the Pacific Northwest.” Forest Ecology and Management 410 (February): 114–25. https://doi.org/10.1016/j.foreco.2018.01.006.

Wood, Connor M., and Stefan Kahl. 2024. “Guidelines for Appropriate Use of BirdNET Scores and Other Detector Outputs.” Journal of Ornithology 165 (3): 777–82. https://doi.org/10.1007/s10336-024-02144-5.

Zipkin, Elise F., J. Andrew Royle, Deanna K. Dawson, and Scott Bates. 2010. “Multi-Species Occurrence Models to Evaluate the Effects of Conservation and Management Actions.” Biological Conservation 143 (2): 479–84. https://doi.org/10.1016/j.biocon.2009.11.016.

2.9 APPENDIX 2.1

Artist attribution: Graphical elements used in figures are original photos and designs by the authors, provided by the Washington State Department of Natural Resources, or obtained under public domain from PhyloPic (Michael Keesey, 2025, phylopic.org), FlatIcon (Freepik Company, 2025, flaticon.com), and Vecteezy (Eezy LLC, 2026, vecteezy.com).

Table A2.1: Passive acoustic monitoring survey effort. Due to the limited availability of ARUs, a rotating deployment schedule was used to record acoustic data continuously (24 hours per day) at a site for up to 10 days. Survey effort is shown per breeding season (i.e., year) across survey dates, number of deployments, and recorded days out of total days per deployment, total recorded days across all sites, and total number of sites surveyed.

Season	Survey date range	Deployments	Rec. days of deployment	Total rec. days	Sites
2020	4/08 to 7/26	8	10/10	2080	200
2021	4/13 to 8/05	8	4/10	832	215
2022	5/22 to 7/27	3	4/10	208	32
2023	5/18 to 7/27	6	10/10	780	80

Table A2.2: Species-specific observations, bioacoustic classifier performance metrics, and detection methods. Naive site occurrence (N site) and survey detections (N detection) are shown across all years. The classifier submodel used within the ensemble is either "target" (OESF v1.0, Jacuzzi and Olden 2025) or "source" (BirdNET v2.4, Kahl et al., 2021). Validation N TP and N TN indicate the number of true positive and true negative samples used in calibration, respectively. Model performance is summarized with AUC PR, area under the precision-recall curve (1.0 is perfect, with no tradeoff between precision and recall, while 0.5 is akin to a random guess)—this metric is robust to imbalanced datasets, and is the preferred summary statistic for bioacoustic data; and also AUC ROC, area under the receiver operating curve, summarizing performance. This metric is provided as standard practice but is not robust to imbalanced data, and should not be exclusively relied upon to interpret performance. The threshold value indicates the prediction score threshold above which the probability of a true positive detection is ≥95%. Precision and recall report the validation dataset proportion of predicted positives that were true positives, and the proportion of true positives that were correctly predicted, respectively. Four detection methods are shown, such that "probabilistic" leverages logistic regression (Platt scaling) to determine the threshold at which Pr(TP)>=0.95. However, some classes cannot fit such a regression because they: (1) report perfect performance from our calibration data (the random sample contained no true negatives)—these classes default to (A) an optimized threshold that maximizes recall while maintaining perfect precision ("precision"), or (B) a naive threshold at the decision boundary 0.5 ("naive"), whichever threshold is higher; (2) report exceptionally poor performance (the random sample contained very few true positives)—these classes must be manually reviewed by a human to determine true presence/absence ("manual"); or (3) are very rare (there are not enough samples available to meaningfully evaluate performance)—these classes also must be manually reviewed by a human to determine true presence/absence ("manual").

Scientific name	Common name	N_site	N_detection	Model	N_TP	N_TN	AUC_PR	AUC_ROC	Threshold	Precision	Recall	Method
Corvus brachyrhynchos	American crow	47	90	source	101	3538	0.972	0.999	0.87	1	0.505	probabilistic
Spinus tristis	American goldfinch	29	38	source	105	3498	0.963	0.999	0.821	0.964	0.514	probabilistic
Turdus migratorius	American robin	224	3717	target	392	3295	0.934	0.984	0.467	0.995	0.518	probabilistic
Haliaeetus leucocephalus	Bald eagle	59	96	source	103	3508	0.993	1	0.758	1	0.816	precision
Patagioenas fasciata	Band-tailed pigeon	219	2178	target	126	3430	0.965	0.994	0.957	0.988	0.635	probabilistic
Hirundo rustica	Barn swallow	38	69	source	113	3474	0.998	1	0.583	1	0.967	precision
Strix varia	Barred owl	207	1492	target	145	3478	0.956	0.998	0.991	0.955	0.586	probabilistic
Megaceryle alcyon	Belted kingfisher	52	119	source	102	3574	0.958	0.998	0.982	0.984	0.598	probabilistic
Pheucticus melanocephalus	Black-headed grosbeak	182	762	source	104	3473	0.989	1	0.497	1	0.827	probabilistic
Setophaga nigrescens	Black-throated gray warbler	222	2547	target	148	3404	0.962	0.998	0.507	0.99	0.649	probabilistic
Certhia americana	Brown creeper	204	2182	source	171	3482	0.945	0.994	0.839	1	0.468	probabilistic
Molothrus ater	Brown-headed cowbird	2	2	source	23	3507	0.713	0.999	Inf	-	-	manual
Perisoreus canadensis	Canada jay	186	737	source	134	3497	0.975	1	0.436	1	0.724	probabilistic
Bombycilla cedrorum	Cedar waxwing	211	1483	source	505	3478	0.996	1	0.586	0.995	0.867	probabilistic
Poecile rufescens	Chestnut-backed chickadee	219	2562	source	109	3460	0.922	0.994	0.772	0.978	0.413	probabilistic
Petrochelidon pyrrhonota	Cliff swallow	2	3	source	3	3461	1	1	Inf	-	-	manual
Chordeiles minor	Common nighthawk	151	609	source	102	3462	0.998	1	0.814	0.989	0.902	probabilistic
Corvus corax	Common raven	224	3228	target	148	3390	0.981	0.995	0.743	1	0.811	probabilistic
Junco hyemalis	Dark-eyed junco	211	1980	target	111	3480	0.966	0.99	0.951	1	0.73	probabilistic
Dryobates pubescens	Downy woodpecker	10	22	source	40	3561	0.629	0.995	Inf	-	-	manual
Streptopelia decaocto	Eurasian collared-dove	1	1	source	39	3481	0.964	1	Inf	-	-	manual
Coccothraustes vespertinus	Evening grosbeak	224	2317	source	106	3452	0.99	1	0.531	0.976	0.783	probabilistic
Regulus satrapa	Golden-crowned kinglet	221	3403	target	322	3370	0.883	0.966	0.928	1	0.363	probabilistic
Zonotrichia atricapilla	Golden-crowned sparrow	17	48	source	102	3475	0.976	0.999	0.85	1	0.549	probabilistic
Bubo virginianus	Great horned owl	1	1	source	1	3517	0.002	0.94	Inf	-	-	manual
Dryobates villosus	Hairy woodpecker	222	2250	target	106	3416	0.97	0.998	0.95	0.987	0.736	probabilistic
Empidonax hammondii	Hammond's flycatcher	219	1609	source	106	3516	0.993	1	0.5	1	0.934	naive
Catharus guttatus	Hermit thrush	84	211	source	110	3512	0.959	0.997	0.734	0.976	0.373	probabilistic
Vireo huttoni	Hutton's vireo	223	2523	target	130	3391	0.964	0.998	0.799	1	0.662	probabilistic
Geothlypis tolmiei	Macgillivray's warbler	28	167	source	88	3537	0.968	0.999	0.924	1	0.523	probabilistic
Brachyramphus marmoratus	Marbled murrelet	46	53	target	135	3539	1	1	Inf	-	-	manual
Falco columbarius	Merlin	5	5	source	8	3508	0.974	1	Inf	-	-	manual
Colaptes auratus	Northern flicker	220	2304	target	106	3409	0.987	1	0.644	1	0.774	probabilistic
Accipiter gentilis	Northern goshawk	6	12	source	29	3522	0.797	0.998	Inf	-	-	manual
Glaucidium gnoma	Northern pygmy-owl	154	516	target	100	3497	0.968	0.999	0.7	0.955	0.64	probabilistic
Stelgidopteryx serripennis	Northern rough-winged swallow	8	12	source	42	3461	1	1	Inf	-	-	manual
Aegolius acadicus	Northern saw-whet owl	83	215	source	90	3503	0.969	0.999	0.976	0.983	0.633	probabilistic
Contopus cooperi	Olive-sided flycatcher	131	461	source	123	3507	0.994	1	0.597	0.99	0.837	probabilistic
Leiothlypis celata	Orange-crowned warbler	46	318	source	114	3494	0.913	0.979	0.86	0.933	0.368	probabilistic
Pandion haliaetus	Osprey	88	194	source	121	3469	1	1	0.585	1	1	precision
Troglodytes pacificus	Pacific wren	224	3653	target	252	3308	0.974	0.997	0.795	1	0.683	probabilistic
Empidonax difficilis	Western flycatcher	223	3357	target	384	3306	0.898	0.974	0.907	0.993	0.367	probabilistic
Dryocopus pileatus	Pileated woodpecker	204	1542	target	113	3475	0.991	1	0.949	0.978	0.788	probabilistic
Spinus pinus	Pine siskin	157	738	source	103	3473	0.968	0.999	0.608	0.983	0.573	probabilistic
Haemorhous purpureus	Purple finch	107	581	target	106	3460	0.989	0.999	0.942	1	0.811	probabilistic
Loxia curvirostra	Red crossbill	223	2496	target	103	3425	0.982	0.999	0.958	1	0.718	probabilistic
Sitta canadensis	Red-breasted nuthatch	216	1564	target	138	3514	0.988	0.999	0.966	0.991	0.768	probabilistic
Buteo jamaicensis	Red-tailed hawk	36	48	source	105	3580	0.899	0.998	0.926	1	0.379	probabilistic
Corthylio calendula	Ruby-crowned kinglet	31	80	source	105	3523	0.946	0.999	0.857	0.981	0.505	probabilistic
Bonasa umbellus	Ruffed grouse	1	2	source	75	3483	0.999	1	Inf	-	-	manual
Selasphorus rufus	Rufous hummingbird	117	516	target	123	3468	0.955	0.997	0.912	1	0.618	probabilistic
Accipiter striatus	Sharp-shinned hawk	66	92	source	117	3508	0.983	1	0.711	0.964	0.684	probabilistic
Melospiza melodia	Song sparrow	36	381	target	115	3457	0.956	0.999	0.924	0.978	0.774	probabilistic
Dendragapus fuliginosus	Sooty grouse	175	896	target	151	3455	0.755	0.949	0.987	0.973	0.238	probabilistic
Pipilo maculatus	Spotted towhee	127	597	target	103	3481	0.924	0.995	0.959	0.981	0.505	probabilistic
Cyanocitta stelleri	Steller's jay	224	2510	source	102	3429	0.901	0.99	0.624	1	0.382	probabilistic
Catharus ustulatus	Swainson's thrush	211	1732	target	118	3429	0.982	0.999	0.693	1	0.763	probabilistic
Myadestes townsendi	Townsend's solitaire	5	5	source	42	3520	0.982	1	Inf	-	-	manual
Setophaga townsendi	Townsend's warbler	175	739	target	119	3526	0.995	1	0.895	1	0.882	probabilistic
Tachycineta bicolor	Tree swallow	17	44	source	101	3500	0.989	1	0.833	1	0.723	probabilistic
Ixoreus naevius	Varied thrush	224	3723	target	569	3262	0.9	0.961	0.847	1	0.439	probabilistic
Chaetura vauxi	Vaux's swift	208	1629	source	105	3420	0.996	1	0.351	0.989	0.857	probabilistic
Tachycineta thalassina	Violet-green swallow	70	160	source	100	3494	0.995	1	0.787	0.989	0.88	probabilistic
Vireo gilvus	Warbling vireo	100	430	source	102	3480	0.988	1	0.518	0.988	0.804	probabilistic
Sialia mexicana	Western bluebird	7	8	source	10	3493	0.985	1	Inf	-	-	manual
Megascops kennicottii	Western screech-owl	75	180	source	93	3485	0.974	0.999	0.899	1	0.602	probabilistic
Piranga ludoviciana	Western tanager	216	1872	target	116	3457	0.968	0.997	0.962	1	0.69	probabilistic
Contopus sordidulus	Western wood-pewee	82	160	source	103	3511	0.99	1	0.641	1	0.748	probabilistic
Zonotrichia leucophrys	White-crowned sparrow	31	253	target	102	3529	0.99	0.998	0.729	1	0.941	probabilistic
Empidonax traillii	Willow flycatcher	22	102	source	102	3495	0.995	1	0.708	1	0.843	precision
Cardellina pusilla	Wilson's warbler	175	1022	target	100	3485	0.944	0.998	0.942	0.938	0.6	probabilistic
Setophaga petechia	Yellow warbler	5	7	source	74	3480	1	1	Inf	-	-	manual

Table A2.3: Local environmental variables selected for consideration as candidate predictors and associated ecological rationale from a literature review. Variables were quantified through habitat surveys and remote sensing geographic information system analysis.

Environmental variable(s)	Spatial scale	Category	Ecological rationale	References
Basal area	Plot	Structure	Indicates forest density and/or age, influencing light availability, vertical stratification, and bird foraging and nesting.	Cushman and McGarigal 2004, James and Shughart 1970
Quadratic mean diameter	Plot	Structure	Reflects average tree size and structural maturity; larger diameter trees provide bark substrates for foraging and nesting cavities.	Sallabanks and Arnett 2005, Cahall et al. 2013, Carey 2003, Hagar et al., 2004
Tree density	Plot	Structure	Reflects stand density and openness, competition for space and light, and availability of perching and nesting resources.	Burivalova et al. 2015, Cahall et al. 2013, Carey 2003, Hagar et al., 2004
Canopy closure, height	Plot	Structure	Affects foraging, sheltering, and nesting opportunities.	Sallabanks and Arnett 2005, MacArthur and MacArthur 1961, Cody 1985
Tree height distribution	Plot	Structure	Proxy for vertical vegetation complexity, may benefit microhabitat diversity and provide important structural features for birds; Increased vertical complexity allows for vertical stratification of foraging substrates and nesting opportunities	Shaw et al. 2002, Cody 1985, Sallabanks and Arnett 2005, Ruggiero et al. 1991
Tree species composition	Plot	Composition	Relative tree dominance reflects differences in bird resource availability.	Cushman and McGarigal 2004, Sallabanks and Arnett 2005, Ruggiero et al. 1991
Snag density	Plot	Structure	Features needed for territory defense, breeding, and/or nesting of bird species (e. g. cavities, perches).	Sallabanks and Arnett 2005, Martin 1995, Franklin & Donato 2020
Downed dead wood volume	Plot	Structure	Foraging and shelter for ground-foragers, insect prey availability for insectivores.	Sallabanks and Arnett 2005, Cody 1985, Price et al., 2020, Donato et al. 2012
Understory cover, composition	Plot	Structure, composition	Provides nesting sites for shrub-nesting species, foraging habitat for ground and shrub foragers, and shelter from predators.	Cushman and McGarigal 2004, Cody 1985, James and Shughart 1970, Martin 1995
Elevation	Plot	Abiotic	Influences climate and vegetation; substantial bird species turnover can occur along elevational gradients.	Irwin 1998, Cushman and McGarigal 2004, Sallabanks and Arnett 2005
Stand area	Stand	Composition	Larger patches may support species with larger home range sizes while reducing edge effects.	McGarigal et al. 2023, Cushman and McGarigal 2004, MacArthur and MacArthur 1961, Wiens 1989
Core area	Stand	Composition	Interior forest specialists rely on core habitat with minimal edge effects.	Sallabanks and Arnett 2005, Wiens 1989, Cody 1985, Kremsater & Bunnell 1999
Distance to edge	Stand	Configuration	Edge proximity is positively associated with generalists and negatively with interior specialists.	Sallabanks and Arnett 2005, Wiens 1989, Cody 1985, Kremsater & Bunnell 1999
Distance to nearest paved road	Landscape	Configuration	Habitat loss and edge effects from roads may benefit or hinder particular bird species.	Sallabanks and Arnett 2005, Cushman and McGarigal 2004, Cody 1985
Distance to nearest perennial fish-bearir	Landscape	Configuration	Riparian-dependent and insectivorous species may benefit from stream density.	Cushman and McGarigal 2004, Cody 1985, Ruggiero et al. 1991
Proportional abundance of cover class	Landscape	Composition	Increased availability of habitat associated with particular species preferences may benefit the use of those species.; greater forest patch types within an area may support unique ecological niches, can also indicate habitat fragmentation, patch heterogeneity.	McGarigal et al. 2023, Cushman and McGarigal 2004, May 1982, Turner & Gardner 2015
Aggregation, shape index	Landscape	Configuration	More complex patch shapes may increase edge habitat and use of associated species, as well as habitat heterogeneity.	Cushman and McGarigal 2004, McGarigal and McComb 1995, Turner & Gardner 2015
Contrast-weighted edge density	Landscape	Configuration	A relative measure of the amount of contrast along the patch perimeter, where high-contrast edges may restrict dispersal and promote edge effects; high edge density is positively associated with generalists and negatively with interior specialists, and can indicate habitat fragmentation.	Cushman and McGarigal 2004, McGarigal et al. 2023, Wiens 1989, Cody 1985

Table A2.4: Model selection results for home range size, including number of estimated parameters K, log-likelihood LL, Akaike Information Criterion corrected for small sample size AIC_c, difference from the best model's AIC_c, and weight.

Model	**K**	**LL**	**AIC_c**	**ΔAIC_c**	**Weight**
Mass	3	-157.18	321.6	0	0.81
Mass + HWI	4	-157.13	324.5	2.87	0.19
HWI	3	-164.35	336	14.35	0.001

Table A2.5: Multi-species occupancy model guild-level mean parameter estimates for effects on detection probability.

Grouping	Guild	Parameter	Variable	Estimate	SD
Community	All species	*μβ1,1*	Precipitation	-0.26 (-0.30, -0.21)	0.02
Community	All species	*μβ2,1*	Temperature	0.16 (0.10, 0.21)	0.03
Community	All species	*μβ3,1*	Day	-0.02 (-0.18, 0.14)	0.08
Community	All species	*μβ4,1*	Day (squared)	-0.22 (-0.35, -0.11)	0.06
Nesting	Cavity, primary	*μβ1,1*	Precipitation	-0.34 (-0.52, -0.15)	0.09
Nesting	Cavity, secondary	*μβ1,2*	Precipitation	-0.31 (-0.52, -0.11)	0.1
Nesting	Ground	*μβ1,3*	Precipitation	-0.11 (-0.20, -0.01)	0.05
Nesting	Shrub	*μβ1,4*	Precipitation	-0.19 (-0.36, -0.04)	0.08
Nesting	Tree	*μβ1,5*	Precipitation	-0.29 (-0.35, -0.22)	0.03
Nesting	Cavity, primary	*μβ2,1*	Temperature	0.21 (-0.05, 0.50)	0.14
Nesting	Cavity, secondary	*μβ2,2*	Temperature	0.05 (-0.14, 0.22)	0.09
Nesting	Ground	*μβ2,3*	Temperature	0.06 (-0.11, 0.24)	0.09
Nesting	Shrub	*μβ2,4*	Temperature	0.01 (-0.31, 0.30)	0.16
Nesting	Tree	*μβ2,5*	Temperature	0.20 (0.13, 0.27)	0.04
Nesting	Cavity, primary	*μβ3,1*	Day	0.05 (-0.38, 0.59)	0.24
Nesting	Cavity, secondary	*μβ3,2*	Day	-0.51 (-0.96, -0.11)	0.21
Nesting	Ground	*μβ3,3*	Day	-0.29 (-1.03, 0.42)	0.36
Nesting	Shrub	*μβ3,4*	Day	0.27 (-0.87, 1.31)	0.54
Nesting	Tree	*μβ3,5*	Day	0.03 (-0.18, 0.22)	0.1
Nesting	Cavity, primary	*μβ4,1*	Day (squared)	0.28 (-0.06, 0.68)	0.18
Nesting	Cavity, secondary	*μβ4,2*	Day (squared)	-0.30 (-0.72, 0.04)	0.19
Nesting	Ground	*μβ4,3*	Day (squared)	-0.31 (-0.57, -0.07)	0.13
Nesting	Shrub	*μβ4,4*	Day (squared)	-0.69 (-1.56, 0.04)	0.39
Nesting	Tree	*μβ4,5*	Day (squared)	-0.25 (-0.43, -0.07)	0.09
Foraging	Aerial	*μβ1,1*	Precipitation	-0.21 (-0.30, -0.14)	0.04
Foraging	Bark	*μβ1,2*	Precipitation	-0.23 (-0.45, -0.01)	0.11
Foraging	Foliage	*μβ1,3*	Precipitation	-0.30 (-0.40, -0.21)	0.05
Foraging	Ground	*μβ1,4*	Precipitation	-0.24 (-0.33, -0.15)	0.05
Foraging	Aerial	*μβ2,1*	Temperature	0.20 (0.11, 0.29)	0.05
Foraging	Bark	*μβ2,2*	Temperature	0.24 (-0.09, 0.58)	0.17
Foraging	Foliage	*μβ2,3*	Temperature	0.18 (0.09, 0.27)	0.05
Foraging	Ground	*μβ2,4*	Temperature	0.07 (-0.08, 0.21)	0.07
Foraging	Aerial	*μβ3,1*	Day	0.00 (-0.35, 0.34)	0.18
Foraging	Bark	*μβ3,2*	Day	0.12 (-0.52, 0.87)	0.34
Foraging	Foliage	*μβ3,3*	Day	0.06 (-0.25, 0.37)	0.16
Foraging	Ground	*μβ3,4*	Day	-0.22 (-0.50, 0.05)	0.14
Foraging	Aerial	*μβ4,1*	Day (squared)	-0.36 (-0.60, -0.13)	0.12
Foraging	Bark	*μβ4,2*	Day (squared)	0.09 (-0.16, 0.54)	0.18
Foraging	Foliage	*μβ4,3*	Day (squared)	-0.31 (-0.56, -0.07)	0.12
Foraging	Ground	*μβ4,4*	Day (squared)	-0.08 (-0.27, 0.12)	0.1

Table A2.6: Multi-species occupancy model guild-level mean parameter estimates for effects on habitat use probability.

Grouping	Guild	Parameter	Variable	Estimate	SD
Community	All species	μα1,1	Initiation	0.38 (0.17, 0.60)	0.11
Community	All species	μα2,1	Thinned	0.13 (0.02, 0.24)	0.06
Community	All species	μα3,1	Mature	0.02 (-0.16, 0.20)	0.09
Community	All species	μα7,1	Elevation	-0.03 (-0.19, 0.12)	0.08
Community	All species	μα8,1	Road	-0.03 (-0.14, 0.06)	0.05
Community	All species	μα9,1	Stream	-0.07 (-0.15, 0.02)	0.04
Community	All species	μα10,1	Year	-0.04 (-0.16, 0.07)	0.06
Community	All species	μα4,1,1	Density (Stem exclusion)	-0.12 (-0.47, 0.23)	0.18
Community	All species	μα4,2,1	Density (Stand initiation)	-0.15 (-0.37, 0.07)	0.11
Community	All species	μα4,3,1	Density (Mature)	0.37 (-0.01, 0.75)	0.19
Community	All species	μα4,4,1	Density (Thinned)	-0.01 (-0.37, 0.36)	0.19
Community	All species	μα5,1,1	QMD (Stem exclusion)	-0.12 (-0.57, 0.33)	0.23
Community	All species	μα5,2,1	QMD (Stand initiation)	0.09 (-0.13, 0.32)	0.12
Community	All species	μα5,3,1	QMD (Mature)	0.08 (-0.19, 0.35)	0.14
Community	All species	μα5,4,1	QMD (Thinned)	-0.98 (-1.49, -0.50)	0.25
Community	All species	μα6,1,1	Hardwood (Stem exclusion)	0.25 (0.09, 0.41)	0.08
Community	All species	μα6,2,1	Hardwood (Stand initiation)	0.08 (-0.08, 0.25)	0.08
Community	All species	μα6,3,1	Hardwood (Mature)	0.11 (-0.00, 0.22)	0.06
Community	All species	μα6,4,1	Hardwood (Thinned)	0.29 (0.13, 0.46)	0.08
Nesting	Cavity, primary	μα1,1	Initiation	0.13 (-0.48, 0.88)	0.34
Nesting	Cavity, secondary	μα1,2	Initiation	0.36 (-0.20, 1.06)	0.31
Nesting	Ground	μα1,3	Initiation	0.59 (0.06, 1.12)	0.26
Nesting	Shrub	μα1,4	Initiation	1.06 (0.08, 2.18)	0.54
Nesting	Tree	μα1,5	Initiation	0.20 (-0.10, 0.51)	0.16
Nesting	Cavity, primary	μα2,1	Thinned	0.28 (-0.22, 0.91)	0.29
Nesting	Cavity, secondary	μα2,2	Thinned	0.03 (-0.37, 0.37)	0.18
Nesting	Ground	μα2,3	Thinned	0.10 (-0.27, 0.44)	0.18
Nesting	Shrub	μα2,4	Thinned	-0.39 (-1.75, 1.11)	0.69
Nesting	Tree	μα2,5	Thinned	0.19 (0.02, 0.35)	0.08
Nesting	Cavity, primary	μα3,1	Mature	0.72 (-0.76, 2.21)	0.72
Nesting	Cavity, secondary	μα3,2	Mature	-0.06 (-0.39, 0.31)	0.18
Nesting	Ground	μα3,3	Mature	-0.08 (-0.54, 0.34)	0.22
Nesting	Shrub	μα3,4	Mature	-1.70 (-3.54, -0.06)	0.84
Nesting	Tree	μα3,5	Mature	0.04 (-0.19, 0.27)	0.11
Nesting	Cavity, primary	μα7,1	Elevation	-0.12 (-1.64, 1.19)	0.69
Nesting	Cavity, secondary	μα7,2	Elevation	0.20 (-0.26, 0.76)	0.26
Nesting	Ground	μα7,3	Elevation	0.04 (-0.45, 0.53)	0.25
Nesting	Shrub	μα7,4	Elevation	-0.46 (-1.37, 0.40)	0.45
Nesting	Tree	μα7,5	Elevation	-0.02 (-0.23, 0.19)	0.11
Nesting	Cavity, primary	μα8,1	Road	0.25 (-0.06, 0.58)	0.16
Nesting	Cavity, secondary	μα8,2	Road	-0.05 (-0.51, 0.45)	0.24
Nesting	Ground	μα8,3	Road	0.03 (-0.26, 0.25)	0.13

Nesting	Shrub	μα8,4	Road	-0.18 (-0.89, 0.54)	0.35
Nesting	Tree	μα8,5	Road	-0.08 (-0.24, 0.08)	0.08
Nesting	Cavity, primary	μα9,1	Stream	0.17 (-0.22, 0.57)	0.2
Nesting	Cavity, secondary	μα9,2	Stream	-0.08 (-0.35, 0.20)	0.14
Nesting	Ground	μα9,3	Stream	0.03 (-0.24, 0.32)	0.14
Nesting	Shrub	μα9,4	Stream	-0.13 (-0.71, 0.41)	0.28
Nesting	Tree	μα9,5	Stream	-0.11 (-0.24, 0.00)	0.06
Nesting	Cavity, primary	μα10,1	Year	-0.06 (-0.53, 0.40)	0.23
Nesting	Cavity, secondary	μα10,2	Year	0.03 (-0.46, 0.36)	0.21
Nesting	Ground	μα10,3	Year	-0.11 (-0.36, 0.11)	0.12
Nesting	Shrub	μα10,4	Year	-0.16 (-0.93, 0.38)	0.32
Nesting	Tree	μα10,5	Year	-0.00 (-0.23, 0.22)	0.11
Nesting	Cavity, primary	μα4,1,1	Density (Stem exclusion)	-0.21 (-1.64, 1.11)	0.7
Nesting	Cavity, primary	μα4,2,1	Density (Stand initiation)	0.43 (-0.66, 1.35)	0.5
Nesting	Cavity, primary	μα4,3,1	Density (Mature)	0.76 (-1.36, 2.92)	1.07
Nesting	Cavity, primary	μα4,4,1	Density (Thinned)	-0.43 (-1.77, 0.95)	0.69
Nesting	Cavity, secondary	μα4,1,2	Density (Stem exclusion)	-0.15 (-1.18, 0.83)	0.52
Nesting	Cavity, secondary	μα4,2,2	Density (Stand initiation)	-0.44 (-1.19, 0.14)	0.33
Nesting	Cavity, secondary	μα4,3,2	Density (Mature)	0.76 (-0.99, 2.19)	0.77
Nesting	Cavity, secondary	μα4,4,2	Density (Thinned)	-0.02 (-1.22, 1.14)	0.61
Nesting	Ground	μα4,1,3	Density (Stem exclusion)	-0.45 (-1.45, 0.46)	0.49
Nesting	Ground	μα4,2,3	Density (Stand initiation)	-0.26 (-1.40, 0.77)	0.54
Nesting	Ground	μα4,3,3	Density (Mature)	-0.32 (-1.41, 0.72)	0.53
Nesting	Ground	μα4,4,3	Density (Thinned)	-0.10 (-1.06, 0.90)	0.5
Nesting	Shrub	μα4,1,4	Density (Stem exclusion)	-0.02 (-2.62, 2.77)	1.36
Nesting	Shrub	μα4,2,4	Density (Stand initiation)	0.07 (-0.81, 0.79)	0.4
Nesting	Shrub	μα4,3,4	Density (Mature)	-0.18 (-2.74, 2.45)	1.29
Nesting	Shrub	μα4,4,4	Density (Thinned)	0.63 (-2.34, 3.52)	1.46
Nesting	Tree	μα4,1,5	Density (Stem exclusion)	0.08 (-0.47, 0.68)	0.29
Nesting	Tree	μα4,2,5	Density (Stand initiation)	-0.20 (-0.46, 0.04)	0.13
Nesting	Tree	μα4,3,5	Density (Mature)	0.61 (0.09, 1.14)	0.27
Nesting	Tree	μα4,4,5	Density (Thinned)	0.01 (-0.54, 0.55)	0.28
Nesting	Cavity, primary	μα5,1,1	QMD (Stem exclusion)	-0.46 (-1.93, 1.06)	0.76
Nesting	Cavity, primary	μα5,2,1	QMD (Stand initiation)	-0.93 (-2.20, 0.23)	0.61
Nesting	Cavity, primary	μα5,3,1	QMD (Mature)	0.73 (-0.76, 2.35)	0.79
Nesting	Cavity, primary	μα5,4,1	QMD (Thinned)	-0.07 (-1.55, 1.51)	0.77
Nesting	Cavity, secondary	μα5,1,2	QMD (Stem exclusion)	0.67 (-0.75, 1.97)	0.68
Nesting	Cavity, secondary	μα5,2,2	QMD (Stand initiation)	0.29 (-0.45, 0.99)	0.36
Nesting	Cavity, secondary	μα5,3,2	QMD (Mature)	0.16 (-0.59, 0.93)	0.39
Nesting	Cavity, secondary	μα5,4,2	QMD (Thinned)	0.43 (-1.33, 2.26)	0.88
Nesting	Ground	μα5,1,3	QMD (Stem exclusion)	-0.41 (-1.51, 0.79)	0.57
Nesting	Ground	μα5,2,3	QMD (Stand initiation)	-0.03 (-0.72, 0.64)	0.35
Nesting	Ground	μα5,3,3	QMD (Mature)	-0.43 (-1.20, 0.32)	0.38

Nesting	Ground	μα5,4,3	QMD (Thinned)	-0.47 (-1.68, 0.75)	0.61
Nesting	Shrub	μα5,1,4	QMD (Stem exclusion)	-1.04 (-3.16, 1.16)	1.08
Nesting	Shrub	μα5,2,4	QMD (Stand initiation)	0.02 (-1.11, 1.09)	0.56
Nesting	Shrub	μα5,3,4	QMD (Mature)	1.26 (-2.70, 4.50)	1.8
Nesting	Shrub	μα5,4,4	QMD (Thinned)	-1.05 (-3.35, 1.22)	1.17
Nesting	Tree	μα5,1,5	QMD (Stem exclusion)	-0.04 (-0.75, 0.66)	0.36
Nesting	Tree	μα5,2,5	QMD (Stand initiation)	0.25 (-0.11, 0.63)	0.19
Nesting	Tree	μα5,3,5	QMD (Mature)	0.16 (-0.33, 0.68)	0.26
Nesting	Tree	μα5,4,5	QMD (Thinned)	-1.68 (-2.46, -0.95)	0.38
Nesting	Cavity, primary	μα6,1,1	Hardwood (Stem exclusion)	0.18 (-0.44, 0.89)	0.34
Nesting	Cavity, primary	μα6,2,1	Hardwood (Stand initiation)	0.24 (-0.35, 0.95)	0.33
Nesting	Cavity, primary	μα6,3,1	Hardwood (Mature)	-0.21 (-1.00, 0.62)	0.41
Nesting	Cavity, primary	μα6,4,1	Hardwood (Thinned)	0.46 (-0.22, 1.27)	0.38
Nesting	Cavity, secondary	μα6,1,2	Hardwood (Stem exclusion)	0.12 (-0.37, 0.63)	0.26
Nesting	Cavity, secondary	μα6,2,2	Hardwood (Stand initiation)	-0.15 (-0.52, 0.22)	0.19
Nesting	Cavity, secondary	μα6,3,2	Hardwood (Mature)	0.21 (-0.27, 0.61)	0.22
Nesting	Cavity, secondary	μα6,4,2	Hardwood (Thinned)	-0.18 (-0.95, 0.72)	0.41
Nesting	Ground	μα6,1,3	Hardwood (Stem exclusion)	0.13 (-0.52, 0.77)	0.32
Nesting	Ground	μα6,2,3	Hardwood (Stand initiation)	0.18 (-0.29, 0.72)	0.25
Nesting	Ground	μα6,3,3	Hardwood (Mature)	0.20 (-0.14, 0.60)	0.18
Nesting	Ground	μα6,4,3	Hardwood (Thinned)	0.11 (-0.39, 0.56)	0.24
Nesting	Shrub	μα6,1,4	Hardwood (Stem exclusion)	0.69 (-0.32, 2.08)	0.6
Nesting	Shrub	μα6,2,4	Hardwood (Stand initiation)	0.10 (-0.54, 0.94)	0.37
Nesting	Shrub	μα6,3,4	Hardwood (Mature)	0.53 (-1.67, 2.65)	1
Nesting	Shrub	μα6,4,4	Hardwood (Thinned)	0.40 (-1.80, 2.18)	0.99
Nesting	Tree	μα6,1,5	Hardwood (Stem exclusion)	0.35 (0.13, 0.58)	0.12
Nesting	Tree	μα6,2,5	Hardwood (Stand initiation)	0.03 (-0.23, 0.32)	0.14
Nesting	Tree	μα6,3,5	Hardwood (Mature)	0.07 (-0.09, 0.25)	0.09
Nesting	Tree	μα6,4,5	Hardwood (Thinned)	0.41 (0.20, 0.64)	0.11
Foraging	Aerial	μα1,1	Initiation	0.43 (0.17, 0.72)	0.14
Foraging	Bark	μα1,2	Initiation	-0.16 (-0.98, 0.67)	0.41
Foraging	Foliage	μα1,3	Initiation	0.80 (0.27, 1.37)	0.28
Foraging	Ground	μα1,4	Initiation	0.11 (-0.38, 0.58)	0.24
Foraging	Aerial	μα2,1	Thinned	0.13 (-0.06, 0.31)	0.09
Foraging	Bark	μα2,2	Thinned	0.23 (-0.43, 1.04)	0.36
Foraging	Foliage	μα2,3	Thinned	0.23 (0.02, 0.43)	0.1
Foraging	Ground	μα2,4	Thinned	-0.00 (-0.41, 0.38)	0.2
Foraging	Aerial	μα3,1	Mature	0.08 (-0.09, 0.26)	0.09
Foraging	Bark	μα3,2	Mature	1.05 (-0.83, 2.84)	0.91
Foraging	Foliage	μα3,3	Mature	-0.07 (-0.43, 0.29)	0.19
Foraging	Ground	μα3,4	Mature	-0.21 (-0.53, 0.11)	0.16
Foraging	Aerial	μα7,1	Elevation	-0.10 (-0.31, 0.12)	0.11
Foraging	Bark	μα7,2	Elevation	-0.33 (-2.12, 1.29)	0.84

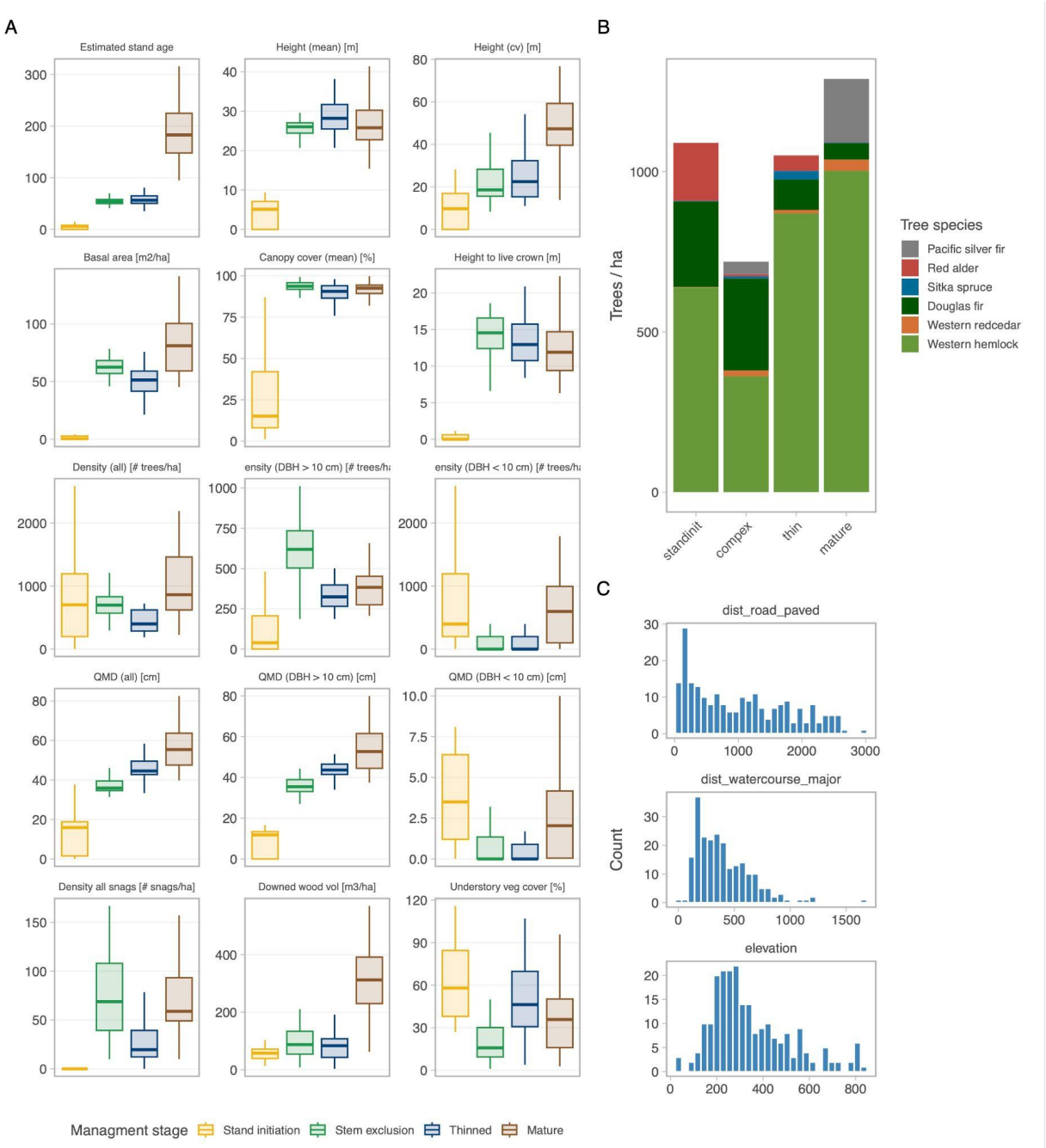

Figure A2.1: Measurements of local habitat conditions derived from field surveys and remote-sensing data at the plot scale: state-specific variation in local habitat structure (A) and mean live tree species composition (B). Distribution of paved road proximity, major watercourse proximity, and elevation across sites (C).

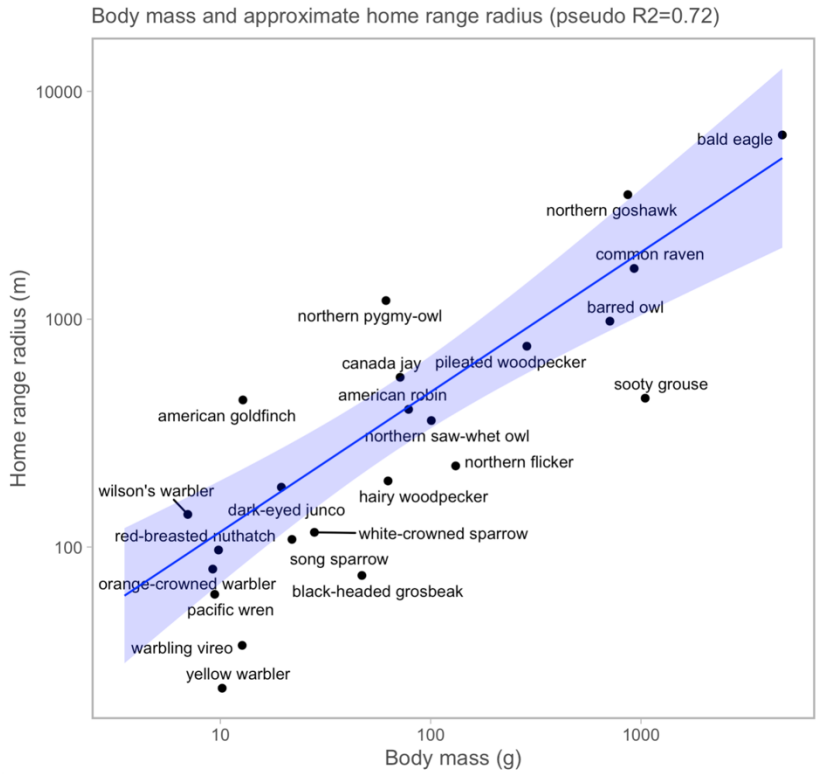

Figure A2.2: Relationship between body mass and home range radius, derived from a generalized linear model expressing home range radius as a function of log-transformed body mass with a gamma error distribution and log link.

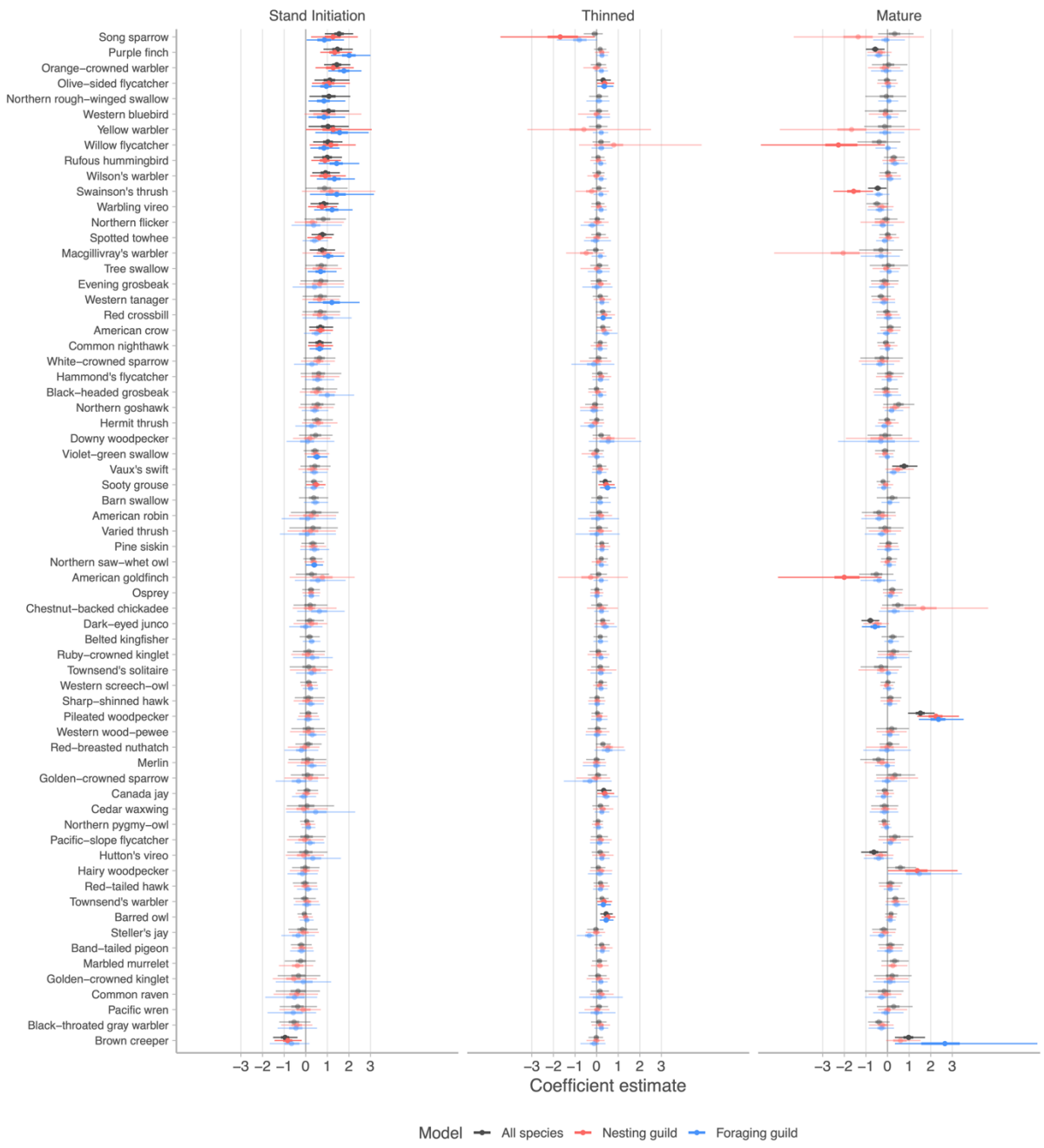

Figure A2.3: Coefficient estimates from three multi-species occupancy models (community, nesting microhabitat, foraging substrate) for the effects of forest developmental stage proportion at the species-specific home range scale at the species level. Posterior means and 95% and 50% Bayesian credible intervals (thin and thick lines, respectively) are shown in opaque color where the 95% BCI excludes zero, indicating strong effects. Covariates were *Z*-scored, and estimates are shown relative to stem exclusion as a baseline stage such that a positive effect indicates a greater probability of habitat use compared to stem exclusion.

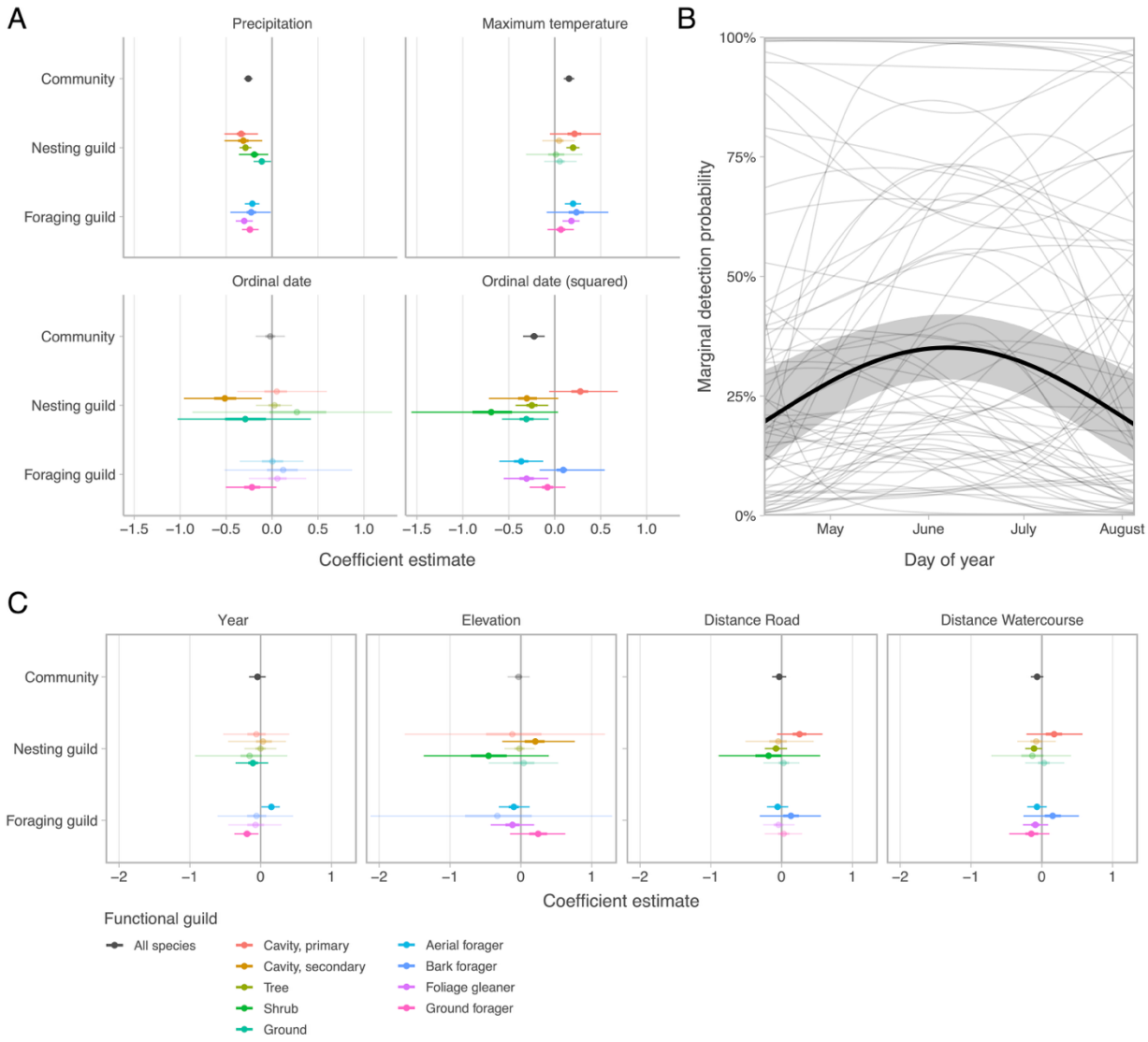

Figure A2.4: Multi-species occupancy model coefficient estimates for additional effects on detection probability (A) and habitat use (C) at the community and functional guild levels, and marginal predictions of detection probability as a function of ordinal date (C) with the bold line showing the community-level mean response with 95% Bayesian credible intervals and ghosted lines showing responses for individual species. Detection parameters include daily precipitation, maximum temperature, and a quadratic effect of ordinal date. Habitat use parameters include year, elevation, distance to the nearest paved road, and distance to the nearest perennial fish-bearing stream. Posterior means and 95% and 50% Bayesian credible intervals are shown in opaque color for guild-specific estimates where the 50% BCI excludes zero, indicating probable effects.

2.10 APPENDIX 2.2

Multi-species occupancy models were specified in JAGS and fit with Markov chain Monte Carlo (MCMC). For each model we ran three chains of length 60,000 after an adaptation phase of 10,000 and burn-in of 20,000, and thinned the posterior chains by 10. Model code is available at the open-source repository github.com/giojacuzzi/avian-acoustic-monitoring-oesf, but is provided below for ease of reference:

```
model {

  ## Community-level (group) hyperpriors
  for (g in 1:G) {

    # Occurrence
    mu.u[g]    ~ dnorm(0, 1/2.25^2)
    sigma.u[g] ~ dt(0, 1/2.25^2, 1) T(0,)
    tau.u[g]   <- 1 / pow(sigma.u[g], 2)

    # Covariate effects on occurrence
    for (s in 1:S) { # estimate stage-specific plot-scale effects for each stage
      mu.alpha_plot1[s,g]      ~ dnorm(0, 1/2.25^2)
      mu.alpha_plot2[s,g]      ~ dnorm(0, 1/2.25^2)
      mu.alpha_plot3[s,g]      ~ dnorm(0, 1/2.25^2)
      sigma.alpha_plot1[s,g]   ~ dt(0, 1/2.25^2, 1) T(0,)
      sigma.alpha_plot2[s,g]   ~ dt(0, 1/2.25^2, 1) T(0,)
      sigma.alpha_plot3[s,g]   ~ dt(0, 1/2.25^2, 1) T(0,)
      tau.alpha_plot1[s,g]     <- 1 / pow(sigma.alpha_plot1[s,g], 2)
      tau.alpha_plot2[s,g]     <- 1 / pow(sigma.alpha_plot2[s,g], 2)
      tau.alpha_plot3[s,g]     <- 1 / pow(sigma.alpha_plot3[s,g], 2)
    }

    mu.alpha_season[g]     ~ dnorm(0, 1/2.25^2)
    mu.alpha_point1[g]     ~ dnorm(0, 1/2.25^2)
    mu.alpha_point2[g]     ~ dnorm(0, 1/2.25^2)
    mu.alpha_point3[g]     ~ dnorm(0, 1/2.25^2)
    mu.alpha_homerange1[g] ~ dnorm(0, 1/2.25^2)
    mu.alpha_homerange2[g] ~ dnorm(0, 1/2.25^2)
    mu.alpha_homerange3[g] ~ dnorm(0, 1/2.25^2)

    sigma.alpha_season[g]     ~ dt(0, 1/2.25^2, 1) T(0,)
    sigma.alpha_point1[g]     ~ dt(0, 1/2.25^2, 1) T(0,)
    sigma.alpha_point2[g]     ~ dt(0, 1/2.25^2, 1) T(0,)
    sigma.alpha_point3[g]     ~ dt(0, 1/2.25^2, 1) T(0,)
    sigma.alpha_homerange1[g] ~ dt(0, 1/2.25^2, 1) T(0,)
    sigma.alpha_homerange2[g] ~ dt(0, 1/2.25^2, 1) T(0,)
    sigma.alpha_homerange3[g] ~ dt(0, 1/2.25^2, 1) T(0,)

    tau.alpha_season[g]     <- 1 / pow(sigma.alpha_season[g], 2)
    tau.alpha_point1[g]     <- 1 / pow(sigma.alpha_point1[g], 2)
    tau.alpha_point2[g]     <- 1 / pow(sigma.alpha_point2[g], 2)
    tau.alpha_point3[g]     <- 1 / pow(sigma.alpha_point3[g], 2)
    tau.alpha_homerange1[g] <- 1 / pow(sigma.alpha_homerange1[g], 2)
```

```
  tau.alpha_homerange2[g] <- 1 / pow(sigma.alpha_homerange2[g], 2)
  tau.alpha_homerange3[g] <- 1 / pow(sigma.alpha_homerange3[g], 2)

  # Detection
  for (s in 1:S) {
    mu.v[s,g]    ~ dnorm(0, 1/2.25^2)
    sigma.v[s,g] ~ dt(0, 1/2.25^2, 1) T(0,)
    tau.v[s,g]   <- 1 / pow(sigma.v[s,g], 2)
  }

  # Covariate effects on detection (unconfirmed true-positive)
  mu.beta_point1[g]    ~ dnorm(0, 1/2.25^2)
  mu.beta_point2[g]    ~ dnorm(0, 1/2.25^2)
  mu.beta_point3[g]    ~ dnorm(0, 1/2.25^2)
  sigma.beta_point1[g] ~ dt(0, 1/2.25^2, 1) T(0,)
  sigma.beta_point2[g] ~ dt(0, 1/2.25^2, 1) T(0,)
  sigma.beta_point3[g] ~ dt(0, 1/2.25^2, 1) T(0,)
  tau.beta_point1[g]  <- 1 / pow(sigma.beta_point1[g], 2)
  tau.beta_point2[g]  <- 1 / pow(sigma.beta_point2[g], 2)
  tau.beta_point3[g]  <- 1 / pow(sigma.beta_point3[g], 2)

  mu.beta_point3_sq[g] ~ dnorm(0, 1/2.25^2)
  sigma.beta_point3_sq[g] ~ dt(0, 1/2.25^2, 1) T(0,)
  tau.beta_point3_sq[g] <- 1 / pow(sigma.beta_point3_sq[g], 2)
}

## Species-level priors
for (i in 1:I) {

  # Stage-invariant covariates
  u[i]            ~ dnorm(mu.u[group[i]], tau.u[group[i]])
  alpha_point1[i] ~ dnorm(mu.alpha_point1[group[i]],tau.alpha_point1[group[i]])
  alpha_point2[i] ~ dnorm(mu.alpha_point2[group[i]],tau.alpha_point2[group[i]])
  alpha_point3[i] ~ dnorm(mu.alpha_point3[group[i]],tau.alpha_point3[group[i]])
  alpha_homerange1[i] ~ dnorm(mu.alpha_homerange1[group[i]],tau.alpha_homerange1[group[i]])
  alpha_homerange2[i] ~ dnorm(mu.alpha_homerange2[group[i]],tau.alpha_homerange2[group[i]])
  alpha_homerange3[i] ~ dnorm(mu.alpha_homerange3[group[i]],tau.alpha_homerange3[group[i]])
  alpha_season[i] ~ dnorm(mu.alpha_season[group[i]],tau.alpha_season[group[i]])

  # Stage- and species-specific covariates
  for (s in 1:S) {
    alpha_plot1[s,i] ~ dnorm(mu.alpha_plot1[s,group[i]], tau.alpha_plot1[s,group[i]])
    alpha_plot2[s,i] ~ dnorm(mu.alpha_plot2[s,group[i]], tau.alpha_plot2[s,group[i]])
    alpha_plot3[s,i] ~ dnorm(mu.alpha_plot3[s,group[i]], tau.alpha_plot3[s,group[i]])
    v[s,i]           ~ dnorm(mu.v[s,group[i]], tau.v[s,group[i]])
  }

  # Detection
  beta_point1[i] ~ dnorm(mu.beta_point1[group[i]],tau.beta_point1[group[i]])
  beta_point2[i] ~ dnorm(mu.beta_point2[group[i]],tau.beta_point2[group[i]])
  beta_point3[i] ~ dnorm(mu.beta_point3[group[i]],tau.beta_point3[group[i]])
  beta_point3_sq[i] ~ dnorm(mu.beta_point3_sq[group[i]],tau.beta_point3_sq[group[i]])
}

## Ecological process (latent occupancy)
for (i in 1:I) { # for each species i
  for (t in 1:Tseason) { # for each season t
    for (j in 1:J) { # for each site j

      logit(psi[j,t,i]) <- u[i] +
```

```
                            alpha_plot1[stage[j],i] * x_alpha_plot1[j,t] +
                            alpha_plot2[stage[j],i] * x_alpha_plot2[j,t] +
                            alpha_plot3[stage[j],i] * x_alpha_plot3[j,t] +
                            alpha_point1[i] * x_alpha_point1[j,t] +
                            alpha_point2[i] * x_alpha_point2[j,t] +
                            alpha_point3[i] * x_alpha_point3[j,t] +
                            alpha_homerange1[i] * x_alpha_homerange1[j,t,i] +
                            alpha_homerange2[i] * x_alpha_homerange2[j,t,i] +
                            alpha_homerange3[i] * x_alpha_homerange3[j,t,i] +
                            alpha_season[i] * x_season[t]

        z[j,t,i] ~ dbern(psi[j,t,i])

        ## Detection model
        for (k in 1:K[j,t]) { # for each survey k during season t at site j

          logit(p11[j,k,t,i]) <- v[stage[j],i] +
                                 beta_point1[i]*x_beta_point1[j,k,t] +
                                 beta_point2[i]*x_beta_point2[j,k,t] +
                                 beta_point3[i]*x_beta_point3[j,k,t] +
                                 beta_point3_sq[i]*pow(x_beta_point3[j,k,t], 2)

          p[j,k,t,i] <- z[j,t,i] * p11[j,k,t,i]

          # Observed outcome
          y[j,k,t,i] ~ dbern(p[j,k,t,i])

          # Simulated replicate for posterior predictive checks
          y_sim[j,k,t,i] ~ dbern(p[j,k,t,i])

          # Deviance (Broms et al., 2016)
          d_obs[j,k,t,i] <- z[j,t,i] * (y[j,k,t,i] * log(p[j,k,t,i]) + (1 - y[j,k,t,i]) * log(1 -
p[j,k,t,i]))
          d_sim[j,k,t,i] <- z[j,t,i] * (y_sim[j,k,t,i] * log(p[j,k,t,i]) + (1 - y_sim[j,k,t,i]) *
log(1 - p[j,k,t,i]))

        } # K surveys

        # Pad jagged array of deviance values with zeros to enable sum below
        for (k in (K[j,t]+1):Kmax) {
          d_obs[j,k,t,i] <- 0
          d_sim[j,k,t,i] <- 0
        }

      } # J sites
    } # Tseason seasons
  } # I species

  ## Derived quantities
  # Deviance of simulated and observed data for posterior predictive check
  D_obs <- -2 * sum(d_obs[1:J,1:Kmax,1:Tseason,1:I])
  D_sim <- -2 * sum(d_sim[1:J,1:Kmax,1:Tseason,1:I])
}
```

Chapter 3. AQUATIC INSECT SUBSIDIES MEDIATE CURRENT AND FUTURE URBANIZATION EFFECTS ON INSECTIVOROUS BIRDS ACROSS SPATIAL SCALES

Publication history: This study was co-authored with Stevan Pekich and Julian D. Olden. At the time that this dissertation was published, this chapter was in review for publication.

3.1 ABSTRACT

Freshwater and riparian ecosystems are tightly coupled by the flow of resource subsidies across aquatic and terrestrial boundaries and are also vulnerable to environmental stressors associated with urban development. Ongoing declines in insectivorous bird populations are attributed in part to reductions in riparian habitat and the availability of aquatic and terrestrial prey. However, the ways in which urbanization alters aquatic subsidies, and how these changes propagate to avian consumers, remain poorly understood, limiting our ability to anticipate future urbanization impacts and inform cross-boundary mitigation strategies. The present study examines how aquatic insect communities, riparian vegetation, and urban land cover influence avian communities during the breeding season by coupling benthic macroinvertebrate surveys with bioacoustic monitoring across streams spanning an urbanization gradient in the Seattle metropolitan area (Washington, USA). Results from multi-species occupancy and structural equation models indicate that stream biotic integrity (B-IBI) is strongly associated with the richness of avian insectivore and migrant guilds, more so than impervious surface cover (ISC) and tree canopy cover (TCC). Urbanization influenced avian richness indirectly through two pathways operating at multiple spatial scales: local-scale ISC reduced riparian TCC, whereas landscape-scale ISC reduced B-IBI, suggesting aquatic subsidies and riparian habitat conditions may mediate the influence of urban stressors on birds. Applying our model to projections of ISC through 2100 indicates that the protection and restoration of riparian vegetation at both local and landscape scales may be necessary to maintain present-day avian richness levels in the face of continued urban development and its negative effect on aquatic subsidies. These findings

highlight how the future conservation of terrestrial and aquatic biodiversity in urban environments is tightly intertwined and dependent on co-management of the landscape

3.2 INTRODUCTION

Freshwater and terrestrial ecosystems face joint biodiversity crises in an increasingly urbanized world. Rivers, streams, and their associated riparian environments support some of the most biodiverse ecological systems on Earth (Balian et al., 2008; Naiman et al., 1993), providing foraging and breeding habitat (Pennington & Blair, 2011), migration and dispersal corridors (Skagen et al., 2005), and climate refugia for many organisms (Seavy et al., 2009). Concurrently, these environments are facing increasing rates of habitat conversion, hydrological alteration, and shifts in climate (Albert et al., 2021; Reid et al., 2019), spurring ongoing and accelerating declines in both freshwater and terrestrial organisms (Finn et al., 2023).

Three-quarters of the world's avifauna are in decline (Johnston et al., 2025; Rosenberg et al., 2019), with growing numbers of species losses due to habitat loss (Bowler et al., 2019), climate change (Nimmo et al., 2015), and parallel reductions in the abundance and composition of prey (Moller, 2019; Tallamy & Shriver, 2021). Projections indicate that rapid human population growth will continue primarily in expanding urban areas (United Nations, 2025; Chen et al., 2020). Such dramatic changes in land use are expected to present commensurate threats to the integrity of riparian ecosystems, depending on the development of environmental policy and action (Martinuzzi et al., 2014; Walsh et al., 2005). Understanding the aquatic-terrestrial linkages that structure interconnected food webs in urban environments can support decision makers working to ensure ecosystem integrity in the face of future urban expansion.

Freshwater and riparian environments are tightly coupled by the reciprocal flow of nutrient subsidies across aquatic-terrestrial boundaries (Figure 3.1; Baxter et al., 2005; Nakano & Murakami, 2001). Terrestrial predators such as birds (Schürings and Olden, 2026; Jackson et al., 2020), bats (Baxter et al., 2005), and spiders (Smith et al., 2007; Kowarik et al., 2023) benefit from the emergence of adult aquatic insects such as mayflies, stoneflies, and caddisflies (Ephemeroptera, Plecoptera, and Trichoptera; EPT), which are in turn supported through the deposition of organic matter from the riparian zone (Tank et al., 2010). Abundant EPT prey

during the breeding season help support the energetic needs of insectivorous birds through the provision of non-nutritionally substitutable highly concentrated essential fatty acids (Shipley et al., 2024; Twining et al., 2018), which enhance breeding success, growth, and fitness (Martin-Creuzburg et al., 2017; Dodson et al., 2016). These subsidies provide migrants with critical resources for refueling and breeding (Trevelline et al., 2018; Macdade et al., 2011), and aerial foragers and foliage gleaners in particular have shown strong responses to emergent prey biomass (Schilke et al., 2020; Iwata et al., 2003). The abundance and composition of bird communities in riparian environments can therefore be directly influenced by the availability and diversity of allochthonous aquatic prey (Schilke et al., 2020; Uesugi & Murakami, 2007).

Cross-boundary linkages are highly vulnerable to environmental stressors that influence aquatic and terrestrial habitat quality (Kautza & Sullivan, 2015; Baxter et al., 2005). There are multiple pathways through which environmental factors can propagate across aquatic and terrestrial ecosystems (Figure 3.1). Aquatic macroinvertebrate communities can shift dramatically in response to anthropogenic land-use change, selecting for biological traits that tolerate urban streams and reducing the diversity and biomass of sensitive EPT taxa (Chen et al., 2023). The removal of vegetation, disruption of overland flow, and alteration of water quality and temperature associated with urban encroachment can alter the magnitude and timing of aquatic insect emergence (Manning & Sullivan, 2021), thereby disrupting foraging and phenological synchrony of avian insectivores (Shipley et al., 2022). Indeed, studies have linked pronounced declines among migrants and aerial insectivores to parallel reductions in aquatic insect populations (Sánchez-Bayo et al., 2019; Nebel et al., 2010).

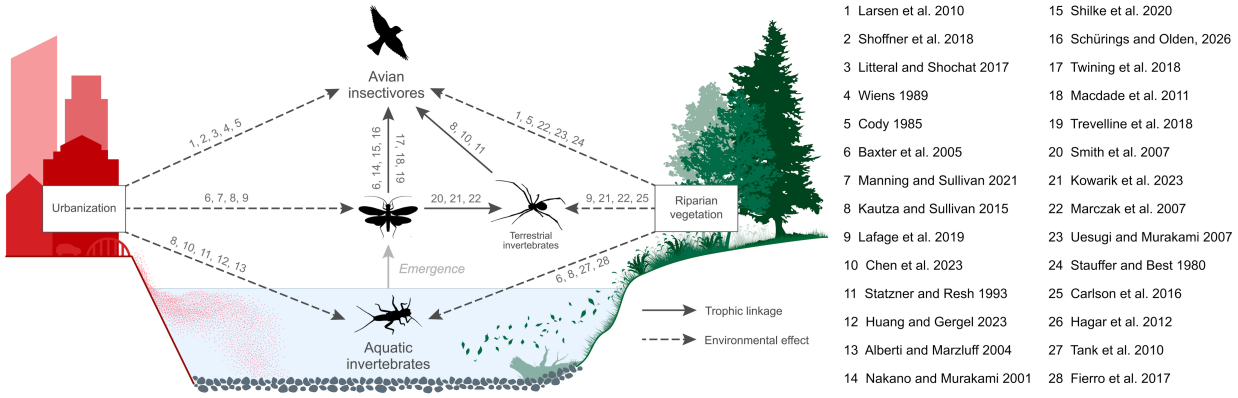

Figure 3.1: Theoretical model illustrating pathways of influence, including trophic linkages and abiotic environmental effects, linking avian insectivores with aquatic macroinvertebrate prey, riparian vegetation, and urbanization stressors across multiple spatial scales.

Mounting evidence suggests that aquatic insect subsidies may mediate the effects of urbanization on bird communities through bottom-up trophic pathways (Schürings and Olden, 2026; Kautza & Sullivan, 2015; Larsen et al., 2010). This process may be particularly important in highly degraded environments where aquatic insects can become disproportionately important foraging resources (Marczak et al., 2007; Nakano & Murakami, 2001). Riparian vegetation may facilitate aquatic-terrestrial linkages (Carlson et al., 2016) by providing critical habitat structure for avian breeding and foraging (Uesugi & Murakami, 2007) while also supporting the persistence of aquatic subsidies (Tank et al., 2010). Consequently, reductions in the quantity and quality of riparian habitat and aquatic prey, driven by urban expansion and conversion to impervious surfaces, may have direct and indirect cascading effects on avian carrying capacity and diversity in riverine systems (Stenroth et al., 2015; Twining et al., 2018; Stauffer & Best, 1980). Improving our understanding of how land conversion alters aquatic resource subsidies and how these changes propagate to avian consumers is critical (Manning & Sullivan, 2021; Greenwood & Booker, 2016; Kautza & Sullivan, 2015), particularly when developing cross-boundary management strategies (Baxter et al., 2005).

Relationships between urbanization and cross-boundary linkages are scale-dependent (Allan, 2004; Huang & Gergel, 2023). Changes in the composition of aquatic subsidies in urban streams are largely explained by land cover composition and configuration within the watershed (Huang & Gergel, 2023; Alberti & Marzluff, 2004), as contiguous impervious surfaces increase stormwater runoff, pollutants, and water temperature (Lafage et al., 2019; Baruch et al., 2018).

At the local scale of a stream reach, removal or degradation of riparian vegetation reduces the input of organic matter to primary consumers and alters hydrology, habitat heterogeneity, and microclimate (Fierro et al., 2017). Similarly, landscape-scale composition, configuration, and connectivity of terrestrial habitats influence the dispersal and persistence of avian populations (Shoffner et al., 2018; Litteral & Shochat, 2017; Marzluff, 2005), whereas nesting and foraging habitat structure and microclimate influence local species composition (Wiens, 1989; Cody, 1985). Consideration of land conversion at both local and landscape scales is therefore essential for understanding its influence on the diversity of avian insectivores and their prey (Lafage et al., 2019).

As urban expansion will drive continued land conversion, there is an urgent need to anticipate future impacts on the subsidy-driven assembly of bird communities to inform cross-boundary mitigation strategies. Multi-scale efforts in freshwater conservation and restoration that seek to bolster aquatic-terrestrial linkages may help to safeguard biodiversity in the face of urbanization (Leal et al., 2020; Amis et al., 2009). However, constraints on land-use management at local and landscape scales pose challenges for the development of effective conservation strategies (Wang et al., 2016). Broad-scale management efforts can be constrained by mixed land ownership, whereas local-scale efforts are feasible given municipal ownership or easement of a stream segment. Conversely, local management may be impossible due to private ownership, while changes to the broader landscape are achievable through regional or watershed management plans by government agencies. The degree to which birds are influenced by the modulation of aquatic subsidies from urbanization at these contrasting management scales requires further investigation.

We aimed to assess the relative influence of land use, riparian habitat condition, and aquatic insect subsidies on avian taxonomic richness in urban streams during the breeding season. Leveraging benthic macroinvertebrate surveys and avian bioacoustic monitoring from streams spanning a gradient of urbanized watersheds in the Seattle metropolitan area of Washington state, USA, we used multi-species occupancy and piecewise structural equation modeling to disentangle the determinants of bird diversity and their aquatic insect prey at multiple spatial scales. We hypothesized that 1) the richness of avian insectivores in streams is supported by aquatic insect prey diversity, 2) this positive linkage helps offset the negative

effects of urbanization, and 3) streams with intact riparian areas and reduced urban landscape conversion support local avian biodiversity by promoting enhanced aquatic insect subsidies.

To estimate future impacts of urban expansion on riparian bird communities, we used projections of impervious surface cover through 2100 to predict changes in the availability of riparian habitat and aquatic insect prey. We also conducted a model sensitivity analysis to evaluate the potential of local-only, landscape-only, and cross-scale management actions to maintain present-day levels of avian insectivore richness through the reduction of impervious surface cover and increase of tree canopy cover. Our results reveal the direct and indirect pathways through which multi-scale riparian conservation and restoration may offer synergistic benefits across ecosystem boundaries to conserve biodiversity amid urban expansion.

3.3 METHODS

3.3.1 Site selection and data collection

This study was conducted within the Seattle metropolitan area of Washington state, USA. Seattle ranks among the fastest-growing metropolitan areas in the United States, with urban sprawl projected to increase impervious surface coverage and the fragmentation and degradation of both terrestrial and aquatic habitats over the course of the century (Puget Sound Regional Council, 2020; Robinson et al., 2005), mirroring trends in urban expansion globally (United Nations, 2025). As much as 90% of riparian habitat in the state has been lost or extensively degraded since the arrival of settlers in the 19th century, yet roughly 85% of the state's terrestrial vertebrate species use riparian habitat during their life histories (Knutson & Naef, 1997).

Local government agencies regularly conduct aquatic macroinvertebrate surveys in streams across the region to track trends in freshwater integrity and habitat quality using a regionally calibrated benthic index of biotic integrity (B-IBI; Sosik et al., 2025; Morley & Karr 2002). B-IBI incorporates multiple metrics to quantify stream biological condition, including the richness of EPT, Diptera, Odonata, Bivalvia, and Gastropoda taxa. The index ranges from 0 ("very poor" condition category, with low diversity dominated by highly tolerant taxa) to 100 ("excellent" condition category, with high diversity comparable to a minimally disturbed reference condition) (Table A3.1), reflecting the quality of potential emergent insect subsidies

(Statzner & Resh, 1993). B-IBI is regularly used to inform water resource management, restoration, and ecological science (Macneale et al., 2020), and research in the region has revealed significant effects of impervious surface and forest cover on B-IBI (Sosik et al., 2025; Alberti et al., 2007) and on avian occurrence and diversity (Marzluff, 2005) at both local and landscape scales (Morley & Karr, 2002).

We selected 50 study streams along an urban-rural gradient from existing B-IBI survey locations (King County, 2025) using stratified random sampling, ensuring comparable sample sizes across reported B-IBI values and areal extent of impervious surfaces at both the local (550 m radial distance) and landscape (5 km) scales (Figure 3.2A, B; Figure A3.1). Total fractional impervious surface cover (ISC), widely used as an effective surrogate for the influence of multiple urbanization stressors (Arnold Jr. & Gibbons, 2007), was calculated from the most recent National Land Cover Database (USGS, 2023a). Candidate sites were restricted to those displaying stable B-IBI values over the past 5 years (non-significant $p > 0.05$ relationships with year as a predictor) and a minimum distance of approximately 1 km from any other site to mitigate spatial autocorrelation.

Benthic macroinvertebrate sampling was conducted by the King County Department of Natural Resources and Parks during low-flow conditions between mid-July and early October of 2024-2025 (for protocol details, see Macneale et al., 2020). B-IBI was obtained for each stream from the most recently available survey year, with values ranging from 0 to 100 (mean 48.2, standard deviation 29.4). B-IBI values were strongly correlated with EPT richness (Pearson's $r = 0.98$, $p < 0.001$, $n = 50$). As such, we used B-IBI as an indicator of both the quality and availability of emergent insect subsidies at the site (Statzner & Resh, 1993).

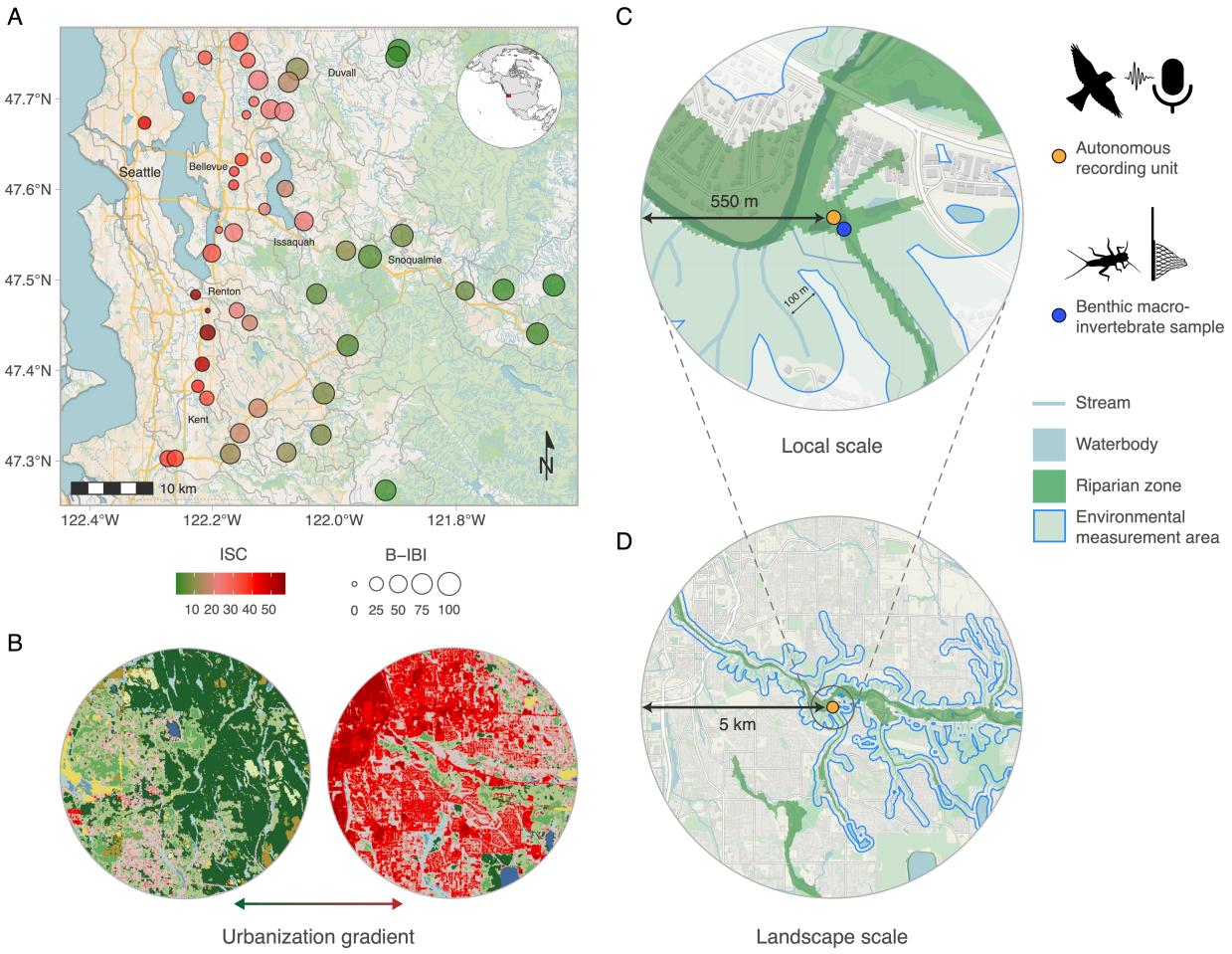

Figure 3.2: Stream sampling methodology. Site locations in the Seattle metropolitan area (A) were sampled across an urbanization gradient of impervious surface cover (ISC) (B). At each site an autonomous recording unit was used to conduct a bioacoustic survey for avian occurrence, co-located with an in-stream macroinvertebrate survey to quantify the benthic index of biotic integrity (B-IBI) (C). Environmental measurements were taken from the riparian zone and connected stream segments and waterbodies, buffered by 100 m to include edge habitat, at local (C) and landscape (D) spatial extents.

We conducted surveys for avian species occurrence using passive acoustic monitoring during the breeding seasons of 2024 and 2025 (mid-June to early August). Bioacoustic surveys can improve the probability of detecting avian species and increase spatiotemporal sample size compared to traditional point-count surveys in structurally heterogeneous environments (Darras et al., 2018) and are increasingly used to assess species richness and community composition (Shonfield & Bayne, 2017). One AudioMoth autonomous recording unit (ARU; Hill et al., 2019) was co-located with each B-IBI survey location at a maximum distance of 100 m from the stream (Figure 3.2C). We deployed each ARU for one season on a tree at breast height at a location to

minimize ambient noise from running water and vehicles, using a plastic bag and desiccant for weatherproofing. ARUs were programmed to record with a 32 kHz sampling rate each day for the first 10 minutes of every half hour from 04:00-11:00 (approximately one hour before sunrise to four hours after sunrise) and 20:00-22:00 (one hour before sunset to two hours after sunset). This schedule surveyed periods when birds are most vocal and active during foraging (Sullivan & Vierling, 2009), while also managing battery usage to record throughout the breeding season for a total of 89 days.

Acoustic monitoring data were processed with the BirdNET convolutional neural network (version 2.4; Kahl et al., 2021) to produce detection predictions for a group of 129 species representing the regional species pool (Table A3.2), as determined from the Cornell Laboratory's eBird regional occurrence database (Fink et al., 2024) and historical observations within the study area (Brown, 1985). We configured the BirdNET classifier with default analysis parameters to produce continuous prediction scores for each species at each site at 3-second intervals. Because the resulting predictions spanned over 13,000 total hours of acoustic data, which could not feasibly be manually reviewed for true detections, we used Platt scaling (Platt, 1999) to calibrate classifier output scores to probabilities following Wood and Kahl (2024). This approach uses a validation dataset of positive and negative examples to fit a species-specific logistic regression model that relates score values to the probability that a prediction is a true positive detection of the species. We assembled the validation dataset by aurally and visually reviewing spectrograms of a random selection of 450 predictions for each species spanning the full range of scores, using Raven Pro (version 1.6; K. Lisa Yang Center for Conservation Bioacoustics, 2024). Examples were annotated by experts as true positive or true negative for species presence when definitive. Logistic regression models fitted to these data were used to derive probabilistic thresholds for each species (Table A3.2), with a minimum threshold of 0.5 representing the classifier's decision boundary between likely true-positive and false-positive detections. Only classifier predictions with a probability of true positive detection greater than or equal to 95% were retained as observations for subsequent analysis. For species with insufficient data or classifier performance to support regression, predictions were manually reviewed to a minimum confidence score of 0.5. To filter out transient species and spurious detections, we discarded detections for species that occurred during fewer than 2 surveys (days) at a site. The resulting binary data represented putative observation histories for each species at each site.

Variables characterizing the composition, configuration, and structure of urban development and vegetation were measured from remote sensing data at local and landscape spatial scales (Table A3.3). We defined the "local" scale as a 550-m radius circle centered on the ARU, thus capturing fine-scale conditions immediately surrounding the riparian area and within the territory of most birds (Brown, 1985), while also corresponding to the 90th percentile of aquatic emergent insect dispersal (Muehlbauer et al., 2014). We defined the "landscape" scale as a 5-km radius circle centered on the ARU, representing the surrounding landscape matrix and roughly corresponding to the upper extent of home range size within the regional avian species pool (Brown, 1985). Variables were measured for each site from an area clipped to the extent of the respective spatial scale, containing mapped riparian area (Abood et al., 2022; 10-m resolution) and all National Hydrography stream segments and waterbodies connected to the surveyed stream (USGS, 2023b), buffered by 100 m to include edge habitat (Figure 3.2C, D). Variables known to shape avian and aquatic macroinvertebrate community composition were calculated (Table A3.3), including ISC and road density (representing the extent of urban development) and forest proportional area, tree canopy cover (TCC), mean canopy height, and foliage height diversity (representing the extent and structural complexity of riparian vegetation). All raster data were available at 30-m resolution. NLCD land-cover classes were aggregated into simplified categories for calculating landscape configuration metrics: developed, vegetated (forest or wetland), and other.

We first explored the variation in and correlations between candidate variables across sites. ISC and road density were strongly correlated within spatial scales (Pearson's $r \geq 0.75$), and pairwise combinations of vegetation variables were highly correlated within spatial scales ($r \geq 0.8$), suggesting that they capture similar aspects of urban development and riparian vegetation structure, respectively. We excluded forest proportional area as a candidate after visual inspection of satellite imagery indicated classification errors between the forest and developed cover categories, particularly in the vicinity of urban streams with greenways that have high TCC and low ISC yet relatively narrow widths. In the interest of parsimony and ecological relevance, we limited predictors to ISC, a measure of urban development from 0 to 100%, and TCC, a measure of riparian vegetation from 0 to 100%. ISC and TCC represent mechanisms directly linked to habitat conditions for birds and benthic macroinvertebrates. ISC reflects the degree of hydrological alteration, pollution, thermal stress, and riparian habitat conversion (Nowak &

Greenfield, 2012; Arnold Jr. & Gibbons, 2007), while TCC reflects habitat vegetation structure, stream shading and temperature moderation, and the magnitude of allochthonous inputs of terrestrial organic matter (Lafage et al., 2019). ISC and TCC are also widely used as key ecological indicators in urban ecology, planning, and restoration (Morley & Karr, 2002; Mincey et al., 2013; Alberti & Marzluff, 2004; Sosik et al., 2025) and support the modeling of future environmental conditions via readily available spatial projections (Bierwagen et al., 2010, Nowak & Greenfield, 2012). All covariates were *Z*-scored prior to model fitting.

To investigate differences in responses among functional groups within the broader avian community, we classified species into groupings based on diet composition, foraging behavior, and migration using the AVONET trait database (Tobias et al., 2022) and diet and foraging literature reviews from the Birds of the World database (Billerman et al., 2025). The diet composition grouping consisted of two guilds, insectivores and other consumers, where the former includes known predators of aquatic insect larvae or their emergent adult forms, as well as species with diet compositions exhibiting all of the following features: 1) dominantly invertebrate prey; with 2) the presence of one or more of the macroinvertebrate taxa surveyed using the B-IBI metric; and 3) aerial, insessorial, or aquatic locomotion while foraging. These criteria feature species that forage in-stream for aquatic macroinvertebrate larvae as a primary source of nutrition, as well as aerial foragers and foliage gleaners that supplement their diets with emergent macroinvertebrates (Nakano & Murakami, 2001), while excluding primarily terrestrial, arboreal, and generalist foragers (Schilke et al., 2020). The foraging behavior grouping consisted of three guilds—insectivorous aerial foragers, insectivorous foliage gleaners, and other foragers (including ground foraging or bark probing insectivores and non-insectivores)—reflecting alternative foraging strategies and niche differentiation within the community (Wiens, 1989). The migration grouping comprised two guilds, migrants and resident or partial migrants, allowing comparison of species that undertake long-distance migration to the study area for breeding, potentially relying more heavily on aquatic subsidies (Trevelline et al., 2018; Macdade et al., 2011).

3.3.2 Multi-species occupancy models

We constructed multi-species occupancy models (MSOM) to account for the imperfect detection of species (i.e., false negatives) across our environmentally heterogeneous survey sites, and to

estimate the effects of B-IBI, ISC, and TCC on the probability of species- and guild-specific site occurrence during the breeding season. We built four MSOMs, each grouping species into guilds according to each of the different functional groupings, as well as a community grouping including all species. Each MSOM was a hierarchical model couched in a Bayesian framework, modeling species-specific latent occurrence and detection parameters as random effects related across guilds with guild-specific distributions (Royle & Dorazio, 2008). For example, the model based on the diet composition grouping included separate hierarchical distributions for species within the insectivore guild and for species within the other consumer guild. As several species exhibit home range sizes beyond the range of ARU detection (Brown, 1985), we relax the assumption of closure and interpret our models as estimating the probability of a species occurring at a site during the breeding season, rather than occupying it (Royle & Dorazio, 2008).

We model the occurrence of species *i* at site *j* using a Bernoulli random variable z_{ij} with probability of occurrence ψ_{ij}, such that $z_{ij} \sim$ Bernoulli(ψ_{ij}). Similarly, the detection or nondetection of species *i* at site *j* during survey *k* is a Bernoulli random variable y_{ijk}. If the species occurs at a site, then $z_{ij} = 1$ and the probability of detection during a survey is p_{ijk}. If the species is absent, then $z_{ij} = 0$ and we assume the probability of detection is 0. Therefore, the product $z_{ij}\, p_{ijk}$ represents the probability of detection (p_{ijk}) depending on the species occurrence (z_{ij}), such that $y_{ijk} \mid z_{ij} \sim$ Bernoulli($z_{ij}\, p_{ijk}$). We model the ecological occurrence state process such that:

(1)

$$logit(\psi_{ij}) = u_i + \alpha_{1,i} * BIBI_j + \alpha_{2,i} * TCC_{local,j} + \alpha_{3,i} * TCC_{land,j} + \alpha_{4,i} * ISC_{local,j} + \alpha_{5,i} * ISC_{land,j}$$

$$u_i \sim \text{Normal}\left(\mu^{(u)}_{g[i]}, \sigma^{(u)}_{g[i]}\right)$$

$$\alpha_{a,i} \sim \text{Normal}\left(\mu^{(\alpha)}_{a,g[i]}, \sigma^{(\alpha)}_{a,g[i]}\right), a = 1, \ldots, 5$$

where u_i is a species-specific occurrence intercept drawn from a guild (g)-specific normal distribution with mean $\mu^{(u)}_g$ and standard deviation $\sigma^{(u)}_g$. Species-specific coefficients α_{ai} are also modeled as guild-level random effects, with means $\mu^{(\alpha)}_{a,g}$ and standard deviations $\sigma^{(\alpha)}_{a,g}$ for $a = 1, \ldots, 5$, corresponding to B-IBI at the local scale, and TCC and ISC at the local and landscape scales. We model the observation process such that:

(2)

$$logit(p_{ijk}) = v_i + \beta_{1,i} * Day_{jk} + \beta_{2,i} * TCC_{local,j} + \beta_{3,i} * ISC_{local,j}$$

$$v_i \sim \text{Normal}\left(\mu^{(v)}_{g[i]}, \sigma^{(v)}_{g[i]}\right)$$

$$\beta_{b,i} \sim \text{Normal}\left(\mu^{(\beta)}_{b,g[i]}, \sigma^{(\beta)}_{b,g[i]}\right), b = 1,2,3$$

where v_i and $\beta_{b,i}$ are species-level random effects drawn from guild-specific distributions, with $\beta_{1:3,i}$ corresponding to coefficients for the (*Z*-scored) day of year and TCC and ISC at the local scale, respectively.

Following Broms et al. (2016) and Northrup and Gerber (2018), we specified weakly informative Normal(0, 2.25^2) hyperpriors on the logit scale for the guild-level means of all occurrence and detection parameters ($\mu^{(u)}_g$ and $\mu^{(v)}_g$) and covariate effects ($\mu^{(\alpha)}_{a,g}$ and $\mu^{(\beta)}_{b,g}$). We used half-Cauchy(0, 2.25) hyperpriors on the logit scale for the corresponding guild-level standard deviations ($\sigma^{(u)}_g$, $\sigma^{(v)}_g$, $\sigma^{(\alpha)}_{a,g}$, $\sigma^{(\beta)}_{b,g}$). We used JAGS (Plummer, 2023) to carry out our Bayesian analysis with Markov chain Monte Carlo (MCMC) and jagsUI (Kellner & Meredith, 2026) to process results. We assessed convergence using Gelman-Rubin diagnostics ($\hat{R} < 1.01$) and visual evaluation of chain histories. We used deviance-based posterior predictive checks (Broms et al., 2016) to assess model fit. Complete model specifications and MCMC configurations are provided in Appendix 3.2.

By modeling occurrence and detection probabilities for individual species and guilds, our MSOM corrects for imperfect detection and supports the robust estimation of community richness (Royle & Dorazio, 2008). For each MCMC iteration, we calculated guild-specific richness at site *j* as the sum of latent occurrence states for all member species of guild *g*, such that $R_{gj} = \sum_{i \in g} z_{ij}$. Total site richness was derived analogously by summing latent occurrence states across all species for each site. Posterior means and 95% Bayesian credible intervals for these measures of richness were then calculated from the resulting posterior distributions and retained to propagate uncertainty through subsequent structural equation modeling of avian richness.

3.3.3 Structural equation modeling

Referencing our theoretical model (Figure 3.1), we predicted that avian richness is influenced by an interconnected network of determinants operating across spatial scales. We predicted that aquatic prey diversity positively affected avian insectivore and migrant guild richness while having no discernible effect on other guilds or total richness. We also predicted that local riparian vegetation had a direct positive effect on B-IBI and avian richness. Finally, we predicted that local-scale urban development (ISC_{local}) had a direct negative effect on local riparian vegetation (TCC_{local}) and an indirect negative effect on avian richness through local vegetation, while landscape-scale development (ISC_{land}) had a direct negative effect on aquatic macroinvertebrate prey diversity (B-IBI) and an indirect negative effect on avian richness through aquatic prey.

We used piecewise structural equation modeling (SEM) to test our predictions and disentangle direct and indirect effects on estimated avian richness (Lefcheck, 2015). Structural equation modeling is a form of path analysis that resolves multivariate relationships among multiple predictor and response variables, enabling tests of hypothesized causal network structures (Fan et al., 2016). We defined a structure linking environmental factors (ISC, TCC), aquatic macroinvertebrate prey (B-IBI), and avian richness through individual component linear models. Logit transformation of predictors with proportional values was used to ensure compatibility with piecewise structural equation modeling, which does not currently support beta-distributed responses (Lefcheck, 2015). Logit-transformed TCC_{local} was modeled as an endogenous linear function of ISC_{local} to reflect riparian habitat loss from urban encroachment. We used an AIC_c-based model selection approach (Hurvich & Tsai, 1989) to evaluate the importance of predictors at different spatial scales among candidate component models using logit-transformed B-IBI (scaled 0-1) and avian richness as endogenous response variables. For each response, using the posterior mean richness for each guild, we fit all possible sets of candidate linear models including both local-scale and landscape-scale measures of ISC and TCC. We examined the top-ranking models ($\Delta AIC_c < 2$) to confirm that variables following our predictions were indeed strongly associated with the response, and retained these component models for use in structural equation modeling.

Structural equation modeling was performed over all posterior draws from the community (all species) grouping MSOM to propagate uncertainty in richness estimates to component model coefficients. We selected the community grouping MSOM to obtain robust

estimates of richness, thereby avoiding the potential for guild-specific hyperpriors in other models to bias estimates of latent occurrence for specific species or functional groups (Pacifici et al., 2014). We fit structural equation models (SEM) using piecewiseSEM (Lefcheck, 2015) and used tests of directed separation to confirm independence claims implicit within the model network structures (i.e., omission of significant paths according to the data). Residuals of component models were inspected for approximate normality. We assessed overall goodness-of-fit using the Fisher's C statistic, where a non-significant p-value ($p > 0.05$) indicates consistency between the observed data and the hypothesized model (Lefcheck, 2015).

3.3.4 Future biodiversity projections and mitigation via stream management

In anticipation of accelerated population and technological growth over the century, the Puget Sound regional growth management strategy directs development toward existing built areas, encouraging infill and redevelopment to increase urban density (Puget Sound Regional Council, 2020). This compact growth pattern is designed to preserve natural resource lands and limit urban encroachment into rural areas while supporting a burgeoning population through expansion of urban housing and transit infrastructure. Within urban growth centers, however, development is expected to reduce terrestrial and aquatic habitat and degrade water quality through the removal of vegetation and conversion of land to impervious surface.

To predict the effect of future urban development on avian insectivore richness and B-IBI in the region, we used decadal projections of ISC from 2020 to 2100 from the Integrated Climate and Land Use Scenarios (ICLUS; US EPA, 2025). ICLUS uses demographic and spatial housing allocation models informed by past land use and transit patterns to forecast ISC at 1-km resolution to assess how changes in land use and climate affect environmental outcomes (Bierwagen et al., 2010). Different forecast scenarios are aligned with the Special Report on Emissions Scenarios storylines describing future population, socioeconomic, and technological trajectories (A1, A2, B1, and B2, roughly corresponding to Representative Concentration Pathways 8.5, 8.5-6.0, 4.5, and 4.5-6.0, respectively). For each scenario and decade, we calculated site-specific local- and landscape-scale projected ISC using the same methodology presented above, downscaling to 30-m resolution. To account for ICLUS model-based discrepancies in estimates of ISC, we calculated the percent relative change from a 2020 baseline (the closest decade to our observations) and applied this factor to the observed present-day ISC

(USGS, 2023a). We excluded four outlier sites along a suburban highway corridor from the analysis that exhibited erroneously low baseline ISC estimates, yielding extremely high adjusted ISC projections. Baseline projections and observed values for the remaining sites were largely concordant (maximum mean ISC difference of 0.03 across scenarios; SD = 0.13). We then used our SEMs to predict TCC, B-IBI, and guild-specific richness in response to ISC changes over time and across scenarios.

Finally, we examined the potential of stream conservation and restoration to mitigate projected losses in avian insectivore richness. We performed a sensitivity analysis for each SEM to determine the level of effort (decrease in ISC and a commensurate increase in TCC) required to maintain present-day richness levels. We constrained simulations to vary at a single spatial scale, holding environmental variables at the other scale constant. Local-only management occurs when changes to the local reach are possible (due to municipal ownership or a stream segment easement), whereas changes to the larger watershed are not (due to mixed or public ownership of surrounding lands). Conversely, landscape-only management is a scenario in which changes to the larger watershed are possible (through regional or watershed-scale management plans by government agencies), whereas changes to the local reach are not (due to private ownership). The effort required at each scale to maintain present-day richness, if possible, indicates the extent to which management across one or multiple spatial scales is necessary to conserve avian biodiversity. As the local scale is nested within the landscape scale, actions at either scale are inherently linked. However, we note that they can be effectively decoupled under practical extents of management. For example, landscape management to protect a forested area from development elsewhere within the watershed may improve B-IBI while not directly altering local riparian conditions. As such, we present these sensitivity analyses to explore trends in avian richness within model parameters, rather than to explicitly evaluate particular management strategies.

3.4 RESULTS

3.4.1 Observed avian communities

We detected 73 bird species across all 50 acoustic survey sites, of which roughly one-third were members of the insectivore guild under the diet composition grouping and roughly one-third were members of the migrant guild under the migration grouping (Table A3.1). Species composition largely overlapped across sites (Jaccard similarity 0.65). Insectivores were largely migratory (65%), primarily neotropical migrants, and foliage gleaning (49%) and aerial (27%) foraging behaviors were most common. Eleven families were represented among insectivores, with warblers (*Parulidae*, 7 species), tyrant flycatchers (*Tyrannidae*, 5), woodpeckers (*Picidae*, 5), and vireos (*Vireonidae*, 3) together accounting for roughly half the total number of insectivorous species. The most frequently observed members of the insectivore guild were the Chestnut-backed Chickadee (*Poecile rufescens*, 96% naïve occurrence), Western Flycatcher (*Empidonax difficilis*, 88%), Western Tanager (*Piranga ludoviciana*, 88%), and Swainson's Thrush (*Catharus ustulatus*, 84%).

3.4.2 Effects on occurrence and detection probability

Multi-species occupancy models (MSOM) provided estimates of occurrence and detectability for each species across each grouping (Figure 3.3, A3.2; Table A3.4, A3.5). Gelman-Rubin statistics ($\hat{R} < 1.01$) and visual inspection of chains indicated convergence for each model, and Bayesian posterior predictive checks (p = 0.49–0.5) indicated sufficient fit. Seasonal survey day strongly negatively affected detection probability for nearly all guilds, reflecting a decline in detectability later in the breeding season. We found no strong evidence that either ISC_{local} or TCC_{local} affected detection probability for any guild, though there was variation in species-specific responses.

By contrast, variation in covariate effects on occurrence was evident and differed substantially across species and guilds. B-IBI had the largest effect size among all occurrence covariates for the insectivore and migrant guilds and was the only guild-level predictor with a 95% Bayesian credible interval excluding zero (Figure 3.3A). Both counterfactual guilds of non-insectivore consumers (diet composition grouping) and resident or partial migrant species (migration grouping) showed no relationship with B-IBI. Insectivorous aerial foragers and

insectivorous foliage gleaners (foraging behavior grouping) and the full community showed a tendency toward increased occurrence with increasing B-IBI (Figure 3.3B), though this pattern was uncertain with credible intervals including zero. We found no clear evidence of an effect of ISC or TCC on bird occurrence probability at either the local or landscape scales across any guild, due to large species-specific differences in functional responses.

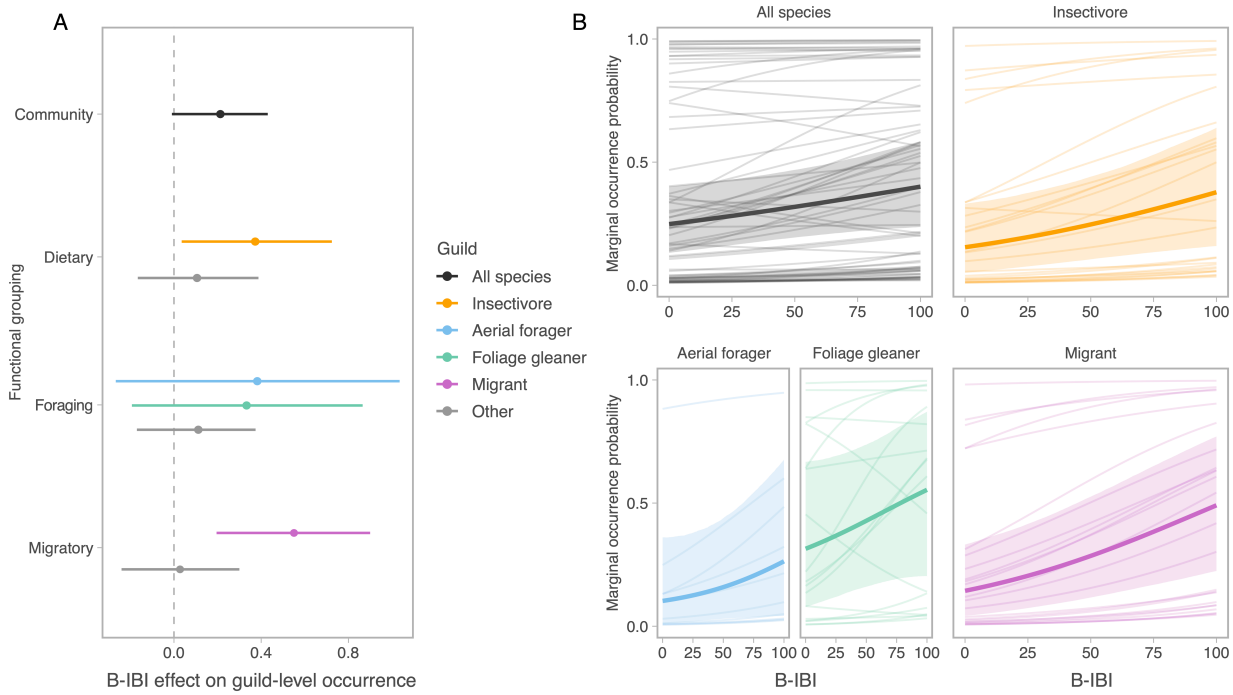

Figure 3.3: Multi-species occupancy modeling results across functional groupings for the benthic index of biotic integrity (B-IBI). (A) Guild-level effects of B-IBI on occurrence probability (posterior means with 95% Bayesian credible intervals). (B) Mean marginal probabilities of occurrence for each guild in relation to B-IBI. Bold lines show responses for guild-level means with shaded 95% Bayesian credible intervals. Ghosted lines show responses for individual species members

Species-specific responses revealed that occurrence was strongly influenced by B-IBI and TCC_{local}. Among the insectivore guild, the Swainson's Thrush (*Catharus ustulatus*) and Black-headed Grosbeak (*Pheucticus melanocephalus*) showed the strongest positive relationships with B-IBI, with 95% credible intervals excluding zero, while mean coefficients for all other members except the Hutton's Vireo (*Vireo huttoni*) were also positive. Species with strong responses to B-IBI within the migrant guild were the Western Wood-pewee (*Contopus sordidulus*), Black-throated Gray Warbler (*Setophaga nigrescens*), Western Tanager (*Piranga ludoviciana*), and

Wilson's Warbler (*Cardellina pusilla*). Under the community grouping, TCC_{local} substantially increased occurrence for the Barred Owl (*Strix varia*), Western Flycatcher (*Empidonax difficilis*), Wilson's Warbler (*Cardellina pusilla*), and Pacific Wren (*Troglodytes pacificus*), and decreased occurrence for the American Goldfinch (*Spinus tristis*) and Downy Woodpecker (*Picoides pubescens*). TCC_{land}, ISC_{land}, and ISC_{local} had no clear effect on any individual species.

3.4.3 Multi-scale pathways of landcover influence on macroinvertebrate and avian diversity

Model selection using AIC_c confirmed the importance of potential predictors for each component linear model in structural equation modeling (Table A3.6). Competitive models indicated strong support for ISC_{land} as a predictor of B-IBI, and divided support between an additional predictor of TCC_{local} or ISC_{local}. We retained TCC_{local} and treated ISC_{local} as an exogenous variable in structural equation modeling. For both insectivore and migrant guilds, B-IBI was consistently the strongest predictor of richness, and support for additional predictors was similarly divided between TCC_{local} and ISC_{local}. We again retained TCC_{local} as the direct predictor in structural equation modeling and treated ISC_{local} as an exogenous variable. TCC_{land} and ISC_{land}, by contrast, were consistently weak predictors of richness. B-IBI was the top-ranked predictor of richness for the aerial foraging guild, though no one predictor clearly dominated at either spatial scale among competitive models, indicating substantial uncertainty. Foliage gleaners and the entire avian community showed mixed support for B-IBI, with no single predictor clearly dominating at either spatial scale across competitive models. In agreement with our hypotheses regarding the causal network of biotic and abiotic factors governing the system (Figure 3.1), we therefore retained the following model structure for use in each structural equation model:

(3)

$$TCC_{local} = \alpha_1 + \beta_1 * ISC_{local} + \varepsilon_{TCC_{local}}$$

$$BIBI = \alpha_2 + \beta_2 * TCC_{local} + \beta_3 * ISC_{land} + \varepsilon_{BIBI}$$

$$Richness_g = \alpha_3 + \beta_4 * BIBI + \beta_5 * TCC_{local} + \varepsilon_{Richness_g}$$

where $Richness_g$ is the estimated posterior richness of avian guild g.

Global goodness-of-fit of the structural equation models was adequate for all guilds (mean Fisher's C 3.72–6.1, $p > 0.05$ on 8 degrees of freedom; Table A3.7), with non-significant tests of directed separation ($p > 0.05$) indicating that the network structure specified was consistent with the observed data. All models shared an identical network structure for abiotic variables, with ISC_{local} exerting a strong negative effect on TCC_{local} and ISC_{land} strongly degrading B-IBI (Figure 3.4, Table 3.1). TCC_{local} was weakly positively associated with B-IBI. These pathways explained a large proportion of the variance in TCC_{local} and B-IBI ($R^2 = 0.73$ and 0.62, respectively).

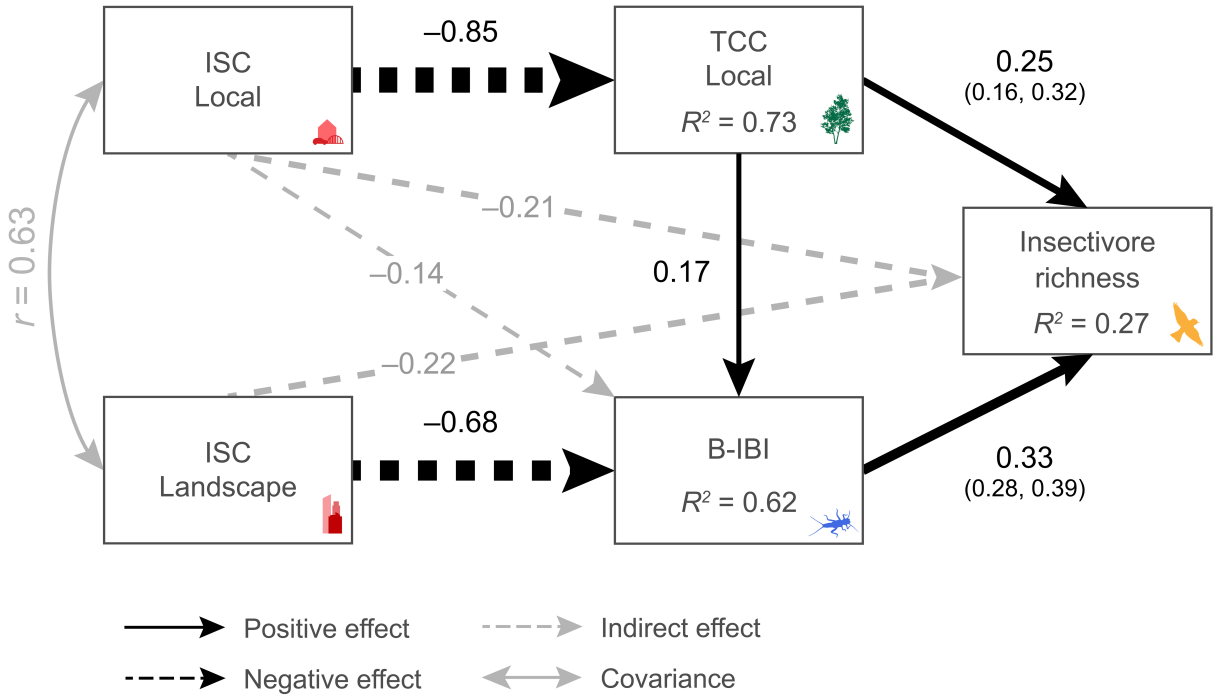

Figure 3.4: Structural equation model illustrating pathways through which urban development (ISC) at local and landscape spatial scales directly and indirectly affected riparian vegetation (TCC), benthic macroinvertebrate prey diversity (B-IBI), and posterior estimates of species richness for the avian insectivore guild, based on data from remote sensing, in-stream surveys, and bioacoustic monitoring. Arrows represent causal pathways between predictor and response variables, with line thickness proportional to the mean estimated standardized effect size. R^2 values show the mean variance of endogenous variables explained by predictors.

Grouping	Response	Predictor	Standardized coefficient	*f*
-	B-IBI	ISC_{land}	–0.68	1
	B-IBI	TCC_{local}	0.17	1
	TCC_{local}	ISC_{local}	–0.85	1
Community	Total richness	B-IBI	0.16 (0.11, 0.21)	1
Community	Total richness	TCC_{local}	0.04 (–0.05, 0.11)	0.83
Dietary	Insectivore richness	B-IBI	0.33 (0.28, 0.39)	1
Dietary	Insectivore richness	TCC_{local}	0.25 (0.16, 0.32)	1
Dietary	Other consumer richness	B-IBI	–0.02 (–0.08, 0.05)	0.71
Dietary	Other consumer richness	TCC_{local}	–0.13 (–0.23, –0.04)	1
Foraging	Aerial forager richness	B-IBI	0.29 (0.19, 0.39)	1
Foraging	Aerial forager richness	TCC_{local}	0.17 (0.01, 0.26)	0.98
Foraging	Foliage gleaner richness	B-IBI	0.11 (0.06, 0.17)	1
Foraging	Foliage gleaner richness	TCC_{local}	0.13 (0.04, 0.19)	0.99
Foraging	Other forager richness	B-IBI	0.08 (0.02, 0.15)	0.99
Foraging	Other forager richness	TCC_{local}	–0.07 (–0.19, 0.02)	0.93
Migratory	Migrant richness	B-IBI	0.4 (0.36, 0.46)	1
Migratory	Migrant richness	TCC_{local}	0.25 (0.17, 0.3)	1
Migratory	Resident and partial migrant richness	B-IBI	–0.07 (–0.13, 0.0)	0.98
Migratory	Resident and partial migrant richness	TCC_{local}	–0.12 (–0.21, –0.04)	1

Table 3.1: Standardized path coefficients for guild-specific structural equation models. Coefficient posterior mean and 95% Bayesian credible intervals are shown. Component models relating the benthic index of biotic integrity (B-IBI) to landscape-scale impervious surface cover (ISC_{land}) and local-scale tree canopy cover (TCC_{local}), and TCC_{local} to ISC_{local}, shared an identical structure across all structural equation models. *f* is the proportion of the posterior with the same sign as the mean, reflecting uncertainty that an effect is positive or negative.

Responses to biotic and abiotic drivers varied markedly among avian guilds. While total community richness showed no definitive response to either B-IBI or TCC and was poorly explained by the model (mean $R^2 = 0.04$), insectivore and migratory guilds showed clear responses to stream conditions. Strong positive effects of B-IBI and moderate positive effects of TCC_{local} on richness were the primary drivers of richness for these guilds. Together, these two predictors explained a moderate proportion of the variance in richness (mean $R^2 = 0.27$ and 0.34 for insectivore and migrant guilds, respectively). However, we found no strong statistical evidence for a cascading indirect effect of TCC_{local} on richness through B-IBI. Aerial foragers exhibited a moderate response to B-IBI ($R^2 = 0.17$), the greatest among foraging guilds, whereas

other foragers showed limited evidence of a response to either aquatic or riparian predictors, as reflected in the low explanatory power of their respective models (R^2 = 0.01-0.05; Table A3.7).

Indirect effects of ISC on insectivore and migrant guild richness operated through two pathways: ISC_{local} reduced TCC_{local}, and ISC_{land} reduced B-IBI. These indirect effects were similar in magnitude, but the B-IBI mediated pathway had greater statistical support. Individually, each indirect negative effect was weaker than the direct positive effects of B-IBI and TCC on richness; however, together they suggest that ISC influences avian richness through multiple pathways.

3.4.4 Multi-scale stream management efforts to mitigate future biodiversity loss

As members of the insectivore guild (diet composition grouping) have the most direct mechanistic ties to stream macroinvertebrate conditions and may thereby reflect the strength of aquatic-terrestrial linkages throughout the broader avian community, we focused our prediction of future urban expansion effects on B-IBI and insectivore guild richness. We present results for ICLUS scenario B1, which aligns most closely with the Puget Sound regional growth management strategy's anticipation of spatially compact yet high rates of population growth and migration in the region, alongside rapid economic growth and technological change (Puget Sound Regional Council, 2020; Bierwagen et al., 2010). Results for other scenarios are provided in the supplementary materials (Figure A3.3B, Table A3.8). The general trends we present below held across scenarios and posterior draws.

Projections indicated that ISC will increase across nearly all streams over the current century. Relative to present-day conditions, both local- and landscape-level ISC are projected to increase on average by roughly an additional 12% of surface area cover by the year 2100, a mean increase of approximately 1.7 times across all streams (Figure A3.3A, Table A3.8). At the most dramatically altered stream, ISC_{local} is expected to increase threefold while ISC_{land} will more than double. Consequently, TCC_{local} is predicted to decrease by up to 27%, representing roughly half of present-day canopy cover (Figure A3.3A). These environmental changes induce shifts in B-IBI (Figure 3.5A, C), with all but the most pristine rural forested streams degrading by as much as 34 points by year 2100. Many streams are expected to experience sufficient degradation to warrant reclassification across multiple condition categories, for example, from “good” to “poor” (Table A3.1). Collectively, these reductions in habitat and prey are predicted to reduce avian

insectivore richness by as many as three species (mean –2.84, 95% credible interval –3.23, –2.38; Figure 3.5B, D).

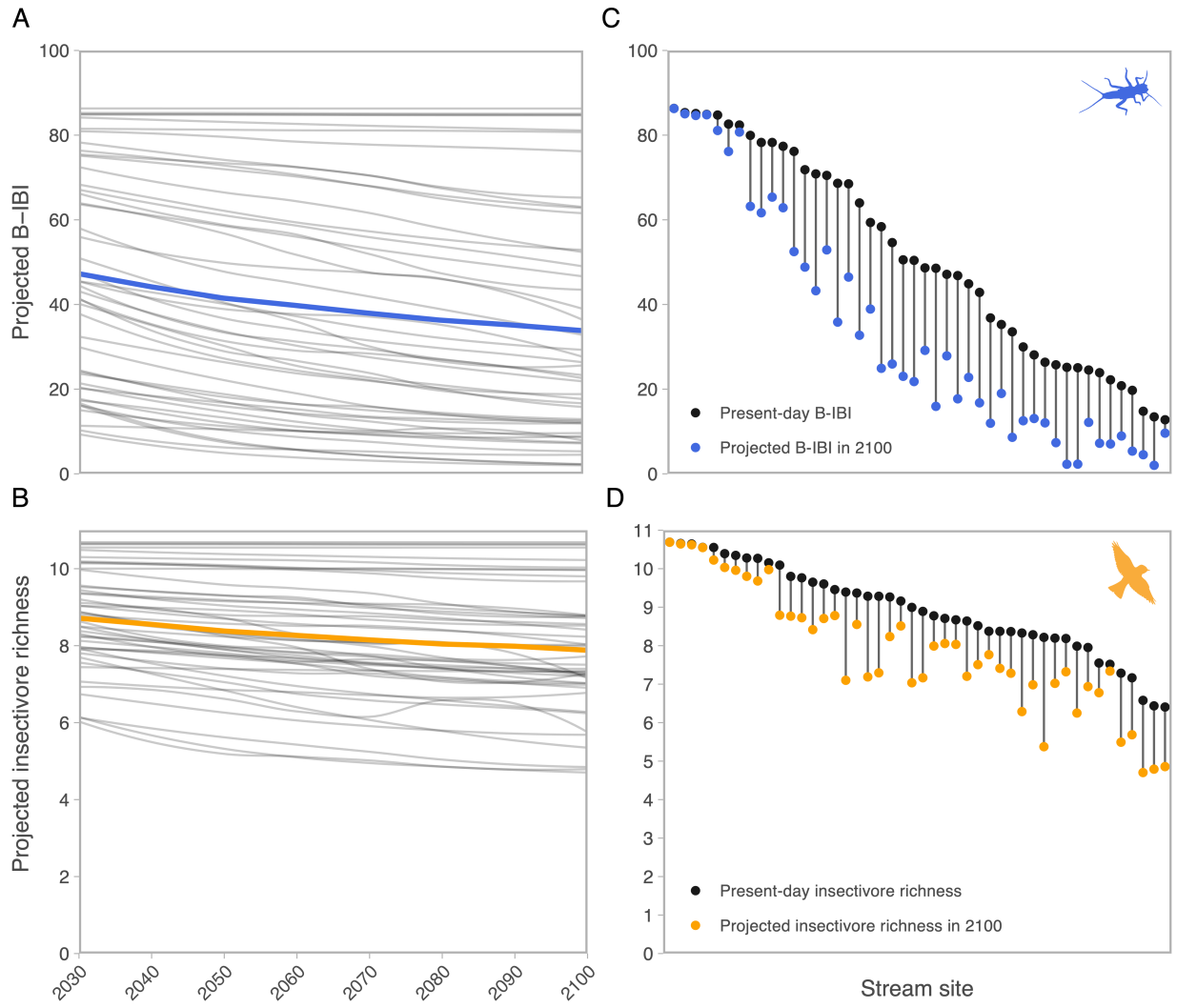

Figure 3.5: Projected future changes in B-IBI (A) and avian insectivore richness (B) over time as a consequence of urban development under the B1 ICLUS scenario, illustrated using an SEM fit to the posterior mean richness. Mean trajectories across all surveyed stream sites are shown in bold color over individual site trajectories. (C,D) Predicted losses in B-IBI and richness in 2100 compared to present-day levels.

We consider two scenarios that aim to maintain present-day levels of species richness: 1) a local-only scenario assuming future landscape-scale urbanization goes unimpeded (e.g., due to a growing population furthering urban sprawl), representing the potential for stream protection

and restoration on public lands and private lands with easements or trusts (Figure 3.6A); and 2) a landscape-only scenario assuming future local-scale urbanization and riparian vegetation cannot be changed within a particular stream reach (e.g., due to private land ownership), representing the potential for conservation action through integrated watershed management plans (Figure 3.6B). We define "restoration" in our model as a reduction in ISC and a commensurate increase in TCC.

A sensitivity analysis of the SEM fit to the posterior mean insectivore richness revealed that landscape-only management required larger reductions in ISC at a greater spatial scale than local-only management. For many streams, even dramatic, complete landscape-scale conservation efforts cannot mitigate the overwhelming impacts of local-scale degradation within a stream reach (Figure 3.6B). By contrast, more streams were able to maintain present richness levels through local-scale management alone (Figure 3.6A). Similarly, the slope of contour lines between scales in Figure 3.6C is less than –1, indicating that modeled richness is more sensitive to reductions in local- rather than landscape-scale ISC. However, neither management approach was sufficient to maintain present-day bird community richness across all streams, as several required management action at one particular scale or both (Figure 3.6C). Across both scales, the magnitude of management action required is not necessarily contingent on the degree of future impairment under a "no action" scenario.

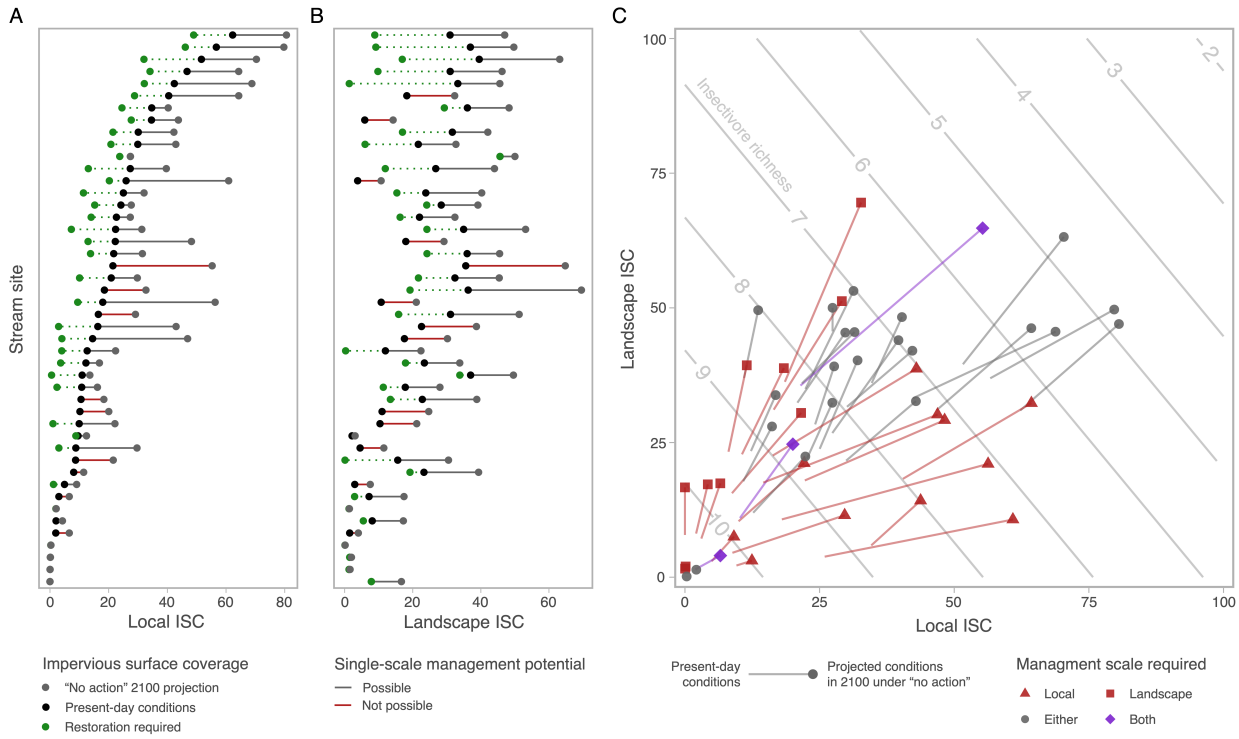

Figure 3.6: Predicted management action at local and landscape scales required to maintain present-day avian richness levels by year 2100, obtained from a sensitivity analysis of the SEM fit to the posterior mean insectivore richness. (A) Local-only scenario, with commensurate increases in riparian vegetation from restoration implied. (B) Landscape-only scenario, with stream sites aligned with (A). (C) Predicted insectivore richness, using posterior mean SEM, across both spatial dimensions of impervious surface cover (ISC). Contours show equal levels of richness. Individual stream trajectories are shown with lines beginning at present-day conditions and ending at projected conditions in 2100 under a "no action" scenario. Streams shown in gray can fully mitigate reductions through single-scale management, at either the local or catchment scale. Those shown in red can only maintain richness via management at the local (triangle) or landscape (square) scale. Those shown in purple require management actions at both scales simultaneously.

3.5 DISCUSSION

Freshwater and riparian environments are tightly coupled by the flow of cross-boundary resource subsidies, such that birds can track and benefit from the seasonal emergence of adult aquatic insect prey. We found that a benthic index of biotic integrity (B-IBI) was strongly associated with the richness of avian insectivores and migrants across urban streams during the breeding season. However, B-IBI was highly vulnerable to degradation from impervious surface cover (ISC), a

surrogate for urban stressors, and reduced tree canopy cover (TCC), reflecting riparian habitat condition. We show that stream biotic integrity and riparian habitat condition mediate the transmission of local- and landscape-scale stressors from urban development to avian communities. We predict declines in B-IBI and avian insectivore richness as a result of projected future urban expansion. However, we found that present-day insectivore diversity can be maintained by provisioning habitat and aquatic subsidies through riparian protection and restoration, although the magnitude and spatial scale of management action required varied by stream context. These findings suggest that multi-scale management strategies are critical to safeguard terrestrial and aquatic biodiversity amid future urbanization.

3.5.1 Pathways of influence on the diversity of avian guilds and aquatic insects

B-IBI demonstrated a clear association with the occurrence of specific functional groups within the larger avian community, most notably insectivores and migrants (Figure 3.3, 3.4). Members of the insectivore guild (under the diet composition grouping) consume aquatic insect larvae or their emergent adult forms as primary or supplemental food sources. As an indicator of the abundance and composition of benthic macroinvertebrate communities, B-IBI is closely related to the quality and availability of these prey subsidies (Statzner & Resh, 1993). Therefore, insectivores in our study system may selectively exploit these resources to support their energetic needs during breeding, growth, and molting (Twining et al., 2018; Martin-Creuzburg et al., 2017; Dodson et al., 2016). As prey availability is inversely related to territory size across many bird species (Hixon, 1980), streams with high levels of B-IBI may increase carrying capacity by supporting higher insectivore densities (Gray, 1993; Wilcox et al., 2021), thereby expanding opportunities for coexistence and facilitating greater taxonomic richness (Hulbert, 2004). Similarly, habitat structural complexity and vegetation density may benefit birds both directly through habitat provision and indirectly through enhanced aquatic subsidies (Baxter et al., 2005), as evidenced in our model (Figure 3.4). The role of foraging behavior in shaping community composition was inconclusive; however, trends toward increased occurrence by aerial foragers and foliage gleaners with improved stream integrity are consistent with previous research (Schilke et al., 2020). It is unclear whether increased richness results from greater niche specialization through increased prey diversity or from reduced resource limitation.

Migratory birds, particularly neotropical insectivores, were especially responsive to B-IBI (Figure 3.3, Table 3.1). While the insectivore guild (under the diet composition grouping) is composed of an ecologically heterogeneous collection of species with disparate foraging strata and diverse prey types, migratory birds (under the migration grouping) share more closely aligned foraging behaviors along riparian corridors (Pennington et al., 2008), higher dependence on aquatic-terrestrial subsidies, and tightly coupled phenological synchrony with prey emergence (Trevelline et al., 2018; Macdade et al., 2011). Migrants undertake long-distance journeys during which seasonal pulses in aquatic subsidies at stopover and breeding sites can provide essential resources for refueling and reproduction (Dodson et al., 2016; Smith et al., 2007). As B-IBI represents the quality of aquatic-terrestrial subsidies and stream integrity as a function of the surrounding watershed, it may serve as an indicator of the broader suite of riparian habitat conditions that migrants track across regional scales. These results support other findings that aquatic-terrestrial subsidies are more strongly associated with avian diversity in riparian environments than habitat composition alone (Wagner & Reynolds, 2019), particularly in highly degraded environments where subsidies can become disproportionately important foraging resources (Marczak et al., 2007; Nakano & Murakami, 2001).

We found that the local avian community within a stream segment was shaped by an interconnected network of environmental determinants operating across spatial scales. The strong influence of landscape-level ISC on B-IBI, and local ISC on TCC, point to cascading effects of urban pressures on birds through the modification of stream and habitat integrity. Although insectivores were most influenced by nearby conditions at the stream reach, the vulnerability of these conditions to pressures from the surrounding landscape indirectly links local avian communities to urban development at broader spatial scales (Sullivan et al., 2020). Moreover, the magnitudes of these indirect pressures rival those of the direct influence of local stream integrity and riparian vegetation alone (Figure 3.4). Therefore, avian diversity in urban streams is contingent on the cumulative effects of urban stressors in the surrounding landscape, and efforts to conserve urban avian diversity must consider the multiple interacting scales at which these stressors operate (Pennington & Blair, 2011).

3.5.2 Implications for urban stream management

Projections of future land use conditions indicate that anthropogenic stressors will continue to increase throughout the Seattle metropolitan area over the current century (Puget Sound Regional Council, 2020; Robinson et al., 2005), resulting in degradation of stream integrity and declines in avian richness (Figure 3.5). By applying our model to projections of ISC through 2100, we anticipate substantial reductions in B-IBI resulting in an estimated loss of up to three bird species from the local riparian community. While we do not directly predict changes in community composition, our occupancy modeling results suggest that reductions in richness will likely be driven by the loss of insectivores and migrants. Streams with the most dramatic changes in avian richness and B-IBI tended to be located on the fringes of semi-urban neighborhoods, or within private forestlands surrounded by an urban matrix—areas that are expected to experience substantial development in the future. While these trends held across ICLUS scenarios, under the B1 compact urban growth scenario we predicted slightly greater increases in local ISC and reductions in richness compared to other scenarios (Table A3.8). As the streams we sampled are mostly located within regionally designated urban growth areas, this reflects the effect of compact development strategies that redirect urbanization from the broader watershed scale to the local scale via infill and redevelopment (Bierwagen et al., 2010).

Efforts to conserve and restore riparian areas safeguard pathways for cross-boundary nutrient exchange and corridors for movement and dispersal, and may buffer against perturbations from urban expansion and densification (Keten et al., 2020; Pennington et al., 2008). Using model simulations, we report that the protection and restoration of urban streams across multiple spatial scales are likely necessary mitigation actions to ensure that present-day avian richness associated with these streams is retained. This approach builds on existing work that leverages SEM to predict the consequences of anthropogenic pressures on aquatic subsidies (Fernandes et al., 2019), extending inference to avian insectivores and quantifying effects across aquatic-terrestrial boundaries. We explored two scenarios to maintain insectivore richness, and found that richness responses were more sensitive to reductions in local- rather than landscape-scale ISC. The local-only scenario was predicted to maintain avian richness in most streams with comparatively small to moderate requirements to decrease impervious surface and increase riparian tree canopy cover (Figure 3.6A). This suggests that municipal and private lands held in easements or trusts may serve as important buffers to maintain both the habitat and aquatic insect

subsidies required to support avian richness amid continued urban development across the broader landscape. By contrast, the landscape-only scenario often required larger reductions in ISC at greater spatial scales to achieve the same status quo outcome for avian species richness (Figure 3.6B). However, unilateral reduction in urban land use from present-day conditions to such an extent is impracticable. Moreover, for many streams, our models indicate that even dramatic, complete landscape-scale restoration efforts will not mitigate the overwhelming impacts of local-scale degradation. This suggests that the cascading benefits of improved stream integrity through integrated watershed management may be better realized when streams are not locally degraded. Additionally, our modeling indicates that the magnitude of action required to maintain richness levels is not necessarily contingent on the magnitude of projected future impairment (Figure 3.6). These findings suggest that local-scale efforts to restore and protect streams in the present are pragmatic strategies to conserve richness with substantially less effort compared to attempts to reverse impacts from already-established urban development in the future.

No single-scale approach was sufficient to conserve avian richness at all streams, however; several depended exclusively on restoration of one scale or both (Figure 3.6). Streams requiring local restoration have relatively low levels of ISC within their surrounding landscape, while those requiring landscape restoration have low ISC locally. Thus, the required spatial scale is often governed by which has the greatest restoration capacity. In extreme cases, streams projected to experience major ISC changes at both scales may be unable to maintain richness through single-scale restoration alone, requiring instead strategies that simultaneously restore both. While we constrained these two scenarios to act independently to explore the spatial scaling of urbanization effects, in practice, both restoration efforts and urban development are inherently linked across spatial scales. Ultimately, restoration at any scale alters local conditions somewhere that strongly shape nesting and foraging habitat structure and microclimate, factors that most strongly influence habitat selection and community composition (Wiens, 1989; Cody, 1985). However, conditions throughout the landscape remain important factors shaping the dispersal and persistence of avian populations that form the regional species pool (Shoffner et al., 2018; Litteral & Shochat, 2017), despite the inconclusive direct landscape-scale effects we report here. Urban landscapes that support persistent avian populations must provide a variety of resources for birds beyond aquatic subsidies alone (Marzluff, 2005). Integrated management

plans are thus critical for balancing the ecological, economic, and social needs throughout an urban watershed (Wang et al., 2016).

Increased urban development is necessary to accommodate growing human populations (United Nations, 2025; Chen et al., 2020). While compact urban growth strategies help preserve natural resource lands by limiting urban encroachment into rural areas, the redirection of growth via infill and redevelopment results in increased ecological impacts in densified areas (Puget Sound Regional Council, 2020). However, the strategic conservation of riparian corridors within urban growth areas may help offset some losses to local biodiversity attributed to densification by protecting aquatic-terrestrial ecosystem linkages (Keten et al., 2020; Pennington et al., 2008), while also buffering against the effects of invasive species (Peller & Altermatt, 2024), and climate change (Seavy et al., 2009). Protecting intact urban forests and increasing riparian habitat complexity, connectivity, and water quality can enhance both aquatic and terrestrial diversity (Wegscheider et al., 2025), while restoring channel-floodplain connectivity and hydrological regimes can enhance the flux of aquatic subsidies (McCabe et al., 2025). Emerging strategies to jump-start the recovery of degraded urban streams through assisted macroinvertebrate recolonization (e.g., “bug seeding”) may contribute to these efforts (Clinton et al., 2022). These cross-ecosystem co-benefits can be magnified by aligning freshwater and terrestrial conservation through co-management of the landscape, supporting ecosystem resilience in the face of future urbanization and climate change (Leal et al., 2020; Amis et al., 2009).

3.5.3 Opportunities for future research

While B-IBI is strongly correlated with EPT richness and serves as a robust indicator of the composition of aquatic insect communities (Statzner & Resh, 1993), it does not directly quantify the biomass or timing of emergent subsidies. The degree to which changes in bird diversity are coupled with the magnitude and temporal flux of emergent subsidies warrants further research. Peak emergence periods can alter the foraging behavior and demographics of insectivores (Baxter et al., 2005), driving increased bird abundance and immigration from upland to riparian habitats (Nakano & Murakami 2001; Uesugi & Murakami 2007). We found that detection probability was highest earlier in the breeding season for most species, a period coinciding with typical peak emergence, and this effect was stronger for insectivores and migrants than for non-insectivores and residents (Figure A3.2). Importantly, our predictions assume that the

relationship between richness and B-IBI will remain constant through time, which may not hold as climate change drives a phenological mismatch between the timing of emergence and bird breeding (Shipley et al., 2022). Reducing thermal pollution through the restoration of hydrological regimes and riparian microclimate refugia may stabilize these effects (Dallas & Ross-Gillespie, 2015). Additionally, the relationship between urban development and B-IBI may not remain constant through time, but is expected to remain strongly negative (Sosik et al., 2025).

The degree to which improved stream integrity benefits birds through access to emergent insects specifically, versus terrestrial arthropods that also benefit from aquatic subsidies, remains unclear. High stream integrity can support greater densities of terrestrial prey and avian insectivores (Smith et al., 2007; Hagar et al., 2012), while stream degradation can impair aquatic resource subsidies to riparian spiders (Kowarik et al., 2023), with cascading effects on avian consumers (Nakano & Murakami, 2001). We observed strong responses to B-IBI for several species with little or no documented predation of aquatic macroinvertebrates (e.g., Black-headed Grosbeak, Black-throated Gray Warbler) that nevertheless exhibit reliance on food webs with aquatic origins (Jackson et al., 2020).

We constrained our analysis to variables widely used as indicator metrics in urban planning and restoration (Morley & Karr, 2002; Mincey et al., 2013) that readily support the prediction of ecological responses to future change (Bierwagen et al., 2010; Nowak & Greenfield, 2012). TCC approximates the prevalence of riparian vegetation in urban streams, but may not capture the structural heterogeneity that birds and emergent insects require for foraging and breeding, or the in-stream microhabitat conditions of aquatic insects. Similarly, ISC may not fully represent the connected surfaces that direct stormwater collection (Han & Burian, 2009), and does not directly quantify human activity, light or noise pollution. The many mechanisms through which urbanization stressors shape aquatic insect and avian communities are increasingly understood (Huang & Gergel, 2023; Shoffner et al., 2018; Baxter et al., 2005), yet investigating the degree to which they propagate across trophic boundaries remains a promising area of research (Bundschuh et al., 2022).

Our study demonstrates the utility of passive acoustic monitoring as a cost-effective approach to supplement existing monitoring programs of urban freshwater ecosystems at large spatiotemporal scales (Arzberger et al., 2025; Shonfield & Bayne, 2017). However, bioacoustic

surveys of avian community composition depend on the robust detection of many species. Importantly, the classifier calibration approach we employed assumes that the species-specific probabilistic threshold for a true positive detection is constant across sites and surveys, which may not hold in heterogeneous soundscapes that vary in space and time. While all calibrated species achieved precision scores of roughly 1 (Table A3.2), suggesting this is not the case in our study, exhaustive manual validation of detections was necessary for several species (e.g., varied thrush, brown-headed cowbird, great horned owl) because of frequent classifier false positive confusion from geophony and anthropophony. We suggest that future community-level bioacoustic surveys conducted across greater spatiotemporal scales consider methods such as transfer learning to enable robust semi-autonomous detection at scale (Jacuzzi & Olden, 2025).

3.5.4 Conclusion

We provide evidence that aquatic insect subsidies mediate current and future urbanization effects on insectivorous birds across spatial scales. Efforts to reinforce and protect cross-boundary ecosystem linkages may be critical to support ecosystem resilience in future urban landscapes. Projected consequences for ecosystem functions resulting from increasing urban development in our study region mirror global urban expansion trends (United Nations, 2025; Chen et al., 2020). Loss of riverine habitat and biota threatens the collapse of ecosystem processes and functions, jeopardizing their ecosystem services for humans (Lynch et al., 2023; Albert et al., 2021). Management strategies that bolster aquatic-terrestrial linkages through the protection and restoration of riparian habitat may mediate the effects of anthropogenic stressors on avian biodiversity, particularly in arid and growing regions experiencing rapid urban development where the provisioning of aquatic subsidies may be disproportionately influential in the persistence of bird populations (Naiman et al., 1993). Therefore, the conservation and restoration of urban streams is a joint priority for supporting the resilience of both aquatic and terrestrial ecosystems (Adams et al., 2013; Amis et al., 2009) and may be essential to curb ongoing parallel declines of insectivorous bird and insect populations worldwide (Tallamy & Shriver, 2021; Rosenberg et al., 2019). Such management efforts must consider the multiple interacting scales and pathways through which urbanization stressors influence avian communities (Pennington & Blair, 2011). Our findings contribute to a growing body of research showing that the future

conservation of terrestrial and aquatic biodiversity in urban environments is tightly intertwined and depends on the co-management of the landscape today.

3.6 ACKNOWLEDGEMENTS

Funding for this study was provided by the Future Rivers National Science Foundation program and the School of Aquatic and Fishery Sciences, University of Washington. We thank Kate Macneale and the King County Department of Natural Resources and Parks (DNRP) for their feedback in study design, and Sarah J Converse for suggestions that improved this manuscript. We also thank all King County DNRP agency scientists and volunteers from the cities of Kirkland, Bellevue, and Redmond for conducting benthic macroinvertebrate sampling, as well as community residents who cooperated with acoustic monitoring. Attributions for graphical elements used in figure illustrations can be found in Appendix 3.1.

3.7 DATA AVAILABILITY

All data and code required to recreate analyses and generate results, figures, and tables are provided through the open-source repository github.com/giojacuzzi/riparian-avian-macroinvert-monitoring-kc.

3.8 REFERENCES

Abood, Sinan A., Linda Spencer, and Michael Wieczorek. 2022. U.S. Forest Service National Riparian Areas Base Map for the Conterminous United States in 2019. U.S. Department of Agriculture, Forest Service. https://www.fs.usda.gov/rds/archive/catalog/RDS-2019-0030.

Adams, Vanessa M., Jorge G. Álvarez-Romero, Josie Carwardine, et al., 2014. "Planning Across Freshwater and Terrestrial Realms: Cobenefits and Tradeoffs Between Conservation Actions." Conservation Letters 7 (5): 425–40. https://doi.org/10.1111/conl.12080.

Albert, James S., Georgia Destouni, Scott M. Duke-Sylvester, et al., 2021. "Scientists' Warning to Humanity on the Freshwater Biodiversity Crisis." Ambio 50 (1): 85–94. https://doi.org/10.1007/s13280-020-01318-8.

Alberti, Marina, Derek Booth, Kristina Hill, et al., 2007. "The Impact of Urban Patterns on Aquatic Ecosystems: An Empirical Analysis in Puget Lowland Sub-Basins." Landscape and Urban Planning 80 (4): 345–61. https://doi.org/10.1016/j.landurbplan.2006.08.001.

Alberti, Marina, and John M. Marzluff. 2004. "Ecological Resilience in Urban Ecosystems: Linking Urban Patterns to Human and Ecological Functions." Urban Ecosystems 7 (3): 241–65. https://doi.org/10.1023/B:UECO.0000044038.90173.c6.

Allan, J. David. 2004. "Landscapes and Riverscapes: The Influence of Land Use on Stream Ecosystems." Annual Review of Ecology, Evolution, and Systematics 35 (Volume 35, 2004): 257–84. https://doi.org/10.1146/annurev.ecolsys.35.120202.110122.

Amis, Mao A., Mathieu Rouget, Mervyn Lotter, and Jenny Day. 2009. "Integrating Freshwater and Terrestrial Priorities in Conservation Planning." Biological Conservation 142 (10): 2217–26. https://doi.org/10.1016/j.biocon.2009.04.021.

Arnold Jr., Chester L., and C. James Gibbons. 1996. "Impervious Surface Coverage: The Emergence of a Key Environmental Indicator." Journal of the American Planning Association 62 (2): 243–58. https://doi.org/10.1080/01944369608975688.

Arzberger, Sophie, Andrew Fairbairn, Michael Hemauer, Maximilian Mühlbauer, Julie Weissmann, and Monika Egerer. 2025. "The Potential of Soundscapes as an Ecosystem Monitoring Tool for Urban Biodiversity." Journal of Urban Ecology 11 (1): juaf002. https://doi.org/10.1093/jue/juaf002.

Balian, E. V., H. Segers, C. Lévèque, and K. Martens. 2008. “The Freshwater Animal Diversity Assessment: An Overview of the Results.” Hydrobiologia 595 (1): 627–37. https://doi.org/10.1007/s10750-007-9246-3.

Baruch, Ethan M., Kristofor A. Voss, Joanna R. Blaszczak, Joseph Delesantro, Dean L. Urban, and Emily S. Bernhardt. 2018. “Not All Pavements Lead to Streams: Variation in Impervious Surface Connectivity Affects Urban Stream Ecosystems.” Freshwater Science 37 (3): 673–84. https://doi.org/10.1086/699014.

Baxter, Colden V., Kurt D. Fausch, and W. Carl Saunders. 2005. “Tangled Webs: Reciprocal Flows of Invertebrate Prey Link Streams and Riparian Zones.” Freshwater Biology 50 (2): 201–20. https://doi.org/10.1111/j.1365-2427.2004.01328.x.

Bierwagen, Britta G., David M. Theobald, Christopher R. Pyke, et al., 2010. “National Housing and Impervious Surface Scenarios for Integrated Climate Impact Assessments.” Proceedings of the National Academy of Sciences 107 (49): 20887–92. https://doi.org/10.1073/pnas.1002096107.

Billerman, S. M., B. K. Keeney, G. M. Kirwan, F. Medrano, N. D. Sly, and M. G. Smith. 2026. “Birds of the World.” Cornell Laboratory of Ornithology. https://doi.org/10.2173/bow.

Bowler, Diana E., Henning Heldbjerg, Anthony D. Fox, Maaike de Jong, and Katrin Böhning-Gaese. 2019. “Long-Term Declines of European Insectivorous Bird Populations and Potential Causes.” Conservation Biology 33 (5): 1120–30. https://doi.org/10.1111/cobi.13307.

Broms, Kristin M., Mevin B. Hooten, and Ryan M. Fitzpatrick. 2016. “Model Selection and Assessment for Multi-Species Occupancy Models.” Ecology 97 (7): 1759–70. https://doi.org/10.1890/15-1471.1.

Brown, E. R. 1985. Management of Wildlife and Fish Habitats in Forests of Western Oregon and Washington. PB-94-188075/XAB. U.S. Department of Agriculture, Forest Service. https://www.osti.gov/biblio/7110353.

Bundschuh, Mirco, Sebastian Pietz, Alexis P. Roodt, and Johanna M. Kraus. 2022. “Contaminant Fluxes across Ecosystems Mediated by Aquatic Insects.” Current Opinion in Insect Science 50 (April): 100885. https://doi.org/10.1016/j.cois.2022.100885.

Carlson, Peter E., Brendan G. McKie, Leonard Sandin, and Richard K. Johnson. 2016. “Strong Land-Use Effects on the Dispersal Patterns of Adult Stream Insects: Implications for

Transfers of Aquatic Subsidies to Terrestrial Consumers." Freshwater Biology 61 (6): 848–61. https://doi.org/10.1111/fwb.12745.

Chen, Guangzhao, Xia Li, Xiaoping Liu, et al., 2020. "Global Projections of Future Urban Land Expansion under Shared Socioeconomic Pathways." Nature Communications 11 (1): 537. https://doi.org/10.1038/s41467-020-14386-x.

Chen, Kai, Stephen R. Midway, Brandon K. Peoples, Beixin Wang, and Julian D. Olden. 2023. "Shifting Taxonomic and Functional Community Composition of Rivers under Land Use Change." Ecology 104 (11): e4155. https://doi.org/10.1002/ecy.4155.

Clinton, Sandra M., Jacqueline Hartman, Kate H. Macneale, and Allison H. Roy. 2022. "Stream Macroinvertebrate Reintroductions: A Cautionary Approach for Restored Urban Streams." Freshwater Science 41 (3): 507–20. https://doi.org/10.1086/721471.

Cody, Martin L. 1981. "Habitat Selection in Birds: The Roles of Vegetation Structure, Competitors, and Productivity." BioScience 31 (2): 107–13. https://doi.org/10.2307/1308252.

Dallas, H. F., and V. Ross-Gillespie. 2015. "Review: Sublethal Effects of Temperature on Freshwater Organisms, with Special Reference to Aquatic Insects." Water SA 41 (5): 712–26. https://doi.org/10.4314/wsa.v41i5.15.

Darras, Kevin, Péter Batáry, Brett Furnas, et al., 2018. "Comparing the Sampling Performance of Sound Recorders versus Point Counts in Bird Surveys: A Meta-Analysis." Journal of Applied Ecology 55 (6): 2575–86. https://doi.org/10.1111/1365-2664.13229.

Dodson, Jenna C., Nicholas J. Moy, and Lesley P. Bulluck. 2016. "Prothonotary Warbler Nestling Growth and Condition in Response to Variation in Aquatic and Terrestrial Prey Availability." Ecology and Evolution 6 (20): 7462–74. https://doi.org/10.1002/ece3.2400.

Fernandes, A. C. P., L. F. Sanches Fernandes, J. P. Moura, R. M. V. Cortes, and F. A. L. Pacheco. 2019. "A Structural Equation Model to Predict Macroinvertebrate-Based Ecological Status in Catchments Influenced by Anthropogenic Pressures." Science of The Total Environment 681 (September): 242–57. https://doi.org/10.1016/j.scitotenv.2019.05.117.

Fierro, Pablo, Carlos Bertrán, Jaime Tapia, et al., 2017. "Effects of Local Land-Use on Riparian Vegetation, Water Quality, and the Functional Organization of Macroinvertebrate Assemblages." Science of The Total Environment 609 (December): 724–34. https://doi.org/10.1016/j.scitotenv.2017.07.197.

Fink, D., A. Johnston, M. Strimas-Mackey, et al., 2025. “eBird Status and Trends, Data Version: 2023.” eBird Status and Trends, Cornell Lab of Ornithology. https://doi.org/10.2173/WZTW8903.

Finn, Catherine, Florencia Grattarola, and Daniel Pincheira-Donoso. 2023. “More Losers than Winners: Investigating Anthropocene Defaunation through the Diversity of Population Trends.” Biological Reviews 98 (5): 1732–48. https://doi.org/10.1111/brv.12974.

Gray, Lawrence J. 1993. “Response of Insectivorous Birds to Emerging Aquatic Insects in Riparian Habitats of a Tallgrass Prairie Stream.” The American Midland Naturalist 129 (2): 288–300. https://doi.org/10.2307/2426510.

Greenwood, M. J., and D. J. Booker. 2016. “Influence of Hydrological Regime and Land Cover on Traits and Potential Export Capacity of Adult Aquatic Insects from River Channels.” Oecologia 180 (2): 551–66. https://doi.org/10.1007/s00442-015-3462-8.

Hagar, Joan C., Judith Li, Janel Sobota, and Stephanie Jenkins. 2012. “Arthropod Prey for Riparian Associated Birds in Headwater Forests of the Oregon Coast Range.” Forest Ecology and Management 285 (December): 213–26. https://doi.org/10.1016/j.foreco.2012.08.026.

Han, Woo Suk, and Steven J. Burian. 2009. “Determining Effective Impervious Area for Urban Hydrologic Modeling.” Journal of Hydrologic Engineering 14 (2): 111–20. https://doi.org/10.1061/(ASCE)1084-0699(2009)14:2(111).

Hill, Andrew P., Peter Prince, Jake L. Snaddon, C. Patrick Doncaster, and Alex Rogers. 2019. “AudioMoth: A Low-Cost Acoustic Device for Monitoring Biodiversity and the Environment.” HardwareX 6 (October): e00073. https://doi.org/10.1016/j.ohx.2019.e00073.

Hixon, Mark A. 1980. “Food Production and Competitor Density as the Determinants of Feeding Territory Size.” The American Naturalist 115 (4): 510–30.

Huang, Jieying, and Sarah E. Gergel. 2023. “Effectiveness of Landscape Indicators for Explaining the Variability of Benthic Macro-Invertebrates in Urban Streams.” Journal of Environmental Management 342 (September): 118130. https://doi.org/10.1016/j.jenvman.2023.118130.

Hurlbert, Allen H. 2004. “Species–Energy Relationships and Habitat Complexity in Bird Communities.” Ecology Letters 7 (8): 714–20. https://doi.org/10.1111/j.1461-0248.2004.00630.x.

Hurvich, Clifford M., and Chih-Ling Tsai. 1989. “Regression and Time Series Model Selection in Small Samples.” Biometrika 76 (2): 297–307. https://doi.org/10.1093/biomet/76.2.297.

Iwata, Tomoya, Shigeru Nakano, and Masashi Murakami. 2003. “Stream Meanders Increase Insectivorous Bird Abundance in Riparian Deciduous Forests.” Ecography 26 (3): 325–37. https://doi.org/10.1034/j.1600-0587.2003.03355.x.

Jackson, Breeanne K., Sarah L. Stock, Leila S. Harris, Joseph M. Szewczak, Lynn N. Schofield, and Michelle A. Desrosiers. 2020. “River Food Chains Lead to Riparian Bats and Birds in Two Mid-Order Rivers.” Ecosphere 11 (6): e03148. https://doi.org/10.1002/ecs2.3148.

Jacuzzi, Giordano, and Julian D. Olden. 2025. “Few-Shot Transfer Learning Enables Robust Acoustic Monitoring of Wildlife Communities at the Landscape Scale.” Ecological Informatics 90 (December): 103294. https://doi.org/10.1016/j.ecoinf.2025.103294.

Johnston, Alison, Amanda D. Rodewald, Matt Strimas-Mackey, et al., 2025. “North American Bird Declines Are Greatest Where Species Are Most Abundant.” Science 388 (6746): 532–37. https://doi.org/10.1126/science.adn4381.

K. Lisa Yang Center for Conservation Bioacoustics at the Cornell Lab of Ornithology. 2026. Raven Pro: Interactive Sound Analysis Software (Version 1.6.5). The Cornell Lab of Ornithology, released. https://www.ravensoundsoftware.com/.

Kahl, Stefan, Connor M. Wood, Maximilian Eibl, and Holger Klinck. 2021. “BirdNET: A Deep Learning Solution for Avian Diversity Monitoring.” Ecological Informatics 61 (March): 101236. https://doi.org/10.1016/j.ecoinf.2021.101236.

Kautza, Adam, and S. Mažeika P. Sullivan. 2015. “Shifts in Reciprocal River-Riparian Arthropod Fluxes along an Urban-Rural Landscape Gradient.” Freshwater Biology 60 (10): 2156–68. https://doi.org/10.1111/fwb.12642.

Kellner, Ken, and Mike Meredith. 2026. jagsUI: A Wrapper Around “rjags” to Streamline “JAGS” Analyses. V. 1.6.3. Released January 10. https://cran.r-project.org/web/packages/jagsUI/index.html.

Keten, Akif, Engin Eroglu, Sertac Kaya, and James T. Anderson. 2020. “Bird Diversity along a Riparian Corridor in a Moderate Urban Landscape.” Ecological Indicators 118 (November): 106751. https://doi.org/10.1016/j.ecolind.2020.106751.

King County Department of Natural Resources and Parks. 2026. “Puget Sound Stream Benthos.” https://pugetsoundstreambenthos.org/.

Knutson, K. Lea, and Virginia L. Naef. 1997. Management Recommendations for Washington’s Priority Habitats: Riparian. Washington Department of Fish & Wildlife. https://wdfw.wa.gov/publications/00029.

Kowarik, Carmen, Dominik Martin-Creuzburg, Kate L. Mathers, Christine Weber, and Christopher T. Robinson. 2023. “Stream Degradation Affects Aquatic Resource Subsidies to Riparian Ground-Dwelling Spiders.” Science of The Total Environment 855 (January): 158658. https://doi.org/10.1016/j.scitotenv.2022.158658.

Lafage, D., E. Bergman, R. L. Eckstein, E. M. Österling, J. P. Sadler, and J. J. Piccolo. 2019. “Local and Landscape Drivers of Aquatic-to-Terrestrial Subsidies in Riparian Ecosystems: A Worldwide Meta-Analysis.” Ecosphere 10 (4): e02697. https://doi.org/10.1002/ecs2.2697.

Larsen, Stefano, Alberto Sorace, and Laura Mancini. 2010. “Riparian Bird Communities as Indicators of Human Impacts along Mediterranean Streams.” Environmental Management 45 (2): 261–73. https://doi.org/10.1007/s00267-009-9419-0.

Leal, Cecília G., Gareth D. Lennox, Silvio F. B. Ferraz, et al., 2020. “Integrated Terrestrial-Freshwater Planning Doubles Conservation of Tropical Aquatic Species.” Science 370 (6512): 117–21. https://doi.org/10.1126/science.aba7580.

Lefcheck, Jonathan S. 2016. “piecewiseSEM: Piecewise Structural Equation Modelling in r for Ecology, Evolution, and Systematics.” Methods in Ecology and Evolution 7 (5): 573–79. https://doi.org/10.1111/2041-210X.12512.

Litteral, Jennifer, and Eyal Shochat. 2017. “The Role of Landscape-Scale Factors in Shaping Urban Bird Communities.” In Ecology and Conservation of Birds in Urban Environments, edited by Enrique Murgui and Marcus Hedblom. Springer International Publishing. https://doi.org/10.1007/978-3-319-43314-1_8.

Lynch, Abigail J., Steven J. Cooke, Angela H. Arthington, et al., 2023. “People Need Freshwater Biodiversity.” WIREs Water 10 (3): e1633. https://doi.org/10.1002/wat2.1633.

Macdade, Lauren S., Paul G. Rodewald, and Kent A. Hatch. 2011. “Contribution of Emergent Aquatic Insects to Refueling in Spring Migrant Songbirds.” The Auk 128 (1): 127–37. https://doi.org/10.1525/auk.2011.10186.

Macneale, Kate, Liora Llewellyn, and Beth Sosik. 2020. King County Freshwater Benthic Macroinvertebrate Sampling and Analysis Plan. (Seattle, WA), June.

Manning, David W. P., and S. Mažeika P. Sullivan. 2021. “Conservation Across Aquatic-Terrestrial Boundaries: Linking Continental-Scale Water Quality to Emergent Aquatic Insects and Declining Aerial Insectivorous Birds.” Frontiers in Ecology and Evolution 9 (February). https://doi.org/10.3389/fevo.2021.633160.

Marczak, Laurie B., Ross M. Thompson, and John S. Richardson. 2007. “Meta-Analysis: Trophic Level, Habitat, and Productivity Shape the Food Web Effects of Resource Subsidies.” Ecology 88 (1): 140–48. https://doi.org/10.1890/0012-9658(2007)88%255B140:mtlhap%255D2.0.co;2.

Martin-Creuzburg, Dominik, Carmen Kowarik, and Dietmar Straile. 2017. “Cross-Ecosystem Fluxes: Export of Polyunsaturated Fatty Acids from Aquatic to Terrestrial Ecosystems via Emerging Insects.” Science of The Total Environment 577 (January): 174–82. https://doi.org/10.1016/j.scitotenv.2016.10.156.

Martinuzzi, Sebastián, Stephanie R. Januchowski-Hartley, Brenda M. Pracheil, et al., 2014. “Threats and Opportunities for Freshwater Conservation under Future Land Use Change Scenarios in the United States.” Global Change Biology 20 (1): 113–24. https://doi.org/10.1111/gcb.12383.

Marzluff, John M. 2005. “Island Biogeography for an Urbanizing World: How Extinction and Colonization May Determine Biological Diversity in Human-Dominated Landscapes.” Urban Ecosystems 8 (2): 157–77. https://doi.org/10.1007/s11252-005-4378-6.

McCabe, Christina L., Christoph D. Matthaei, and Jonathan D. Tonkin. 2025. “The Ecological Benefits of More Room for Rivers.” Nature Water 3 (3): 260–70. https://doi.org/10.1038/s44221-025-00403-0.

Mincey, Sarah K., Mikaela Schmitt-Harsh, and Richard Thurau. 2013. “Zoning, Land Use, and Urban Tree Canopy Cover: The Importance of Scale.” Urban Forestry & Urban Greening 12 (2): 191–99. https://doi.org/10.1016/j.ufug.2012.12.005.

Møller, Anders Pape. 2019. “Parallel Declines in Abundance of Insects and Insectivorous Birds in Denmark over 22 Years.” Ecology and Evolution 9 (11): 6581–87. https://doi.org/10.1002/ece3.5236.

Morley, Sarah A., and James R. Karr. 2002. “Assessing and Restoring the Health of Urban Streams in the Puget Sound Basin.” Conservation Biology 16 (6): 1498–509.

Muehlbauer, Jeffrey D., Scott F. Collins, Martin W. Doyle, and Klement Tockner. 2014. “How Wide Is a Stream? Spatial Extent of the Potential ‘Stream Signature’ in Terrestrial Food Webs Using Meta-Analysis.” Ecology 95 (1): 44–55. https://doi.org/10.1890/12-1628.1.

Naiman, Robert J., Henri Décamps, and Michael Pollock. 1993. “The Role of Riparian Corridors in Maintaining Regional Biodiversity.” Ecological Applications 3 (2): 209–12. https://doi.org/10.2307/1941822.

Nakano, Shigeru, and Masashi Murakami. 2001. “Reciprocal Subsidies: Dynamic Interdependence between Terrestrial and Aquatic Food Webs.” Proceedings of the National Academy of Sciences 98 (1): 166–70. https://doi.org/10.1073/pnas.98.1.166.

Nebel, Silke, Alex Mills, Jon D. McCracken, and Philip D. Taylor. 2010. “Declines of Aerial Insectivores in North America Follow a Geographic Gradient.” Avian Conservation and Ecology 5 (2): art1. https://doi.org/10.5751/ACE-00391-050201.

Nimmo, Dale G., Angie Haslem, James Q. Radford, Mark Hall, and Andrew F. Bennett. 2016. “Riparian Tree Cover Enhances the Resistance and Stability of Woodland Bird Communities during an Extreme Climatic Event.” Journal of Applied Ecology 53 (2): 449–58. https://doi.org/10.1111/1365-2664.12535.

Northrup, Joseph M., and Brian D. Gerber. 2018. “A Comment on Priors for Bayesian Occupancy Models.” PLOS ONE 13 (2): e0192819. https://doi.org/10.1371/journal.pone.0192819.

Nowak, David J., and Eric J. Greenfield. 2012. “Tree and Impervious Cover Change in U.S. Cities.” Urban Forestry & Urban Greening 11 (1): 21–30. https://doi.org/10.1016/j.ufug.2011.11.005.

Pacifici, Krishna, Elise F. Zipkin, Jaime A. Collazo, Julissa I. Irizarry, and Amielle DeWan. 2014. “Guidelines for a Priori Grouping of Species in Hierarchical Community Models.” Ecology and Evolution 4 (7): 877–88. https://doi.org/10.1002/ece3.976.

Peller, Tianna, and Florian Altermatt. 2024. “Invasive Species Drive Cross-Ecosystem Effects Worldwide.” Nature Ecology & Evolution 8 (6): 1087–97. https://doi.org/10.1038/s41559-024-02380-1.

Pennington, Derric N., and Robert B. Blair. 2011. “Habitat Selection of Breeding Riparian Birds in an Urban Environment: Untangling the Relative Importance of Biophysical Elements and Spatial Scale.” Diversity and Distributions 17 (3): 506–18. https://doi.org/10.1111/j.1472-4642.2011.00750.x.

Pennington, Derric N., James Hansel, and Robert B. Blair. 2008. “The Conservation Value of Urban Riparian Areas for Landbirds during Spring Migration: Land Cover, Scale, and Vegetation Effects.” Biological Conservation 141 (5): 1235–48. https://doi.org/10.1016/j.biocon.2008.02.021.

Platt, John. 2000. “Probabilistic Outputs for Support Vector Machines and Comparisons to Regularized Likelihood Methods.” Adv. Large Margin Classif. 10 (June).

Plummer, Martyn. 2023. “JAGS - Just Another Gibbs Sampler.” https://mcmc-jags.sourceforge.io/.

Puget Sound Regional Council. 2020. VISION 2050: Final Supplemental Environmental Impact Statement. https://www.psrc.org/sites/default/files/2022-02/v2050finalseis-march2020.pdf.

Reid, Andrea J., Andrew K. Carlson, Irena F. Creed, et al., 2019. “Emerging Threats and Persistent Conservation Challenges for Freshwater Biodiversity.” Biological Reviews 94 (3): 849–73. https://doi.org/10.1111/brv.12480.

Robinson, Lin, Joshua P. Newell, and John M. Marzluff. 2005. “Twenty-Five Years of Sprawl in the Seattle Region: Growth Management Responses and Implications for Conservation.” Landscape and Urban Planning 71 (1): 51–72. https://doi.org/10.1016/j.landurbplan.2004.02.005.

Rosenberg, Kenneth V., Adriaan M. Dokter, Peter J. Blancher, et al., 2019. “Decline of the North American Avifauna.” Science 366 (6461): 120–24. https://doi.org/10.1126/science.aaw1313.

Royle, J. Andrew, and Robert M. Dorazio. 2008. Hierarchical Modeling and Inference in Ecology: The Analysis of Data from Populations, Metapopulations and Communities. Academic Press. https://doi.org/10.1016/B978-0-12-374097-7.X0001-4.

Sánchez-Bayo, Francisco, and Kris A. G. Wyckhuys. 2019. “Worldwide Decline of the Entomofauna: A Review of Its Drivers.” Biological Conservation 232 (April): 8–27. https://doi.org/10.1016/j.biocon.2019.01.020.

Schilke, Paul R., Mireia Bartrons, Jessica M. Gorzo, et al., 2020. “Modeling a Cross-Ecosystem Subsidy: Forest Songbird Response to Emergent Aquatic Insects.” Landscape Ecology 35 (7): 1587–604. https://doi.org/10.1007/s10980-020-01038-0.

Schürings, Christian, and Julian D. Olden. 2026. “Cross-Ecosystem Linkages between Freshwater Insects and Riparian Birds across the USA.” Nature Ecology & Evolution 10 (5): 961–72. https://doi.org/10.1038/s41559-026-03041-1.

Seavy, Nathaniel E., Thomas Gardali, Gregory H. Golet, et al., 2009a. “Why Climate Change Makes Riparian Restoration More Important than Ever: Recommendations for Practice and Research.” Special Theme: Climate Change and Ecological Restoration. Ecological Restoration 27 (3): 330–38. https://doi.org/10.3368/er.27.3.330.

Seavy, Nathaniel E., Thomas Gardali, Gregory H. Golet, et al., 2009b. “Why Climate Change Makes Riparian Restoration More Important than Ever: Recommendations for Practice and Research.” Special Theme: Climate Change and Ecological Restoration. Ecological Restoration 27 (3): 330–38. https://doi.org/10.3368/er.27.3.330.

Shipley, J. Ryan, Rebecca Oester, Margaux Mathieu-Resuge, et al., 2024. “Consumer Biodiversity Increases Organic Nutrient Availability across Aquatic and Terrestrial Ecosystems.” Science 386 (6719): 335–40. https://doi.org/10.1126/science.adp6198.

Shipley, J. Ryan, Cornelia W. Twining, Margaux Mathieu-Resuge, et al., 2022. “Climate Change Shifts the Timing of Nutritional Flux from Aquatic Insects.” Current Biology 32 (6): 1342-1349.e3. https://doi.org/10.1016/j.cub.2022.01.057.

Shoffner, Alexandra, Andrew M. Wilson, Wenwu Tang, and Sara A. Gagné. 2018. “The Relative Effects of Forest Amount, Forest Configuration, and Urban Matrix Quality on Forest Breeding Birds.” Scientific Reports 8 (1): 17140. https://doi.org/10.1038/s41598-018-35276-9.

Shonfield, Julia, and Erin Bayne. 2017. “Avian Conservation and Ecology: Autonomous Recording Units in Avian Ecological Research: Current Use and Future Applications.” Avian Conservation and Ecology 12 (1). https://doi.org/10.5751/ACE-00974-120114.

Skagen, Susan K., Jeffrey F. Kelly, Charles van Riper Iii, et al., 2005. “Geography of Spring Landbird Migration through Riparian Habitats in Southwestern North America.” The Condor. 107: 212--227. https://research.fs.usda.gov/treesearch/29525.

Smith, Robert J., Frank R. Moore, and Christopher A. May. 2007. “Stopover Habitat Along the Shoreline of Northern Lake Huron, Michigan: Emergent Aquatic Insects as a Food Resource for Spring Migrating Landbirds.” The Auk 124 (1): 107–21. https://doi.org/10.1093/auk/124.1.107.

Sosik, Elizabeth A., Kate H. Macneale, and Sean P. Sullivan. 2025. “Surprising Improvements in Stream Biotic Integrity despite Increased Urban Development and Warming Temperatures.” Freshwater Science 44 (4): 475–92. https://doi.org/10.1086/737227.

Statzner, Bernhard, and Vincent H. Resh. 1993. “Multiple-Site and-Year Analyses of Stream Insect Emergence: A Test of Ecological Theory.” Oecologia 96 (1): 65–79. https://doi.org/10.1007/BF00318032.

Stauffer, F., and Louis B. Best. 1980. “Habitat Selection by Birds of Riparian Communities: Evaluating Effects of Habitat Alterations.” The Journal of Wildlife Management 44 (1): 1–15. https://doi.org/10.2307/3808345.

Stenroth, Karolina, Lina E. Polvi, Emma Fältström, and Micael Jonsson. 2015. “Land-Use Effects on Terrestrial Consumers through Changed Size Structure of Aquatic Insects.” Freshwater Biology 60 (1): 136–49. https://doi.org/10.1111/fwb.12476.

Sullivan, S. Mažeika P., Joseph W. Corra, and Jeffry T. Hayes. 2021. “Urbanization Mediates the Effects of Water Quality and Climate on a Model Aerial Insectivorous Bird.” Ecological Monographs 91 (2): e01442. https://doi.org/10.1002/ecm.1442.

Sullivan, S. Mažeika P., and Kerri T. Vierling. 2009. “Experimental and Ecological Implications of Evening Bird Surveys in Stream-Riparian Ecosystems.” Environmental Management 44 (4): 789–99. https://doi.org/10.1007/s00267-009-9318-4.

Tallamy, Douglas W., and W. Gregory Shriver. 2021. “Are Declines in Insects and Insectivorous Birds Related?” Ornithological Applications 123 (1): duaa059. https://doi.org/10.1093/ornithapp/duaa059.

Tank, Jennifer L., Emma J. Rosi-Marshall, Natalie A. Griffiths, Sally A. Entrekin, and Mia L. Stephen. 2010. “A Review of Allochthonous Organic Matter Dynamics and Metabolism

in Streams." Journal of the North American Benthological Society 29 (1): 118–46. https://doi.org/10.1899/08-170.1.

Tobias, Joseph A., Catherine Sheard, Alex L. Pigot, et al., 2022. "AVONET: Morphological, Ecological and Geographical Data for All Birds." Ecology Letters 25 (3): 581–97. https://doi.org/10.1111/ele.13898.

Trevelline, Brian K., Tim Nuttle, Brandon D. Hoenig, Nathan L. Brouwer, Brady A. Porter, and Steven C. Latta. 2018. "DNA Metabarcoding of Nestling Feces Reveals Provisioning of Aquatic Prey and Resource Partitioning among Neotropical Migratory Songbirds in a Riparian Habitat." Oecologia 187 (1): 85–98. https://doi.org/10.1007/s00442-018-4136-0.

Twining, Cornelia Wingfield, Jeremy Ryan Shipley, and David W. Winkler. 2018. "Aquatic Insects Rich in Omega-3 Fatty Acids Drive Breeding Success in a Widespread Bird." Ecology Letters 21 (12): 1812–20. https://doi.org/10.1111/ele.13156.

Uesugi, Akane, and Masashi Murakami. 2007. "Do Seasonally Fluctuating Aquatic Subsidies Influence the Distribution Pattern of Birds between Riparian and Upland Forests?" Ecological Research 22 (2): 274–81. https://doi.org/10.1007/s11284-006-0028-6.

United Nations. 2025. World Urbanization Prospects 2025: Summary of Results. United Nations. https://desapublications.un.org/publications/world-urbanization-prospects-2025-summary-results.

U.S. Environmental Protection Agency. 2025. "ICLUS v1.3 Estimated Percent Impervious Surface for the Conterminous USA." https://catalog.data.gov/dataset/iclus-v1-3-estimated-percent-impervious-surface-for-the-conterminous-usa12.

U.S. Geological Survey. 2023a. "Annual NLCD Collection." https://doi.org/10.5066/P94UXNTS.

U.S. Geological Survey. 2023b. "National Hydrography Dataset." https://www.usgs.gov/national-hydrography/national-hydrography-dataset.

Wagner, Marlene A., and John D. Reynolds. 2019. "Salmon Increase Forest Bird Abundance and Diversity." PLOS ONE 14 (2): e0210031. https://doi.org/10.1371/journal.pone.0210031.

Walsh, Christopher J., Allison H. Roy, Jack W. Feminella, Peter D. Cottingham, Peter M. Groffman, and Raymond P. Morgan. 2005. "The Urban Stream Syndrome: Current Knowledge and the Search for a Cure." Journal of the North American Benthological Society 24 (3): 706–23. https://doi.org/10.1899/04-028.1.

Wang, Guangyu, Shari Mang, Haisheng Cai, et al., 2016. “Integrated Watershed Management: Evolution, Development and Emerging Trends.” Journal of Forestry Research 27 (5): 967–94. https://doi.org/10.1007/s11676-016-0293-3.

Washington Department of Fish and Wildlife. 2025. Washington’s State Wildlife Action Plan: 2025 Update. Olympia, Washington.

Wegscheider, B., N. K. Rideout, W. A. Monk, M. A. Gray, R. Steeves, and D. J. Baird. 2025. “Modeling Nature-Based Restoration Potential across Aquatic–Terrestrial Boundaries.” Conservation Biology 39 (5): e70046. https://doi.org/10.1111/cobi.70046.

Wiens, John A. 1989. The Ecology of Bird Communities: Volume 2: Processes and Variations. Vol. 2. Cambridge Studies in Ecology. Cambridge University Press. https://doi.org/10.1017/CBO9780511608568.

Wilcox, Kirsten A., Marlene A. Wagner, and John D. Reynolds. 2021. “Salmon Subsidies Predict Territory Size and Habitat Selection of an Avian Insectivore.” PLOS ONE 16 (7): e0254314. https://doi.org/10.1371/journal.pone.0254314.

Wood, Connor M., and Stefan Kahl. 2024. “Guidelines for Appropriate Use of BirdNET Scores and Other Detector Outputs.” Journal of Ornithology 165 (3): 777–82. https://doi.org/10.1007/s10336-024-02144-5.

3.9 APPENDIX 3.1

Artist attribution: Graphical elements used in figures are original designs by the authors or obtained under public domain from PhyloPic (Michael Keesey, 2025, phylopic.org), FlatIcon (Freepik Company, 2025, flaticon.com), and Vecteezy (Eezy LLC, 2026, vecteezy.com), and were created by T. Michael Keesey, Guillaume Dera, and Prespa Research Group.

Table A3.1: B-IBI biological condition categories, adapted from Karr et al. 1986 by Morley 2000. B-IBI incorporates multiple metrics to quantify stream biological condition, including the richness of EPT, Diptera, Odonata, Bivalvia, and Gastropoda taxa. The index ranges from 0 ("very poor" condition category, with low diversity dominated by highly tolerant taxa) to 100 ("excellent" condition category, with high diversity comparable to a minimally disturbed reference condition).

B-IBI	Biological condition	Description
[80, 100]	Excellent	Comparable to least disturbed reference condition; overall high taxa diversity, particularly of mayflies, stoneflies, caddis flies, long-lived, clinger, and intolerant taxa. Relative abundance of predators high.
[60, 80)	Good	Slightly divergent from least disturbed condition; absence of some long-lived and intolerant taxa; slight decline in richness of mayflies, stoneflies, and caddis flies; proportion of tolerant taxa increases.
[40, 60)	Fair	Total taxa richness reduced - particularly intolerant, long-lived, stonefly, and clinger taxa; relative abundance of predators declines; proportion of tolerant taxa continues to increase.
[20, 40)	Poor	Overall taxa diversity depressed; proportion of predators greatly reduced as is long-lived taxa richness; few stoneflies or intolerant taxa present; dominance by three most abundant taxa often very high.
[0, 20)	Very Poor	Overall taxa diversity very low and dominated by a few highly tolerant taxa; mayfly, stonefly, caddis fly, clinger, long-lived, and intolerant taxa largely absent; relative abundance of predators very low.

Table A3.2: Regional species pool for acoustic monitoring, including bioacoustic classifier performance and observation histories. Values shown include the number of stream sites at which a species was observed ("Sites"), the naïve occurrence probability ("Naïve occurrence"), the number of vocalization detections ("Detections"), the area under the precision-recall curve ("PR AUC"), the area under the receiver operating characteristic curve ("ROC AUC"), score threshold value from 0.0-1.0 at which probability of a true positive detection is greater than or equal to 95% ("Threshold Pr(TP) ≥ 0.95"), precision and recall at that threshold ("Threshold precision", "Threshold recall", respectively), minimum threshold considered ("Min threshold"), and precision and recall at that minimum threshold ("Min threshold precision", "Min threshold recall", respectively).

Scientific name	Common name	Sites	Naive occurrence	Detections	PR AUC	ROC AUC	Threshold Pr(TP) ≥ 0.95	Threshold precision	Threshold recall	Min threshold	Min threshold precision	Min threshold recall
Turdus Migratorius	American Robin	50	1	286547	0.99	0.99	0.72	0.96	0.71	0.5	0.83	1
Junco Hyemalis	Dark-Eyed Junco	50	1	30353	-	-	-	-	-	-	-	-
Cyanocitta Stelleri	Steller's Jay	49	0.98	31189	-	-	-	-	-	-	-	-
Poecile Rufescens	Chestnut-Backed Chickadee	48	0.96	292	1	0.83	0.47	0.99	1	0.5	0.99	1
Corvus Brachyrhynchos	American Crow	48	0.96	75321	-	-	-	-	-	-	-	-
Poecile Atricapillus	Black-Capped Chickadee	47	0.94	24905	0.95	0.96	0.93	1	0.42	0.5	0.49	1
Colaptes Auratus	Northern Flicker	47	0.94	20512	-	-	-	-	-	-	-	-
Bombycilla Cedrorum	Cedar Waxwing	47	0.94	5423	-	-	-	-	-	-	-	-
Melospiza Melodia	Song Sparrow	46	0.92	43559	-	-	-	-	-	-	-	-
Pipilo Maculatus	Spotted Towhee	45	0.9	58492	-	-	-	-	-	-	-	-
Dryobates Pubescens	Downy Woodpecker	44	0.88	2195	-	-	-	-	-	-	-	-
Empidonax Difficilis	Pacific-Slope Flycatcher	44	0.88	95716	-	-	-	-	-	-	-	-
Piranga Ludoviciana	Western Tanager	44	0.88	18897	1	0.99	0.74	1	0.85	0.5	0.92	0.97
Certhia Americana	Brown Creeper	43	0.86	182	1	-	0	1	1	0.5	1	1
Catharus Ustulatus	Swainson's Thrush	42	0.84	233436	1	-	0.5	1	1	0.5	1	0.84
Regulus Satrapa	Golden-Crowned Kinglet	41	0.82	9886	0.96	0.94	0.91	1	0.5	0.5	0.81	0.97
Sitta Canadensis	Red-Breasted Nuthatch	38	0.76	20808	0.89	0.85	0.9	1	0.23	0.5	0.71	0.95
Dryobates Villosus	Hairy Woodpecker	34	0.68	945	0.95	0.94	0.8	1	0.46	0.5	0.77	0.88
Psaltriparus Minimus	Bushtit	32	0.64	2007	-	-	-	-	-	-	-	-
Thryomanes Bewickii	Bewick's Wren	31	0.62	3109	-	-	-	-	-	-	-	-
Pheucticus Melanocephalus	Black-Headed Grosbeak	28	0.56	4913	0.99	0.93	0.62	1	0.71	0.5	0.97	0.82
Corvus Corax	Common Raven	27	0.54	4633	0.97	0.96	0.61	1	0.63	0.5	0.91	0.95
Troglodytes Pacificus	Pacific Wren	25	0.5	60493	-	-	-	-	-	-	-	-
Dryocopus Pileatus	Pileated Woodpecker	23	0.46	752	0.97	0.94	0.88	0.95	0.59	0.5	0.67	1
Haemorhous Purpureus	Purple Finch	22	0.44	1680	0.93	0.96	0.93	1	0.57	0.5	0.45	1
Cardellina Pusilla	Wilson's Warbler	21	0.42	9155	0.95	0.88	0.78	0.99	0.4	0.5	0.92	0.84
Empidonax Hammondii	Hammond's Flycatcher	21	0.42	2975	-	-	-	-	-	-	-	-
Setophaga Nigrescens	Black-Throated Gray Warbler	20	0.4	808	1	-	0.5	1	1	0.5	1	1
Megaceryle Alcyon	Belted Kingfisher	20	0.4	1034	0.96	0.97	0.97	1	0.66	0.5	0.44	1
Vireo Gilvus	Warbling Vireo	19	0.38	16351	0.97	0.92	0.67	1	0.56	0.5	0.96	0.75
Spinus Tristis	American Goldfinch	19	0.38	1023	0.99	0.98	0.65	1	0.82	0.5	0.92	0.96
Passer Domesticus	House Sparrow	19	0.38	1668	0.89	0.95	0.93	1	0.29	0.5	0.4	1
Haemorhous Mexicanus	House Finch	18	0.36	257	0.96	0.96	0.87	1	0.59	0.5	0.63	1
Calypte Anna	Anna's Hummingbird	17	0.34	1552	0.98	0.96	0.81	1	0.73	0.5	0.83	0.9
Contopus Sordidulus	Western Wood-Pewee	15	0.3	9174	0.99	0.89	0.72	0.99	0.59	0.5	0.96	0.86
Vireo Huttoni	Hutton's Vireo	15	0.3	825	-	-	-	-	-	-	-	-
Spinus Pinus	Pine Siskin	14	0.28	767	-	-	-	-	-	-	-	-
Haliaeetus Leucocephalus	Bald Eagle	13	0.26	1067	-	-	-	-	-	-	-	-
Tachycineta Thalassina	Violet-Green Swallow	12	0.24	1827	-	-	-	-	-	-	-	-
Pandion Haliaetus	Osprey	12	0.24	68	1	-	0	1	1	0.5	1	1
Buteo Jamaicensis	Red-Tailed Hawk	10	0.2	40	1	-	0	1	1	0.5	1	1
Strix Varia	Barred Owl	10	0.2	412	0.85	0.9	0.99	1	0.34	0.5	0.32	1
Chordeiles Minor	Common Nighthawk	7	0.14	104	0.63	0.65	1	1	0.02	0.5	0.33	1
Accipiter Cooperii	Cooper's Hawk	7	0.14	38	1	-	1	-	0	0.5	1	1
Bubo Virginianus	Great Horned Owl	7	0.14	34	1	-	1	-	0	0.5	1	1
Empidonax Traillii	Willow Flycatcher	4	0.08	7048	0.98	0.85	0.59	0.99	0.54	0.5	0.97	0.65
Loxia Curvirostra	Red Crossbill	4	0.08	28	1	-	1	-	0	0.5	1	1
Coccothraustes Vespertinus	Evening Grosbeak	4	0.08	40	0.85	0.92	0.98	1	0.08	0.5	0.42	1
Setophaga Petechia	Yellow Warbler	3	0.06	196	0.91	0.81	0.5	0.95	0.18	0.5	0.95	0.18
Vireo Cassinii	Cassin's Vireo	3	0.06	16	1	-	0	1	1	0.5	1	1
Anas Platyrhynchos	Mallard	3	0.06	18	1	-	1	-	0	0.5	1	1
Branta Canadensis	Canada Goose	3	0.06	208	0.95	0.95	0.86	0.96	0.5	0.5	0.7	1
Geothlypis Trichas	Common Yellowthroat	2	0.04	14	1	-	1	-	0	0.5	1	1
Leiothlypis Celata	Orange-Crowned Warbler	2	0.04	10	1	-	1	-	0	0.5	1	1
Chaetura Vauxi	Vaux's Swift	2	0.04	44	1	-	0	1	1	0.5	1	0.97
Contopus Cooperi	Olive-Sided Flycatcher	2	0.04	600	0.99	0.97	0.62	0.99	0.78	0.5	0.98	0.9
Ixoreus Naevius	Varied Thrush	2	0.04	20	1	-	0	1	1	0.5	1	1
Cinclus Mexicanus	American Dipper	2	0.04	8	0.5	0.59	1	-	0	0.5	0.17	1
Selasphorus Rufus	Rufous Hummingbird	2	0.04	12	1	-	0	1	1	0.5	1	1
Patagioenas Fasciata	Band-Tailed Pigeon	2	0.04	10	1	-	1	-	0	0.5	1	1
Falco Sparverius	American Kestrel	2	0.04	8	0.75	0.75	0.95	-	0	0.5	0.5	0.75
Glaucidium Gnoma	Northern Pygmy-Owl	2	0.04	66	0.82	0.86	0.99	0.75	0.09	0.5	0.55	1
Setophaga Coronata	Yellow-Rumped Warbler	1	0.02	26	1	-	0	1	1	0.5	1	1
Geothlypis Tolmiei	Macgillivray's Warbler	1	0.02	4	1	-	1	-	0	0.5	1	1
Larus Glaucescens	Glaucous-Winged Gull	1	0.02	16	1	-	1	-	0	0.5	1	1
Charadrius Vociferus	Killdeer	1	0.02	22	1	-	1	-	0	0.5	1	1
Molothrus Ater	Brown-Headed Cowbird	1	0.02	12	1	-	0	1	1	0.5	1	1
Sphyrapicus Ruber	Red-Breasted Sapsucker	1	0.02	28	0.8	0.61	0.9	-	0	0.5	0.75	0.26
Actitis Macularius	Spotted Sandpiper	1	0.02	6	0.97	0.85	0.76	1	0.8	0.5	0.83	1
Butorides Virescens	Green Heron	1	0.02	24	1	-	0	1	1	0.5	1	1
Falco Columbarius	Merlin	1	0.02	14	0.93	0.98	0.95	1	0.57	0.5	0.28	1
Zenaida Macroura	Mourning Dove	1	0.02	4	1	-	1	-	0	0.5	1	1
Megascops Kennicottii	Western Screech-Owl	1	0.02	14	1	-	1	-	0	0.5	1	1

Table A3.3: Variables characterizing urban development and vegetation at local and landscape scales. Values for mean, standard deviation, and range of each variable at each spatial scale are provided alongside data sources.

Variable	Local mean (SD), range	Landscape mean (SD), range	Data source
Impervious surface cover, ISC (%)	20.6 (15.5), 0.0-62.3	22.9 (15.9), 0.0-57.4	National Land cover Database 2023 (USGS)
Road density (m/km^2)	7788.2 (4856.5), 373.7-21665.6	6594.9 (2642.5), 1862.5-12008.6	United States Census Bureau 2024
Forest proportional area (%)	33.8 (30.8), 0.0-99.7	30.9 (28.1), 0.0-92.3	National Land cover Database 2023 (USGS)
Tree canopy cover , TCC (%)	50.2 (13.2), 23.1-77.6	45.4 (14.0), 20.6-73.0	Abood et al., 2022 (USFS)
Canopy height mean (m)	24.7 (4.6), 18.2-37.7	23.4 (4.3), 17.8-33.6	Vogeler et al. 2023 (NASA)
Foliage height diversity	2.7 (0.2), 2.4-3.1	2.6 (0.2), 2.2-3.0	Vogeler et al. 2023 (NASA)

Table A3.4: Guild-level effects on occurrence probability $\mu^{(\alpha)}_{a,g}$ (posterior means with 95% Bayesian credible intervals) across multi-species occupancy model groupings. Variables include the benthic index of biotic integrity B-IBI, local tree canopy cover TCC_{local}, landscape TCC_{land}, local impervious surface cover ISC_{local}, and landscape ISC_{land}

Grouping	Guild	Parameter	Variable	Estimate	SD
Community	All species	$\mu_{\alpha 1,1}$	B-IBI	0.21 (-0.01, 0.43)	0.11
Dietary	Insectivore	$\mu_{\alpha 1,1}$	B-IBI	0.37 (0.04, 0.72)	0.18
Dietary	Other consumer	$\mu_{\alpha 1,2}$	B-IBI	0.11 (-0.17, 0.39)	0.14
Foraging	Aerial forager	$\mu_{\alpha 1,1}$	B-IBI	0.38 (-0.27, 1.03)	0.33
Foraging	Foliage gleaner	$\mu_{\alpha 1,2}$	B-IBI	0.33 (-0.19, 0.87)	0.27
Foraging	Other forager	$\mu_{\alpha 1,3}$	B-IBI	0.11 (-0.17, 0.37)	0.14
Migratory	Migrant	$\mu_{\alpha 1,1}$	B-IBI	0.55 (0.20, 0.90)	0.18
Migratory	Resident, partial migrant	$\mu_{\alpha 1,2}$	B-IBI	0.03 (-0.24, 0.30)	0.14
Community	All species	$\mu_{\alpha 2,1}$	TCC_{local}	0.01 (-0.26, 0.28)	0.14
Dietary	Insectivore	$\mu_{\alpha 2,1}$	TCC_{local}	0.15 (-0.25, 0.56)	0.2
Dietary	Other consumer	$\mu_{\alpha 2,2}$	TCC_{local}	-0.09 (-0.44, 0.26)	0.18
Foraging	Aerial forager	$\mu_{\alpha 2,1}$	TCC_{local}	0.27 (-0.61, 1.25)	0.46
Foraging	Foliage gleaner	$\mu_{\alpha 2,2}$	TCC_{local}	0.04 (-0.50, 0.58)	0.27
Foraging	Other forager	$\mu_{\alpha 2,3}$	TCC_{local}	-0.08 (-0.43, 0.27)	0.18
Migratory	Migrant	$\mu_{\alpha 2,1}$	TCC_{local}	0.19 (-0.24, 0.63)	0.22
Migratory	Resident, partial migrant	$\mu_{\alpha 2,2}$	TCC_{local}	-0.09 (-0.42, 0.25)	0.17
Community	All species	$\mu_{\alpha 3,1}$	TCC_{land}	0.01 (-0.24, 0.27)	0.13
Dietary	Insectivore	$\mu_{\alpha 3,1}$	TCC_{land}	0.00 (-0.39, 0.40)	0.2
Dietary	Other consumer	$\mu_{\alpha 3,2}$	TCC_{land}	0.06 (-0.31, 0.43)	0.19
Foraging	Aerial forager	$\mu_{\alpha 3,1}$	TCC_{land}	0.23 (-0.48, 0.97)	0.37
Foraging	Foliage gleaner	$\mu_{\alpha 3,2}$	TCC_{land}	-0.17 (-0.67, 0.34)	0.26
Foraging	Other forager	$\mu_{\alpha 3,3}$	TCC_{land}	0.03 (-0.33, 0.39)	0.18
Migratory	Migrant	$\mu_{\alpha 3,1}$	TCC_{land}	0.02 (-0.40, 0.47)	0.23
Migratory	Resident, partial migrant	$\mu_{\alpha 3,2}$	TCC_{land}	0.00 (-0.33, 0.34)	0.17
Community	All species	$\mu_{\alpha 4,1}$	ISC_{local}	-0.03 (-0.26, 0.21)	0.12
Dietary	Insectivore	$\mu_{\alpha 4,1}$	ISC_{local}	-0.12 (-0.49, 0.26)	0.19
Dietary	Other consumer	$\mu_{\alpha 4,2}$	ISC_{local}	0.00 (-0.29, 0.29)	0.15
Foraging	Aerial forager	$\mu_{\alpha 4,1}$	ISC_{local}	-0.10 (-0.95, 0.64)	0.4
Foraging	Foliage gleaner	$\mu_{\alpha 4,2}$	ISC_{local}	-0.20 (-0.67, 0.27)	0.24
Foraging	Other forager	$\mu_{\alpha 4,3}$	ISC_{local}	0.02 (-0.26, 0.32)	0.15
Migratory	Migrant	$\mu_{\alpha 4,1}$	ISC_{local}	-0.07 (-0.46, 0.35)	0.21
Migratory	Resident, partial migrant	$\mu_{\alpha 4,2}$	ISC_{local}	-0.02 (-0.30, 0.26)	0.14
Community	All species	$\mu_{\alpha 5,1}$	ISC_{land}	0.16 (-0.16, 0.49)	0.16
Dietary	Insectivore	$\mu_{\alpha 5,1}$	ISC_{land}	0.04 (-0.49, 0.57)	0.26
Dietary	Other consumer	$\mu_{\alpha 5,2}$	ISC_{land}	0.25 (-0.17, 0.68)	0.22
Foraging	Aerial forager	$\mu_{\alpha 5,1}$	ISC_{land}	0.10 (-1.00, 1.14)	0.54
Foraging	Foliage gleaner	$\mu_{\alpha 5,2}$	ISC_{land}	0.17 (-0.46, 0.78)	0.31
Foraging	Other forager	$\mu_{\alpha 5,3}$	ISC_{land}	0.14 (-0.31, 0.55)	0.22
Migratory	Migrant	$\mu_{\alpha 5,1}$	ISC_{land}	0.15 (-0.40, 0.70)	0.27
Migratory	Resident, partial migrant	$\mu_{\alpha 5,2}$	ISC_{land}	0.14 (-0.27, 0.55)	0.21

Table A3.5: Guild-level effects on detection probability $\mu^{(\beta)}_{b,g}$ (posterior means with 95% Bayesian credible intervals) across multi-species occupancy model groupings. Variables include seasonal survey day, local tree canopy cover TCC_{local}, and local impervious surface cover ISC_{local}.

Grouping	Guild	Parameter	Variable	Estimate	SD
Community	All species	$\mu_{\beta 1,1}$	Day	-0.64 (-0.79, -0.50)	0.07
Dietary	Insectivore	$\mu_{\beta 1,1}$	Day	-0.83 (-1.09, -0.57)	0.13
Dietary	Other consumer	$\mu_{\beta 1,2}$	Day	-0.54 (-0.71, -0.36)	0.09
Foraging	Aerial forager	$\mu_{\beta 1,1}$	Day	-0.49 (-1.09, 0.15)	0.31
Foraging	Foliage gleaner	$\mu_{\beta 1,2}$	Day	-0.98 (-1.23, -0.75)	0.12
Foraging	Other forager	$\mu_{\beta 1,3}$	Day	-0.52 (-0.70, -0.34)	0.09
Migratory	Migrant	$\mu_{\beta 1,1}$	Day	-1.02 (-1.29, -0.74)	0.14
Migratory	Resident, partial migrant	$\mu_{\beta 1,2}$	Day	-0.47 (-0.62, -0.32)	0.08
Community	All species	$\mu_{\beta 2,1}$	TCC_{local}	0.11 (-0.04, 0.27)	0.08
Dietary	Insectivore	$\mu_{\beta 2,1}$	TCC_{local}	0.30 (-0.13, 0.72)	0.21
Dietary	Other consumer	$\mu_{\beta 2,2}$	TCC_{local}	0.00 (-0.13, 0.14)	0.07
Foraging	Aerial forager	$\mu_{\beta 2,1}$	TCC_{local}	0.49 (-1.00, 2.01)	0.75
Foraging	Foliage gleaner	$\mu_{\beta 2,2}$	TCC_{local}	0.07 (-0.17, 0.32)	0.12
Foraging	Other forager	$\mu_{\beta 2,3}$	TCC_{local}	0.09 (-0.06, 0.25)	0.08
Migratory	Migrant	$\mu_{\beta 2,1}$	TCC_{local}	0.28 (-0.18, 0.74)	0.24
Migratory	Resident, partial migrant	$\mu_{\beta 2,2}$	TCC_{local}	0.03 (-0.10, 0.18)	0.07
Community	All species	$\mu_{\beta 3,1}$	ISC_{local}	0.00 (-0.15, 0.16)	0.08
Dietary	Insectivore	$\mu_{\beta 3,1}$	ISC_{local}	-0.01 (-0.39, 0.41)	0.2
Dietary	Other consumer	$\mu_{\beta 3,2}$	ISC_{local}	0.04 (-0.12, 0.19)	0.08
Foraging	Aerial forager	$\mu_{\beta 3,1}$	ISC_{local}	0.44 (-0.88, 1.86)	0.68
Foraging	Foliage gleaner	$\mu_{\beta 3,2}$	ISC_{local}	-0.13 (-0.46, 0.21)	0.17
Foraging	Other forager	$\mu_{\beta 3,3}$	ISC_{local}	0.05 (-0.13, 0.22)	0.09
Migratory	Migrant	$\mu_{\beta 3,1}$	ISC_{local}	-0.07 (-0.49, 0.38)	0.22
Migratory	Resident, partial migrant	$\mu_{\beta 3,2}$	ISC_{local}	0.06 (-0.10, 0.22)	0.08

Table A3.6: Top-ranking candidate linear component models ($\Delta AIC_c < 2$) among endogenous response variables (B-IBI and avian guilds).

Response	B-IBI	ISC Land	ISC Local	TCC Land	TCC Local	K	LL	AICc	Δ AICc	Weight
B-IBI	N/A	-7.18	-1.97			4	-73.09	155.10	0.00	0.23
B-IBI	N/A	-7.32			0.52	4	-73.10	155.10	0.02	0.23
B-IBI	N/A	-8.38				3	-74.32	155.20	0.09	0.22
All species						2	-155.53	315.31	0.00	0.21
All species	0.58					3	-154.68	315.88	0.57	0.16
All species					1.27	3	-155.11	316.74	1.43	0.10
All species			-4.51			3	-155.12	316.76	1.45	0.10
All species		-2.87				3	-155.35	317.23	1.92	0.08
All species				0.70		3	-155.37	317.27	1.96	0.08
Predator	0.55				1.31	4	-114.28	237.45	0.00	0.20
Predator	0.55		-4.59			4	-114.43	237.76	0.30	0.17
Predator	0.79					3	-115.80	238.12	0.67	0.14
Aerial forager	0.25					3	-71.59	149.71	0.00	0.19
Aerial forager	0.19				0.34	4	-70.99	150.87	1.16	0.10
Aerial forager		-2.54				3	-72.20	150.93	1.21	0.10
Aerial forager				0.65		3	-72.35	151.22	1.51	0.09
Aerial forager	0.18			0.30		4	-71.20	151.29	1.58	0.08
Aerial forager	0.20		-0.93			4	-71.27	151.43	1.72	0.08
Aerial forager	0.18	-1.05				4	-71.33	151.55	1.84	0.07
Foliage Gleaner			-3.08			3	-108.24	223.01	0.00	0.16
Foliage Gleaner						2	-109.46	223.18	0.18	0.15
Foliage Gleaner					0.77	3	-108.48	223.49	0.48	0.13
Foliage Gleaner	0.24					3	-108.55	223.62	0.61	0.12
Foliage Gleaner			-3.97	-0.41		4	-108.01	224.92	1.91	0.06
Migrant	0.68				1.30	4	-112.77	234.43	0.00	0.24
Migrant	0.69		-4.19			4	-113.16	235.20	0.78	0.16
Migrant	0.92					3	-114.36	235.24	0.81	0.16

Table A3.7: Structural equation modeling results for guild-specific models representing urbanization effects on avian communities through modifications to riparian habitat and stream integrity. Results are shown for MSOM posterior mean and 95% credible interval, unless specified otherwise. Low value of Fisher's C and a non-significant p-value ($p > 0.05$) indicate consistency between model structure and the observed data. R^2 shows the mean variance explained for each endogenous response variable with 95% credible interval. The B-IBI and TCC_{local} component models shared the same structure across all structural equation models.

Grouping	**Guild model**	**Fisher's C**	**P-value median (range)**	**d.f.**	**Endogenous variables**	**R2**
-	-	-	-	-	B-IBI TCClocal	0.62 0.73
Community	All species	4.63 (3.81, 5.66)	0.8 (0.47–0.93)	8	Richness	0.04 (0.02, 0.06)
Dietary	Predator Other consumer	4.18 (3.24, 5.33) 6.1 (4.83, 7.66)	0.84 (0.41–0.94) 0.64 (0.22–0.88)	8	Richness	0.27 (0.21, 0.32) 0.02 (0.0, 0.05)
Migratory	Migrant Resident, partial migrant	3.72 (3.02, 4.71) 5.05 (4.05, 6.34)	0.88 (0.57–0.94) 0.76 (0.34–0.93)	8	Richness	0.34 (0.28, 0.38) 0.03 (0.01, 0.06)
Foraging	Aerial forager Foliage gleaner Other forager	4.11 (3.14, 5.73) 5.87 (4.59, 7.2) 4.88 (3.73, 6.39)	0.86 (0.33–0.94) 0.66 (0.26–0.93) 0.78 (0.3–0.94)	8	Richness	0.17 (0.09, 0.22) 0.05 (0.02, 0.08) 0.01 (0, 0.03)

Table A3.8: Projected changes to impervious surface cover (ISC) and tree canopy cover (TCC) variables from present-day conditions at local and landscape scales by year 2100 across the Integrated Climate and Land Use Scenarios (ICLUS). In addition to mean, max, and minimum values, the multiplicative change factor is shown for ISC and TCC.

ICLUS scenario	ISC local mean	ISC land mean	ISC local mean factor	ISC land mean factor	ISC local max factor	ISC land max factor	TCC local min	TCC local min factor	B-IBI min	Insectivore richness min
B1	0.12	0.12	1.71	1.72	3.37	2.81	-0.27	0.48	-0.34	-2.84 (-3.23, -2.38)
A1	0.1	0.1	1.6	1.58	4.03	2.09	-0.22	0.54	-0.33	-2.08 (-2.36, -1.75)
A2	0.11	0.12	1.75	1.82	3.17	2.96	-0.27	0.44	-0.35	-2.65 (-3.0, -2.26)
B2	0.1	0.9	1.61	1.61	4.5	2.75	-0.25	0.47	-0.27	-2.15 (-2.49, -1.81)

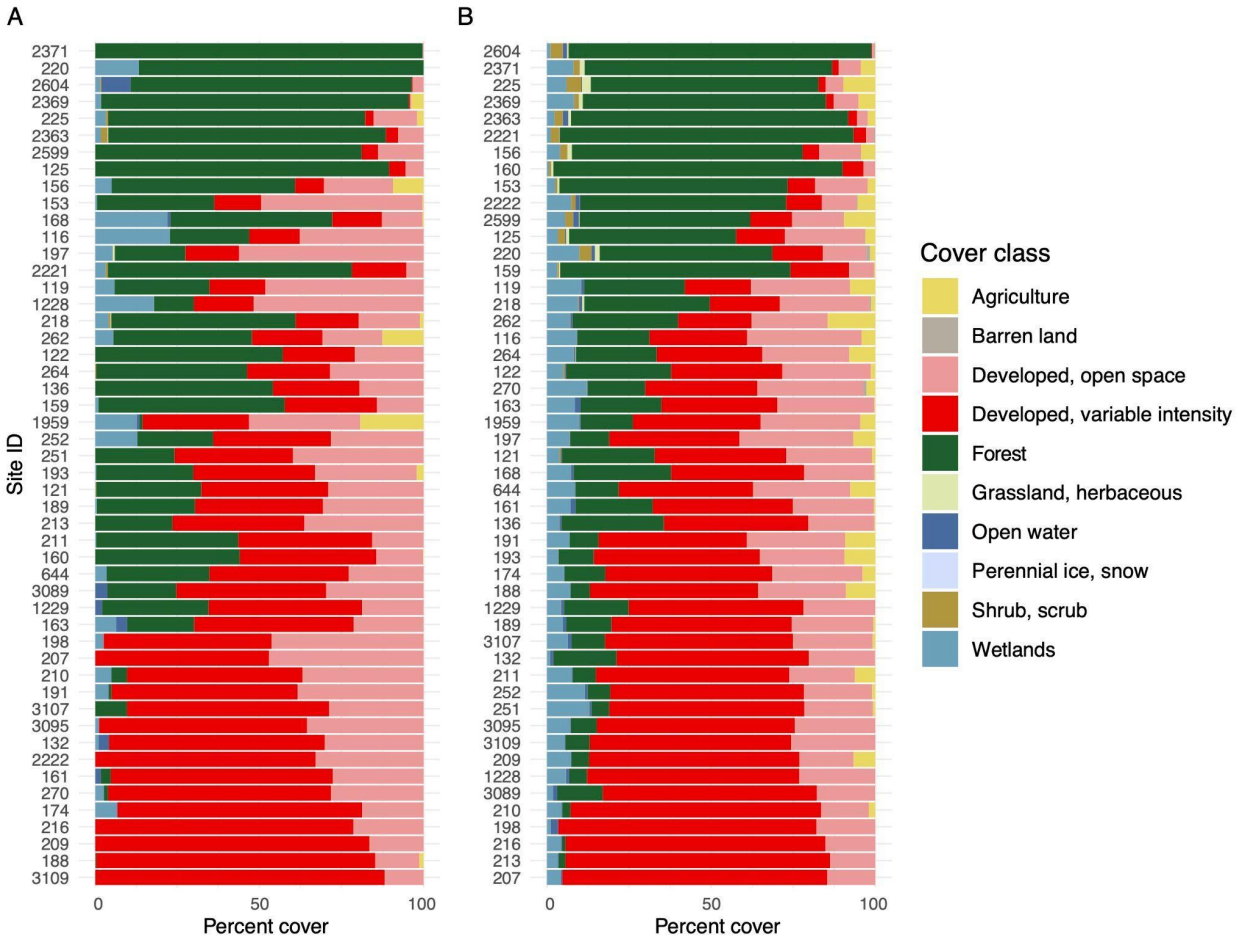

Figure A3.1. National Land Cover Dataset land cover proportion across sites selected with stratified random sampling, at local (A) and landscape (B) spatial scales.

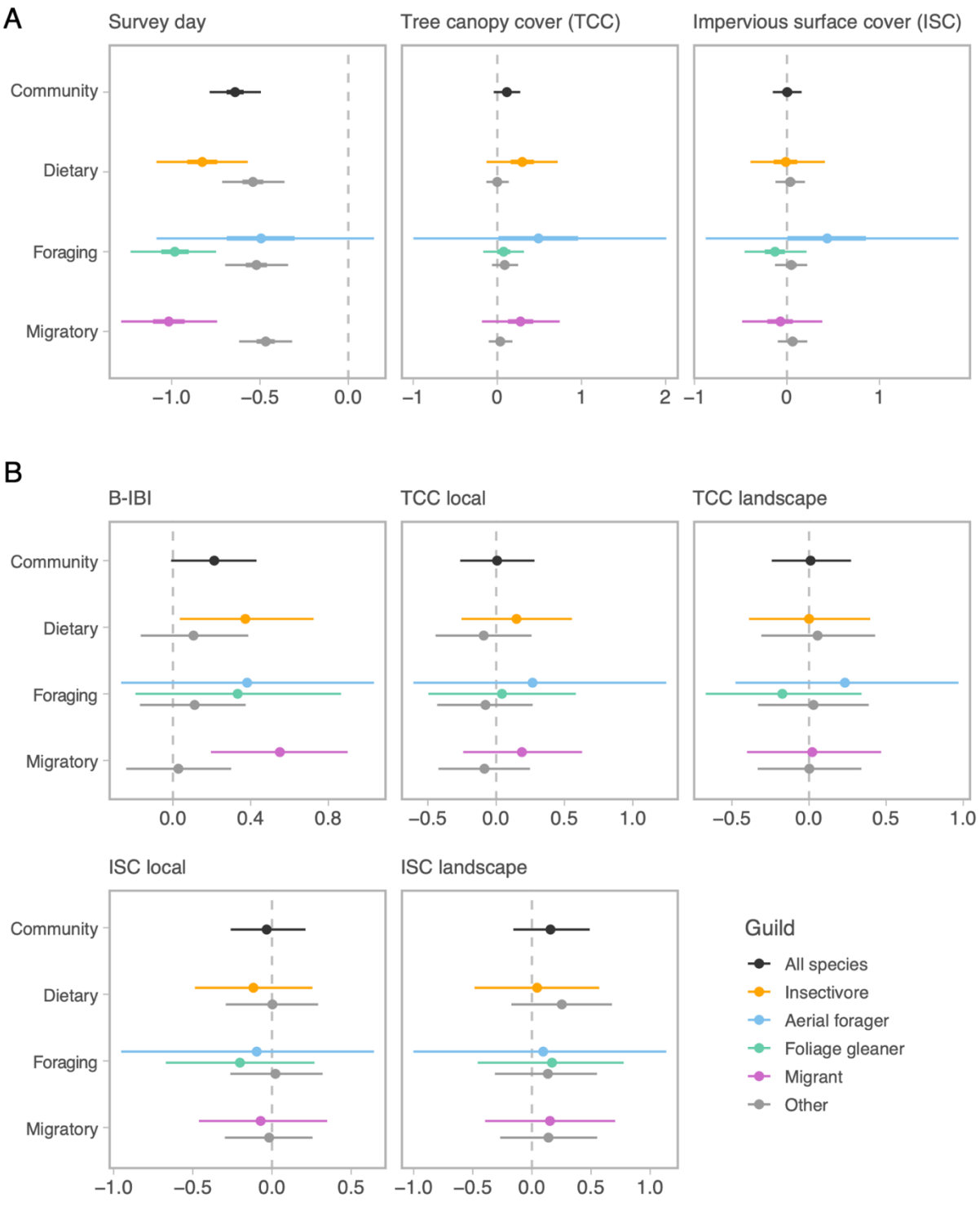

Figure A3.2: Guild-level effects of covariates on detection (A) and occurrence (B) probability across multi-species occupancy model functional groupings, shown as posterior means with 95% Bayesian credible intervals.

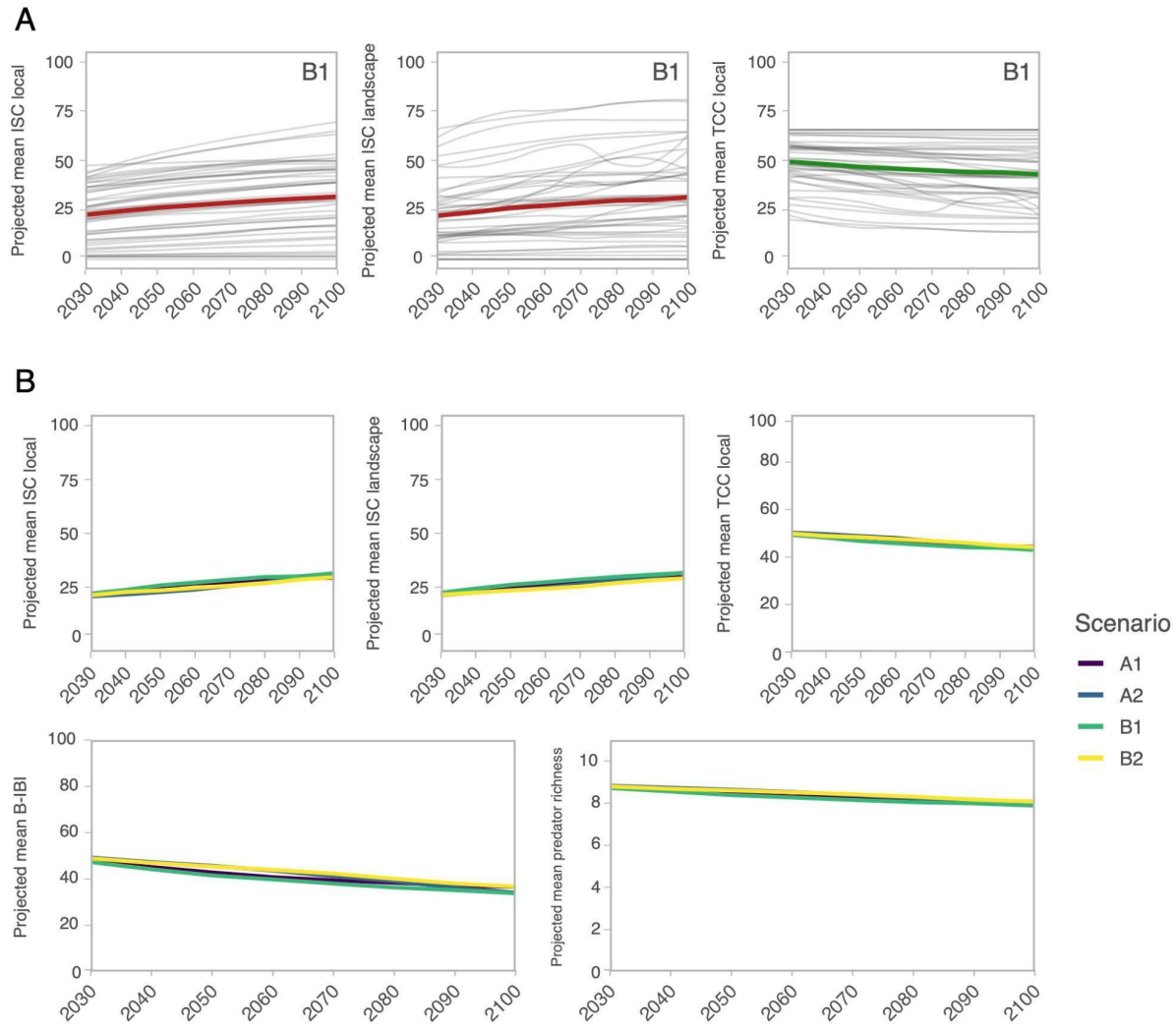

Figure A3.3. (A) Projections for impervious surface cover at the local and landscape scales, and predicted tree canopy cover at the local scale, for ICLUS scenario B1. (B) Projected environmental and ecological outcomes across scenarios, shown as mean trends across all sites.

3.10 APPENDIX 3.2

Multi -species occupancy models were specified in JAGS and fit with Markov chain Monte Carlo (MCMC). For each model we ran three chains of length 30,000 after an adaptation phase of 5,000 and burn-in of 10,000, and thinned the posterior chains by 3. Model code is available at the open-source repository github.com/giojacuzzi/riparian-avian-macroinvert-monitoring-kc, but is provided below for ease of reference:

```
model{

  ## Community (group) level hyperpriors
  for (g in 1:G) {
    # Occurrence
    mu.u[g]    ~ dnorm(0, 1/2.25^2)
    sigma.u[g] ~ dt(0, 1/2.25^2, 1) T(0,)
    tau.u[g] <- sigma.u[g]^-2

    # Covariate effects on occurrence
    mu.alpha1[g]    ~ dnorm(0, 1/2.25^2)
    mu.alpha2[g]    ~ dnorm(0, 1/2.25^2)
    mu.alpha3[g]    ~ dnorm(0, 1/2.25^2)
    mu.alpha4[g]    ~ dnorm(0, 1/2.25^2)
    mu.alpha5[g]    ~ dnorm(0, 1/2.25^2)
    sigma.alpha1[g] ~ dt(0, 1/2.25^2, 1) T(0,)
    sigma.alpha2[g] ~ dt(0, 1/2.25^2, 1) T(0,)
    sigma.alpha3[g] ~ dt(0, 1/2.25^2, 1) T(0,)
    sigma.alpha4[g] ~ dt(0, 1/2.25^2, 1) T(0,)
    sigma.alpha5[g] ~ dt(0, 1/2.25^2, 1) T(0,)
    tau.alpha1[g] <- sigma.alpha1[g]^-2
    tau.alpha2[g] <- sigma.alpha2[g]^-2
    tau.alpha3[g] <- sigma.alpha3[g]^-2
    tau.alpha4[g] <- sigma.alpha4[g]^-2
    tau.alpha5[g] <- sigma.alpha5[g]^-2

    # Detection
    mu.v[g]    ~ dnorm(0, 1/2.25^2)
    sigma.v[g] ~ dt(0, 1/2.25^2, 1) T(0,)
    tau.v[g] <- sigma.v[g]^-2

    # Covariate effects on detection
    mu.beta1[g]    ~ dnorm(0, 1/2.25^2)
    mu.beta2[g]    ~ dnorm(0, 1/2.25^2)
    mu.beta3[g]    ~ dnorm(0, 1/2.25^2)
    sigma.beta1[g] ~ dt(0, 1/2.25^2, 1) T(0,)
    sigma.beta2[g] ~ dt(0, 1/2.25^2, 1) T(0,)
    sigma.beta3[g] ~ dt(0, 1/2.25^2, 1) T(0,)
    tau.beta1[g]  <- sigma.beta1[g]^-2
    tau.beta2[g]  <- sigma.beta2[g]^-2
    tau.beta3[g]  <- sigma.beta3[g]^-2

  } # G groups
```

```
  ## Species level priors
  for (i in 1:I) {

      # Occupancy
      u[i]      ~ dnorm(mu.u[group[i]], tau.u[group[i]])
      alpha1[i] ~ dnorm(mu.alpha1[group[i]],tau.alpha1[group[i]])
      alpha2[i] ~ dnorm(mu.alpha2[group[i]],tau.alpha2[group[i]])
      alpha3[i] ~ dnorm(mu.alpha3[group[i]],tau.alpha3[group[i]])
      alpha4[i] ~ dnorm(mu.alpha4[group[i]],tau.alpha4[group[i]])
      alpha5[i] ~ dnorm(mu.alpha5[group[i]],tau.alpha5[group[i]])

      # Detection
      v[i]     ~ dnorm(mu.v[group[i]], tau.v[group[i]])
      beta1[i] ~ dnorm(mu.beta1[group[i]],tau.beta1[group[i]])
      beta2[i] ~ dnorm(mu.beta2[group[i]],tau.beta2[group[i]])
      beta3[i] ~ dnorm(mu.beta3[group[i]],tau.beta3[group[i]])

  } # I species

  for (i in 1:I) { # for each species i
      for (j in 1:J) { # for each site j

              # Ecological process model for latent occurrence z
              logit(psi[j,i]) <- u[i] +
                alpha1[i]*x_alpha1[j] +
                alpha2[i]*x_alpha2[j] +
                alpha3[i]*x_alpha3[j] +
                alpha4[i]*x_alpha4[j] +
                alpha5[i]*x_alpha5[j]

              z[j,i] ~ dbern(psi[j,i])

              for (k in 1:K[j]) { # for each survey k during season t at site j

                  ## Observation model, assuming no false positives

                  # p11 is true-positive detection probability given z = 1
                  logit(p11[j,k,i]) <- v[i] +
                    beta1[i]*x_beta1[j,k] +
                    beta2[i]*x_beta2[j,k] +
                    beta3[i]*x_beta3[j,k]

                  p[j,k,i] <- z[j,i] * p11[j,k,i]

                  # Observed outcome
                  y[j,k,i] ~ dbern(p[j,k,i])

                  # Simulated replicate for posterior predictive checks
                  y_sim[j,k,i] ~ dbern(p[j,k,i])

                  # Deviance (Broms et al. 2016)
                  d_obs[j,k,i] <- z[j,i] * (y[j,k,i] * log(p[j,k,i]) + (1 - y[j,k,i]) * log(1 -
p[j,k,i]))
                  d_sim[j,k,i] <- z[j,i] * (y_sim[j,k,i] * log(p[j,k,i]) + (1 - y_sim[j,k,i]) *
log(1 - p[j,k,i]))

              } # K surveys

              # Pad jagged array of deviance values with zeros to enable sum below
              for (k in (K[j]+1):Kmax) {
```

```
                d_obs[j,k,i] <- 0
                d_sim[j,k,i] <- 0
            }

      } # J sites
  } # I species

  ## Derived quantities

  # Deviance of simulated and observed data for posterior predictive check
  D_obs <- -2 * sum(d_obs[1:J,1:Kmax,1:I])
  D_sim <- -2 * sum(d_sim[1:J,1:Kmax,1:I])
}
```